

University of Groningen

## Neurogenerative diseases and the Protein quality control system

Seidel, Kay

**IMPORTANT NOTE:** You are advised to consult the publisher's version (publisher's PDF) if you wish to cite from it. Please check the document version below.

*Document Version*

Publisher's PDF, also known as Version of record

*Publication date:*

2011

[Link to publication in University of Groningen/UMCG research database](#)

*Citation for published version (APA):*

Seidel, K. (2011). *Neurogenerative diseases and the Protein quality control system*. [Thesis fully internal (DIV), University of Groningen]. [S.n.].

### Copyright

Other than for strictly personal use, it is not permitted to download or to forward/distribute the text or part of it without the consent of the author(s) and/or copyright holder(s), unless the work is under an open content license (like Creative Commons).

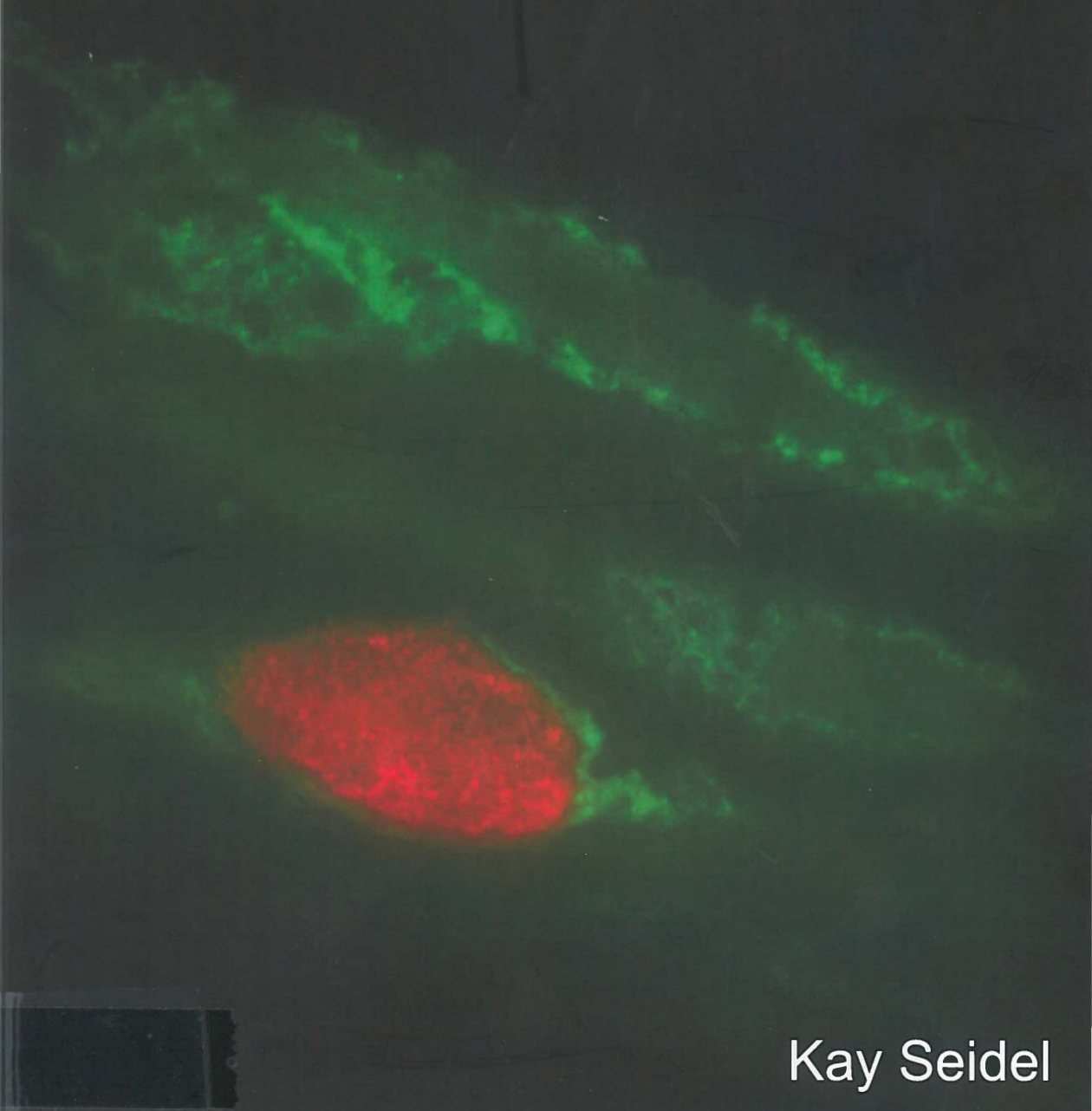
The publication may also be distributed here under the terms of Article 25fa of the Dutch Copyright Act, indicated by the "Taverne" license. More information can be found on the University of Groningen website: <https://www.rug.nl/library/open-access/self-archiving-pure/taverne-amendment>.

### Take-down policy

If you believe that this document breaches copyright please contact us providing details, and we will remove access to the work immediately and investigate your claim.

Downloaded from the University of Groningen/UMCG research database (Pure): <http://www.rug.nl/research/portal>. For technical reasons the number of authors shown on this cover page is limited to 10 maximum.

# Neurodegenerative diseases and the protein quality control system



Kay Seidel

# **Neurodegenerative diseases and the protein quality control system**

**Kay Seidel**

*The Studies in this thesis were supported by:*

The Research School of Behavioural and Cognitive Neurosciences  
(BCN)

J.K. de Cock stichting

The Deutsche Forschungsgemeinschaft (DFG)

The Deutsche Heredo-Ataxie-Gesellschaft (DHAG)

The ADCA-Vereniging Nederland

The Bernd Fink-Stiftung

The Prinses Beatrix Fonds

**ISBN: 978-90-367-5107-0**



## Stellingen

1. While controlled aggregation of proteins is often suggested as being cytoprotective (Arrasate et al., 2004), aggregation within neuronal processes is toxic and detrimental to neuronal health (Gunawardena and Goldstein, 2005; Wooten et al., 2006; Seidel et al., 2010) meaning that aggregate prevention or clearance at the earliest possible state may be the preferred way to go in searches for therapy
2. Neurodegeneration in Polyglutamine diseases has 2 components: a general component that arises from a toxic gain-of-function protein aggregation pathology and that is cell- and tissue-type independent and a specific component that arises from the loss or gain of function of the disease-specific protein that determines tissue specificity of the disease (Helmlinger et al., 20006; Duncan et al., 2011, This thesis).
3. Neuronal death in polyQ diseases results not from a single cause, but from cumulative stress build up, encompassing blocking axonal transport, continuous pressure on the protein quality control system, transcriptional dysregulation and other sources (this thesis).
4. It is needless to state that a human disease can never be accurately replicated in an animal model and that studies in animal models therefore have to be carefully designed to answer specific questions (de Jong and Maina, 2010). At the same time, carefully designed studies in animal models are indispensable to develop and test new concepts of ongoing disease processes and possible treatments.
5. Post mortem analysis of human tissue is not only essential for the diagnosis and the initial description of diseases, but through careful analysis it can provide further insight into underlying disease processes.
6. The idea to include a (christian) creator god as a scientific theory as proposed by some schools is incompatible with the principles of science that deal with the analysis of the measurable world. Since a godly intervention is not measurable, creationism thus has no place in the biological sciences at all (Greener, 2007).
7. Since Europe is running out of natural resources, knowledge becomes our primary asset: it is therefore of utmost importance to provide free education for everyone.
8. The Schengen area not only facilitates travel and commerce but also scientific exchange, while the drawbacks are often overdramatized and in reality, marginal (Studie über den erweiterten Schengenraum, Bundeskriminalamt, 2009).
9. The results of many studies, which were financed by public grants, are published in scientific journals, which are often prohibitively expensive and not available to the general public. Yet, the same public already paid for this research, and is entitled to its results. Thus, results from publically funded research should be available to everyone, for free.
10. Germans have the tendency to write overly long, verbose and contrived sentences in an attempt to articulate all their thoughts and opinions on a given subject, without breaking up the structure of the sentence or dividing the subject into different sentences, instead resorting to subordinate clauses and complex wording, often erring on the wrong side of both readability and information density (this thesis).

|   |
|---|
| U |
| M |
| C |
| G |

Bibliotheek  
Groningen



**rijksuniversiteit  
 groningen**

# **Neurodegenerative diseases and the Protein quality control system**

Proefschrift

ter verkrijging van het doctoraat in de  
Medische Wetenschappen  
aan de Rijksuniversiteit Groningen  
op gezag van de  
Rector Magnificus, dr. E. Sterken,  
in het openbaar te verdedigen op  
maandag 10 oktober 2011  
om 12.45 uur

|             |   |
|-------------|---|
| Centrale    | U |
| Medische    | M |
| Bibliotheek | C |
| Groningen   | G |

door

**Kay Seidel**

geboren op 13 februari 1978  
te Siegen, Duitsland

Promotores: Prof. dr. H.H. Kampinga

Copromotores: Dr. W.F.A. den Dunnen  
Dr. U. Rüb

Beoordelingscommissie: Prof. dr. B. Kremer  
Prof. dr. H.W.G.M. Boddeke  
Prof. dr. G. Auburger



*To my parents*

*and my friends*



# Table of Contents

---

|   |   |            |
|---|---|------------|
| <b>Chapter 1</b>                          | Introduction I: The neurodegenerative diseases  | <b>1</b>   |
| <b>Chapter 2</b>                          | Involvement of the auditory brainstem system in spinocerebellar ataxia type 2 (SCA2), type 3 (SCA3) and type 7 (SCA7).    | <b>23</b>  |
| <b>Chapter 3</b>                          | First Appraisal of Brain Pathology Owing to A30P Mutant Alpha Synuclein   | <b>47</b>  |
| <b>Chapter 4</b>                          | Axonal inclusions in spinocerebellar ataxia type 3  | <b>71</b>  |
| <b>Chapter 5</b>                          | Introduction II: The protein quality control system   | <b>95</b>  |
| <b>Chapter 6</b>                          | The p62 antibody reveals cytoplasmic protein aggregates in spinocerebellar ataxia type 6 (SCA6)                           | <b>113</b> |
| <b>Chapter 7</b>                          | Cellular protein quality control and the evolution of aggregates in SCA3  | <b>127</b> |
| <b>Chapter 8</b>                          | The HSPB8-Bag3 chaperone complex is upregulated in astrocytes in the human brain affected by protein aggregation diseases | <b>149</b> |
| <b>Chapter 9</b>                          | Discussion and future perspectives  | <b>189</b> |
| <b>Abstracts (Dutch, English, German)</b> |   | <b>207</b> |
| <b>Acknowledgements</b>                   |   | <b>224</b> |
| <b>Curriculum vitae</b>                   |   | <b>226</b> |

---



# **Chapter 1**

---

## **Introduction:**

### **The Neurodegenerative diseases**

---



## Contents

---

|            |   |           |
|------------|---|-----------|
| <b>1.1</b> | <b>The neurodegenerative diseases</b>   | <b>3</b>  |
| <b>1.2</b> | <b>The Tauopathies: Alzheimer's disease</b>                                   | <b>5</b>  |
| <b>1.3</b> | <b>The Synucleinopathies: Parkinson's disease</b>                             | <b>8</b>  |
| <b>1.4</b> | <b>The Polyglutamine diseases</b>   | <b>10</b> |
| <b>1.5</b> | <b>Aim of the studies, Part 1 (Protein aggregation and Neurodegeneration)</b> | <b>16</b> |

## 1.1 The Neurodegenerative diseases

The neurodegenerative diseases are characterized by the progressive dysfunction and death of neuronal cells, often in a conserved and disease specific manner. While many more diseases can affect the brain, by convention any disease with a known vascular (e.g. Morbus Binswanger), toxic (e.g. Morbus Wernicke-Korsakow), infectious (e.g. syphilis) or autoimmune (e.g. multiple sclerosis) cause is excluded from this group. There is a grey area concerning the prion diseases, which are by their nature infective, but since the infectious particle is a protein and not an organism or a virus, these are typically also included in the neurodegenerative diseases [16].

The symptoms of a neurodegenerative disease are highly specific, usually with disease-typical cardinal and secondary symptoms, corresponding to the underlying neurodegeneration. This degeneration can also lead to observable loss of volume of affected brain regions or to the formation of scar tissue within the central nervous tissue consisting mainly of astroglia, and commonly referred to as astrogliotic scar [41]. Most neurodegenerative disorders have a fixed set of degenerating areas, often even a sequence in which the different systems are affected. However, subtypes with slight alterations in the pathological process are known to exist, e.g. juvenile SCA3 (see below) has a slightly different set of symptoms than the adult onset form [12, 16]. Furthermore, the same brain sites can be affected by different diseases, leading to partial overlap in symptoms (see chapter 2). The symptom of parkinsonism for example is caused by loss of neurons in the substantia nigra [28]. It is primarily associated with Parkinson's disease, but may also occur in spinocerebellar ataxia 3 (SCA3) or multiple system atrophy [12].

Neurodegenerative diseases are often accompanied by marked histological changes and are frequently associated with the presence of protein aggregates [50, 53]. These aggregates primarily consist primarily of a disease typical protein, although other components may be sequestered into the aggregate. They exhibit a high amount of beta-sheet structures as well as beta cross links, and are resistant to detergents, which is why they are usually referred to as insoluble [53]. Protein aggregations can be visualized by diverse histochemical and immunohistochemical methods. While aggregates are present in most of the neurodegenerative diseases, the direct connection to the degenerative process is still under investigation. Initial studies attributed toxic properties to the aggregates themselves, however, more recent research focuses on 1) oligomeric precursor aggregates, 2) the prion like properties of disease proteins, 3) stress to the protein quality control caused by the aggregates as well as 4) sequestration of vital factors into the aggregate [9].

The diseases that are of interest for this thesis will be presented in more detail in the following part of the chapter (Alzheimer's disease, Parkinson's disease, Huntington's disease and Spinocerebellar Ataxia types 2, 3, 6 and 7). The experimental 3 chapters following the introduction of the diseases are concerned with the link between protein aggregation and neurodegeneration: The degeneration of the central auditory systems in the spinocerebellar ataxias Type 2, 3 and 7 (chapter 2), the aggregation and

degeneration pattern of a rare case of familial Parkinson's disease (Chapter 3), as well as the occurrence of axonal aggregations of ataxin-3 in spinocerebellar ataxia type 3 (chapter 4).

| Disease Protein        | Disease   |
|------------------------|---|
| tau                    | Alzheimer's disease, Pick's disease, Agyrophilic grain disease, Progressive supranuclear palsy, Corticobasal degeneration, Frontotemporal dementia, Frontotemporal dementia with parkinsonism linked to chromosome 17 |
| alpha-synuclein        | Parkinson's disease, Lewy Body dementia, Multiple system atrophy  |
| TDP43                  | Subfoms of Frontotemporal dementia  |
| Prion protein          | Creutzfeld Jakob disease, variant Creutzfeld Jakob disease, kuru  |
| Beta amyloid           | Alzheimer's disease, Cerebral amyloid angiopathy  |
| Polyglutamine Proteins | Huntington's disease, dentatorubroplidoluysian atrophy, spinobulbar muscular atrophy, spinocerebellar ataxia 1, 2, 3, 6, 7 and 17   |

**Table 1.1: Disease proteins and diseases**

This table depicts disease proteins, as well as the diseases associated with them. Note that Polyglutamine proteins are not related, but share a polyglutamine sequence within their aminoacid sequences

These chapters are followed by an introduction into the core concepts of the cellular protein quality control systems and how they affect different neurodegenerative diseases (chapter 5) and experimental chapters on how components of the protein quality systems are altered in post-mortem brain tissue (chapters 6-8).

## **1.2. The tauopathies: Alzheimer's disease**

The tauopathies are a group of diseases marked by the intracellular aggregation of the tau protein (table 1.1), of which 6 splicing variants are known. Tau localizes to microtubules, where it acts as a stabilizing agent [17, 20]. The protein is highly expressed in the human brain. Under certain conditions the tau protein can become hyperphosphorylated, which causes it to assemble into characteristic paired helical filaments which in turn assemble into larger aggregates, which have proven to be detrimental to the cell [3, 21].

In Alzheimer's disease (AD) the hyperphosphorylated tau protein aggregates into typical flame shaped neurofibrillary tangles (Fig. 1.2A). Additionally, the disease also displays aggregations of another disease typical protein, the amyloid-beta protein, which aggregates into extracellular plaques. These plaques display a characteristic development from unordered diffuse stainings to plaques with a highly condensed amyloid-beta core positive for the amyloid-beta 40 isoform (Fig. 1.2B-D) [15].

AD is not only the most prevalent tauopathy, but also the most frequent neurodegenerative disease known [31]. Its incidence is 0.5%-0.8% overall and increases drastically with age. AD is mostly idiopathic, but certain genetic risk factors (e.g. ApoE4) as well as mutations resulting in true familial forms (e.g. APP, PSEN) are known to exist [5, 35, 43]. The protein aggregation follows a conserved pattern, which is covered by the staging system proposed by Braak and Braak [7]. The areas affected in the earliest stages are the entorhinal /transentorhinal cortex, as well as the hippocampus (Fig. 1.1).

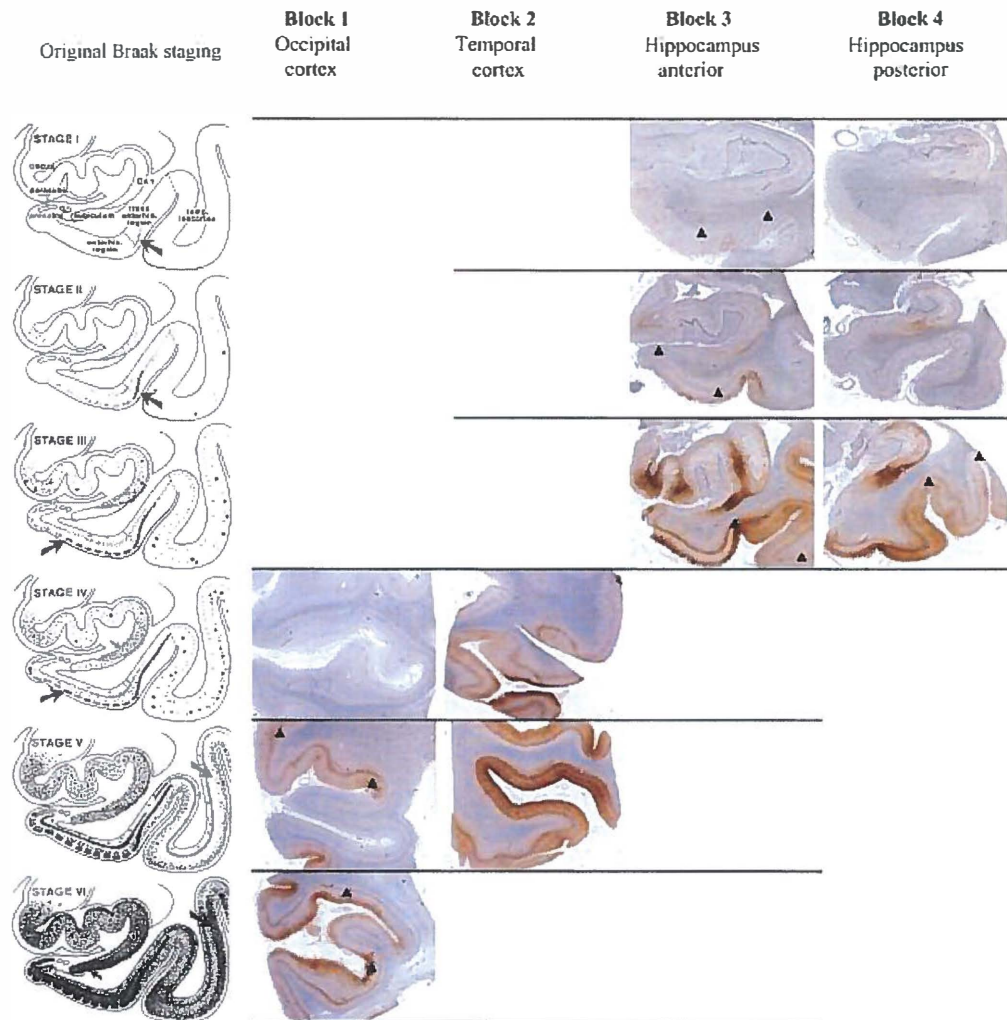


**Figure 1.1: Alzheimer staging and correlation to Abeta pathology in different brain areas**  
The left column depicts spreading of pathology in the Hippocampal area of AD patients, grey shades indicate pathology, arrows depict leading characteristics. 4 columns to the right depict micrographs of tau staining from the anterior and posterior hippocampus as well as the temporal and occipital cortices. The arrowheads indicate borders for the relevant neuroanatomical regions for each given stage.

(adapted from Alafuzoff et al. 2008; Braak and Braak, 1995)

AD patients present with progressive dementia and memory loss. Usually, at the time of diagnosis the brain already exhibits marked neurodegeneration. These symptoms correlate well with the early and grave affection of the entorhinal/transentorhinal cortex as well as the CA1-4 regions of the hippocampus, which are involved in memory formation and processing. In later stages, the neuronal loss becomes macroscopically visible [31].

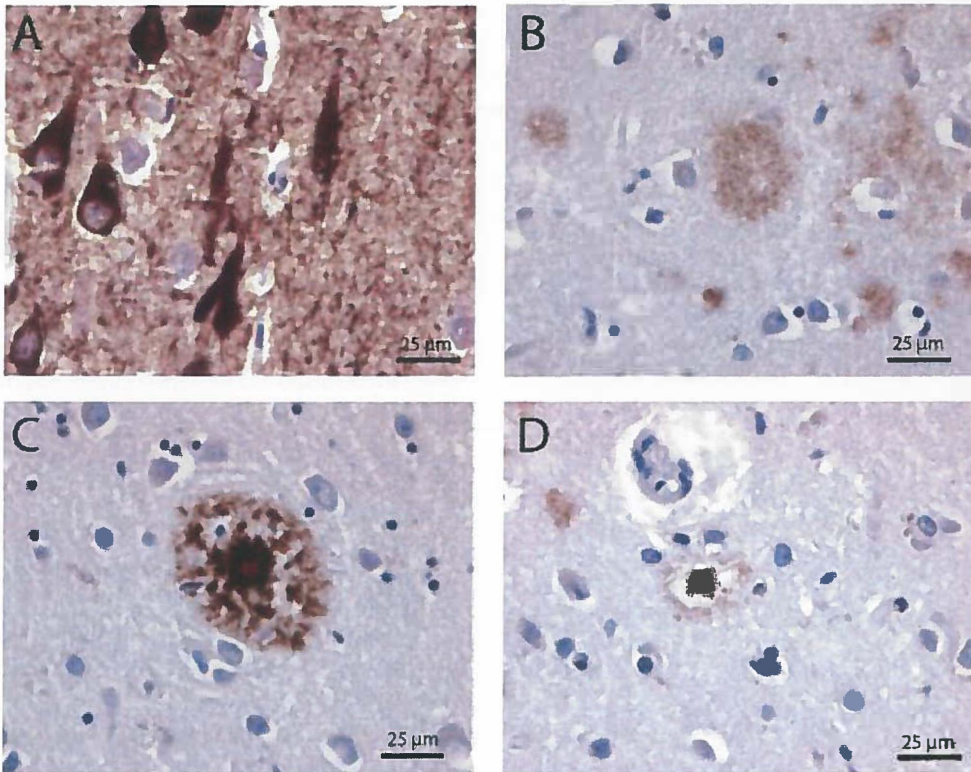


**Figure 1.2: Protein Aggregation in Alzheimer's disease**

(A) Typical flame shaped neurofibrillary tangles as seen in the Hippocampus of Alzheimer's disease, reactive for the AT-8 antibody, which is specific for the hyperphosphorylated form of the tau protein. B-D) Abeta plaques in different stages. (B) depicts the early diffuse form, (C) depicts a mature plaque with a visible core and (D) a "burnt out" structure with only the core remaining.



### 1.3. The synucleinopathies: Parkinson's disease

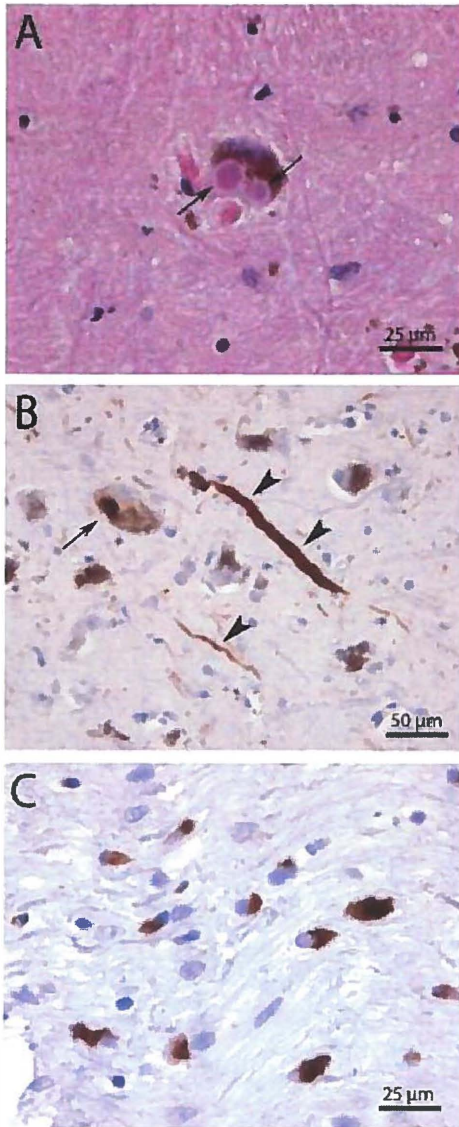


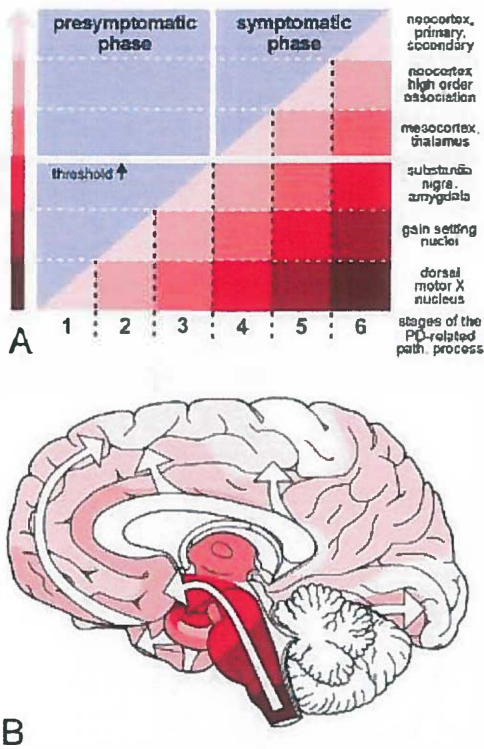
**Figure 1.3: Aggregates of Parkinson's disease**

(A) Eosinophilic Lewy bodies in a pigment-rich neuron of the substantia nigra (arrows). (B) Lewy body (arrow) and Lewy neurites (arrowheads) stained with an anti-alpha synuclein antibody. (C) Oligodendroglial coiled bodies stained with an anti-alpha synuclein antibody.

The synucleinopathies are marked by aggregation of the alpha-synuclein protein (table 1.1). Alpha-synuclein itself is highly expressed in the human brain, and is mainly located in the synaptic terminals, where it localizes to the lipid membranes of synaptic vesicles. The alpha synuclein positive aggregates exist in different forms: the rounded lewy bodies located in neuronal somata, the elongated, neuritic lewy neurites as well as the oligodendroglial coiled bodies and astrocytic aggregates (Fig. 1.3). The types of aggregates and their distribution in the affected brain depend on the disease [37].

The most prevalent synucleinopathy known is Parkinson's disease (PD), a motor disease of old age with serious non-motor symptoms. PD exhibits Lewy bodies, Lewy neurites, diffuse astroglial aggregates and oligodendroglial coiled bodies (Fig. 1.3) [28]. As has been shown recently, the alpha-synuclein aggregation "invades" healthy neuronal areas and even transplants over time, the method of propagation is however still unknown [34]. A theoretical explanation for this is permissive templating, a model where oligomeric aggregates of alpha-synuclein enter cells by unknown means and, given a permissive cell environment, act as a template for further aggregation of alpha-synuclein protein, resulting in macroscopically visible alpha-synuclein aggregates [24].

PD has an incidence of 1% at age 65, with an increasing prevalence in older ages [28]. The majority of all cases of PD are idiopathic. However, several other causes are known such as chemically induced as well as inheritable forms, three of which are located within the disease protein alpha-synuclein (A30P, E46K, A53T) [32, 42, 58]. Since these mutations are very rare and have only recently been discovered, pathological data in these familial forms is scarce (chapter 3).



The sequence in which the protein aggregation affect the patient brain is very specific, and has been staged (Fig. 1.4) [8]. Aside from the possible compromitation of neuronal function by aggregates there is a pronounced neurodegeneration of specific catecholaminergic neuron groups, most prominently the substantia nigra and the locus coeruleus. This leads to a marked, macroscopically visible discoloration of the aforementioned areas [28]. This results in a loss of input into the basal ganglio thalamocortical loop, an important motor control system. Clinically, PD patients exhibit hypokinesia and tremor as primary symptoms, furthermore they may exhibit rigidity, flexed posture, freezing and loss of postural reflexes. PD patients exhibit a good and sustained response to dopamine replacement therapeutics, such as Levodopa [28].



#### 1.4. The Polyglutamine diseases: Huntington's disease and the Spinocerebellar ataxia types 2, 3, 6 and 7

The polyglutamine diseases are a set of genetically and clinically diverse diseases (table 1.1). They are all caused by the expansion of a polymorphic CAG repeat sequence within a disease specific protein. Except for this CAG repeat, the disease proteins show no significant sequence homologies and are otherwise unrelated. The diseases are inheritable, in a dominant manner, and new mutations of the disease locus are rare [38, 46].

Onset and severity of the diseases are closely and inversely related to the length of the polyCAG sequence, with a longer expansion beyond a certain threshold leading to an earlier onset of the disease symptoms (Figure 1.5) [23]. Furthermore, an already elongated sequence has the tendency to expand further in following generations, in a process is known as anticipation. Anticipation does not happen in SCA6, which is known for its very short CAG repeat length [38].

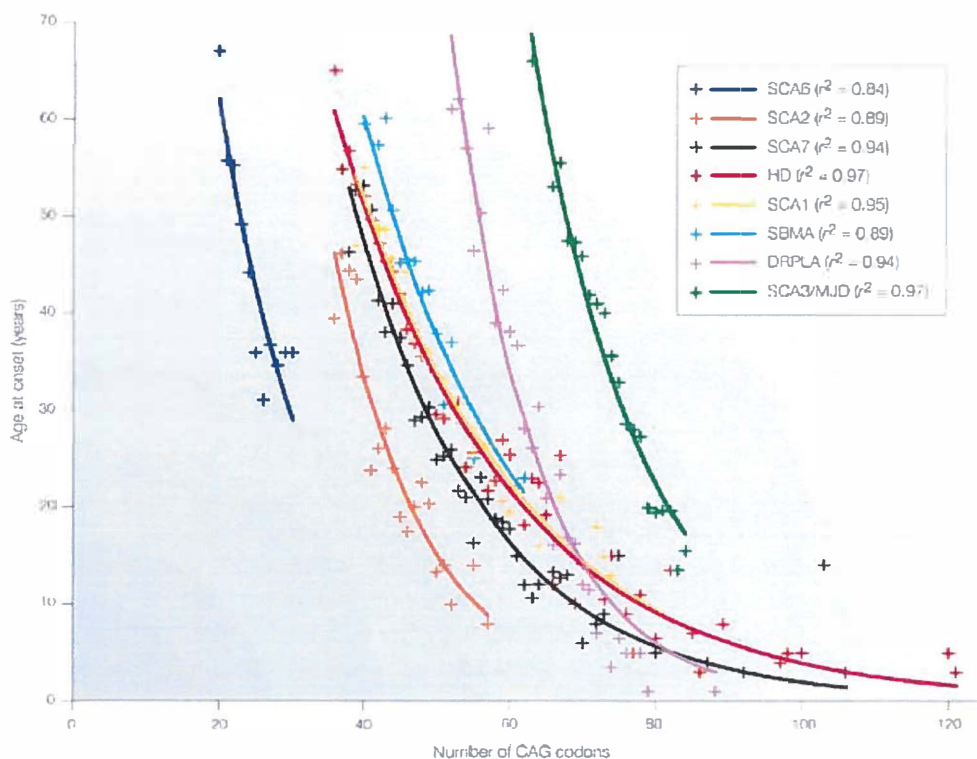


**Figure 1.5: Age of onset related to CAG-repeat length in several polyglutamine diseases**  
Several ages of onset were compiled from literature and correlated to CAG repeats lengths (+). From these data points disease specific curves were compiled.

(reproduced from Gusella and MacDonald, 2000)

The CAG sequence within the disease gene is translated into a polyglutamine (PolyQ) sequence. The extension of this sequence alters the biochemical properties of the diseased protein and relates to its propensity to cause aggregation. The disease phenotype is most likely caused by this toxic gain of function of the protein, as the disease is dominant and there is no clear gene dosage effect. In the majority of the polyQ diseases, protein aggregates are recognizable [38, 39, 57].

All polyQ diseases lead to neuronal degeneration. Although a certain overlap exists between several of the diseases, specific symptoms help to differentiate the disease. The same is true for the underlying degeneration. Most theories link the disease protein's increased propensity to aggregate with neuronal death, however, no mechanism has been clearly identified. While initial theories proposed a role of the large, visible, nuclear protein inclusions, more recent works propose oligomers or small aggregates as the toxic species. In addition, disturbance of axonal transport processes or/and other related and unrelated cellular functions rather than neuronal loss per se may be the cause for – at least the earlier – clinical manifestations of the disease [36, 51].

### *Huntington's disease*

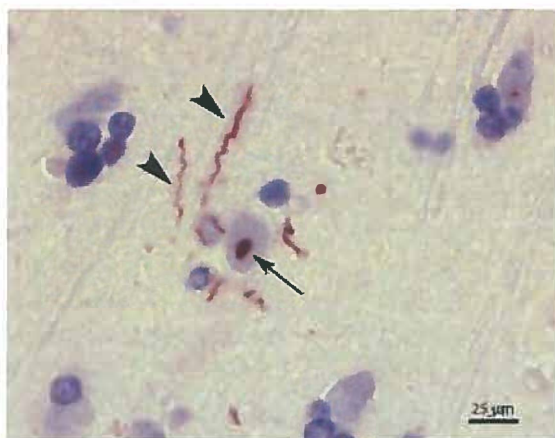


**Figure 1.6: Polyglutamine aggregates in Huntington's disease**

Depicted here are p62 positive polyglutamine aggregates in Huntington's disease, axonal aggregates (arrowheads) have been described in Huntington's disease earlier, NNI (arrow) are also known in SCA1, 3 and 7.

HD is the most common polyQ disease worldwide [25]. It is caused by an expansion of the CAG repeat within the huntingtin gene. In healthy individuals, this sequence has less than 36 repeats, with 36-40 repeats there is incomplete penetrance, a repeat length beyond 40 results in the disease phenotype [25, 55]. The age of onset correlates inversely to the CAG repeat length. While shorter repeats do not result in the disease phenotype recent reports show an increased propensity of any CAG repeat length beyond 28 to expand in following generations [55].

Huntingtin in its native state is a 348 kDa protein, and completely soluble [13]. The protein is expressed in moderate amounts in both neuronal and non neuronal tissue, and has been implicated to have an important role in early neuronal development, transport

and transcription processes [10, 25]. Htt knockout mutants are not viable, mouse htt  $-/-$  mutants die before day 9 of embryogenesis [10].

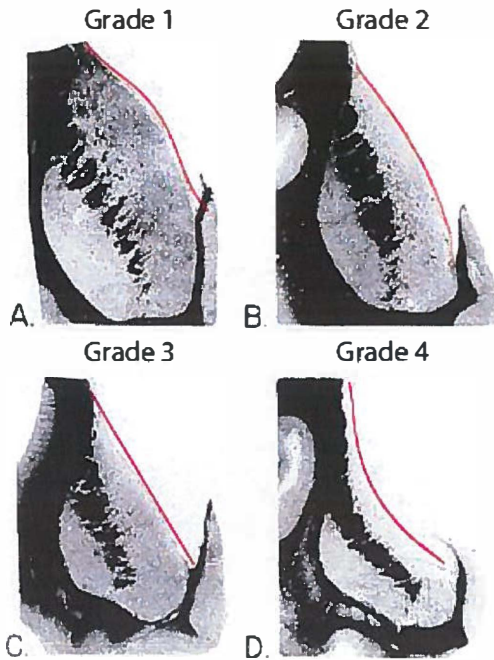


**Figure 1.7: Grading of Huntington's disease**

Huntington's disease is graded by the shape of the severely affected striatum, with neuronal loss and gliosis. In grade 1 patients and controls no macroscopic change is visible, the nucleus appears convex (A). Grade 2 patients exhibiting slight reduction of the nuclear volume, with a less convex outline (B). Grade 3 patients display marked neuronal and volume loss resulting in a straight borderline (C). Grade 4 patients display almost total atrophy of the nucleus, resulting in a concave outline (D).

(adapted from Vonsattel et al., 1985)

Expanded huntingtin is known to aggregate into dot like neuronal nuclear inclusion bodies (NNI) and elongated axonal aggregates (Fig. 1.6) [13]. The link between NNI and neurodegeneration is still unclear and may represent a late event in disease progression, maybe leading to or associated with neuronal death. Axonal aggregates of disease proteins however might be detrimental to neuronal function in an earlier stage of the disease and ultimately culminate in or lead to NNI [22]. Whether axonal aggregates are also formed in other polyQ diseases has as of yet not been systematically investigated (chapter 4).

Jerky, uncontrollable movements, referred to as chorea, are present in the majority of HD patients, but can be transitory in early onset cases. Further symptoms include mental decline with executive dysfunction and depression, rigidity, motor impersistence, dysphagia as well as oculomotor symptoms [25, 29, 55]. The symptoms are progressive and can be linked to the graded pathology. Patients usually die after an average of 20 years after diagnosis due to complications from falling, dysphagia, cachexia and aspiration [29].

HD mainly affects the medium spiny neurons of the striatum but affects further parts of the brain during the progression of the disease, which leads to a mass loss and dilation of the ventricles readily recognizable by imaging techniques. Secondary locations of degeneration include the cerebral cortex, thalamus, hypothalamus, hippocampus,

brainstem, as well as the cerebellar Purkinje cell layer [25, 54, 55]. The disease has been graded into 4 stages (Fig. 1.7) [54]

### *Spinocerebellar ataxia type 2*

SCA2 is caused by the expansion of the protein ataxin-2. The disease is one of the more frequent spinocerebellar ataxias, with a very large prevalence in the Holguin province of Cuba [2]. Healthy patients have a CAG repeat length of 31 or less, 32-34 repeats lead to incomplete penetrance, while a longer expansion results in the fully fledged disease phenotype [27, 33, 38, 40, 49].

Ataxin-2 is a 140kDa protein, which is unrelated to other polyQ proteins. The protein is expressed widely in neuronal as well as non-neuronal tissue, with its function still being unresolved. It exhibits several RNA interacting motifs, associates with other RNA interacting proteins and localizes to RNA containing stress granules. In centrifugation experiments, it localizes to the fraction of the endoplasmatic reticulum [33].

The main symptoms of SCA2 are gait ataxia/dysarthria or rigidity/bradykinesia coupled with early and marked slowing of saccades. Further symptoms include myoclonus or fasciculation like movements, diminished reflexes, frequent cramps and tremor. Since these symptoms can occur in other diseases, the final diagnosis is usually carried out genetically [33, 38, 40, 49].

The disease pathology affects the medulla oblongata, pons, thalamus and cranial nerves and leads to a pallor of the substantia nigra. The degeneration results in a pronounced loss of volume. The ataxia exhibited by most patients is caused by the olivo-ponto-cerebellar degeneration. The affection of several ingestion related brain areas leads to dysphagia, aspiration and finally to death by aspiration pneumonia [33]. Furthermore, affection of the auditory pathways will be described in chapter 2.

### *Spinocerebellar ataxia type 3*

SCA3 is the most common type of spinocerebellar ataxia [49]. It is caused by an expansion of the PolyCAG sequence in the ATXN3 gene, which codes for the ataxin-3 protein. In healthy conditions, the polyCAG stretch has 12-40 repeats, while a repeat length of 53+ shows full penetrance and leads to disease phenotype [40].

Ataxin-3 is a protein widely expressed in neuronal and non neuronal tissue. Its function in healthy conditions is still subject to research. Recent studies elucidated a de-ubiquitinating function, as well as 2 ubiquitin interacting motifs. Likewise, it has been revealed that ataxin-3 is necessary for the correct formation of muscle tissue in mice, by stabilizing several key factors at the protein level [14, 56].

Protein aggregations, with mutant ataxin-3 as primary component, have been described before in SCA3, most prominently in the form of NNI [57]. They are a frequent and ubiquitous occurrence in SCA3, in fact, end stage cases often exhibit NNI in the majority of the central nervous neurons, regardless if the area is affected by neurodegeneration or not [47]. While a direct link between NNI and neurodegeneration has been suggested earlier, it was not possible to correlate neuronal loss with the distribution of NNI [47]. However, as other studies in animal models point out, nuclear localization is important for ataxin-3 toxicity [6]. Yet, several alternative sources of stress to the neurons have been suggested [22, 51].

The cardinal symptoms of SCA3 are limb, stance and trunk ataxia. This is accompanied by several other symptoms such as dysarthria, dysphagia, oculomotor dysfunctions, pyramidal signs, dystonia, bradykinesia, lower motor neuron neuropathy, peripheral neuropathy and rarely parkinsonism [45, 49]. Furthermore, affection of the auditory pathways will be described in chapter 2. In late stages the dysphagia becomes more prominent, leading to continued aspiration and resulting in death by aspiration pneumonia [48]

Patients exhibit a pronounced neuronal loss within the brainstem and parts of the mesencephalon. The neurodegeneration is severe and leads to a loss of brain volume which is macroscopically visible, especially of the brain nerves, which often are severely degenerated. The causative grey matter loss affects all of the major brain nerve nuclei, motor and somatosensory pathways, and the cerebellar Purkinje cell layer as well as deep cerebellar nuclei.

#### *Spinocerebellar ataxia type 6*

In comparison to the other polyQ diseases SCA6 is a relatively milder disease. Although the disease symptoms are still grave, it is rarely life determining [38, 40, 49]. The disease is caused by the comparatively short expansion of a polyQ repeat in CACNA1A, a voltage gated calcium channel [44]. Even in disease cases, the expansion is usually too short to detect the disease protein with a polyQ specific antibody, and protein aggregation is still debated (see chapter 6) [52].

The disease symptoms usually encompass a cerebellar ataxia accompanied by dysarthria and gaze evoked nystagmus. Other noncerebellar symptoms are less frequent, but can include a decreased vibration and positions sense, impaired eye movements and, later in the course of the disease, spasticity and hyperreflexia. The symptoms progress slowly and are usually compatible with a normal life span [38, 40, 49].

The primary site of degeneration is the cerebellum with affection of the Purkinje cell layer as well as the deep cerebellar nuclei, the atrophy is macroscopically observable. Extracerebellar sites of degeneration include motor and sensor systems of the



brainstem and the midbrain, as well as loss of giant Betz motoneurons of the cerebral cortex [19].

#### *Spinocerebellar ataxia type 7*

Spinocerebellar ataxia type 7 is one of the less frequent SCAs, and caused by the expansion within the ATXN-7 gene [49]. This gene is known for its strong tendency for anticipation, which leads to large leaps in CAG repeat length between generations coupled with a comparatively high incidence of new mutations [11]

The disease gene ATXN-7 has a toxic threshold of 34 repeats. Expansions beyond this threshold result in the fully fledged disease phenotype. 34-36 repeats result in an incomplete penetrance, while a repeat length of 28-33 does not result in any disease phenotype but show a strong tendency for anticipation. Expansions of more than 300 repeats have been reported, which result in infant onset and rapid death [11]. Its normal function is related to the formation of the STAGA complex, which controls the transcription of a number of genes, several of which are important for correct eye function [26].

Apart from a marked cerebellar ataxia, dysarthria and dysphagia, SCA7 patients present with a distinct and progressive loss of vision, due to affection of the retina [4]. This results in blindness in advanced cases, which sets the disease clearly apart from any of the other PolyQ disorders. These symptoms may be accompanied by brisk reflexes and oculomotor abnormalities [38, 40, 49].

Neuronal loss and gliosis are present in the cerebellum, the medulla oblongata, the pons, and to a lesser extent in the globus pallidus, substantia nigra, and red nucleus. The retinal atrophy is marked and unique among the spinocerebellar ataxias. SCA7 cases exhibit NNIs, although those are rare compared to SCA3 or HD [38, 40, 49]. An additional affection of the auditory systems will be described in chapter 2.

### **1.5. Aim of the studies, Part 1 (Protein aggregation and Neuro-degeneration)**

In many neurodegenerative diseases, the aggregation of a disease typical protein is coupled with the death of neurons. This may result in a macroscopically visible atrophy of white and grey matter areas.

To study the underlying connection between disease protein aggregation and neurodegeneration, biological models are necessary. Unlike the study of human tissue which can only provide snapshots of the disease situation, biological models can provide the opportunity to study different, even presymptomatic stages and allow for in vivo imaging. However given the length of the pathological process, which can easily exceed 10 years in most of the neurodegenerative diseases, compared with the life expectancy of a lab animal or a culture models, and the complexity of the human brain compared with these models, it is clear that these disease models are difficult to establish. This is why examination of the pathoanatomy in the diseases human brain provides a necessary baseline.

Neurodegenerative diseases often exhibit grave and life determining symptoms, especially in the later stages, which can mask some of the more discrete clinical manifestations. In order to maximize the quality of life of the late stage patients, any hint of additional symptoms which may be overlooked in standard clinical care is appreciated. Pathoanatomical investigation can provide those hints by investigating brain areas with a known function and comparing those with the clinical picture.

#### **1) Involvement of the auditory brainstem system in spinocerebellar ataxia type 2 (SCA2), type 3 (SCA3) and type 7 (SCA7)**

SCA2, 3 and 7 are known for their severe motor phenotype, which dominate the clinical picture, and marked atrophy of the brainstem and the somatomotor and –sensor components known to be affected in the spinocerebellar ataxias. To enable better care for the patients, investigation of other possibly affected systems located in the brainstem is warranted, as in this case, the auditory system.

#### **2) First appraisal of brain pathology owing to A30P mutant alpha-synuclein.**

Since the discovery of the PD causing alpha-synuclein mutants, these have seen intensive use in diverse PD models (Krüger et al., 1998). A comparison between idiopathic and inherited PD is necessary to validate the use of these models.

#### **3) Axonal inclusions in spinocerebellar ataxia type 3.**

Axonal aggregates, as known from HD, have been suggested as inhibitors of axonal transport (Di Figlia et al., 1997, Gunawardena and Goldstein, 2005). Huntington's disease is known to express axonal aggregations. This study investigates, if these potentially dangerous structures are present in the polyQ disease SCA3 as well.

## References

1. Alafuzoff I, Arzberger T, Al-Sarrai S, Bodi I, Bogdanovic N, Braak H, Bugiani O, Del-Tredici K, Ferrer I, Gelpi E, Giaccone G, Graeber MB, Ince P, Kamphorst W, King A, Korkolopoulou P, Kovács GG, Larionov S, Meyronet D, Monoranu C, Parchi P, Patsouris E, Roggendorf W, Seilhean S, Tagliavini F, Stadelmann C, Streichenberger N, Thal DR, Wharton SB, Kretzschmar H. *Brain Pathol* 2008;18:484-496.
2. Auburger G, Orozco-Diaz G, Capote R, Gispert S, Perez M, Cueto M, Meneses M, Farrall M, Williamson R, Chamberlain S, Heredero L. Autosomal dominant ataxia: Genetic evidence for locus heterogeneity from a Cuban founder effect population. *Am J Hum Genet* 1990;46:1163-1177.
3. Ballatore C, Lee VM, Trojanowski JQ. Tau mediated neurodegeneration in Alzheimer's disease and related disorders. *Nat Rev Neurosci* 2007;8:663-672.
4. Benomar A, Le Guern E, Dürr A, Ouhabi H, Stevanin G, Yahyaoui M, Chkili T, Agid Y, Brice A. Autosomal-dominant cerebellar ataxia with retinal degeneration (ADCA type II) is genetically different from ADCA type I. *Ann Neurol* 1994;35:439-444.
5. Bertram L, Tanzi R. Alzheimer type dementia. In: Dickson DW, editor. *Neurodegeneration: The molecular pathology of dementia and movement disorders*. Basel: ISN Neuropath Press; 2003;40-46.
6. Bichelmeier U, Schmidt T, Hübener J, Boy J, Rüttiger L, Häbig K, Poths S, Bonin M, Knipper M, Schmidt WJ, Wilbertz J, Wolbutg H, Laccone F, Riess O. Nuclear localization of ataxin-3 is required for the manifestation of symptoms in SCA3: in vivo evidence. *J Neurosci*. 2007;27:7418-28.
7. Braak H, Braak E. Staging of Alzheimer's disease-related neurofibrillary changes. *Neurobiol Aging* 1995;16:271-278.
8. Braak H, Del Tredici K, Rüb U, De Vos RA, Jansen Steur EN, Braak E. Staging of brain pathology related to sporadic Parkinson's disease. *Neurobiol Aging* 2003;24:197-211.
9. Bucciantini M, Giannoni E, Chiti F, Baroni F, Formigli L, Zurdo J, Taddei N, Ramponi G, Dobson CM, Stefani M. Inherent toxicity of aggregates implies a common mechanism for protein misfolding diseases. *Nature* 2002;416:507-511.
10. Cattaneo E, Zuccato C, Tartari M. Normal Huntingtin function: an alternative approach to Huntington's disease. *Nat Rev Neurosci* 2005;6:919-930.



11. David G, Abbas N, Stevanin G, Dürr A, Yvert G, Cancel G, Weber C, Imbert G, Saudou F, Antoniou E, Drabkin H, Denmill R, Giunti P, Benomar A, Wood N, Ruberg M, Agid Y, Mandel JL, Brice A. Cloning of the SCA7 gene reveals a highly unstable CAG repeat expansion. *Nat Genet* 1997;17:65-70.
12. Dickson DW, editor. *Neurodegeneration: The molecular pathology of dementia and movement disorders*. Basel: ISN Neuropath Press; 2003.
13. DiFiglia M, Sapp E, Chase KO, Davies SW, Bates GP, Vonsattel JP, Aronin N. Aggregation of huntingtin in neuronal intranuclear inclusions and dystrophic neurites in Brain. *Science* 1997;277:1990-1993.
14. do Carmo Costa M, Bajanca F, Rodriguez AJ, Tome RJ, Cothals G, Macedo-Ribeiro S, Paulson HL, Logarinho E, Maciel P. Ataxin-3 plays a role in the mouse myogenic differentiation through regulation of integrin subunit levels. *PLoS One* 2010;5:e11728
15. Duyckaerts C, Dickson DW. Neuropathology of Alzheimer's disease. In: Dickson DW, editor. *Neurodegeneration: The molecular pathology of dementia and movement disorders*. Basel: ISN Neuropath Press; 2003;47-65.
16. Ellison D, Love S, Chimelli L, Harding B, Lowe J, Roberts GW, Vinter HV, editors. *Neuropathology*. Barcelona: Mosby international; 1998.
17. Garcia ML, Cleveland DW. 2001. Going new places using an old MAP: microtubules and human neurodegenerative disease. *Curr Opin Cell Biol* 13:41-48.
18. Gibb WR. Functional neuropathology in Parkinson's disease. *Eur Neurol* 1997;38 Suppl 2:21-25
19. Gierga K, Scheelhaas HJ, Brunt ER, Seidel K, Scherzed W, Egensperger R, de Vos RA, den Dunnen W, Ippel PF, Petrasch-Parwez E, Deller T, Schöls L, Rüb U. Spinocerebellar ataxia type 6 (SCA6): neurodegeneration goes beyond the known brain predilection sites. *Neuropathol Appl Neurobiol* 2009; 35:515-527.
20. Goedert M, Hasegawa M. The Tauopathies: Toward an experimental animal model. *Am J Pathol* 1999 January; 154: 1-6.
21. Goedert M, Spillantini MG, Jakes R, Crowther RA, Vanmchelen E, Probst A, Götz J, Bürki K, Cohen P. Molecular dissection of the paired helical filament. *Neurobiol Aging* 1995;16:325-334.

22. Gunawardena S, Goldstein LS. Polyglutamine diseases and transport problems: deadly traffic jams on neuronal highways. *Arch Neurol* 2005;62:46-51.
23. Gusella JF, MacDonald ME. Molecular genetics: unmasking polyglutamine triggers in neurodegenerative disease. *Nat Rev Neurosci* 2000;1:109-115.
24. Hardy J, Expression of normal sequence pathogenic proteins for neurodegenerative disease contributes to disease risk: 'permissive templating' as a general mechanism underlying neurodegeneration. *Biochem Soc Trans* 2005;33:578-581.
25. Hedreen JC, Roos RAC. Huntington's disease. In *Neurodegeneration: The molecular Pathology of Dementia and Movement Disorders*. Ed DW Dickson. Basel: ISN Neuropath Press; 2003;229-41.
26. Helmlinger D, Hardy S, Abou-Sleymane G, Eberlin A, Bowman AB, Gansmüller A, Picaud S, Zhogby HY, Trottier Y, Tora L, Devys D. Glutamine-expanded ataxin-7 alters TFTC/STAGA recruitment and chromatin structure leading to photoreceptor dysfunction. *PLoS Biol* 2006;4:e67
27. Hernandez A, Magarino C, Gispert S, Santos N, Lunkes A, Orozco G, Heredero L, Beckmann J, Auburger G. Genetic mapping of the spinocerebellar ataxia 2 (SCA2) locus on chromosome 12q23-q24.1. *Genomics* 1995;25:433-435.
28. Jellinger KA, Mizuno Y. Parkinson's disease. In: Dickson DW, editor. *Neurodegeneration: The molecular pathology of dementia and movement disorders*. Basel: ISN Neuropath Press; 2003;159-187.
29. Kagel M, Leopold NA. Dysphagia in Huntington's disease: a 16-year retrospective. *Dysphagia* 1992;7:106-114.
30. Kawaguchi Y, Okamoto T, Taniwaki M, Aizawa M, Inoue M, Katayama S, Kawakami H, Nakamura S, Nishimura M, Akiguchi I, Kimura J, Narumiya S, Kakizuka A. CAG expansions in a novel gene for Machado-Joseph disease at chromosome 14q32.1. *Nat Genet* 1994;8:221-228.
31. Knopman D. Alzheimer type dementia. In: Dickson DW, editor. *Neurodegeneration: The molecular pathology of dementia and movement disorders*. Basel: ISN Neuropath Press; 2003;24-39.
32. Krüger R, Kuhn W, Müller T, Woitalla D, Graeber M, Kosel S, Przuntek H, Eppelen JT, Schöls L, and Riess O. Ala30Pro mutation in the gene encoding alpha-synuclein in Parkinson's disease. *Nature Genet* 1998;18:106-108.

33. Lastres-Becker I, Rüb U, Auburger G. Spinocerebellar ataxia 2 (SCA2). *Cerebellum* 2008;7:115-24
34. Li JY, Englund E, Holton JL, Soulet D, Hagell P, Lees AJ, Lashley T, Quinn NP, Rehnkrone S, Björklund A, Widner H, Revesz T, Lindvall O, Brundin P. Lewy bodies in grafted neurons in subjects with Parkinson's disease suggest host to-to-graft disease propagation. *Nat Med* 2008;14:501-503.
35. McGowan E, Eriksen J, Hutton M. A decade of modeling Alzheimer's disease in transgenic mice. *Trends Genet* 2006;22:281-289.
36. Michalik A, van Broeckhoven C. Pathogenesis of polyglutamine disorders: aggregation revisited. *Hum Mol Genet* 2003;12 Spec No 2: R173-186.
37. Norris EH, Giasson BI, Lee VM. Alpha-synuclein: normal function and role in neurodegenerative diseases. *Curr Top Dev Biol* 2004;60:17-54.
38. Orr HT, Zoghbi HY. Trinucleotide repeat disorders. *Annu Rev Neurosci* 2007;30: 575-621.
39. Paulson H. Protein fate in neurodegenerative proteinopathies: Polyglutamine diseases join the (mis)fold. *Am J Hum Genet* 1999;64:339-345.
40. Paulson H. The spinocerebellar ataxias. *J Neuroophthalmol* 2009;29:227-237.
41. Pekny M, Nilsson M. Astrocyte activation and reactive gliosis. *Glia* 2005;50:427-434.
42. Polymeropoulos MH, Lavedan C, Leroy E, Ide SE, Dehejia A, Dutra A, Pike B, Root H, Rubenstein J, Boyer R, Stenroos ES, Chandrasekharappa S, Athanassiadou A, Papapetropoulos T, Johnson WG, Lazzarini AM, Duvoisin RC, Di Iorio G, Golbe LI, Nussbaum RL. Mutation in the alpha-synuclein gene identified in families with Parkinson's disease. *Science* 1997;276:2045-2047.
43. Price DL, Sisodia SS. Mutant genes in familial Alzheimer's disease and transgenic models. *Annu Rev Neurosci* 1998;21:479-505.
44. Riess O, Rüb U, Pastore A, Bauer P, Schöls L. SCA3: neurological features, pathogenesis and animal models. *Cerebellum* 2008;7:125-137.
45. Riess O, Schöls L, Bottger H, Nolte D, Vieira-Saecker AM, Schimming C, Kreuz F, Macek M Jr, Kresova A, Macek M Sen, Klockgether T, Zühlke C, Laccone FA. SCA6 is caused by moderate CAG expansion in the alpha1A-voltage-dependent calcium channel gene. *Hum Mol Genet* 1997;6:1289-1293.

46. Ross CA. Introduction to Trinucleotide Repeat Disorders. In: Dickson DW, editor. *Neurodegeneration: The molecular pathology of dementia and movement disorders*. Basel: ISN Neuropath Press; 2003;226-228.
47. Rüb U, Brunt ER, Petrasch-Parwez E, Schöls L, Theegarten D, Auburger G, Seidel K, Schultz C, Gierga K, Paulson H, von Broeckhoven C, Deller T, deVos RA. Degeneration of ingestion-related brainstem nuclei in spinocerebellar ataxia type 2, 3, 6 and 7. *Neuropathol Appl Neurobiol* 2006a; 32: 635-649.
48. Rüb U, de Vos RA, Brunt ER, Sebestény T, Auburger G, Bohl J, Ghebemedhin E, Gierga K, Seidel K, den Dunnen W, Heinsen H, Paulson H, Deller T. Spinocerebellar ataxia type 3 (SCA3): thalamic neurodegeneration occurs independently from thalamic ataxin-3 immunopositive neuronal intranuclear inclusions. *Brain Pathol* 2006b;16:218-227.
49. Schöls L, Bauer P, Schmidt T, Schulte T, Riess O. Autosomal dominant cerebellar ataxias: clinical features, genetics, and pathogenesis. *Lancet Neurol* 2004;3:291-304.
50. Soto C. Unfolding the role of protein misfolding in neurodegenerative diseases. *Nat Rev Neurosci* 2003;4:49-60.
51. Takahashi T, Katada S, Onodera O. Polyglutamine diseases: where does toxicity come from? What is toxicity? Where are we going? *J Mol Cell Biol* 2010;2:180-191.
52. Trottier Y, Lutz Y, Stevanin G, Imbert G, Devys D, Cancel G, Saudou F, Weber C, David G, Tora L, Agid Y, Brice A, Mandel JL. Polyglutamine expansion as a pathological epitope in Huntington's disease and four dominant cerebellar ataxias. *Nature* 1995;378:403-406.
53. Vekrellis K, Stefanis L. Protein aggregation and the UPS. In: *The Proteasome in Neurodegeneration*. Eds Stefanis L, Keller JN. New York: Springer; 2003;40-55.
54. Vonsattel JP, Myers RH, Stevens TJ, Ferrante RJ, Bird ED, Richardson EP jr. Neuropathological classification of Huntington's disease. *J Neuropathol Exp Neurol* 1985;44:559-577.
55. Walker FO. Huntington's disease. *Lancet* 2007;369:218-228.
56. Winborn BJ, Travis SM, Todi SV, Scaglione KM, Xu P, Williams AJ, Cohen RE, Peng J, Paulson HL. The deubiquitinating enzyme ataxin-3, a

- polyglutamine disease protein, edits Lys63 linkages in mixed linkage ubiquitin chains. *J Biol Chem* 2008;183:26436-26443.
57. Yamada M, Sato T, Tsuji S, Takahashi H. CAG repeat disorder models and human neuropathology: similarities and differences. *Acta Neuropathol* 2008;208:71-86
58. Zarranz JJ, Alegre J, Gomez-Esteban JC, Lezcano E, Ros R, Ampuero I, Vidal L, Hoenicka J, Rodriguez O, Atares B, Llorenz V, Gomez Tortosa E, del Ser T, Munoz DG, de Yebenes JG. The new mutation, E64K, of alpha-synuclein causes Parkinsonism and Lewy body dementia. *Ann Neurol* 2004;55:164-173.

## Chapter 2

---

# Involvement of the auditory brainstem system in spinocerebellar ataxia type 2 (SCA2), type 3 (SCA3), and type 7 (SCA7)

---

<sup>1</sup> Seidel K, <sup>1</sup> Hoche F, <sup>2</sup> Brunt ER, <sup>3</sup> Auburger G, <sup>4</sup> Schöls L, <sup>5</sup> Bürk K, <sup>6</sup> de Vos RA<sup>7</sup>, den Dunnen W, <sup>1</sup> Bechmann I, <sup>8</sup> Egensperger R, <sup>9, 10</sup> Van Broeckhoven C, <sup>1</sup> Gierga K, <sup>1</sup> Deller T, <sup>1</sup> Rüb U

<sup>1</sup> *Institute of Clinical Neuroanatomy, J. W. Goethe University, D-60590 Frankfurt/Main, Germany*

<sup>2</sup> *Department of Neurology, University Medical Center Groningen, University of Groningen, NL-5970 RB Groningen, The Netherlands*

<sup>3</sup> *Section Molecular Genetics, Department of Neurology, J. W. Goethe University, D-60590 Frankfurt/Main, Germany*

<sup>4</sup> *Center of Neurology and Hertie-Institute for Clinical Brain Research, University of Tübingen, D-72076 Tübingen, Germany*

<sup>5</sup> *Institute of Cell Biology, Department of Immunology, University of Tübingen, D-72076 Tübingen, Germany*

<sup>6</sup> *Laboratorium Pathologie Oost Nederland, NL-7512 AD Enschede, The Netherlands*

<sup>7</sup> *Department of Pathology and Laboratory Medicine, University Medical Center Groningen, University of Groningen, NL-5970 RB Groningen, The Netherlands*

<sup>8</sup> *Institute of Pathology and Neuropathology, University Hospital Essen, D-45122, Germany*

<sup>9</sup> *Neurodegenerative Brain Diseases Group, Department of Molecular Genetics, VIB; and*

<sup>10</sup> *University of Antwerp, BE-2610 Antwerpen, Belgium*

## Summary

**Aims:** The spinocerebellar ataxias type 2 (SCA2), type 3 (SCA3) and type 7 (SCA7) are clinically characterized by progressive and severe ataxic symptoms, dysarthria, dysphagia, oculomotor impairments, pyramidal and extrapyramidal manifestations, and sensory deficits. Although recent clinical studies reported additional disease signs suggesting involvement of the brainstem auditory system, this has never been studied in detail in SCA2, SCA3 or SCA7.

**Methods:** We performed a detailed pathoanatomical investigation of unconventionally thick tissue sections through the auditory brainstem nuclei (i.e. nucleus of the inferior colliculus, nuclei of the lateral lemniscus, superior olive, cochlear nuclei) and auditory brainstem fiber tracts (i.e. lateral lemniscus, trapezoid body, dorsal acoustic stria, cochlear portion of the vestibulocochlear nerve) of clinically diagnosed and genetically confirmed SCA2, SCA3 and SCA7 patients.

**Results:** Examination of unconventionally thick serial brainstem sections stained for lipofuscin pigment and Nissl material revealed a consistent and widespread involvement of the auditory brainstem nuclei in the SCA2, SCA3, and SCA7 patients studied. Serial brainstem tissue sections stained for myelin showed loss of myelinated fibers in two of the auditory brainstem fiber tracts (i.e. lateral lemniscus, trapezoid body) in a subset of patients.

**Conclusions:** The involvement of the auditory brainstem system offers plausible explanations for the auditory impairments detected in some of our and other SCA2, SCA3 and SCA7 patients upon bedside examination or neurophysiological investigation. However, further clinical studies are required to resolve the striking discrepancy between the consistent involvement of the brainstem auditory system observed in this study and the comparatively low frequency of reported auditory impairments in SCA2, SCA3 and SCA7 patients.

**Key words:** auditory system - brainstem - brainstem auditory evoked potentials - polyglutamine diseases - spinocerebellar ataxias



## Introduction

The spinocerebellar ataxias type 2 (SCA2), type 3 (SCA3) and type 7 (SCA7) represent progressive and currently untreatable ataxic disorders and owing to the underlying genetic defect are assigned to the group of CAG-repeat or polyglutamine disorders [19, 34, 48]. As is the case with all of the other currently known CAG-repeat or polyglutamine disorders SCA2, SCA3 and SCA7 are molecular biologically characterized by the presence of expanded and meiotic unstable CAG-repeats at specific gene loci (SCA2: chromosome 12q23-p24.1; SCA3: chromosome 14q24.3-q32.2; SCA7: chromosome 3p12-p21), which encode the disease specific proteins harboring an elongated polyglutamine tract (SCA2: ataxin-2; SCA3: ataxin-3; SCA7: ataxin-7) [9, 17-20, 22, 37, 48]. The normal SCA2 allele contains 14-31, the normal SCA3 allele 12-47, and the normal SCA7 allele 4-35 CAG-repeats. In affected patients and at-risk carriers the mutated SCA2 allele is expanded to approximately 35-64, the mutated SCA3 allele to 52-84, and the mutated SCA7 allele to 38-72 CAG-repeats [9, 17-20, 22, 37, 48]. Owing to a pronounced meiotic instability of the SCA7 CAG-repeat extreme expansions of over 200 CAG-repeats may occur in infantile SCA7 patients [20, 22].

The clinical pictures of advanced SCA2, SCA3 and SCA7 patients along with severe ataxia consistently include dysarthria and dysphagia, pyramidal and extrapyramidal motor disorders, specific oculomotor disorders and somatosensory deficits [6, 9, 11, 14, 19, 20, 22, 34, 47, 48]. In addition, recent clinical studies have shown that in SCA2, SCA3 and SCA7 patients disease symptoms may occur suggesting involvement of the auditory brainstem nuclei (i.e. impaired hearing and altered brainstem auditory evoked potentials) [1, 9, 12, 16, 19, 20, 22, 36, 47]. In the present study, we performed a detailed pathoanatomical investigation of the auditory brainstem system in clinically diagnosed and genetically confirmed SCA2, SCA3 and SCA7 patients in order to test the hypothesis that this system is among the targets of the degenerative processes of SCA2, SCA3 and SCA7.

## Patients and methods

In the present post-mortem study we examined the brains of twelve patients with clinically diagnosed and genetically confirmed spinocerebellar ataxia (SCA) (three SCA2 patients: 2 females, 1 male; mean age at disease onset:  $30.33 \pm 25.5$  years; mean age at death:  $56.0 \pm 31.5$  years - seven SCA3 patients: 2 females, 5 males; mean age at disease onset:  $33.9 \pm 13.9$  years; mean age at death:  $56.0 \pm 18.9$  years - two SCA7 patients: 1 female, 1 male; mean age at disease onset:  $41.5 \pm 12.0$  years; mean age at death:  $67.0 \pm 14.1$  years; Table 1) and thirteen age and gender-matched control individuals without medical histories of neurological or psychiatric diseases (3 females 10 males; mean age at death:  $57.15 \pm 15.9$  years; Table 1). The examination of these brains was approved by the ethical board of the Faculty of Medicine at the J. W. Goethe University of Frankfurt/Main, Germany.



| Case | Age | Gender | Clinical diagnosis | CAG  | Onset of initial symptoms | Duration of disease |
|------|-----|--------|--------------------|------|---------------------------|---------------------|
| 1    | 25  | F      | SCA2               | 52   | 6                         | 19                  |
| 2    | 55  | M      | SCA2               | 40   | 30                        | 25                  |
| 3    | 88  | F      | SCA2               | 36   | 55                        | 33                  |
| 4    | 24  | M      | SCA3               | 81   | 13                        | 11                  |
| 5    | 45  | M      | SCA3               | 69   | 25                        | 20                  |
| 6    | 52  | M      | SCA3               | 69   | 30                        | 22                  |
| 7    | 56  | M      | SCA3               | 74   | 30                        | 26                  |
| 8    | 60  | M      | SCA3               | 73   | 38                        | 22                  |
| 9    | 75  | F      | SCA3               | 68   | 46                        | 28                  |
| 10   | 80  | F      | SCA3               | 65   | 55                        | 25                  |
| 11   | 57  | M      | SCA7               | 47   | 33                        | 24                  |
| 12   | 77  | F      | SCA7               | 39   | 50                        | 27                  |
| 13   | 17  | M      | Control            | n.d. | -                         | -                   |
| 14   | 40  | M      | Control            | n.d. | -                         | -                   |
| 15   | 50  | M      | Control            | n.d. | -                         | -                   |
| 16   | 53  | M      | Control            | n.d. | -                         | -                   |
| 17   | 54  | M      | Control            | n.d. | -                         | -                   |
| 18   | 57  | M      | Control            | n.d. | -                         | -                   |
| 19   | 60  | M      | Control            | n.d. | -                         | -                   |
| 20   | 61  | M      | Control            | n.d. | -                         | -                   |
| 21   | 63  | M      | Control            | n.d. | -                         | -                   |
| 22   | 65  | M      | Control            | n.d. | -                         | -                   |
| 23   | 69  | F      | Control            | n.d. | -                         | -                   |
| 24   | 74  | F      | Control            | n.d. | -                         | -                   |
| 25   | 80  | F      | Control            | n.d. | -                         | -                   |

**Table 2.1: Synopsis of the SCA patients and control individuals studied.**

Patient number, age at death (years), gender (F= female; M = Male), clinical diagnosis (SCA2 = spinocerebellar ataxia type 2, SCA3 = spinocerebellar ataxia type 3, SCA7 = spinocerebellar ataxia type 7), number of expanded CAG repeats (CAG) in the diseased SCA2, SCA3 or SCA7 allele, age at onset of initial disease symptoms (years), and duration of SCA2, SCA3 or SCA7 (years) (n.d. – not determined).

The clinical records of all SCA patients described progressive gait, stance, and limb ataxia, as well as dysarthria and saccadic smooth pursuits. In addition, eleven of them showed dysmetrical horizontal saccades (cases 1-8, 10-12; Table 1) and suffered from progressive dysphagia (cases 1, 3-12; Table 1). Disease symptoms noticed in the medical records of the SCA patients suggesting involvement of the auditory brainstem system included: loss of wave III of brainstem auditory evoked potentials (BAEP) at age 14 (case 1; Table 1), reduced peak V of BAEP at age 29 (case 5; Table 1), and reduced hearing detected upon bedside examination at age 47 (case 11; Table 2.1).

Genetic examination of the CAG-repeat expansion in the mutated alleles confirmed the clinical diagnosis in all of the SCA patients under consideration (Table 2.1) [9, 10, 17, 18, 37].

### *Tissue preparation*

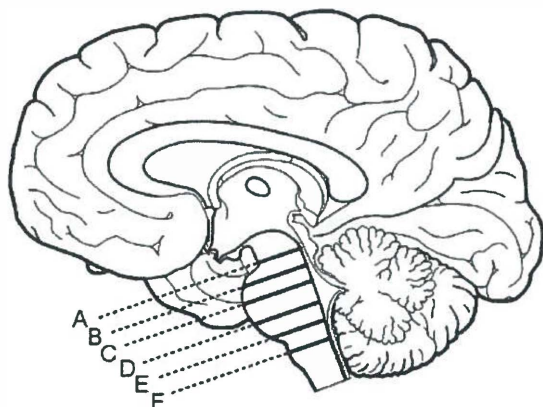


**Figure 2.1: The levels of the gray and white matter components of the human brainstem auditory pathway**

Median view of a mediosagittal section through the human brain. The sectional planes of the schematized horizontal sections through the brain stem presented in Figures 2 A-F are indicated by lines (plane of the section in Figure 2 A = line A; plane of the section in Figure 2 B = line B; plane of the section in Figure 2 C = line C; plane of the section in Figure 2 D = line D; plane of the section in Figure 2 E = line E; plane of the section in Figure 2 F = line F).

Autopsy was performed in the SCA patients within  $21.08 \pm 13.0$  h and in the control individuals within  $20.4 \pm 10.1$  h postmortem. Subsequent to the fixation of the brains of the SCA patients and control individuals in a 4% aqueous formaldehyde solution, the brainstems together with the cerebella were cut perpendicular to the brain axis of Meynert at the level of the inferior colliculus. Thereafter, the brainstems were removed from the cerebella by sagittal sections through the cerebellar peduncles, embedded in polyethylene glycol (PEG 1000, Merck, Darmstadt, Germany) [50], and cut into complete sets of serial 100- $\mu$ m thick horizontal sections. The first set of serial free-floating sections underwent a combined staining for lipofuscin pigment (aldehyde fuchsin) and Nissl material (Darrow red) [5, 39, 45] and was used for the anatomical identification of the auditory brainstem nuclei [2, 27-30, 33, 38, 55] (Figs. 2.1, 2.2; 2.3A, D; 2.4A, D) and for the assessment of their

neurodegeneration in the SCA patients. In each instance, the second set of serial free-floating sections was stained according to a modified Heidenhain procedure to highlight brainstem auditory pathways (Figs. 2.1, 2.2; 2.5A, D) [15, 38]. The third set of serial free-floating sections of the SCA patients and control individuals was immunostained with a rabbit polyclonal antibody against glial fibrillary acidic protein (GFAP; 1.500, Dako, Germany) to visualize reactive astrogliosis. In the SCA2 patients and three control individuals the fourth set of serial free-floating sections was immunolabelled with the monoclonal mouse anti-polyglutamine antibody 1C2 (1:1000, Chemicon, Temecula, CA, USA) to highlight intraneuronal proteins aggregates harboring an expanded polyglutamine tract [54]. Furthermore, immunocytochemistry was performed to assess the presence of neuronal intranuclear aggregates (NI) consisting of the pathologically altered forms of the disease proteins ataxin-3 or ataxin-7. Therefore, the fourth set of serial free-floating serial brainstem sections of the SCA3

patients and three control individuals were immunostained with a polyclonal anti-ataxin-3 antibody (1:2000) [35], whereas this same set of serial sections of the SCA7 patients and of two control individuals was immunostained with a polyclonal anti-ataxin-7 antibody (1:2000) [21].

The specificity of the immunolabelling was assessed by omission of the primary antibodies. Incubation with the primary antibodies was performed for 12 h at room temperature followed by incubation with biotinylated anti-rabbit immunoglobulins for 1.5 h at room temperature. Bound antigens were visualized with the AB-complex (Vectastain, Vector Laboratories, Burlingame, California, USA) and 3,3'-diaminobenzidine-tetra-HCl/H<sub>2</sub>O<sub>2</sub> (DAB, D5637 Sigma, Taufkirchen, Germany).

The extent of degeneration of the auditory brainstem nuclei, myelin loss of auditory brainstem fiber tracts and reactive astrogliosis in the SCA patients was scored as none discernible (-), obvious (+), or severe (++) (Tables 2.2, 2.3). The presence of intraneuronal aggregates with an expanded polyglutamine tract in the SCA2 patients and the occurrence of NI in the SCA3 and SCA7 patients was classified as absent (-) or present (+) (Table 2.2). The neuropathological findings of the two SCA7 patients have been recently reported [40, 42].

Owing to the small numbers of SCA2 and SCA7 patients studied, detailed statistical analysis was only performed in the SCA3 patients. To this end, Kendall's rank correlation coefficient tau ( $\tau$ ) was applied to determine whether the extent of the degeneration of the auditory brainstem nuclei and fiber tracts was dependent upon either the individual length of the CAG-repeats in the mutated SCA3 allele or the duration of the disease [9].

### **Anatomical remarks**

#### *Nucleus of the inferior colliculus*

The *inferior colliculus* represents the caudal elevation of the midbrain tectal plate and contains the ovoid *nucleus of the inferior colliculus (NIC)* (Fig. 2.2A). The *NIC* borders ventrally on the lateral lemniscus (*LL*) and medially on the periaqueductal gray. In primates the *NIC* harbors predominantly small-sized oval, spindle-shaped or triangular nerve cells, which tend to be orientated in its caudal portion predominantly with their long axis directed dorsomedially and in its rostral portions in a haphazard manner [2, 28, 30, 33, 38, 55].

#### *Nuclei of the lateral lemniscus*

The nuclei of the lateral lemniscus are embedded in the *LL* and comprise a *dorsal nucleus of the lateral lemniscus (DNLL)* and a poorly developed *ventral nucleus of the lateral lemniscus (VNLL)* (Figs. 2.2B, C; 2.3A; 2.5A). The *DNLL* is located between

the sagulum and the lateral parabrachial nucleus (Figs. 2.2 B), reaches the caudal pole of the midbrain pedunculo-pontine and is built up of medium-sized, loosely arranged oval or multipolar nerve cells. The *VNLL* also harbors medium-sized, loosely arranged round or oval cells, as well as a dense glial network. Its caudal portion lies in the ventrolateral part of the pons and is dorsally related to the superior cerebellar peduncle (Figs. 2.2C; 2.3A: 2.5A), whereas its rostral portion lies in the dorsolateral part of the pontine tegmentum, approximates the lateral parabrachial nucleus and assumes an oblong outline with the long axes directed dorsoventrally [2, 28, 30, 33, 38, 55].

### *Superior olive*

The human *superior olive* (*SO*) is situated in the ventrolateral corner of the caudal pontine tegmentum, is largely embedded into the trapezoid body and consists of a prominent *medial superior olive* (*MSO*), a reduced *lateral superior olive* (*LSO*), and a surrounding *periolivary cell group* (*PO*) (Figs. 2.2D; 2.3D). The *MSO* represents a vertical and slender column of about three transversely oriented neurons in width. These medium-sized spindle-shaped neurones of the *MSO* are surrounded by a dense glial network (Figs. 2.2D; 2.3D). The *LSO* lies dorsolateral to the *MSO* and is composed of medium-sized, round or ovoid nerve cells (Figs. 2.2D; 2.3D). The *PO* form a hollow sphere surrounding the *MSO* and *LSO* and consists of predominantly medium-sized round or ovoid nerve cells (Figs. 2.2D; 2.3 D) [2, 27-30, 33, 38, 55].

### *Cochlear nuclei*

The cochlear nuclei are located at the pontomedullary junction and comprise a dorsal and a ventral subnucleus. The *dorsal cochlear nucleus* (*DC*) lies on the dorsolateral surface of the inferior cerebellar peduncle (*ICP*) and along with a small number of giant nerve cells harbors predominantly medium-sized and elongated nerve cells, most of which are arranged with their long axes parallel to the dorsolateral surface of the *ICP* (Figs. 2.2E, F; 2.4A). The most ventrally situated nerve cells of the *DC* are intimately related to the *ventral cochlear nucleus* (*VC*) (Figs. 2.2E, F). The pear-shaped *VC* lies at the ventrolateral aspect of the *ICP*, is penetrated by the *cochlear fibers of the vestibulocochlear nerve* (*VIIIc*), which are passing to the *DC*, and is built up of medium-sized, multipolar ovoid or round nerve cells, the majority of which are directed with their long axes dorsomedially. The rostral portion of the *VC* is divided by the entering *vestibular division of the vestibulocochlear nerve* (*VIIIv*) into a medial and a lateral subdivision (Figs. 2.2E, F; 2.4D) [2, 28, 30, 33, 38, 55].

### *Brainstem auditory fiber tracts*

The *cochlear division of the vestibulocochlear nerve* (*VIIIc*) enters the lateroventral aspect of the brainstem near the pontomedullary sulcus and provides the auditory impulses from the spiral ganglion destined for the cochlear nuclei (Figs. 2.2E, F). The auditory channels, which arise from the cochlear nuclei predominantly terminate in the *NIC* and converge via the *dorsal acoustic stria* (*DAS*), *trapezoid body* (*TZ*), and the *lateral lemniscus* (*LL*) (Figs. 2.2A-E; 2.5A, C) towards this midbrain nucleus. The transversely oriented *TZ* and *DAS* originate from the dorsal and ventral cochlear nuclei (Figs. 2.2D, E), whereby the *TZ* crosses the ventral part of the pontine tegmentum and continues at the lateral part of the pontine tegmentum as the *LL* (Fig. 2.2D; 2.5C). The

*DAS* originates from the DC (Figs. 2.2E), passes over the ICP, and traverses the pontine reticular formation to reach the contralateral SO, where it also passes over into the LL. The LL, containing the nuclei of the same name, is situated in the lateral parts of the rostral pons and caudal midbrain. It ascends to the *IC*, where most of its fibers terminate (Figs. 2.2A-C; 2.5A). Finally, the link between the auditory brainstem system and the thalamic medial geniculate body is provided by the *brachium of the inferior colliculus (BIC)*, which leaves the *IC* [2, 28, 30, 33, 38, 55].

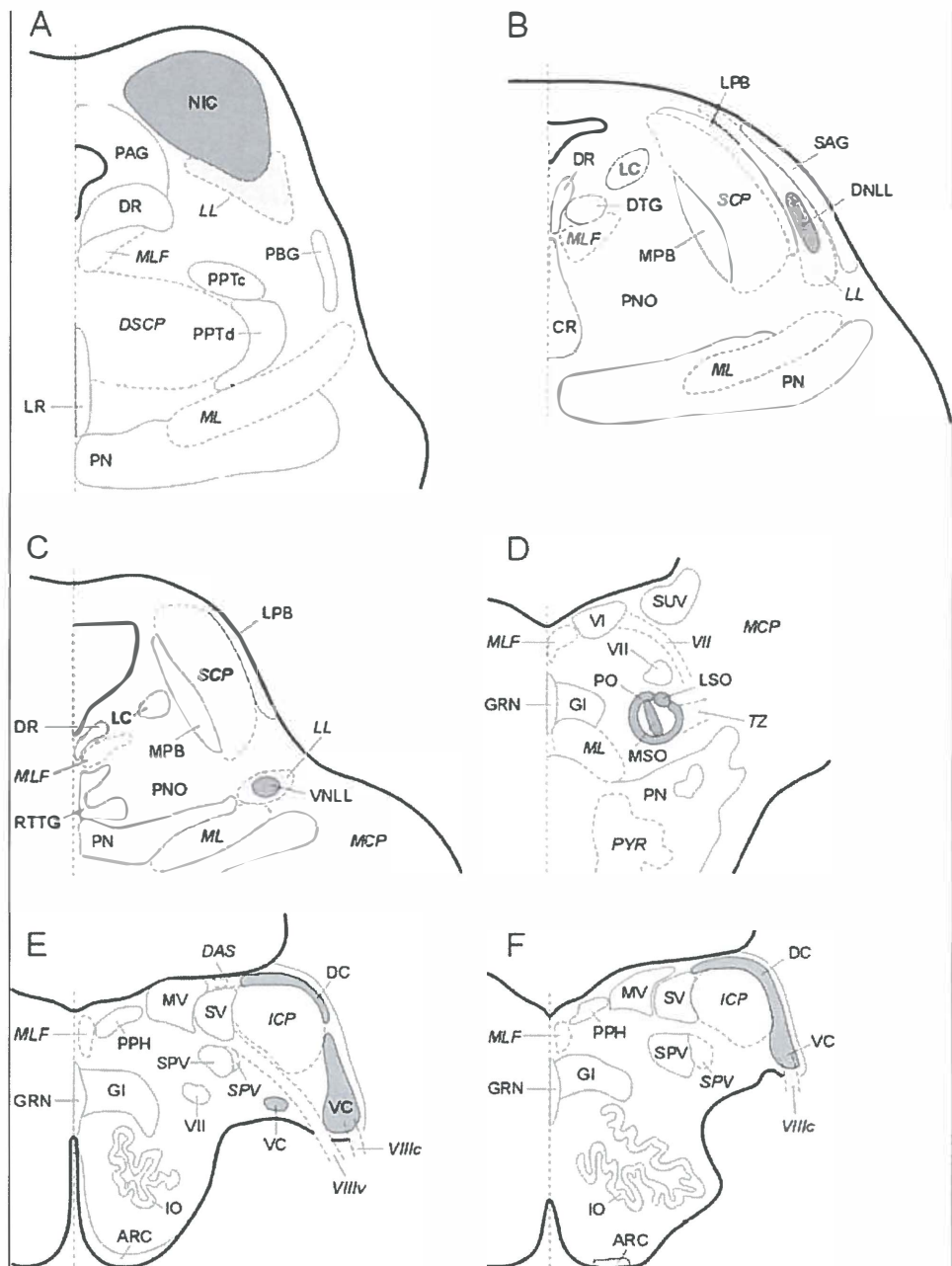


**Figure 2.2 (previous page): The gray and white matter components of the human brainstem auditory pathway.**

Auditory brainstem nuclei are underlined by gray shading and auditory brainstem fiber tracts by light gray shading. **(A)** Schematized frontal section through the caudal midbrain showing the nucleus of the inferior colliculus (NIC) and the lateral lemniscus (*LL*). **(B)** Schematized horizontal section through the rostral pons with the lateral lemniscus (*LL*) and the dorsal nucleus of the lateral lemniscus (DNLL). **(C)** Schematized horizontal section through the caudal pons showing the lateral lemniscus (*LL*) and the ventral nucleus of the lateral lemniscus (VNLL). **(D)** Schematized horizontal section through the pontomedullary junction with the medial superior olive (MSO), lateral superior olive (LSO), and the periolivary cell group (PO), and trapezoid body (*TZ*). **(E)** Schematized horizontal section through the most rostral portion of the medulla oblongata depicting the dorsal acoustic stria (*DAS*), the cochlear (*VIIIc*) and vestibular divisions (*VIIIv*) of the vestibulocochlear nerve, and the dorsal (DC) and ventral cochlear nuclei (VC). **(F)** Schematized horizontal section through the rostral medulla oblongata depicting the cochlear division of the vestibulocochlear nerve (*VIIIc*), and the dorsal (DC) and ventral cochlear nuclei (VC).

(Abbreviations: ARC – Arcuate nucleus; CR – Central raphe nucleus; *DAS* – Dorsal acoustic stria; DC – Dorsal cochlear nucleus; DNLL – Dorsal nucleus of the lateral lemniscus; DR – Dorsal raphe nucleus; *DSCP* – Decussatio of the superior cerebellar peduncle; DTG – Dorsal tegmental nucleus; GI – Gigantocellular reticular nucleus; GRN – Great raphe nucleus; *ICP* – Inferior cerebellar peduncle; IO – Inferior olive; LC – Locus coeruleus; *LL* – Lateral lemniscus; LPB – Lateral parabrachial nucleus; LR – Linear raphe nucleus; LSO – Lateral superior olive; *MCP* – Medial cerebellar peduncle; *ML* – Medial lemniscus; *MLF* – Medial longitudinal fascicle; MPB – Medial parabrachial nucleus; MSO – Medial superior olive; MV – Medial vestibular nucleus; NIC – Nucleus of the Inferior colliculus; PAG – Periaqueductal gray; PBG – Parabigeminal nucleus; PN – Pontine nuclei; PNO – Pontine reticular formation, oral subnucleus; PO – Periolivary cell group; PPH – Prepositus hypoglossal nucleus; PPTc – Pedunculopontine nucleus, compact part; PPTd – Pedunculopontine nucleus, diffuse part; *PYR* – Pyramidal tract; RTTG – Reticulotegmental nucleus of the pons; SAG – Sagulum; *SCP* – Superior cerebellar peduncle; SPV – Spinal trigeminal nucleus; *SPV* – Spinal trigeminal tract; SUV – Superior vestibular nucleus; SV – Spinal vestibular nucleus; *TZ* – Trapezoid body; VC – Ventral cochlear nucleus; VNLL – Ventral nucleus of the lateral lemniscus; VI – Abducens nucleus; VII – Facial nucleus; *VII* – Facial nerve; *VIIIc* – Cochlear division of the vestibulocochlear nerve; *VIIIv* – Vestibular division of the vestibulocochlear nerve)



## Results

### *Degenerative findings*

The auditory brainstem nuclei consistently underwent neurodegeneration in our SCA patients. The inferior colliculus (IC) showed marked neuronal loss in two of the SCA2, in all SCA3 and in one of the SCA7 patients, while it was severely in another SCA7 patient (Tables 2.1, 2.2). An additional marked to severe neuronal loss was observed in the dorsal and ventral nuclei of the lateral lemniscus of the SCA2, SCA3 and SCA7 patients (Tables 2.1, 2.2; Figs. 2.2 A-C). Among the auditory brainstem nuclei studied, the nuclei of the superior olive underwent the most severe degeneration. They were more or less devoid of nerve cells in one of the SCA2, five of the SCA3 and in one of the SCA7 patients (Tables 2.1, 2.2; Figs. 2.3 D-F). In the remaining SCA2, SCA3 and SCA7 patients the medial superior olive, lateral superior olive and the periolivary cell group were markedly involved (Tables 2.1, 2.2). The dorsal and ventral cochlear nuclei, likewise, were consistently degenerated and showed a marked to serious loss of nerve cells in all of the SCA patients under consideration (Tables 2.1, 2.2; Figs. 2.4A-F).



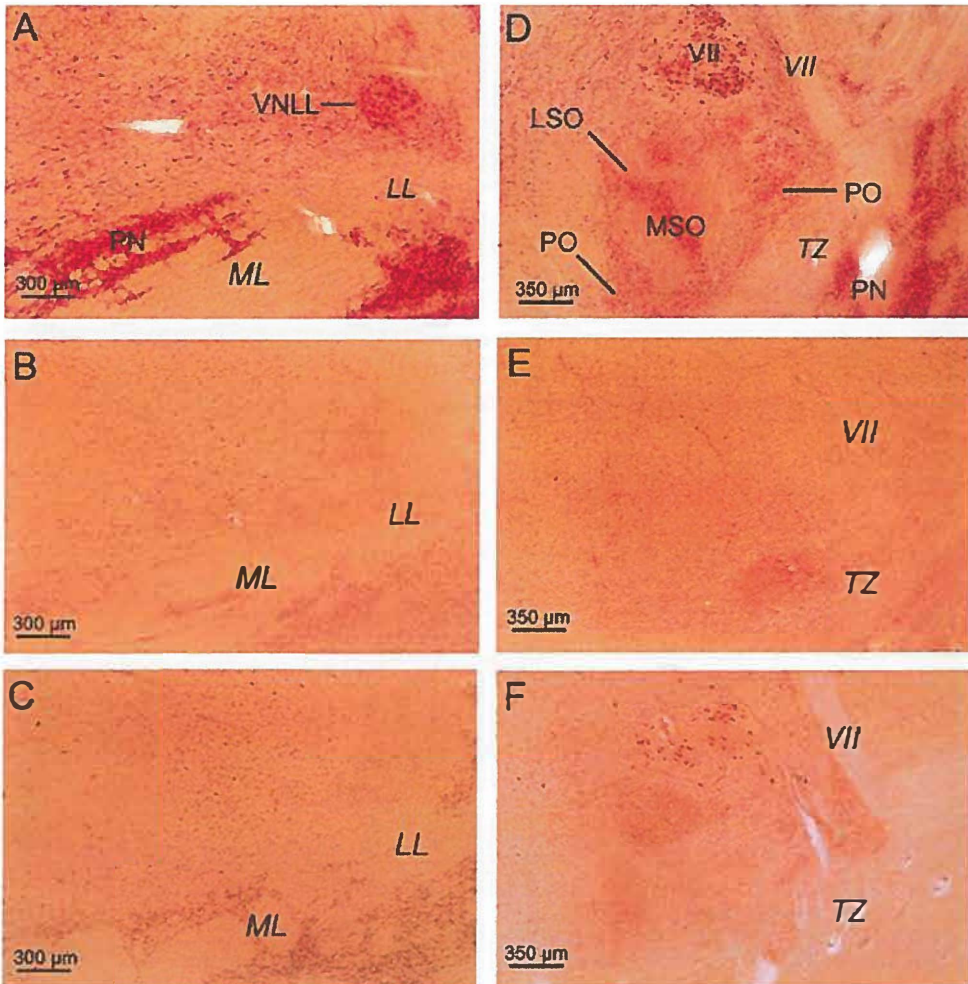


**Figure 2.3: The ventral nucleus of the lateral lemniscus and the superior olive in SCA2, SCA3 and SCA7**

Horizontal sections through (A) the caudal pons of a representative 54-year-old male control case (case 17; Table 1) and (D) the pontomedullary junction with (A) the ventral nucleus of the lateral lemniscus (VNLL) and (D) the medial superior olive (MSO), lateral superior (LSO) and periolivary cell group (PO). (B) Degenerated VNLL of a 24-year-old male SCA3 patient (case 4; Tables 1, 2) and (C) of a 57-year-old male SCA7 patient (case 11; Tables 1, 2). (E) Severe neuronal loss in all three subnuclei of the superior olive in a 25-year-old female SCA2 patient (case 1; Tables 1, 2) and (F) in an 80-year-old female SCA3 patient (case 10; Tables 1, 2). Note the additional degeneration of the facial nucleus (VII) in both SCA patients. For topographical orientation, see figures 2 C, D. (A-F: aldehyde fuchsin-Darrow red staining, 100  $\mu$ m PEG sections).

(Abbreviations: LSO – Lateral superior olive; ML – Medial lemniscus; MSO – Medial superior olive; PN – Pontine nuclei; PO – Periolivary cell group; LL – Lateral lemniscus; TZ – Trapezoid body; VNLL – Ventral nucleus of the lateral lemniscus; VII – Facial nerve; VII – Facial nucleus).

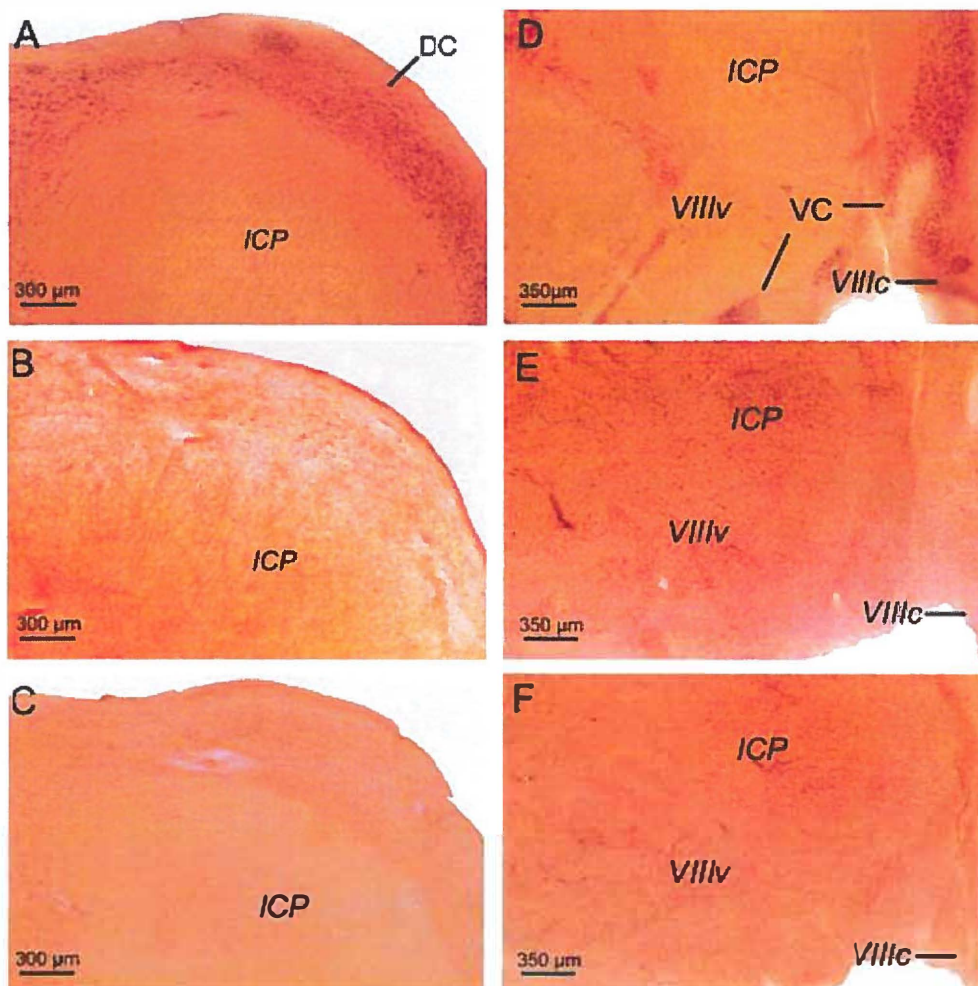


**Figure 2.4: The dorsal and ventral cochlear nuclei in SCA2, SCA3 and SCA7**

Horizontal sections through the rostral medulla oblongata of a 63-year-old male control case without any previous medical history of neurological or psychiatric disease (case 21; Table 1) showing (A) the dorsal cochlear nucleus (DC) and (D) the ventral cochlear nucleus (VC). (B) Severe neurodegeneration of the DC of a 25-year-old female SCA2 patient (case 1; Tables 1-2) and (C) obvious involvement of the DC of a 57-year-old male SCA7 patient (case 11; Tables 1, 2). (E) Severe neuronal loss in the VC of a 45-year-old male SCA3 patient (case 5; Tables 1, 2) and (F) in an 77-year-old female SCA7 patient (case 12; Tables 1, 2). For topographical orientation, see figures 2 E, F. (A-F: aldehyde-fuchsin-Darrow red staining, 100 μm PEG sections).

(Abbreviations: DC – Dorsal cochlear nucleus; VC – Ventral cochlear nucleus; ICP – Inferior cerebellar peduncle; VIIIc – Cochlear division of the vestibulocochlear nerve; VIIIv – Vestibular division of the vestibulocochlear nerve).

Loss of myelinated fibers in the auditory brainstem pathways was confined to the lateral lemniscus and trapezoid body of our SCA patients. Loss of myelinated fibers was observed in the lateral lemniscus of one SCA2, five SCA3 and in the two SCA7 patients (Tables 2.1, 2.3; Figs. 2.5A, B). The trapezoid body was involved in one SCA2, two SCA3 and in the two SCA7 patients (Tables 2.1, 2.3; Figs. 2.5C, D).

Application of Kendall's rank correlation coefficient tau ( $\tau$ ) revealed that the extent of the degeneration of the auditory brainstem nuclei and fiber tracts in the SCA3 patients was independent of the individual length of the CAG-repeats in the mutated SCA3 allele and the duration of the disease (all P values > 0.10).

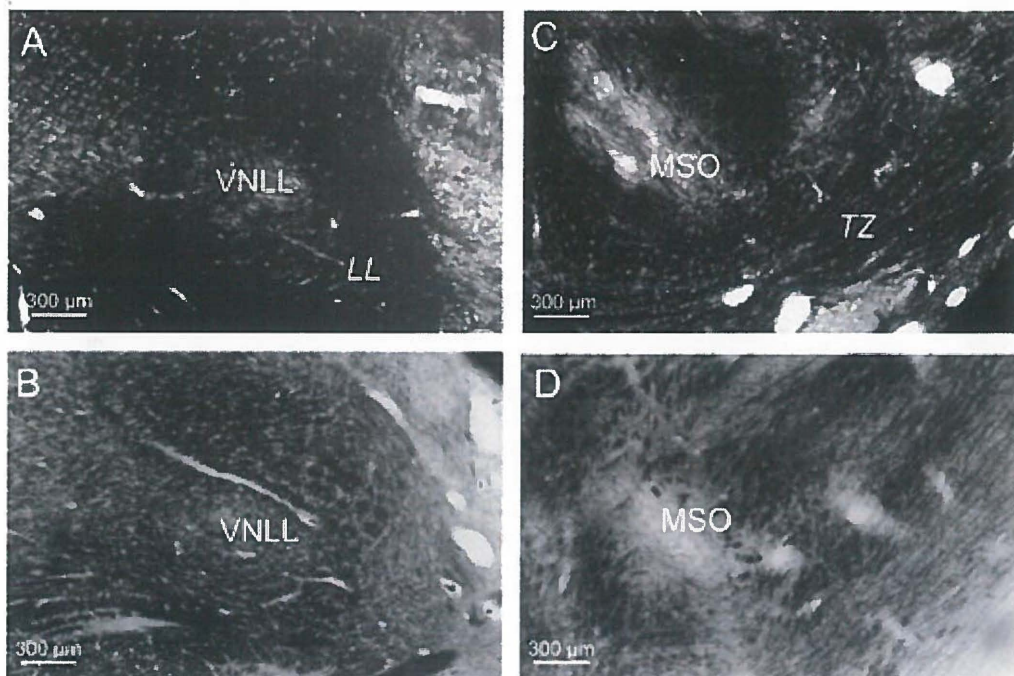


**Figure 2.5: Myelin loss in the lateral lemniscus and trapezoid body in SCA3 and SCA7 patients**  
Horizontal sections through (A) the caudal pons and (C) the pontomedullary junction of a 57-year-old male control case without a medical history of neurological or psychiatric disease (case 18; Table 1) showing (A) the lateral lemniscus (LL), and (C) the trapezoid body (TZ). (B) Loss of myelinated fibers in the LL of a 45-year-old female SCA3 patient (case 5; Tables 1, 3) and (D) in the TZ of a 57-year-old male SCA7 patient (case 11; Tables 1, 3). For topographical orientation, see figures 1 C, D. (A–D: modified Heidenhain staining, 100 µm PEG sections).

(Abbreviations: VNLL – Ventral nucleus of the lateral lemniscus; MSO – Medial superior olive; LL – Lateral lemniscus; TZ – Trapezoid body).

| Case |    | (IC) | (DNLL) | (VNLL) | (MSO) | (LSO) | (PO) | (DC) | (VC) |
|------|----|------|--------|--------|-------|-------|------|------|------|
| 1    | N  | +    | ++     | ++     | ++    | ++    | ++   | ++   | ++   |
|      | NI | -    | -      | -      | -     | -     | -    | -    | -    |
| 2    | N  | -    | +      | +      | +     | +     | +    | +    | +    |
|      | NI | -    | -      | -      | -     | -     | -    | -    | -    |
| 3    | N  | +    | +      | +      | +     | +     | +    | +    | +    |
|      | NI | -    | -      | -      | -     | -     | -    | -    | -    |
| 4    | N  | +    | ++     | ++     | ++    | ++    | +    | +    | +    |
|      | NI | +    | +      | +      | +     | +     | +    | +    | +    |
| 5    | N  | +    | +      | +      | +     | +     | ++   | ++   | ++   |
|      | NI | +    | +      | +      | +     | +     | +    | +    | +    |
| 6    | N  | +    | +      | +      | +     | +     | +    | +    | +    |
|      | NI | +    | +      | +      | +     | +     | +    | +    | +    |
| 7    | N  | +    | +      | +      | ++    | ++    | +    | +    | +    |
|      | NI | +    | +      | +      | +     | +     | +    | +    | +    |
| 8    | N  | +    | +      | +      | ++    | ++    | +    | +    | +    |
|      | NI | +    | +      | +      | +     | +     | +    | +    | +    |
| 9    | N  | +    | +      | +      | ++    | ++    | ++   | +    | +    |
|      | NI | +    | +      | +      | +     | +     | +    | +    | +    |
| 10   | N  | +    | +      | +      | ++    | ++    | ++   | ++   | ++   |
|      | NI | +    | +      | +      | +     | +     | +    | +    | +    |
| 11   | N  | +    | ++     | ++     | ++    | ++    | +    | ++   | ++   |
|      | NI | +    | +      | +      | +     | +     | +    | +    | +    |
| 12   | N  | ++   | ++     | ++     | +     | +     | +    | +    | +    |
|      | NI | +    | +      | +      | +     | +     | +    | +    | +    |

**Table 2.2: Neurodegeneration**

Extent of neurodegeneration (N) (none discernible -, obvious +, severe ++) and presence of immunoreactive neuronal intranuclear neuronal inclusions (NI) (absent -, present +) in the auditory brainstem nuclei of the SCA2, SCA3 and SCA7 patients studied.

(Abbreviations: IC – Inferior colliculus; DNLL – Dorsal nucleus of the lateral lemniscus; VNLL– Ventral nucleus of the lateral lemniscus; MSO – Medial superior olive; LSO – lateral superior olive; PO – periolivary group; DC – dorsal cochlear nucleus; VC – ventral cochlear nucleus).



| Case | Lateral lemniscus<br>(LL) | Trapezoid body<br>(TZ) | Dorsal acoustic<br>stria<br>(DAS) | Vestibulocochlear<br>nerve, cochlear portion<br>(VIIIc) |
|------|---------------------------|------------------------|-----------------------------------|---|
| 1    | +                         | +                      | -                                 | -   |
| 2    | -                         | -                      | -                                 | -   |
| 3    | -                         | -                      | -                                 | -   |
| 4    | -                         | -                      | -                                 | -   |
| 5    | +                         | -                      | -                                 | -   |
| 6    | +                         | -                      | -                                 | -   |
| 7    | +                         | +                      | -                                 | -   |
| 8    | +                         | -                      | -                                 | -   |
| 9    | -                         | -                      | -                                 | -   |
| 10   | +                         | +                      | -                                 | -   |
| 11   | +                         | +                      | -                                 | -   |
| 12   | +                         | +                      | -                                 | -   |

**Table 2.3: Loss of myelinated fibers**

Extent of loss of myelinated fibers (none discernible -, obvious +, severe ++) in the auditory brainstem fiber tracts of the SCA2, SCA3 and SCA7 patients studied.

### *Associated tissue changes*

GFAP-immunoreactive astrocytes were present in all auditory brainstem nuclei of all SCA patients studied (data not shown), whereas no intraneuronal nuclear or cytoplasmic protein aggregates harboring an expanded polyglutamine tract could be detected in the auditory brainstem nuclei of the SCA2 patients, all of the auditory brainstem nuclei of all SCA3 patients displayed ataxin-3 immunopositive neuronal intranuclear aggregates and those of all SCA7 patients ataxin-7 immunopositive neuronal intranuclear aggregates (Tables 2.1, 2.2).

## Discussion

In the present pathoanatomical study we confirmed the hypothesis that the brainstem auditory system, along with the vestibular, oculomotor, somatosensory, ingestion-related and precerebellar brainstem systems [11, 12, 39, 40-46] is among the consistent targets of the degenerative processes of SCA2, SCA3 and SCA7. Such a consistent and severe impairment of the auditory brainstem system, to the best of our knowledge, has never before been reported in other human neurodegenerative diseases. In Alzheimer's disease for example only minor and inconsistent pathological changes have been detected in a subset of auditory brainstem nuclei of some affected patients [32, 49].

The majority of auditory brainstem nuclei were more severely involved in our SCA2 patients and SCA7 patients with the longest CAG-repeats in the mutated alleles, and involvement of auditory brainstem fiber tracts was confined to our SCA2 patient with the longest CAG-repeat in the mutated SCA2 allele. Close inspection of our data and statistical analysis revealed no consistent correlations between the extent of degeneration of the auditory brainstem nuclei and fiber tracts and the individual length of CAG-repeats or the disease duration in our sample of SCA2, SCA3 and SCA7 patients. In view of these findings the nature of the relationship between these two factors and the course of the pathological processes of SCA2, SCA3 and SCA7 is still an open question.

The involvement of the auditory brainstem system seen in our study offers plausible explanations for the auditory disease signs detected in some of our and other SCA2, SCA3 and SCA7 patients upon bedside examination or neurophysiological investigation [1, 9, 12, 16, 19, 20, 22, 36, 47]. In addition, this consistent involvement may also suggest that auditory dysfunctions such as impairments of perception of the frequency, intensity, and temporal patterns of sounds, disturbed analysis of spatial attributes of sound sources (i.e. location, distance and movement), impaired discriminative (signal/noise) hearing, impaired speech discrimination, or pathologically altered brainstem auditory evoked potentials (BAEPs) [2, 23, 25-27, 29, 53, 55] may represent common SCA2, SCA3 and SCA7 disease signs.

However, there is a striking discrepancy between the consistent involvement of the brainstem auditory system and the low frequency of reports of impaired hearing in our and other SCA2, SCA3 and SCA7 patients. The following reasons may account for the rarity of such reports: (1) The pathology in the auditory brainstem system in some affected cases may not suffice to cause clinically relevant auditory dysfunctions. (2) The clinical picture of SCA2, SCA3 and SCA7 patients is dominated by progressive ataxic symptoms, dysarthria and dysphagia and in some SCA7 patients also by visual impairments. Accordingly, more subtle sensory disease symptoms often may escape the attention of affected patients and/or their caregivers [29]. (3) Clinicians still are unaware of the involvement of the auditory brainstem system in SCA2, SCA3 and SCA7. Therefore, it is conceivable that they do not expect auditory symptoms and are not inclined to perform detailed clinical or extensive neurophysiological examinations. (4) The patients' self-reports regarding the presence of auditory dysfunctions may be

inaccurate and less reliable [5, 8, 50, 51], and even detailed bedside examination may fail in detecting auditory impairments [3]. For all of these reasons, further clinico-pathological studies are required to resolve the discrepancy between the consistent involvement of the brainstem auditory pathway and the low frequency of reports of auditory impairments in the SCA2, SCA3 and SCA7. Along with the question of the prevalence of auditory impairments, from a clinical point of view, such studies should address the following questions: (1) Are SCA2, SCA3 and SCA7 associated only with subclinical auditory impairments or with auditory impairments of clinical relevance, which further reduce the quality of life of the severely handicapped patients [7, 8, 52]? (2) Is the communication with affected SCA2, SCA3 and SCA7 patients not only hampered by dysarthria, but also by concomitant auditory dysfunctions [8]? (3) Do auditory dysfunctions along with the well-known immobility and dysarthria contribute to the reduced social interaction of SCA2, SCA3 and SCA7 patients [7, 8, 29, 51, 52]? (4) Do auditory impairments along with visual deficits encroach spatial orientation in affected SCA2, SCA3 and SCA7 patients [7]?

The majority of studies concerning the structure-function relationship of the auditory brainstem system have been performed in experimental animal studies [2, 55]. In view of the anatomical differences between the auditory brainstem system of humans and of animals, however, it is difficult to apply the results of animal studies to humans [25, 27-29, 55]. Although it is well-known that the auditory spatial field is recreated in the auditory brainstem system, the exact mechanisms of and the brainstem structures contributing to the analyses of attributes of sound sources in humans are not entirely known [23, 28, 30, 53, 55]. In addition, while BAEPs can be used to assess the brainstem auditory pathway [2], controversy exists over the generators of the various wave components of the human BAEPs [2, 23, 25, 27, 55]. Accordingly, loss of wave III of the BAEPs in one of our SCA2 patients (case 1; Table 2.2) can be interpreted as a possible consequence of damage to the cochlear nuclei or to the nuclei of the superior olive, and the reduction of peak V of the BAEPs in one of our SCA3 patients (case 5; Tables 2.1-3) as a result of the neuronal loss in the inferior colliculus or loss of myelinated fibers in the lateral lemniscus.

Although we have recently shown in a case study that the auditory brainstem system may also be involved in spinocerebellar ataxia type 4 [13], SCA2, SCA3, and SCA7 currently represent the sole known neurodegenerative diseases associated with a consistent and considerable pathology in the auditory brainstem system. They are genetically well-defined neurodegenerative diseases, thus facilitating unequivocal identification of affected patients and at-risk individuals and recruiting of appropriate test persons for clinical studies. Considering the 'natural experiment' in the auditory brainstem system described in our study these ataxic diseases offer the unique opportunity for detailed clinico-pathological studies of the human auditory brainstem system. Such studies may clarify the unresolved questions regarding the occurrence of auditory disease signs in SCA2, SCA3 and SCA7 and improve our knowledge with



respect to the analyses of sound source attributes and the generators of auditory evoked potentials within the human brainstem.

### **Acknowledgements**

This study was supported by grants from the Deutsche Forschungsgemeinschaft (RU 1215/1-2), the Deutsche Heredo-Ataxie-Gesellschaft (DHAG), the ADCA-Vereniging Nederland, and the Bernd Fink-Stiftung (Düsseldorf, Germany). The skillful assistance of M. Babl, A. Biczysko, M. Bouzrou, B. Meseck-Selchow (tissue processing and immunohistochemistry), and M. Hütten (technical support) is thankfully acknowledged.

## References

1. Abele M, Bürk K, Andres F, Topka H, Laccone F, Bösch S, Brice A, Cancel G, Dichgans J, Klockgether T. Autosomal dominant cerebellar ataxia type I. Nerve conduction and evoked potential studies in families with SCA1, SCA2 and SCA3. *Brain* 1997;120:2141-2148.
2. Biacabe B, Chevallier JM, Avan P, Bonfils P. Functional anatomy of auditory brainstem nuclei: application to the anatomical basis of brainstem auditory evoked potentials. *Auris Nasus Larynx* 2001;28:85-94.
3. Boatman DF, Miglioretti DL, Eberwein C, Alidoost M, Reich SG. How accurate are bedside hearing tests? *Neurology* 2007;68:1311-1314.
4. Bortz J, Lienert GA, Boehnke K. Verteilungsfreie Methoden in der Biostatistik. Berlin: Springer, 1990
5. Braak H, Rüb U, Del Tredici K. Involvement of precerebellar nuclei in multiple system atrophy. *Neuropathol Appl Neurobiol* 2003;29:60-76.
6. Bürk K, Abele M, Fetter M, Dichgans J, Skalej M, Laccone F, Didierjean O, Brice A, Klockgether T. Autosomal dominant cerebellar ataxia type I clinical features and MRI in families with SCA1, SCA2 and SCA3. *Brain* 1996;119:1497-1505.
7. Chia EM, Mitchell P, Rochtchina E, Foran S, Golding M, Wang JJ. Association between vision and hearing impairments and their combined effects on quality of life. *Arch Ophthalmol* 2006;124:1465-1470.
8. Dalton DS, Cruickshanks KJ, Klein BE, Klein R, Wiley TL, Nondahl DM. The impact of hearing loss on quality of life in older adults. *Gerontologist* 2003;43:661-668.
9. David G, Abbas N, Stevanin G, Dürr A, Yvert G, Cancel G, Weber C, Imbert G, Saudou F, Antoniou E, Drabkin H, Gemmill R, Giunti P, Benomar A, Wood N, Ruberg M, Agid Y, Mandel JL, Brice A. Cloning of the SCA7 gene reveals a highly unstable CAG repeat expansion. *Nat Genet* 1997;17:65-70.
10. Del-Favero J, Krols L, Michalik A, Theuns J, Lofgren A, Gossens D, Wehnert A, Van den Bossche D, Van Zand K, Backhovens H, van Regenmorter N, Martin JJ, Van Broeckhoven C. Molecular genetic analysis of autosomal dominant cerebellar ataxia with retinal degeneration (ADCA type II) caused by CAG triplet repeat expansion. *Hum Mol Genet* 1998;7:177-186

11. Dürr A, Smadja D, Cancel G, Lezin A, Stevanin G, Mikol J, Bellance R, Buisson GG, Chneiweiss H, Dellanave J, Agid Y, Brice A, Vernant JC. Autosomal dominant cerebellar ataxia type I in Martinique (French West Indies). Clinical and neuropathological analysis of 53 patients from three unrelated SCA2 families. *Brain* 1995;118:1573-1581.
12. Dürr A, Stevanin G, Cancel G, Duyckaerts C, Abbas N, Didierjean O, Chneiweiss H, Benomar A, Lyon-Caen O, Julien J, Serdaru M, Penet C, Agid Y, Brice A. Spinocerebellar ataxia 3 and Machado-Joseph disease: clinical, molecular, and neuropathological features. *Ann Neurol* 1996;39:490-499.
13. Hellenbroich Y, Gierga K, Reusche E, Schwinger E, Deller T, de Vos RA, Zühlke C, Rüb U. Spinocerebellar ataxia type 4 (SCA4): Initial pathoanatomical study reveals widespread cerebellar and brainstem degeneration. *J Neural Transm* 2006;113:829-843.
14. Holmberg M, Duyckaerts C, Dürr A, Cancel G, Gourfinkel-An I, Damier P, Faucheux B, Trottier Y, Hirsch EC, Agid Y. Spinocerebellar ataxia type 7 (SCA7): a neurodegenerative disorder with neuronal intranuclear inclusions. *Hum Mol Genet* 1998;7:913-918.
15. Hutchins B, Weber JT. A rapid myelin stain for frozen sections: modification of the Heidenhain procedure. *J Neurosci Methods* 1983;7:289-294.
16. Ikeda K, Kubota S, Isashiki Y, Eiraku N, Osame M, Nakagawa M. Machado-Joseph disease with retinal degeneration and dementia. *Acta Neurol Scand* 2001;104:402-405.
17. Imbert G, Saudou F, Yvert G, Devys D, Trottier Y, Garnier JM, Weber C, Mandel JL, Cancel G, Abbas N, Dürr A, Didierjean O, Stevanin G, Agid Y, Brice A. Cloning of the gene for spinocerebellar ataxia 2 reveals a locus with high sensitivity to expanded CAG/glutamine repeats. *Nat Genet* 1996;14:285-291.
18. Kawaguchi Y, Okamoto T, Taniwaki M, Aizawa M, Inoue M, Katayama S, Kawakami H, Nakamura S, Nishimura M, Akiguchi I, Kimura J, Narumiya S, Kakizuka A. CAG expansions in a novel gene for Machado-Joseph disease at chromosome 14q32.1. *Nat Genet* 1994;8:221-228.
19. Klockgether T. Ataxias. In *Textbook of clinical neurology*, 2nd edn. Ed. CG Goetz. Philadelphia: Saunders, 2003:741-57.
20. Lebre AS, Brice A. Spinocerebellar ataxia 7 (SCA7). *Cytogenet Genome Res* 2003;100:154-163.

21. Mauger C, Del-Favero J, Ceuterick C, Lübke U, Van Broeckhoven C, Martin JJ. Identification and localization of ataxin-7 in brain and retina of a patient with cerebellar ataxia type II using anti-peptide antibody. *Brain Res Mol Brain Res* 1999;74:35-43.
22. Michalik A, Martin JJ, Van Broeckhoven C. Spinocerebellar ataxia type 7 associated with pigmentary retinal dystrophy. *Eur J Hum Genet* 2004;12:2-15.
23. Møller AR. Neural mechanisms of BAEP. In *Functional neuroscience: Evoked potentials and magnetic fields*, 1st edn. Eds. C Barber, GG Celesia, I Hashimoto, R Kakigi. Amsterdam: Elsevier Science, 1999:27-35.
24. Møller MB. Audiological examination. *J Clin Neurophysiol* 1994;11:309-18.
25. Møller AR, Jho HD, Yokota M, Jannetta PJ. Contribution from crossed and uncrossed brainstem structures to the brainstem auditory evoked potentials: a study in humans. *Laryngoscope* 1995;105:596-605.
26. Moore DR. Anatomy and physiology of binaural hearing. *Audiology* 1991;30:125-134.
27. Moore JK. Organization of the human superior olivary complex. *Microsc Res Techn* 2000;51:403-412.
28. Moore JK. The human auditory brain stem: a comparative view. *Hear Res* 1987;29:1-32.
29. Moore JK, Moore RY. A comparative study of the superior olivary complex in the primate brain. *Folia Primat* 1971;16:35-51.
30. Nieuwenhuys R. Anatomy of the auditory pathways, with emphasis on the brain stem. *Adv Otorhinolaryngol* 1984;34:25-38.
31. Nondahl DM, Cruickshanks KJ, Wiley TL, Tweed TS, Klein R, Klein BEK. Accuracy of self-reported hearing loss. *Audiology* 1998;37:295-301.
32. Ohm TG, Braak H. Auditory brainstem nuclei in Alzheimer's disease. *Neurosci Lett* 1989;96:60-63.
33. Olszewski J, Baxter D. *Cytoarchitecture of the human brain stem*. Basel: Karger, 1982
34. Paulson H, Ammache Z. Ataxia and hereditary disorders. *Neurol Clin* 2001;19:759-82.

35. Paulson HL, Perez MK, Trottier Y, Trojanowski JQ, Subramony SH, Das SS, Vig P, Mandel JL, Fischbeck KH, Pittman RN. Intranuclear inclusions of expanded polyglutamine protein in spinocerebellar ataxia type 3. *Neuron* 1997;19:333-44.
36. Perretti A, Santoro L, Lanzillo B, Filla A, De Michele G, Barbieri F, Martino G, Ragno M, Coccozza S, Caruso G. Autosomal dominant cerebellar ataxia type I: multimodal electrophysiological study and comparison between SCA1 and SCA2 patients. *J Neurol Sci* 1996;142:45-53.
37. Pulst SM, Nechiporuk A, Nechiporuk T, Gispert S, Chen XN, Lopes-Cendes I, Pearlman S, Starkman S, Orozco-Diaz G, Lunkes A, DeJong P, Rouleau GA, Auburger G, Korenberg JR, Figueroa C, Sahba S. Moderate expansion of a normally biallelic trinucleotide repeat in spinocerebellar ataxia type 2. *Nat Genet* 1996;14:269-76.
38. Riley HA. An atlas of the basal ganglia, brain stem and spinal cord based on myelin-stained material. Baltimore: Williams & Wilkins, 1943
39. Rüb U, Brunt ER, Del Turco D, De Vos RA, Gierga K, Paulson H, Braak H. Guidelines for the pathoanatomical examination of the lower brain stem in ingestive and swallowing disorders and its application to a dysphagic spinocerebellar ataxia type 3 patient. *Neuropathol Appl Neurobiol* 2003;29:1-13.
40. Rüb U, Brunt ER, Gierga K, Seidel K, Schultz C, Schöls L, Auburger G, Heinsen H, Ippel PF, Glimmerveen WF, Wittebol-Post D, Arai K, Deller T, De Vos RA. Spinocerebellar ataxia type 7 (SCA7): first report of a systematic neuropathological study of the brain of a patient with a very short expanded CAG-repeat. *Brain Pathol* 2005;15:287-295.
41. Rüb U, Brunt ER, Petrasch-Parwez E, Schöls L, Theegarten D, Auburger G, Seidel K, Schultz C, Gierga K, Paulson H, van Broeckhoven C, Deller T, de Vos RA. Degeneration of ingestion-related brainstem nuclei in spinocerebellar ataxia type 2, 3, 6 and 7. *Neuropathol Appl Neurobiol* 2006;32:635-49.
42. Rüb U, Brunt ER, Seidel K, Gierga K, Mooy CM, Kettner M, Van Broeckhoven C, Bechmann I, La Spada AR, Schöls L, den Dunnen W, de Vos RA, Deller T. Spinocerebellar ataxia type 7 (SCA7): Widespread brain damage in an adult onset patient with progressive visual impairments in comparison to an adult onset patient without visual impairments. *Neuropathol Appl Neurobiol* 2008;34:155-68.
43. Rüb U, Bürk K, Schöls L, Brunt ER, de Vos RA, Diaz GO, Gierga K, Ghebremedhin E, Schultz C, Del Turco D, Mittelbronn M, Auburger G, Deller

- T, Braak H. Damage to the reticulotegmental nucleus of the pons in spinocerebellar ataxia type 1, 2, and 3. *Neurology* 2004;63:1258-1263.
44. Rüb U, Gierga K, Brunt ER, de Vos RA, Bauer M, Schöls L, Bürk K, Auburger G, Bohl J, Schultz C, Vuksic M, Burbach GJ, Braak H, Deller T. Spinocerebellar ataxias types 2 and 3: degeneration of the pre-cerebellar nuclei isolates the three phylogenetically defined regions of the cerebellum. *J Neural Transm* 2005;112:1523-1545.
  45. Rüb U, Schultz C, Del Tredici K, Gierga K, Reifenberg G, De Vos RA, Seifried C, Braak H, Auburger G. Anatomically based guidelines for systematic investigation of the central somatosensory system and their application to a spinocerebellar ataxia type 2 (SCA2) patient. *Neuropathol Appl Neurobiol* 2003;29:418-433
  46. Rüb U, Seidel K, Özerden I, Gierga K, Brunt ER, Schöls L, de Vos RA, den Dunnen W, Schultz C, Auburger G, Deller T. Consistent affection of the central somatosensory system in spinocerebellar ataxia type 2 and type 3 and its significance for clinical symptoms and rehabilitative therapy. *Brain Res Rev* 2007;53 235-249.
  47. Schöls L, Amoiridis G, Büttner T, Przuntek H, Epplen JT, Riess O. Autosomal dominant cerebellar ataxia: phenotypic differences in genetically defined subtypes? *Ann Neurol* 1997;42:924-932.
  48. Schöls L, Bauer P, Schmidt T, Schulte T, Riess O. Autosomal dominant cerebellar ataxias: clinical features, genetics, and pathogenesis. *Lancet Neurol* 2004;3:291-304.
  49. Sinha UK, Hollen KM, Rodriguez R, Miller CA. Auditory system degeneration in Alzheimer's disease. *Neurology* 1993;43:779-785.
  50. Smithson KG, MacVicar BA, Hatton GI. Polyethylene glycol embedding: a technique compatible with immunocytochemistry, enzyme histochemistry, histofluorescence and intracellular staining. *J Neurosci Methods* 1983;7:27-41.
  51. Sindhusake D, Mitchell P, Smith W, Golding M, Newall P, Hartley D, Rubin G. Validation of self-reported hearing loss. The Blue Mountains hearing study. *Int J Epidemiol* 2001;3:1371-1378.
  52. Sloan FA, Ostermann J, Brown DS, Lee PP. Effects of changes in self-reported vision on cognitive, affective, and functional status and living arrangements among the elderly. *Am J Ophthalmol* 2005;140:618-627.

53. Tollin DJ. The lateral superior olive: a functional role in sound source localization. *Neuroscientist* 2003;9:127-143.
54. Trottier Y. Antibody-based detection of CAG repeat expansion containing genes. *Methods Mol Biol* 2003;217:83-89.
55. Webster WR, Garey LJ. Auditory system. In *The human nervous system*. Ed. G. Paxinos. San Diego: Academic Press, 1990:889-944.



## Chapter 3

---

# First Appraisal of Brain Pathology Owing to A30P Mutant Alpha-Synuclein

---

Kay Seidel<sup>1\*</sup>, Ludger Schöls, MD<sup>2\*</sup>, Silke Nuber, PhD<sup>3</sup>, Elisabeth Petrasch-Parwez, MD<sup>4</sup>, Kristin Gierga, MD<sup>5</sup>, Zbigniew Wszolek, MD<sup>6</sup>, Dennis Dickson, MD<sup>7</sup>, Wei P. Gai, PhD, MD<sup>8</sup>, Antje Bornemann, MD<sup>9</sup>, Olaf Riess, MD<sup>3</sup>, Abdelhaq Rami, PhD<sup>10</sup>, Wilfried F. A. den Dunnen, MD<sup>11</sup>, Thomas Deller, MD<sup>1</sup>, Udo Rüb, MD<sup>1\*\*</sup>, Rejko Krüger, MD<sup>2\*\*</sup>

<sup>1</sup> *Institute of Clinical Neuroanatomy, Dr Senckenberg Anatomy, Goethe University, Frankfurt am Main, Germany*

<sup>2</sup> *Center of Neurology and Hertie-Institute for Clinical Brain Research, University of Tübingen, Tübingen, Germany*

<sup>3</sup> *Department of Medical Genetics, University of Tübingen, Tübingen, Germany*

<sup>4</sup> *Neuroanatomy and Molecular Brain Research, Ruhr-University Bochum, Bochum, Germany*

<sup>5</sup> *Department of Neuropathology, Heinrich-Heine-University, Düsseldorf, Germany*

<sup>6</sup> *Department of Neurology, Mayo Clinic, Jacksonville, FL;*

<sup>7</sup> *Neuropathology Laboratory, Mayo Clinic, Jacksonville, FL;*

<sup>8</sup> *Department of Human Physiology, Flinders University School of Medicine, Bedford Park, Australia;*

<sup>9</sup> *Institute of Brain Research, University of Tübingen, Tübingen, Germany;*

<sup>10</sup> *Institute for Cellular and Molecular Anatomy, Goethe University, Frankfurt am Main, Germany*

<sup>11</sup> *Department of Pathology and Medical Biology, University Medical Center Groningen, University of Groningen, Groningen, the Netherlands.*

Published in: *Annals of Neurology* 2010;67:684-689

**Abstract**

Familial Parkinson disease (PD) due to the A30P mutation in the *SNCA* gene encoding alpha-synuclein is clinically associated with PD symptoms. In this first pathoanatomical study of the brain of an A30P mutation carrier, we observed neuronal loss in the substantia nigra, locus coeruleus, and dorsal motor vagal nucleus, as well as widespread occurrence of alpha-synuclein immunopositive Lewy bodies, Lewy neurites, and glial aggregates. Alpha-synuclein aggregates ultrastructurally resembled Lewy bodies, and biochemical analyses disclosed a significant load of insoluble alpha-synuclein, indicating neuropathological similarities between A30P disease patients and idiopathic PD, with a more severe neuropathology in A30P carriers.

**Introduction**

The identification of the SNCA gene on chromosome 4q21-23 encoding alpha-synuclein as the first gene responsible for autosomal dominantly inherited Parkinson disease (PD) and the subsequent characterization of 3 point mutations in this gene — A53T, E46K, and A30P— revealed a close clinical relationship between familial PD and idiopathic PD (IPD) [13, 15, 16, 26]. Together with familial forms of PD due to multiplications of the SNCA gene, these 3 point mutations have attracted neuropathological interest, because of hopes that insights into the pathomechanisms of inherited PD could be helpful to unravel the unknown pathogenesis of the frequent synucleinopathy IPD [22]. Contrasting the close clinical similarities, the neuropathological relationship between familial PD caused by mutations in the alpha-synuclein–encoding SNCA gene and IPD is not well understood, because neuropathological data on familial PD are limited [8, 15, 26]. To gain more insight into the neuropathology of familial PD, we performed the first pathoanatomical study of the brain of an A30P mutation carrier in the SNCA gene.

**Subjects and Methods**

The 69-year-old male index patient from the German A30P family received diagnosis of PD at the age of 54 years and was successfully treated with L-dopa for the next 2 years [12]. The clinical course until age 65 years included occurrences of L-dopa -related complications (ie, hallucinations). With further disease progression, the patient lost independence in all activities of daily living and was unable to walk without assistance. During the last years prior to his death, the patient also suffered from a progressive cognitive decline. At the age of 69 years, he became mutistic, dysphagic, and bedridden, and was kept alive by percutaneous endoscopic gastrostomy (PEG). He died of respiratory failure in a poor state of general health.

The brains of the A30P patient and 6 control individuals (1 female, 5 males; mean age at death 60.7 ± 12.8 years) were examined in accordance with the Ethics Committee guidelines of the Faculty of Medicine at Goethe University of Frankfurt am Main (Table 3.1). The brain of the A30P patient displayed severe depigmentation of the substantia nigra, and a slight atrophy of the frontal, temporal, and parietal cerebral lobes (Fig 3.1B).

|              | Controls   | IPD    | IPD    | DLB    | A30P   | A53T   |
|--------------|------------|--------|--------|--------|--------|--------|
| N            | 2          | 1      | 1      | 1      | 1      | 1      |
| Sex          | Male       | Male   | Female | Male   | Male   | Female |
| PD duradtion | -          | 5 yrs  | 6 yrs  | 2 yrs  | 13 yrs | 9 yrs  |
| Age at Death | 74.8 years | 63 yrs | 75 yrs | 76 yrs | 69 yrs | 71 yrs |
| Braak stage  | -          | 3      | 5      | 4-5    | 6      | 6      |

**Table 3.1:** Table 6: Clinical and pathological characteristics of brain donors used for biochemical studies.

After fixation of the brains by immersion in 4% buffered formaldehyde solution, the cerebral, cerebellar, and brainstem tissue blocks of the A30P patient and of 5 control cases were embedded in polyethylene glycol (PEG 1000, Merck, Darmstadt, Germany). The first set of serial tissue sections were stained for lipofuscin pigment (aldehyde fuchsin) and Nissl material (Darrow red), and employed for anatomical orientation and the assessment of neurodegeneration [4]. The second set of tissue sections was treated with a rabbit polyclonal antibody against glial fibrillary acidic protein (GFAP) (1:500, Dako, Glostrup, Denmark) to highlight reactive astrogliosis. A third set of serial sections was used to visualize LBs, LNs, and glial inclusions by means of immunoreactions for alpha-synuclein [6]. The fourth set of serial tissue sections was immunostained with the anti-tau antibody AT8 (1:2000; Innogenetics, Ghent, Belgium) or PHF-1 (1:2000; kind gift of P. Davies, Albert Einstein College of Medicine, New York, USA) to visualize tau-immunopositive cytoskeletal changes related to Alzheimer's disease (AD) or other known human tauopathies. In addition, an advanced silver pyridine Campbell-Switzer method was applied to recommended tissue sections of the A30P patient to identify  $\beta$ -amyloid deposits [3, 23]. The tissue sections stained with primary antibodies against GFAP, alpha-synuclein, and tau were incubated with a secondary biotinylated antibody (1:200) directed against the primary antibody for 1.5h at room temperature. Immunoreactions were visualized with the AB complex (Vectastain, Vector Laboratories, Burlingame, USA) and 3,3'-diaminobenzidine-tetra-HCl/H<sub>2</sub>O<sub>2</sub> (DAB, D5637 Sigma, Taufkirchen, Germany). Omission of the primary antibodies resulted in non-staining.

The severity of neuronal loss and the frequency of alpha-synuclein-immunopositive Lewy bodies (LBs), Lewy neurites (LNs), and glial inclusions in the brain of the A30P index patient were semiquantitatively assessed (not discernible, -; slight, +; marked, ++; severe, +++; Tables 3.2–3.6).

Subcellular fractionation of frontal or entorhinal cortex tissue from the A30P patient, 1 patient from a Greek-American kindred carrying the A53T mutation in the *SNCA* gene [16], 1 patient with dementia with Lewy bodies (DLB), 2 IPD patients, and 2 control individuals (Table 1) was performed as described previously [6,24]. Western blots using 3 different antibodies against alpha-synuclein (N-terminus: PA1-38705, Affinity Bioreagents, Golden, CO; NAC domain: Mc42, Translabs, UK; C-terminus:15G7; AG Scientific, San Diego, CA) were reproduced 3 times with similar results, with each sample loaded at least 2 times on different blots.

Electron microscopy was performed to elucidate the ultrastructure of neuronal alpha-synuclein aggregates in the substantia nigra, basal nucleus of Meynert, and dorsal motor vagal nucleus (DMV) of the A30P patient and 1 patient with IPD as control (female; age at death, 76 years; disease duration, 26 years; Braak stage 5) as described previously [12].

## Results

Investigation of pigment-Nissl stained tissue sections revealed neuronal loss in the pars compacta of the substantia nigra (Fig 3.1D, E), locus coeruleus, and DMV (Fig 3.1F, G). LBs and LB-like inclusions occurred as spherical, reniform, or globose neuronal inclusions with smooth surfaces (Fig 3.2A). LNs had a club-or corkscrew-shaped appearance, or were short and stubby or slender, elongated, and thread-like (Fig 3.2A). Alpha-synuclein-immunopositive LBs were present in all areas of the cerebral cortex (neocortex: predominantly in layers V and VI; ento-and transentorhinal regions: predominantly in layers II, III, V, and VI; subiculum, presubiculum, hippocampal CA1, CA2, and CA3 sectors: predominantly in pyramidal layers) (Fig 3.1A, B), in all nuclei of the basal forebrain, basal ganglia, amygdala, and hypothalamus (Fig 3.3C, D), in select regions of the thalamus (Fig 3.3E–H), subthalamus (Fig 3.4A), and brainstem (Fig 3.4B–F), and in the cerebellum (Tables 3.2-3.6).

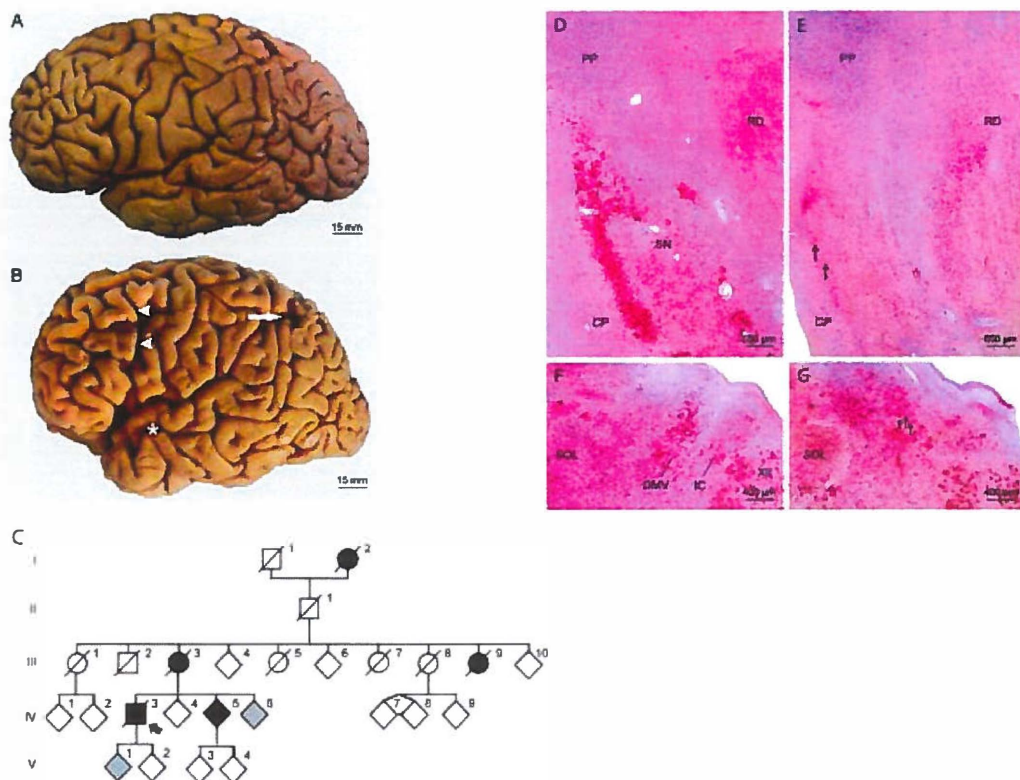


**Figure 3.1: Macroscopic brain aspects in A30P and A30P mutation-related nerve cell loss**

(A) Lateral aspect of the left cerebral hemisphere of a 53-year-old male individual without a prior medical history of neurological or psychiatric disease. (B) Lateral aspect of the left cerebral hemisphere from the A30P index patient. Note the widened sulci of the frontal (*arrowheads*), temporal (*asterisk*), and parietal lobes (*arrow*). (C) Pedigree of the German A30P family indicating the deceased index patient (*black arrow*; *filled black symbols*: affected family members according to the United Kingdom Parkinson's Disease Brain Bank criteria; *filled gray symbols*: individuals displaying subtle extrapyramidal symptoms; *circles*: females; *squares*: males; *oblique slashes*: deceased individuals; *open symbols*: healthy family members). (D) Frontal section through the rostral midbrain of a typical 59-year-old male control case with the dorsal portion of the substantia nigra (SN). (E) Severely degenerated SN of the A30P index patient. (F) Horizontal section through the mid portion of the medulla oblongata of an 84-year-old male control case showing the dorsal motor vagal nucleus (DMV). (G) Markedly degenerated DMV of the A30P index patient. Arrows point to surviving nerve cells. D–G: aldehyde fuchsin-Darrow red staining, 100µm PEG sections. I = first generation; II = second generation; III = third generation; IV = fourth generation; V = fifth generation; PP = peripeduncular nucleus; RD = red nucleus; CP = cerebral peduncle; SOL = solitary tract; IC = intercalate nucleus; XII = hypoglossal nucleus.



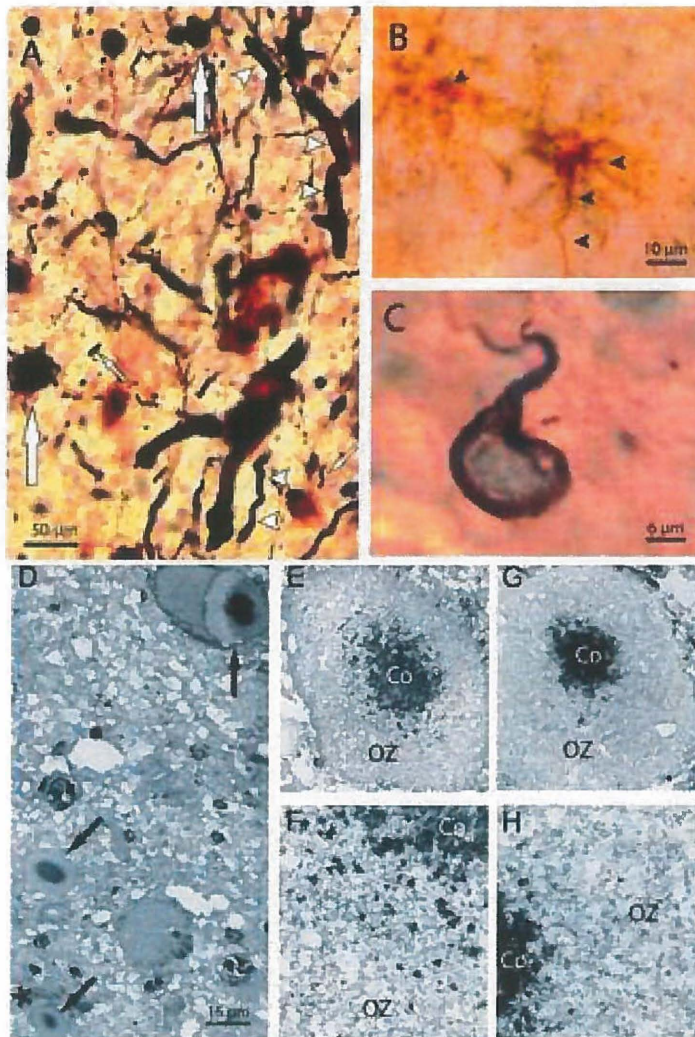


**Figure 3.2: Alpha-synuclein immunocytochemical and electron microscopic findings in the A30P index patient**

(A) Lewy bodies (LBs) (*large arrows*) and Lewy neurites (*arrowheads*) in the dorsal motor vagal nucleus. Small arrows point to coiled bodies. (B) Gleason score glial fibrillary acidic protein (GFAP)-immunopositive astrocytes in the transentorhinal cortex containing alpha-synuclein immunopositive deposits (*arrowheads*). (C) Substantia nigra: Typical coiled-up alpha-synuclein immunopositive oligodendroglial inclusion (brown) surrounding the nucleus (blue) of the affected oligodendrocyte. (D) The dorsal motor vagal nucleus of the A30P patient exhibits various LBs (*arrows*) with a dark inner core and a ring-like light outer zone. (E, F) Electron micrograph of the LB in the lower left corner of D (*asterisk*). The LB shows a dense granular core (Co), surrounded by a lighter outer zone (OZ), which contains loosely arranged filaments (F). (G, H) Electron micrograph of an LB found in an idiopathic Parkinson disease case. Note the high structural similarity of the LBs from both cases. (A) Anti-alpha-synuclein immunocytochemistry; (B) anti-GFAP (3,3'-diaminobenzidine [DAB], brown)/anti-alpha-synuclein (SK4700, blue-gray) double immunostaining; (C) antitransferrin (SK4700, blue-gray)/anti-alpha-synuclein (DAB, brown) double immunostaining; (A–C) 100µm PEG sections; (D) toluidine blue-stained semithin section, 0.75µm; (E–H) uranyl acetate and lead citrate contrasted ultrathin section, 100nm).



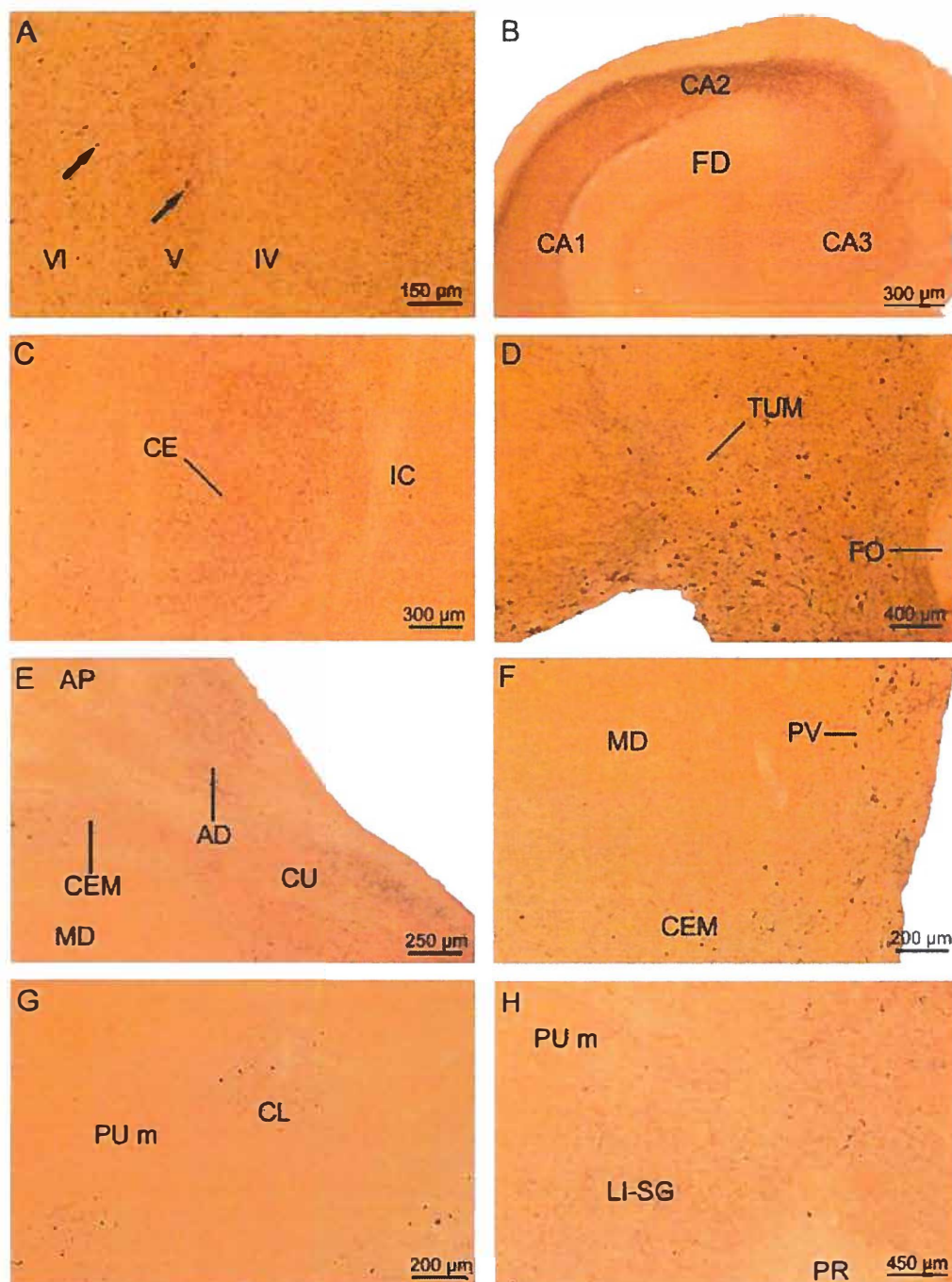


**Figure 3.3 (previous page): Predominantly neuronal alpha-synuclein immunopositive inclusion bodies in the cerebral cortex, amygdala, hypothalamus, and thalamus)**

(A) Allocortical entorhinal region: abundant alpha-synuclein immunopositive LBs in the deep layers V and VI (arrows). (B) Allocortical hippocampus: Severe affection of the CA1, CA2, and CA3 sectors and slight affection of the fascia dentata (FD) by alpha-synuclein immunopositive neuronal inclusions bodies. (C) Amygdala: Close-meshed network of alpha-synuclein immunopositive LBs and LNs in the central nucleus (CE) and markedly affected intercalated nucleus (IC). (D) Hypothalamus: Remarkable involvement of the tuberomammillary nucleus (TUM). (E) Dense mesh of alpha-synuclein immunopositive LBs and LNs in the intralaminar central medial (CEM) and cucullar (CU) thalamic nuclei, as well as in the anterodorsal nucleus (AD) of the thalamus. Note the additional slight involvement of the thalamic anteroprincipal (AP) and mediodorsal nuclei (MD). (F) Severe affection of the thalamic intralaminar central medial (CEM) nucleus and the paraventricular nuclei (PV). (G) Selective vulnerability of the islands of the intralaminar central lateral nucleus (CL) of the thalamus intermingled among the nearly unaffected nerve cells of the medial subnucleus of the pulvinar (PU m). (H) Dense network of LBs and LNs in the limitans-suprageniculate complex (LI-SG) lying at the border between the thalamus and the midbrain. Note the marked involvement of the pretectum (PR). (A-H: anti-alpha-synuclein immunocytochemistry, 100  $\mu$ m PEG sections). Abbreviations: AD – Anterodorsal nucleus of the thalamus; AP – Anteroprincipal nucleus of the thalamus; CA1 – CA1 sector of the hippocampus; CA2 – CA2 sector of the hippocampus; CA3 – CA3 sector of the hippocampus; CE – Central nucleus of the amygdala; CEM – Central medial nucleus of the thalamus; CL – Central lateral nucleus of the thalamus; CU – Cucullar nucleus of the thalamus; FD – Fascia dentata; FO – Fornix; IC – Intercalate nucleus of the amygdala; LI-SG – Limitans-suprageniculate-complex of the thalamus; MD – Mediodorsal nucleus of the thalamus; PR – Pretectum; PU m – Pulvinar, medial subnucleus; PV – Paraventricular nuclei of the thalamus; TUM – Tuberomammillary nucleus of the hypothalamus; IV – Cortical layer IV; V – Cortical layer V; VI – Cortical layer VI

In the thalamus, basal nucleus of Meynert, substantia nigra, DMV, gigantocellular reticular nucleus, raphes magnus nucleus, and intermediate reticular zone, we observed alpha-synuclein-immunopositive neurons without LBs or LNs. These neurons, however, were characterized by the presence of fine alpha-synuclein-immunopositive, slightly brownish, and loosely scattered cytoplasmic granules sparing the nucleus and often extending into the processes of nerve cells. In addition, alpha-synuclein immunopositivity and/or LB-like inclusions were observed in central nervous white matter components (Fig 3.2E–H).

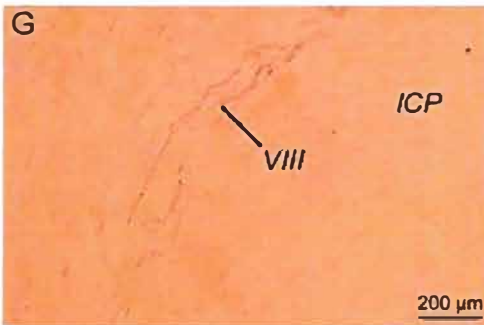
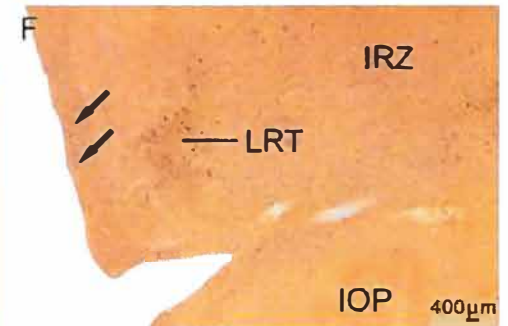
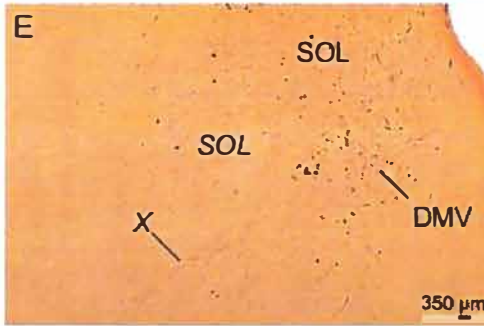
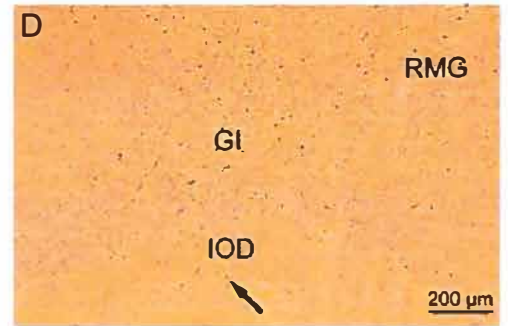
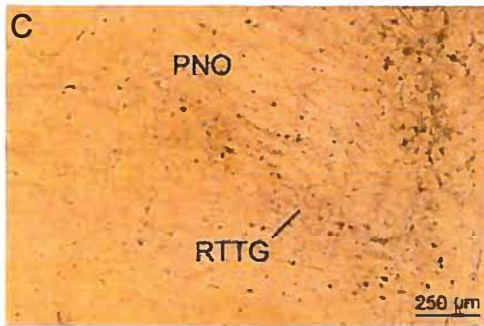
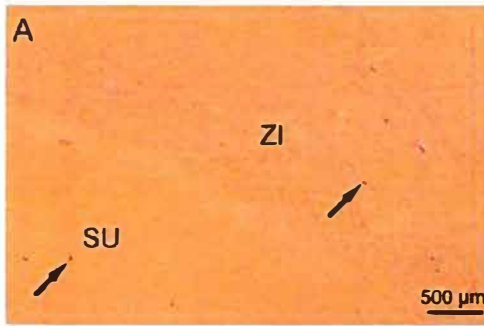


**Figure 3.4 (previous page): Alpha-synuclein immunopositive neuronal and oligodendroglial inclusions in subthalamic and brainstem nuclei, as well as alpha-synuclein immunopositive brainstem fiber tracts**

(A) Abundance of alpha-synuclein immunopositive neuronal (arrow) and oligodendroglial inclusions in the zona incerta (ZI) and slightly affected subthalamic nucleus (SU) (arrow). (B) High prevalence of alpha-synuclein immunopositive LBs (arrow), LNs, and coiled bodies in the substantia nigra (SN). Note the considerable affection of the red nucleus (RD). (C) Dense network of alpha-synuclein immunopositive LBs and LNs in the precerebellar reticulotegmental nucleus of the pons (RTTG) and markedly affected oral subnucleus of the pontine reticular formation (PNO). (D) Large amounts of LBs and LNs in the raphe magnus (RMG) and gigantocellular reticular nuclei (GI). Additional LBs (arrow) are present in the dorsal accessory subnucleus of the inferior olive (IOD). (E) Severe affection of the dorsal motor vagal (DMV) and solitary nuclei (SOL), as well as alpha-synuclein immunopositive vagal nerve (X). (F) Severe alpha-synuclein immunopositive inclusion body pathology in the intermediate reticular zone (IRZ) and the precerebellar lateral reticular nucleus (LRT). Note the alpha-synuclein immunopositive fibers of the dorsal spinocerebellar tract (arrows). Alpha-synuclein immunopositive (G) vestibular nerve (VIII) and (H) olivocerebellar fibers (arrowheads). (A-H: anti-alpha-synuclein immunocytochemistry, 100  $\mu$ m PEG sections). Abbreviations: DMV – Dorsal motor vagal nucleus; ICP – Inferior cerebellar peduncle; IOD – Inferior olive, dorsal accessory subnucleus; IOP – Inferior olive, principal subnucleus; IRZ – Intermediate reticular zone; GI – Gigantocellular reticular nucleus; LRT – Lateral reticular nucleus; PNO – Pontine reticular formation, oral subnucleus; RD – Red nucleus; RMG – Raphe magnus nucleus; RTTG – Reticulotegmental nucleus of the pons; SN – Substantia Nigra; SOL – Solitary nuclei; SOL – Solitary tract; SU – Subthalamic nucleus; ZI – Zona incerta; VIII – Vestibular nerve; X – Vagal nerve

Alpha-synuclein-immunopositive coiled bodies (Fig 3.2A, C; Fig 3.2A, B) and glial fibrillary acidic protein-immunopositive astrocytes were present in all gray and white matter components of the telencephalon, diencephalon, brainstem, and cerebellum of the A30P patient. Anti-alpha-synuclein/anti-transferrin double immunostaining confirmed the purely oligodendroglial localization of the coiled bodies, and AT8 and PHF-1 immunostaining excluded their tau immunoreactivity (Fig 3.2C). Alpha-synuclein-immunopositive and tau-negative astrocytes (Fig 3.2B) occurred in all nuclei of the amygdala and the septum, striatum, claustrum, select thalamic nuclei (ie, central lateral nucleus, limitanssupragenulate complex), temporal neocortex, and ento- and transentorhinal regions. No colocalization of tau with alpha-synuclein was observed in neurons and oligodendrocytes of the dorsal raphe nucleus and the intermediate reticular zone (Fig 3.5).



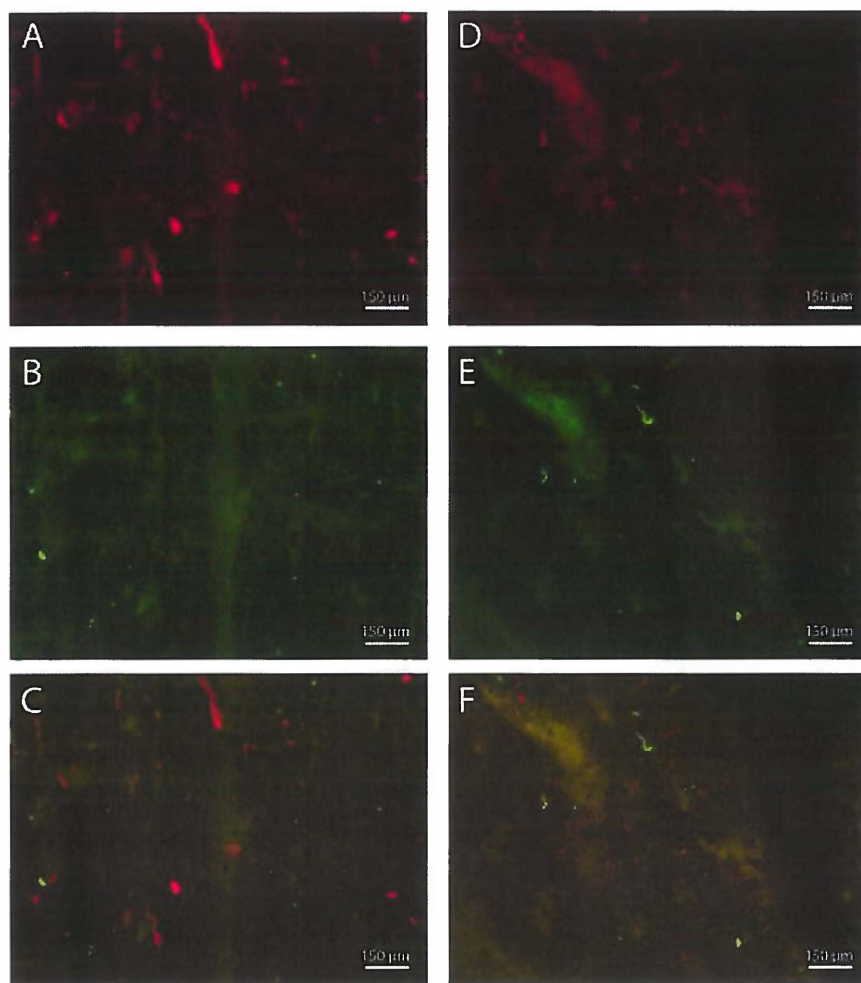


**Figure 3.5: No colocalization of alpha-synuclein and tau pathologies in the dorsal raphe nucleus and intermediate reticular zone of the A30P patient**

Immunofluorescent images displaying concomitant (A) alpha-synuclein and (B) tau inclusion pathologies in the intermediate reticular zone of the A30P patient, which (C) do not colocalize. (D) The alpha-synuclein and (E) tau aggregates likewise (F) do not colocalize in the dorsal raphe nucleus of the A30P patient. (A-F: Immunofluorescence staining of alpha-synuclein inclusion pathology with alexa 568 chromogen (red) and tau inclusion pathology with alexa 488 (green), 100 µm PEG sections).

The Alzheimer disease (AD)-related cortical cytoskeletal pathology as assessed by AT8 and PHF-1 immunostaining corresponded to Braak stage II, and the brain  $\beta$ -amyloidosis to phase 1 of the schema proposed by Thal and colleagues [3,23].

Ultrastructural studies confirmed neuronal loss in the substantia nigra and DMV nucleus. The majority of remaining nigral neurons underwent dark cell degeneration. Several surviving nigral neurons displayed round somatic inclusions with a denser

center and a lighter outer zone as a correlate of LBs. In the DMV nucleus, LBs were detected with a dark dense core (Fig 3.2D) and a broad lighter outer zone reflecting the classical brainstem type of LB [11]. They were frequently localized in the cytoplasm of nerve cells, but also occurred in the neuropil, suggesting dendritic or axonal localization. Electron microscopy revealed a dense dark granular center and a ring-like outer zone with abundant fibrils (Fig 3.2E, F), similar to the ultrastructural characteristics of LBs from an IPD patient (Braak stage 5; Fig 3.2G, H).

Biochemical sequential extraction of alpha-synuclein of frontal cortex of controls, DLB patients, IPD patients (Braak stage 3 and stage 5), the A30P patient and an A53T patient revealed soluble monomeric alpha-synuclein in all samples (Tris-HCl; Fig. 3.6A). The presence of monomeric and oligomeric alpha-synuclein species in the urea fraction was not observed in controls and disclosed insolubility of alpha-synuclein that was most prominent in the A30P case and DLB patient (Fig 3.6A). A30P alpha-synuclein insolubility was prominent in both the entorhinal and frontal cortex of the A30P patient substantiating immunohistochemically determined LB load in these 2 brain areas (Fig 3.6B).

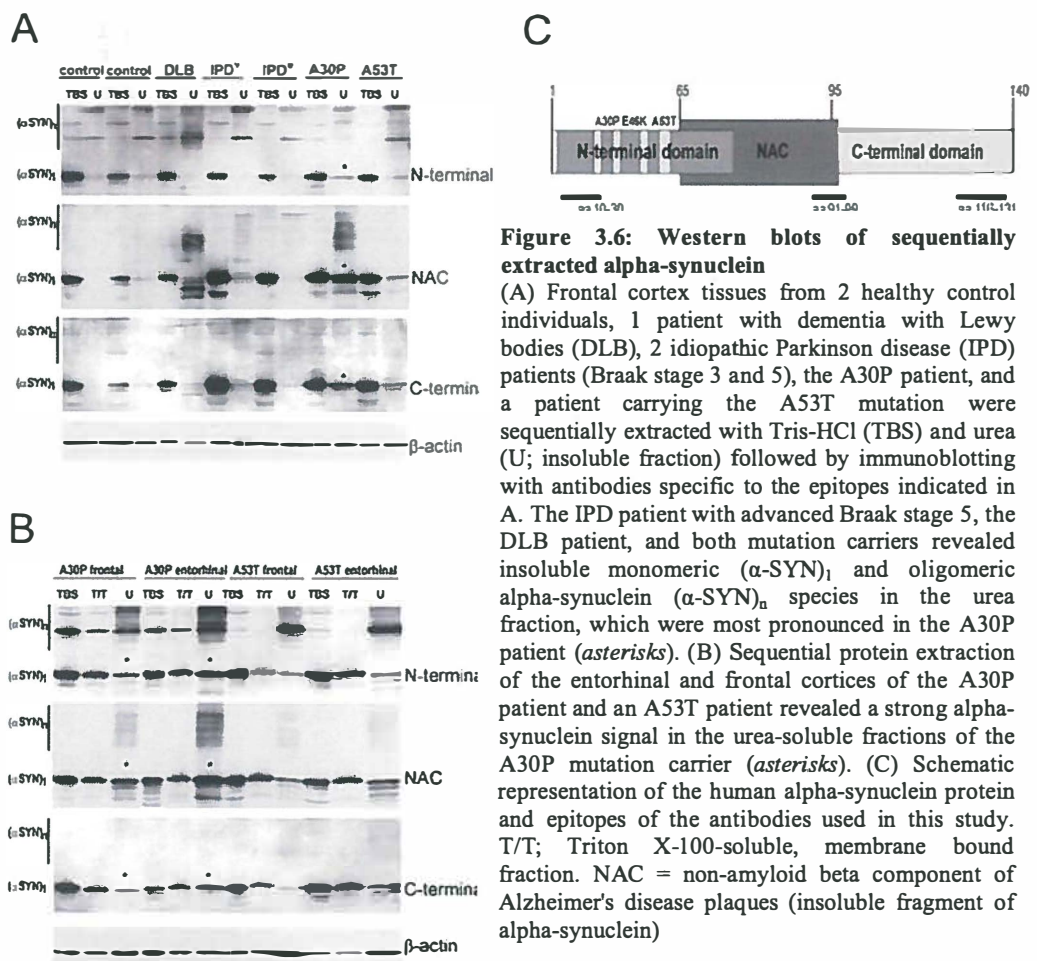


**Figure 3.6: Western blots of sequentially extracted alpha-synuclein**

(A) Frontal cortex tissues from 2 healthy control individuals, 1 patient with dementia with Lewy bodies (DLB), 2 idiopathic Parkinson disease (IPD) patients (Braak stage 3 and 5), the A30P patient, and a patient carrying the A53T mutation were sequentially extracted with Tris-HCl (TBS) and urea (U; insoluble fraction) followed by immunoblotting with antibodies specific to the epitopes indicated in A. The IPD patient with advanced Braak stage 5, the DLB patient, and both mutation carriers revealed insoluble monomeric ( $\alpha$ -SYN)<sub>1</sub> and oligomeric alpha-synuclein ( $\alpha$ -SYN)<sub>n</sub> species in the urea fraction, which were most pronounced in the A30P patient (asterisks). (B) Sequential protein extraction of the entorhinal and frontal cortices of the A30P patient and an A53T patient revealed a strong alpha-synuclein signal in the urea-soluble fractions of the A30P mutation carrier (asterisks). (C) Schematic representation of the human alpha-synuclein protein and epitopes of the antibodies used in this study. T/T; Triton X-100-soluble, membrane bound fraction. NAC = non-amyloid beta component of Alzheimer's disease plaques (insoluble fragment of alpha-synuclein)

|                        | Central nervous gray component       | L   | C  |
|------------------------|--------------------------------------|-----|----|
| <b>Cerebral cortex</b> | Frontal neocortex                    | ++  | +  |
|                        | Temporal neocortex                   | ++  | +  |
|                        | Parietal neocortex                   | ++  | +  |
|                        | Occipital neocortex                  | ++  | +  |
|                        | Cingulate gyrus                      | ++  | +  |
|                        | Insula                               | ++  | ++ |
|                        | Entorhinal cortex                    | ++  | +  |
|                        | Transentorhinal cortex               | ++  | +  |
|                        | Presubiculum                         | +   | +  |
|                        | Parasubiculum                        | +   | +  |
|                        | Subiculum                            | ++  | +  |
|                        | Hippocampus – CA1 sector             | ++  | +  |
|                        | Hippocampus – CA2 sector             | ++  | +  |
|                        | Hippocampus – CA3 sector             | ++  | +  |
|                        | Hippocampus – Fascia dentata         | +   | +  |
| <b>Basal forebrain</b> | Anterior olfactory nucleus           | ++  | +  |
|                        | Clastrum                             | +++ | +  |
|                        | Septal nuclei                        | ++  | +  |
|                        | Bed nucleus of the stria terminalis  | +++ | ++ |
|                        | Nuclei of the diagonal band of Broca | +++ | +  |
|                        | Basal nucleus of Meynert             | +++ | +  |
| <b>Basal ganglia</b>   | Ventral striatum                     | ++  | ++ |
|                        | Ventral pallidum                     | ++  | ++ |
|                        | Caudate nucleus                      | +   | ++ |
|                        | Putamen                              | +   | +  |
|                        | Pallidum                             | +   | ++ |
| <b>Amygdala</b>        | Medial nucleus                       | ++  | +  |
|                        | Central nucleus                      | +++ | +  |
|                        | Intercalated nucleus                 | ++  | +  |
|                        | Periamygdaloid cortex                | ++  | +  |
|                        | Accessory basal nucleus              | +++ | +  |
|                        | Basal nuclei                         | ++  | +  |
|                        | Lateral nucleus                      | ++  | +  |
|                        | Accessory cortical nucleus           | +++ | +  |
|                        | Transitory zone                      | ++  | +  |
|                        | Granular nucleus                     | +++ | +  |

**Table 3.1:** Distribution and extent of alpha-synuclein immunopositive neuronal and oligodendroglial inclusions in the cerebral cortex, basal forebrain, basal ganglia and amygdala of the A30P index patient affected by both LBs and/or LNs and coiled bodies (L, Lewy bodies and/or Lewy neurites; C, coiled bodies; not discernible 0, mild +, marked ++, severe +++).



|                     | Central Nervous Grey component                       | L   | C |
|---------------------|--|-----|---|
| <b>Thalamus</b>     | Anterodorsal nucleus                                 | +++ | + |
|                     | Anteroprecipal nucleus                               | +   | + |
|                     | Ventral anterior nucleus                             | ++  | + |
|                     | Central medial nucleus                               | +++ | + |
|                     | Mediodorsal nucleus                                  | +   | + |
|                     | Parataenial nucleus                                  | ++  | + |
|                     | Paraventricular nuclei                               | +++ | + |
|                     | Paracentral nucleus                                  | ++  | + |
|                     | Cucullar nucleus                                     | +++ | + |
|                     | Laterodorsal nucleus                                 | +   | + |
|                     | Centromedian nucleus                                 | +   | + |
|                     | Parafascicular nucleus                               | ++  | + |
|                     | Subparafascicular nucleus                            | +++ | + |
|                     | Ventral lateral nucleus                              | +   | + |
|                     | Ventral posterior lateral nucleus                    | +   | + |
|                     | Ventral posterior medial nucleus                     | +   | + |
|                     | Ventral posterior medial nucleus, parvocellular part | +   | + |
|                     | Lateral posterior nucleus                            | +   | + |
|                     | Lateral geniculate body                              | +   | + |
|                     | Medial geniculate body                               | +++ | + |
|                     | Central lateral nucleus                              | +   | + |
|                     | Pulvinar, anterior nucleus                           | +   | + |
|                     | Pulvinar, medial nucleus                             | +   | + |
|                     | Pulvinar, lateral nucleus                            | +   | + |
|                     | Pulvinar, inferior nucleus                           | +++ | + |
|                     | Limitans-suprageniculate complex                     | ++  | + |
|                     | Reticular nucleus                                    |     |   |
| <b>Hypothalamus</b> | Periventricular preoptic nucleus                     | +   | + |
|                     | Paraventricular nucleus                              | +   | + |
|                     | Median preoptic area                                 | +   | + |
|                     | Supraoptic nucleus                                   | +   | + |
|                     | Intermediate nucleus                                 | +   | + |
|                     | Lateral hypothalamic area                            | +   | + |
|                     | Anterior hypothalamic area                           | +   | + |
|                     | Arcuate nucleus                                      | +   | + |
|                     | Dorsomedial nucleus                                  | +   | + |
|                     | Ventromedial nucleus                                 | +   | + |
|                     | Mammillary nuclei                                    | +   | + |
|                     | Tuberomammillary nucleus                             | ++  | + |
|                     | Lateral tuberal nucleus                              | +   | + |
|                     | Posterior hypothalamic area                          | ++  | + |
|                     | Supramammillary nucleus                              | ++  | + |

**Table 3.2:** Distribution and extent of alpha-synuclein immunopositive neuronal and oligodendroglial inclusions in the thalamus and hypothalamus of the A30P index patient affected by both LBs and/or LNs (L, Lewy bodies and/or Lewy neurites; C, coiled bodies; not discernible 0, mild +, marked ++, severe +++).

|                           | <b>Central Nervous Grey component</b>                            | <b>L</b> | <b>C</b> |
|---------------------------|--|----------|----------|
| <b>Subthalamic nuclei</b> | Zona incerta   | +++      | ++       |
|                           | Subthalamic nucleus  | +        | +        |
| <b>Midbrain</b>           | Central gray   | +++      | +        |
|                           | Superior colliculus  | +        | +        |
|                           | Dorsal raphe nucleus   | +++      | +        |
|                           | Pedunculopontine nucleus   | +++      | +        |
|                           | Parabigeminal nucleus  | +        | +        |
|                           | Trochlear nucleus  | +        | +        |
|                           | Interpeduncular nucleus  | ++       | +        |
|                           | Ventral tegmental area   | +++      | +        |
|                           | Substantia nigra   | ++       | ++       |
|                           | Inferior colliculus  | ++       | +        |
|                           | Edinger-Westphal nucleus   | ++       | +        |
|                           | Oculomotor nucleus   | +        | +        |
|                           | Red nucleus  | +        | +        |
|                           | Rostral interstitial nucleus of the medial longitudinal fascicle | ++       | +        |
|                           | Nucleus of the posterior commissure                              | ++       | +        |
|                           | Peripeduncular nucleus   | +++      | +        |
|                           | Pretectum  | ++       | ++       |
| <b>Pons</b>               | Pontine nuclei   | +        | ++       |
|                           | Mesencephalic trigeminal nucleus                                 | +        | +        |
|                           | Locus coeruleus  | ++       | +        |
|                           | Parabrachial nuclei  | ++       | +        |
|                           | Pontine reticular formation, oral nucleus                        | ++       | +        |
|                           | Dorsal raphe nucleus   | ++       | +        |
|                           | Reticulotegmental nucleus of the pons                            | +++      | +        |
|                           | Superior vestibular nucleus                                      | ++       | +        |
|                           | Primary trigeminal nucleus                                       | +        | +        |
|                           | Motor trigeminal nucleus   | +        | +        |
|                           | Pontine reticular formation, caudal nucleus                      | ++       | +        |
|                           | Central raphe nucleus  | +++      | +        |
|                           | Abducens nucleus   | +        | +        |
|                           | Raphe interpositus nucleus                                       | ++       | +        |
|                           | Lateral vestibular nucleus                                       | ++       | +        |
|                           | Parvocellular reticular nucleus                                  | ++       | +        |
|                           | Facial nucleus   | +        | +        |
|                           | Superior olive   | +        | +        |
|                           | Prepositus hypoglossal nucleus                                   | +++      | +        |
|                           | Dorsal paramedian nucleus  | +        | +        |
|                           | Arcuate nucleus  | +        | +        |
|                           | Spinal trigeminal nucleus  | ++       | +        |
|                           | Dorsal paragigantocellular reticular nucleus                     | ++       | +        |
|                           | Gigantocellular reticular nucleus                                | +++      | +        |
|                           | Cochlear nuclei  | +        | +        |
|                           | Raphe magnus nucleus   | +++      | +        |

**Table 3.3:** Distribution and extent of alpha-synuclein immunopositive neuronal and oligodendroglial inclusions in subthalamic nuclei, the midbrain and pons of the A30P index patient affected by both LBs and/or LNs (L, Lewy bodies and/or Lewy neurites; C, coiled bodies; not discernible 0, mild +, marked ++, severe +++).

|                          | Central Nervous Grey component | L   | C |
|--------------------------|--------------------------------|-----|---|
| <b>Medulla oblongata</b> | Inferior olive                 | +   | + |
|                          | Medial vestibular nucleus      | ++  | + |
|                          | Spinal vestibular nucleus      | ++  | + |
|                          | Solitary nuclei                | +++ | + |
|                          | Dorsal motor vagal nucleus     | +++ | + |
|                          | Intercalate nucleus            | ++  | + |
|                          | Hypoglossal nucleus            | +   | + |
|                          | Medial reticular nucleus       | ++  | + |
|                          | Intermediate reticular zone    | ++  | + |
|                          | Medial reticular nucleus       | ++  | + |
|                          | Lateral reticular nucleus      | ++  | + |
|                          | External cuneate nucleus       | +   | + |
|                          | Cuneate nucleus                | +   | + |
|                          | Gracile nucleus                | +   | + |
| <b>Cerebellum</b>        | Purkinje cell layer            | +   | + |
|                          | Granular cell layer            | +   | + |
|                          | Dentate nucleus                | +   | + |
|                          | Fastigial nucleus              | +   | + |

**Table 3.4:** Distribution and extent of alpha-synuclein immunopositive neuronal and oligodendroglial inclusions in the medulla oblongata and cerebellum of the A30P index patient affected by both LBs and/or LNs (L, Lewy bodies and/or Lewy neurites; C, coiled bodies; not discernible 0, mild +, marked ++, severe +++).

| Central nervous white component        | IF | C  |
|--|----|----|
| White matter – Frontal cerebral lobe   | +  | +  |
| White matter – Temporal cerebral lobe  | +  | +  |
| White matter – Parietal cerebral lobe  | +  | +  |
| White matter – Occipital cerebral lobe | +  | +  |
| Fornix                                 | +  | +  |
| Internal capsule                       | +  | +  |
| External capsule                       | +  | +  |
| Extreme capsule                        | +  | +  |
| Triangular area of Wernicke            | +  | +  |
| Anterior commissure                    | +  | +  |
| Mammillothalamic tract                 | +  | +  |
| Habenulo-interpeduncular tract         | +  | +  |
| Posterior commissure                   | +  | +  |
| Cerebral peduncle                      | +  | +  |
| Oculomotor nerve                       | +  | +  |
| Lateral lemniscus                      | +  | +  |
| Medial lemniscus                       | +  | +  |
| Medial longitudinal fascicle           | +  | +  |
| Superior cerebellar peduncle           | +  | +  |
| Pontocerebellar fibres                 | +  | +  |
| Medial cerebellar peduncle             | +  | +  |
| Abducens nerve                         | ++ | +  |
| Facial nerve                           | +  | +  |
| Spinal trigeminal tract                | +  | +  |
| Dorsal acoustic stria                  | +  | +  |
| Vestibulocochlear nerve                | ++ | +  |
| Inferior cerebellar peduncle           | +  | +  |
| Olivocerebellar fibers                 | ++ | +  |
| External arcuate fibers                | ++ | +  |
| Solitary tract                         | +  | +  |
| Vagal nerve                            | ++ | +  |
| Hypoglossal nerve                      | ++ | +  |
| Dorsal spinocerebellar tract           | ++ | ++ |
| Ventral spinocerebellar tract          | ++ | +  |
| Gracile fascicle                       | +  | +  |
| Cuneate fascicle                       | +  | +  |
| Cerebellar white matter                | +  | +  |

**Table 3.5:** Extent of alpha-synuclein immunoreactive fibers in the central nervous white matter components of the A30P index patient showing additional oligodendroglial inclusions (IF, immunoreactive fibers; C, coiled bodies; not discernible 0, mild +, marked ++, severe +++).

## Discussion

Our study provides first insights into the pathoanatomy of familial PD caused by the A30P mutation in the *SNCA* gene and demonstrates a widespread central nervous occurrence of alpha-synuclein-immunopositive inclusions and the advantage of investigations of complete tissue series for the identification of more subtle pathological alterations [4, 15].

Application of sensitive immunostaining methods revealed tau-immunoreactive cortical cytoskeletal pathology in the index patient. Because no additional tau-positive neuronal and glial inclusions associated with other known human tauopathies were observed, the cortical tau pathology most likely corresponded to the early Braak AD stage II [3]. In addition, alpha-synuclein immunocytochemistry in the A30P patient did not reveal features of neuronal inclusions or the distribution pattern of alpha-synuclein-immunopositive oligodendroglial inclusions typical for multiple system atrophy [4].

As in IPD, the A30P patient's brain showed neuronal loss in the substantia nigra, DMV, and locus coeruleus and displayed recognized neuronal pathologies (ie, LBs, LNs, and LB-like inclusions) in brain structures typically affected in IPD (e.g. neo- and allocortex, thalamus, cerebellum, substantia nigra, pedunculopontine nucleus, DMV), as well as in brainstem nuclei and central nervous fiber tracts that are not or are only less severely affected in IPD (e.g. rostral interstitial nucleus of the medial longitudinal fascicle, reticulotegmental nucleus of the pons, medial vestibular nucleus, spinocerebellar tracts, and cerebellar peduncles) [5, 21]. In addition, as in IPD, alpha-synuclein-immunopositive astroglial and oligodendroglial inclusions were present in the A30P patient [25].

Among the currently known brain pathologies reported in familial PD forms caused by mutations or multiplications in the *SNCA* gene, the brain pathology of the A30P index patient most closely resembled the brain alterations observed in IPD individuals [8,9,15,26]. Neuropathological discrepancies that strengthen the pathogenic role of A30P mutant alpha-synuclein and may indicate different etiopathogenic mechanisms included: (1) substantial and more severe load of alpha-synuclein aggregates in the cerebellum and precerebellar and oculomotor brainstem nuclei than in IPD; and (2) presence of more glial aggregates, named coiled bodies, in the A30P brain than in IPD. The presence of concurrent tau pathology in A53T mutation carriers or the accumulation of alpha-synuclein and tau within the same neuronal aggregates in carriers of alpha-synuclein multiplications underscore important discrepancies between IPD patients and the A30P mutation carrier studied here [8, 9].

Considering the current knowledge in the field of functional neuroanatomy the pathoanatomical abnormalities seen in the A30P patient studied here can account for the clinical and paraclinical disease signs recorded in his medical history. These include: (1) neurodegeneration of the substantia nigra for parkinsonian features, postural instability, decreased striatal F-dopa uptake in the F-DOPA PET scan, and striatal hypometabolism in the FDG PET scan [6, 1, 11]; (2) presence of neuronal

inclusions in the reticulotegmental nucleus of the pons for saccadic horizontal smooth pursuits [20]; (3) occurrence of neuronal inclusions in the rostral interstitial nucleus of the medial longitudinal fascicle for vertical gaze palsy [14]; (4) occurrence of neuronal inclusions in the abducens nucleus and nerve for diplopia in the horizontal plane [14]; (5) atrophy of the frontal, temporal, and parietal lobes for cortical hypometabolism in the FDG PET scan and neuropsychological deficits (i.e., executive dysfunctions: impaired word fluency; verbal, logical, and visual memory deficits; visuospatial and visuoperceptive impairments) [1, 2]; (6) atrophy of the frontal, temporal, and parietal lobes, degeneration of the locus coeruleus, and occurrence of prosencephalic and brainstem neuronal inclusions (allocortex, insula, cingulate gyrus, basal forebrain nuclei, amygdala, limbic nuclei of the thalamus, ventral tegmental area) for progressive cognitive decline [6, 10]; (7) degeneration of the dorsal motor vagal nucleus and occurrence of neuronal inclusions in ingestion-related brainstem structures (i.e. trigeminal, parvocellular reticular, dorsal motor vagal, hypoglossal, and solitary nuclei, intermediate reticular zone, facial and vagal nerves, solitary tract) for dysphagia [19].

A pathological relationship between the alpha-synuclein pathology of A30P and IPD is also supported (1) by our ultrastructural analyses of LBs in the A30P mutation carrier in comparison to an IPD patient, and (2) by our biochemical findings, which showed insolubility of alpha-synuclein in the A30P patient and in IPD patients. This insolubility reflects a substantial aggregate forming capacity of A30P mutant alpha-synuclein and contrasts with previous in vitro observations on fibril formation of different mutant alpha-synuclein species [7].

In summary, the pathological similarities between the A30P patient and IPD strongly support the view that familial PD caused by the A30P mutation in the *SNCA* gene not only is closely related to IPD clinically, but also pathologically. Although additional postmortem A30P studies are required to ultimately define this neuropathological relationship, our study provides major implications for the validation of transgenic animal models for PD.

### **Acknowledgment**

This study was supported by the Deutsche Forschungsgemeinschaft (RU 1215/1-2, KR2119/3-1) and the Federal Ministry for Education and Research (01GS01834, R.K. and O.R.).

We thank the A30P family for their continued support and interest in this project; P. Davies for the donation of the PHF-1 antibody; M. Babl, B. Meseck-Selchow, M. Bouzrou for processing of tissue sections and immunocytochemistry; M. Löbbecke-Schuhmacher for electron microscopy; and M. Hütten for secretarial assistance.

## References

1. Alexander GE, Crutcher MD, DeLong MR. Basal ganglia-thalamocortical circuits: parallel substrates for motor, oculomotor, "prefrontal" and "limbic" functions. *Prog Brain Res* 1990;85:119-146.
2. Blazquez Alisente JL, Paul Laprediza N, Munoz Cespedes JM. Attention and executive processes in neuropsychological rehabilitation of the visuospatial processes. *Rev Neurol* 2004;38:487-495.
3. Braak H, Braak E. Neuropathological staging of Alzheimer-related changes. *Acta Neuropathol* 1991;82:239-259.
4. Braak H, Rüb U, Del Tredici K. Involvement of precerebellar nuclei in multiple system atrophy. *Neuropathol Appl Neurobiol* 2003;29:60-76.
5. Braak H, Del Tredici K. *Neuroanatomy and pathology of sporadic Parkinson's disease*. Berlin, Heidelberg: Springer, 2009.
6. Braak H, Del Tredici K, Rüb U, de Vos RA, Jansen Steur EN, Braak E. Staging of brain pathology related to sporadic Parkinson's disease. *Acta Neuropathol* 2003; 24:197-211.
7. Conway KA, Harper JD, Lansbury PT. Accelerated in vitro fibril formation by a mutant alpha-synuclein linked to early-onset Parkinson disease. *Nat Med* 1998;4:1318-1320.
8. Duda JE, Giasson BI, Mabon ME, Miller DC, Dolbe LI, Lee VM, Trojanowski JQ. Concurrence of alphasynuclein and tau brain pathology in the Contursi kindred. *Acta Neuropathol* 2002;104:7-11.
9. Gwinn-Hardy K, Mehta ND, Farrer M, Maraganore D, Muentner M, Yen SH, Hardy J, Dickson DW. Distinctive neuropathology revealed by alpha-synuclein antibodies in hereditary parkinsonism and dementia linked to chromosome 4p. *Acta Neuropathol* 2000;99:663-672.
10. Jellinger KA, Mizuno Y. Parkinson's disease. In: Dickson DW, editor. *Neurodegeneration: The molecular pathology of dementia and movement disorders*. Basel: ISN Neuropath Press, 2003. p. 159-187.
11. Kosaka K. Lewy bodies in cerebral cortex, report of three cases. *Acta Neuropathol* 1978;42:127-134.
12. Krüger R, Kuhn W, Leenders KL, Sprengelmeyer R, Müller T, Woitalla D, Portman AT, Maguire RP, Veema L, Schröder U Schöls L, Epplen JT, Riess



- O, Przuntek H. Familial parkinsonism with synuclein pathology: clinical and PET studies of A30P mutation carriers. *Neurology* 2001;56:1355–1362.
13. Krüger R, Kuhn W, Müller T, Woitalla D, Graeber M, Kösel S, Przuntek H, Epplen JT, Schöls L, Riess O. Ala30Pro mutation in the gene encoding alpha-synuclein in Parkinson's disease. *Nat Genet* 1998;18:106–108.
  14. Leigh RJ, Zee DS. The neurology of eye movements, 4th edn. Oxford: Oxford University Press, 2006.
  15. Markopoulou K, Dickson DW, McComb RD, Wszolek ZK, Katechlidou L, Avery L, Stansbury MS, Chase BA. Clinical, neuropathological and genotypic variability in SNCA A53T familial Parkinson's disease: variability in familial Parkinson's disease. *Acta Neuropathol* 2008;116:25–35.
  16. Markopoulou K, Wszolek ZK, Pfeiffer RF. A Greek-American kindred with autosomal dominant, levodopa-responsive parkinsonism and anticipation. *Ann Neurol* 1995;38:373–378.
  17. Petrasch-Parwez A, Nguyen HP, Löbbecke-Schumacher M, Habbes HW, Wiczorek S, Riess O, Andres KH, Dermietzel R, Von Hörsten S. Cellular and subcellular localization of Huntingtin aggregates in the brain of a rat transgenic for Huntington disease. *J Comp Neurol* 2007;501:716–730.
  18. Polymeropoulos MH, Lavedan C, Leroy E, Ide SE, Dehejia A, Dutra A, Pike B, Root H, Rubenstein J, Boyer R, Stenroos ES, Chandrasekharappa S, Athanassiadou A, Papapetropoulos T, Johnson WG, Lazzarini AM, Duvoisin RC, Di Iorio G, Golbe LI, Nussbaum RL. Mutation in the alpha-synuclein gene identified in families with Parkinson's disease. *Science* 1997;276:2045–2047.
  19. Rüb U, Brunt ER, Del Turco D, de Vos RA, Gierga K, Paulson H, Braak H. Guidelines for the pathoanatomical examination of the lower brain stem in ingestive and swallowing disorders and its application to a dysphagic spinocerebellar ataxia type 3 patient. *Neuropathol Appl Neurobiol* 2003;29:1–13.
  20. Rüb U, Bürk K, Schöls L, Brunt ER, de Vos RA, Diaz GO, Gierga K, Ghebremedhin E, Schultz C, Del Turco D, Mittelbronn M, Auburger G, Deller T, Braak H. Damage to the reticulotegmental nucleus of the pons in spinocerebellar ataxia type 1, 2, and 3. *Neurology* 2004;63:1258–1263.
  21. Rüb U, Del Tredici K, Schultz C, Ghebremedhin E, de Vos RA, Jansen Steur E, Braak H. Parkinson's disease: the thalamic components of the limbic loop

- are severely impaired by alpha-synuclein immunopositive inclusion body pathology. *Neurobiol Aging* 2002;23:245–254.
22. Schiesling C, Kieper N, Seidel K, Krüger R. Familial PD-genetics, clinical phenotype and neuropathology in relation to the common sporadic form of the disease. *Neuropathol Appl Neurobiol* 2008;34:255–271.
  23. Thal DR, Rüb U, Orantes M, Braak H. Phases of Abeta-deposition in the human brain and its relevance for the development of AD. *Neurology* 2002;58:1791–1800.
  24. Tofaris GK, Razzaq A, Ghetti B, Lilley KS, Spillantini MG. Ubiquitination of alphasynuclein in Lewy bodies is a pathological event not associated with impairment of proteasome function. *J Biol Chem* 2003;278: 44405–44411.
  25. Wakabayashi K, Hayashi S, Yoshimoto M, Kudo H, Takahashi H. NACP/alphasynuclein-positive filamentous inclusions in astrocytes and oligodendrocytes of Parkinson's disease brains. *Acta Neuropathol* 2000;99:14–20.
  26. Zarranz JJ, Alegre J, Gomez-Estaban JC, Lezcano E, Ros R, Ampuero I, Vidal L, Hoenicka J, Rodriguez O, Atarés B, Llorens V, Gomez Tortosa E, del Ser T, Muñoz DG, de Yebenes JG. The new mutation, E46K, of alpha-synuclein causes Parkinson and Lewy body dementia. *Ann Neurol* 2004;55:164–173.



## Chapter 4

---

# Axonal inclusions in spinocerebellar ataxia type 3

---

Kay Seidel<sup>1,2</sup>, Wilfred FA den Dunnen<sup>1</sup>, Christian Schultz<sup>2,7</sup>, Henry Paulson<sup>3</sup>, Stefanie Frank<sup>2</sup>, Rob de Vos<sup>4</sup>, Ewout R Brunt<sup>5</sup>, Thomas Deller<sup>2</sup>, Harm H Kampinga<sup>6</sup>, Udo Rüb<sup>2</sup>

<sup>1</sup> Department of Pathology and Medical Biology, University Medical Centre Groningen, University of Groningen, Hanzeplein 1, 9713 RB, Groningen, the Netherlands.

<sup>2</sup> Institute of Clinical Neuroanatomy, Dr. Senckenberg Anatomy, J. W. Goethe University, Theodor-Stein-Kai 7, D-60590, Frankfurt/Main, Germany.

<sup>3</sup> Department of Neurology, University of Michigan, 1500 E. Medical Centre Drive, MI4819, Ann Arbor, Michigan, USA.

<sup>4</sup> Laboratorium Pathologie Oost Nederland, Burgemeester Edo Bergsmalaan 1, 7512 AD, Enschede, the Netherlands.

<sup>5</sup> Department of Neurology, University Medical Centre Groningen, University of Groningen, Hanzeplein 1, 9713 RB, Groningen, the Netherlands.

<sup>6</sup> Department of Cell Biology, University of Groningen, Antonius Deusinglaan 1, 9713 AV, Groningen, the Netherlands.

<sup>7</sup> Section of Neuroanatomy, Center for Biomedicine and Medical Technology Mannheim (CBTM), Medical Faculty Mannheim, Ruprecht Karls-University Heidelberg, Ludolf-Krehl-Strasse 13-17, D- 68167, Mannheim, Germany

## **Abstract**

Protein aggregation is a major pathological hallmark of many neurodegenerative diseases including the polyglutamine diseases. Aggregation of the mutated form of the disease protein ataxin-3 into neuronal nuclear inclusions is well described in the polyglutamine disorder spinocerebellar ataxia type 3 (SCA3 or Machado-Joseph disease). In contrast, nothing is known regarding the occurrence of neuropil aggregates in SCA3. Therefore, we performed a systematic immunohistochemical study of serial thick sections through the brains of seven clinically diagnosed and genetically confirmed SCA3 patients. Using antibodies against ataxin-3, p62, ubiquitin, the polyglutamine marker 1C2 as well as the universal aggregation marker TDP-43 we analyzed the neuronal localization, composition and distribution of neuropil aggregates within the brain of these SCA3 patients. The analysis revealed an axonal localization of the neuropil aggregates and their widespread occurrence in fiber tracts of the functional and neurotransmitter systems known to undergo neurodegeneration during SCA3. Similar to neuronal nuclear inclusions, the axonal aggregates were ubiquitinated and immunopositive for the proteasome and autophagy associated shuttle protein p62, indicating an involvement of the neurons' protein quality control system in the occurrence of these aggregates. Rare TDP-43 positive axonal inclusions were also observable. Based on these novel observations we hypothesize that axonal inclusions may be detrimental to axonal transport mechanisms and contribute to the degeneration of nerve cells which occurs in SCA3, due to the good correlation between affected fiber tracts and degenerating neuronal nuclei.

## Introduction

Spinocerebellar ataxia type 3 (SCA3) is an autosomal dominantly inherited progressive neurodegenerative disease. It usually begins in adulthood and is associated with gait, stance, and limb ataxia, dysarthria, dysphagia, oculomotor dysfunction, pyramidal and extrapyramidal signs, peripheral neuropathy, as well as aspiration pneumonia due to dysphagia [1, 9, 27, 33, 39].

Along with dentatorubral-pallidoluysian atrophy, Huntington's disease, spinobulbar muscular atrophy and the spinocerebellar ataxias types 1, 2, 6, 7 and 17, SCA3 belongs to the polyglutamine diseases [21, 25, 27, 40, 45]. These severe neurodegenerative diseases are caused by expanded and meiotically unstable CAG-repeat sequences at disease-specific gene loci encoding elongated polyglutamine sequences in the disease protein [21, 25, 40]. The SCA3 disease gene, *ATXN3*, codes for the disease protein ataxin-3 [20], contains 12-40 CAG-repeats in healthy individuals and approximately 53+ CAG-repeats in affected SCA3 patients and at-risk carriers [27]. Onset and severity of SCA3 correlates with the length of the expanded CAG-repeats [11].

Ataxin-3 is widely expressed in neuronal and non-neuronal tissue [3, 29, 48] and tends to aggregate into neuronal nuclear inclusion bodies (NNIs) in vitro and in vivo when the polyglutamine sequence is expanded. It is well-known that these NNIs of the disease protein are ubiquitinated, contain other proteins, including heat shock proteins (HSPs) and transcription factors [18, 26, 29, 30, 38, 51], are frequently observed in brain tissue of SCA3 patients and are regarded as an important morphological hallmark of neurodegeneration in animal models [5]. However, the exact role of NNIs in neuronal cell death that occurs in SCA3 remains uncertain [24, 52]. Since, however, NNIs are present in degenerated as well as spared brain regions in advanced SCA3, NNIs are not thought to be directly pathogenic in affected nerve cells [35].

Building on our initial findings of uncommon large ataxin-3 immunopositive aggregates in the neuropil of the cell poor pontine reticular brainstem formation of several SCA3 patients, we performed the first systematical study of these neuropil aggregates and report here their axonal localization, composition and brain distribution. The ataxin-3 immunopositive axonal inclusions newly described in the present study are also immunopositive for ubiquitin and p62 (Sequestosome-1, SQSTM-1), but immunonegative for hyperphosphorylated tau and alpha-synuclein.

## Patients and Methods

### *Patients and control individuals*

In the present investigation we studied the brains of seven patients with clinically and genetically diagnosed SCA3 (5 males, 2 females, mean age at death  $58.1 \pm 13.9$  years), along with the brains from two individuals without medical histories of neuropsychiatric diseases (Tab. 1). These two brains were employed as negative controls for the immunohistochemical analyses.

Informed consent was obtained from all patients, in accordance with the medical ethical committee of the University Medical Centre Groningen, the Netherlands, where the autopsies were performed. The ethical board of the Faculty of Medicine at the Johann Wolfgang Goethe University of Frankfurt/Main, Germany, also approved the examination of the brains.

All of the SCA3 patients suffered from gait, stance and limb ataxia, dysarthria, dysphagia and a variety of oculomotor dysfunctions. Genetical diagnosis was carried out in all SCA3 patients by genotyping the DNA extracted from peripheral lymphocytes with polymorphic dinucleotide repeat sequences that flank the specific ataxin-3 gene loci [20, 50]. In the SCA3 patients studied, the length of the normal CAG-repeats varied from 14 to 27, while the pathologically expanded CAG-repeats varied from 62 to 81 (Tab. 1).

| Case          | Age at death (yrs) | Gender | CAG-repeat length | Age at disease onset (yrs) | Disease duration (yrs) |
|---------------|--------------------|--------|-------------------|----------------------------|------------------------|
| SCA3 patients |                    |        |                   |                            |                        |
| 1             | 24                 | M      | 23/81             | 13                         | 11                     |
| 2             | 45                 | M      | 21/69             | 25                         | 20                     |
| 3             | 52                 | M      | 14/69             | 30                         | 22                     |
| 4             | 56                 | M      | 25/74             | 30                         | 26                     |
| 5             | 62                 | F      | 20/73             | 35                         | 27                     |
| 6             | 80                 | F      | 27/65             | 55                         | 25                     |
| 7             | 85                 | M      | 21/62             | 59                         | 26                     |
| Control cases |                    |        |                   |                            |                        |
| 8             | 87                 | M      | n.d.              | -                          | -                      |
| 9             | 74                 | F      | n.d.              | -                          | -                      |

**Table 4.1:** Information on SCA3 patients and healthy controls.

Patient number, age of death (years), gender (F, female; M, male), number of CAG-repeats in the healthy/diseased SCA3 allele, age at onset of initial disease symptoms (years) and duration of disease (years) (n.d. not determined)

### *Brain tissue preparation*

The brains of all SCA3 patients and control individuals were fixed in a 4% phosphate-buffered, aqueous formaldehyde solution (pH 7.4). Thereafter, tissue blocks from the left cerebral hemispheres and brainstems were embedded in polyethylene glycol (PEG



1000, Merck, Darmstadt, Germany) [44] and cut into sets of uninterrupted series of 100  $\mu\text{m}$ -thick frontal sections (cerebral tissue blocks) or 100  $\mu\text{m}$ -thick horizontal sections (brainstem tissue blocks) [8, 32]. Brainstem tissue blocks from case 7 were also embedded in paraffin and cut into 10  $\mu\text{m}$  thick horizontal sections.

In each instance, one set of cerebral and brainstem serial sections was stained with Darrow red for Nissl material and aldehyde-fuchsin for lipofuscin pigment and used for topographical orientation and assessment of neurodegeneration [8].

### *Immunohistochemistry*

For the identification and subcellular localization of neuropil aggregates, we employed the anti-ataxin-3 antibody [29] on select 100  $\mu\text{m}$  cerebral and brainstem sections (see Tab. 2 for a list of the primary antibodies). The primary incubation lasted 20h at room temperature. This was followed by incubation with a secondary, biotin conjugated antibody for 90 minutes at room temperature (1:300). Subsequently, we used the ABC-complex (Vectastain, Vector Laboratories, Burlingame, CA, USA) and 3,3'-diaminobenzidine-tetra-HCl/ $\text{H}_2\text{O}_2$  (DAB, D5637 Sigma, Taufkirchen, Germany) to visualize positive immunoreactions, resulting in a brown staining.

Double immunostaining procedures were employed to examine the intraaxonal localization, topographical distribution and composition of neuropil aggregates. Axonal markers (i.e. the AT270 antibody, directed against the cytoskeletal protein tau; the anti-neurofilament antibody, directed against neuron specific intermediate filaments [15, 43]) were used to ascertain axonal localization of neuropil aggregates. Additional monoclonal antibodies were applied as whole cell markers to identify protein aggregates within neurites of serotonergic (i.e. PH8, directed against tryptophan hydroxylase), as well as dopaminergic or noradrenergic neurons (i.e. MAB 152, directed against tyrosine hydroxylase) [4, 17].

In addition to the polyclonal rabbit anti-ataxin-3 antibody, we employed the monoclonal 1H9 anti-ataxin-3 [48], TDP-43 [47] and the 1C2 polyglutamine antibodies as aggregate markers [49]. The possible association of the axonal aggregates of SCA3 with the proteasomal shuttle protein p62, known to contribute to aggregations in human neurodegenerative diseases, was investigated with an antibody directed against p62 [7, 12, 22, 23, 41, 42]. Axonal and whole cell stainings were visualized with SK4700, aggregation markers with DAB.

For double immunostaining we followed the single staining procedure as described above. After the DAB staining reaction, the slides were rinsed carefully and incubated with an additional primary antibody (axonal or whole cell marker) for 20h at room temperature, followed by incubation with a secondary antibody at room temperature for 90min. This second staining reaction was then visualized with the SK 4700 Kit (Linaris, D-97877 Wertheim, Germany), resulting in a blue-grey staining.

Double immunofluorescent staining was applied to ascertain 1C2 and TDP-43 positivity of axonal aggregates, and to investigate the colocalization of ataxin-3 aggregates with components of the protein quality control and degradation pathways, or with the disease proteins of human tauopathies and synucleinopathies. For this, sections were treated for 10 min with 0.06% sudan-black for quenching of autofluorescence. Subsequently, the sections were incubated with both the monoclonal mouse and polyclonal rabbit primary antibodies for 20h at room temperature, followed by secondary incubation for 90min with Alexa 488, Alexa 568 or Alexa 594 conjugated secondary antibodies (1:1000, Invitrogen, Carlsbad, CA, USA). Both the primary and the secondary antibodies were applied simultaneously. We used the 1C2 antibody to confirm the presence of proteins with an expanded polyglutamine sequence in the axonal aggregates [49]. Ubiquitin [10] and p62 antibodies were employed to investigate a possible colocalization of axonal ataxin-3 aggregates with components of the protein quality control and degradation pathways. The anti-tau AT8 antibody and an anti-alpha-synuclein antibody [6, 14] were used to examine the association of axonal ataxin-3 aggregates with the hyperphosphorylated tau or alpha-synuclein proteins.

Several of the listed antibodies required pre-treatment for antigen retrieval. To unmask hidden epitopes when using the 1H9 antibody, sections were autoclaved in 10 mM citrate buffer (pH 6.0) for 20 minutes. For the anti-neurofilament and anti-p62 antibodies we employed 10 mM citrate buffer (pH 6.0) at 90 °C for 30 minutes. For the anti-alpha-synuclein antibody we used 100% formic acid at room temperature. For the 1C2/neurofilament double immunostaining we employed 3x10 minutes microwaving in tris Buffer (pH 9.0), followed by 3 minutes treatment in 99% formic acid at room temperature. The specificity of the immunolabelling was verified by omission of the primary antibodies which resulted in complete absence of immunopositive structures.

| Detection                          | Clone    | Host species      | Dil.   | Source                                      | Goal                                       |
|------------------------------------|----------|-------------------|--------|---|--|
| Ataxin-3                           | -        | Rabbit polyclonal | 1:750  | Henry Paulson laboratory                    | Aggregate marker                           |
| Ataxin-3, epitope E214-L233        | 1H9      | Mouse monoclonal  | 1:2500 | Chemicon (Millipore), Billerica, MA, USA    | Aggregate marker                           |
| Ubiquitin                          | p4d1     | Mouse monoclonal  | 1:750  | Cell Signaling Technology, Danvers, MA, USA | Aggregate/ proteasomal activity marker     |
| P62                                | Sc-25575 | Rabbit polyclonal | 1:100  | Santa Cruz, Delaware, CA, USA               | Aggregate/ proteasomal activity marker     |
| Polyglutamine stretch              | 1C2      | Mouse monoclonal  | 1:2000 | Chemicon (Millipore), Billerica, MA, USA    | Aggregate marker                           |
| Alpha-synuclein                    | -        | Sheep polyclonal  | 1:2000 | W.P Gai laboratory                          | Aggregate marker                           |
| Hyperphosphorylated tau            | AT8      | Mouse monoclonal  | 1:2000 | Innogenics, Ghent, Belgium                  | Aggregate marker                           |
| Microtubule-associated protein tau | AT270    | Mouse monoclonal  | 1:3000 | Pierce Endogen, Rockford, IL, USA           | Axonal marker                              |
| Neurofilament                      | ab 30309 | Rabbit polyclonal | 1:100  | Abcam, Cambridge, UK                        | Axonal marker                              |
| Tryptophan hydroxylase             | PH8      | Mouse monoclonal  | 1:1000 | Chemicon (Millipore), Billerica, MA, USA    | Serotonergic cell marker                   |
| Tyrosine hydroxylase               | MAB152   | Rabbit polyclonal | 1:2000 | Chemicon (Millipore), Billerica, MA, USA    | Dopaminergic and noradrenergic cell marker |
| TDP-43                             | -        | Rabbit polyclonal | 1:1000 | Georg Auburger laboratory                   | Aggregate marker                           |

**Table 4.2: Information on the primary antibodies.**

Antigen detected by antibody, clone or catalogue designation (omitted with donated antibodies), host species and clone type, working dilution for the antibody, source of the antibody, specific goal of the antibody usage

### *Evaluation of the distribution of axonal aggregates*

The severity of the axonal ataxin-3 pathology was assessed in select tissue sections. If a given tract bore an axonal inclusion at least once in all sections investigated in one patient, the fiber tract's axonal pathology was scored as mild for this patient (score: 1). If it contained single aggregates in the majority of the investigated sections or 3 or more aggregates in a single section of a given patient, axonal pathology was rated as moderate (score: 2). If a tract displayed 3 or more aggregates in more than half of all sections of one patient, axonal pathology was rated as severe (score: 3).

### *Statistics*

SPSS version 16.0 was used for statistical analysis. Bivariate correlations between patient data and morphological findings were evaluated using Spearman's Rho. Two-tailed tests were performed and considered significant at  $p < 0.05$ .

### **Results**

In contrast to the control individuals, the combined application of the tau-antibody AT270 [15], as axonal marker, and the rabbit anti-ataxin-3 antibody [29], as a marker of ataxin-3 protein aggregation, revealed intensively labelled intra-axonal inclusion bodies in all seven SCA3 patients (Fig. 1; Tab. 3).

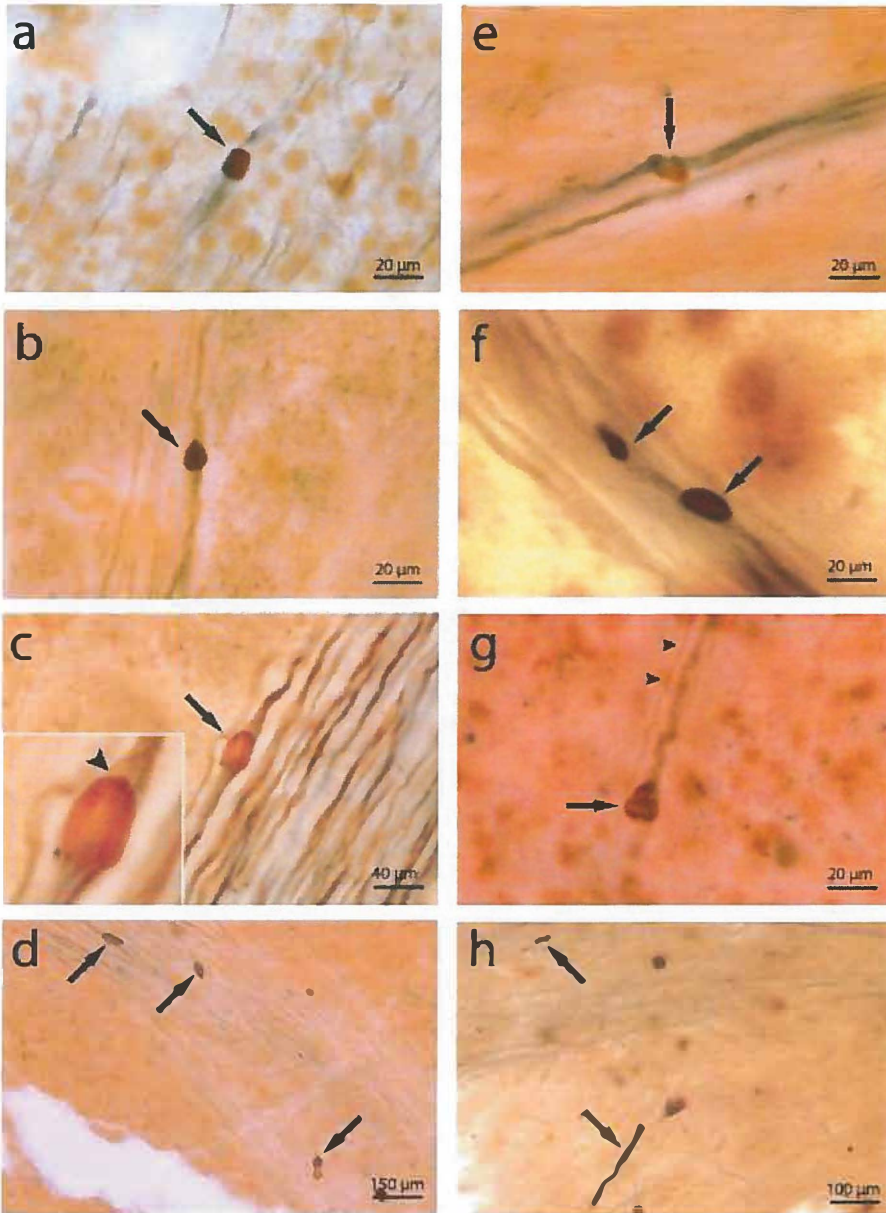


**Figure 4.1: Double immunostainings with anti-ataxin-3 and the axonal marker AT270**

Stainings show axonal aggregates (arrows) in the pyramidal tract (a), oculomotor nerve (b), facial nerve (c, d), hypoglossal nerve (e-g) and nigrostriatal tract (h) of representative SCA3 patients. Axonal aggregates can vary in regards to morphology between ovoid (a-d), elongated (h) or irregular (e, g). Size is also variable, from small (e) to several times the axonal diameter (c, d, g). Note the pallor of the tau staining, indicating axonal dilation (arrowhead) (c), and the comparatively large axonal diameter compared to the unaffected neighbouring axons (arrowheads) (g). Eccentric placement of inclusions in the axon is rarely observable (arrow) (e). (a-h: Anti-ataxin-3 immunostaining with DAB - brown; AT270 stain with SK4700 - blue-grey; 100  $\mu$ m PEG sections)



Except for the external and extreme capsules and the hippocampal alveus, all of the evaluated brain fiber tracts were at least mildly affected by these axonal inclusions (Tab. 3). Among the most severely affected fiber tracts were the medial longitudinal fascicle, and the rubrospinal and nigrostriatal tracts. Additional consistently affected fiber tracts included the cranial nerves (oculomotor, trigeminal, facial, vagal and hypoglossal nerves), the cuneate and gracile fascicles, the lateral lemniscus, the central tegmental tract, the internal arcuate fibers, the dorsal spinocerebellar tract, the lenticular ansa and the inferior thalamic peduncle (Figs 1-6; Tab. 3).

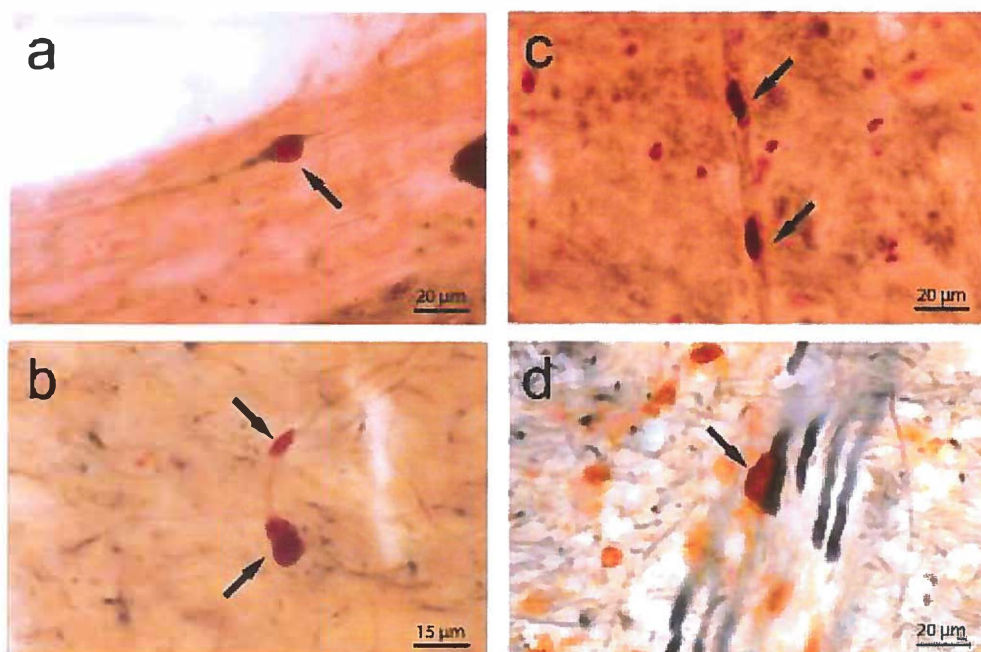


**Figure 4.2: Combined immunostainings with anti-ataxin-3 and anti-tryptophan hydroxylase or anti-tyrosine hydroxylase antibodies**

Stainings depict axonal aggregates (arrows) in serotonergic nerve cells of the caudal raphe nuclei (a, b), dopaminergic nerve cells of the substantia nigra (c) and noradrenergic nerve cells of the locus coeruleus of a typical SCA3 patient (d). Note the ataxin-3 immunopositive aggregate in the axonal hillock of a neuron of the caudal raphe nuclei (arrow) (b). (a, b: Anti-ataxin-3 immunostaining with DAB - brown; PH8 immunostaining with SK4700 - blue-grey; c, d: Anti-ataxin-3 immunostaining with DAB - brown; Anti-TH immunostaining with SK4700 - blue-grey; 100  $\mu$ m PEG sections)

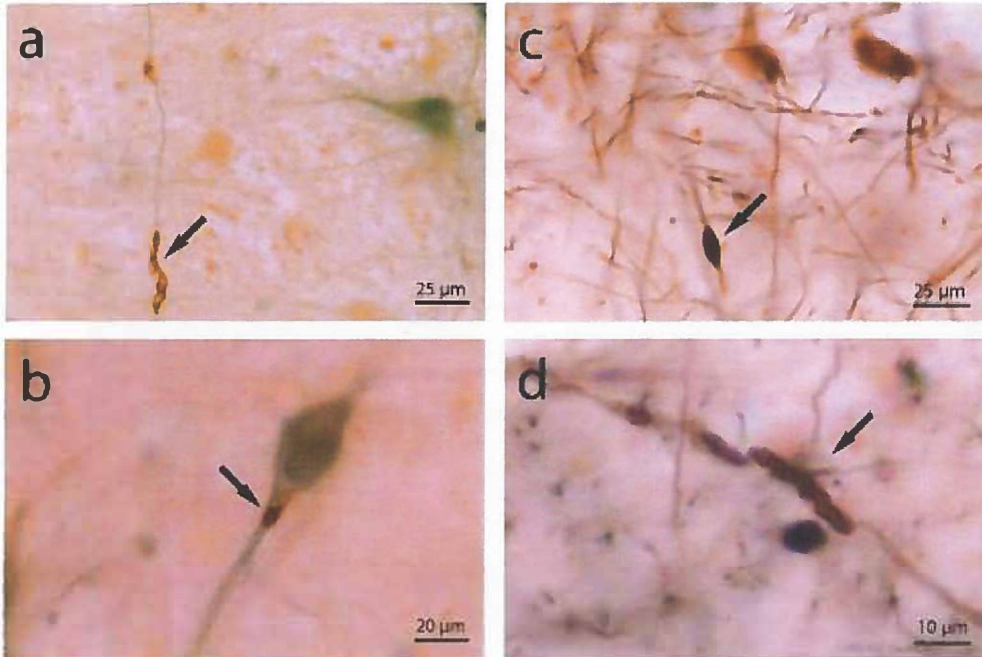


**Figure 4.3 Combined immunostaining with AT270/p62 and AT270/ataxin-3**

p62 immunopositive axonal aggregates (arrows) in the hypoglossal nerve (a) and in neurites within the substantia nigra of a representative SCA3 patient (b). Ataxin-3 immunopositive axonal aggregates (arrows) in the hypoglossal nerve of a typical SCA3 patient (c, d). (a, b: Anti-p62 immunostaining staining with DAB - brown; AT270 staining with SK 4700 - blue-grey; c, d: 1H9 anti-ataxin-3 immunostaining with DAB - brown; Anti-neurofilament immunostaining with SK 4700 - blue-grey; 100 μm PEG sections)

Most axonal aggregates were irregular in shape (Figs. 1e, g), some were ovoid (Figs. 1a-d), or elongated and displayed a neuritic-like shape (Figs. 1f, h). The size of axonal aggregates varied from approximately the diameter of the corresponding axon (Fig. 1b) to a size substantially larger than the normal axonal diameter (Figs. 1c, d, g). These larger aggregates were often accompanied by a comparative thickening of the corresponding axon (Figs. 1c, g). Sometimes thinning of the tau staining within the affected axon, proximal to the aggregations was visible, which indicates a dilation of the axonal structure (Fig. 1c). Ataxin-3 immunopositive axonal aggregates could be observed in all portions of the affected axons (i.e. axon hillock, proximal, middle and distal portions of the axon) (Fig. 2b). Several of the affected axons displayed numerous abnormal aggregates (Figs. 1d, f; 2a, d). Double immunostainings with the 1H9 or anti-p62 antibodies as aggregate markers and the anti-neurofilament or AT270 antibodies as an axonal markers yielded identical staining results (Figs. 3 a-d). A few TDP-43 positive axonal inclusions were also observable (data not shown).



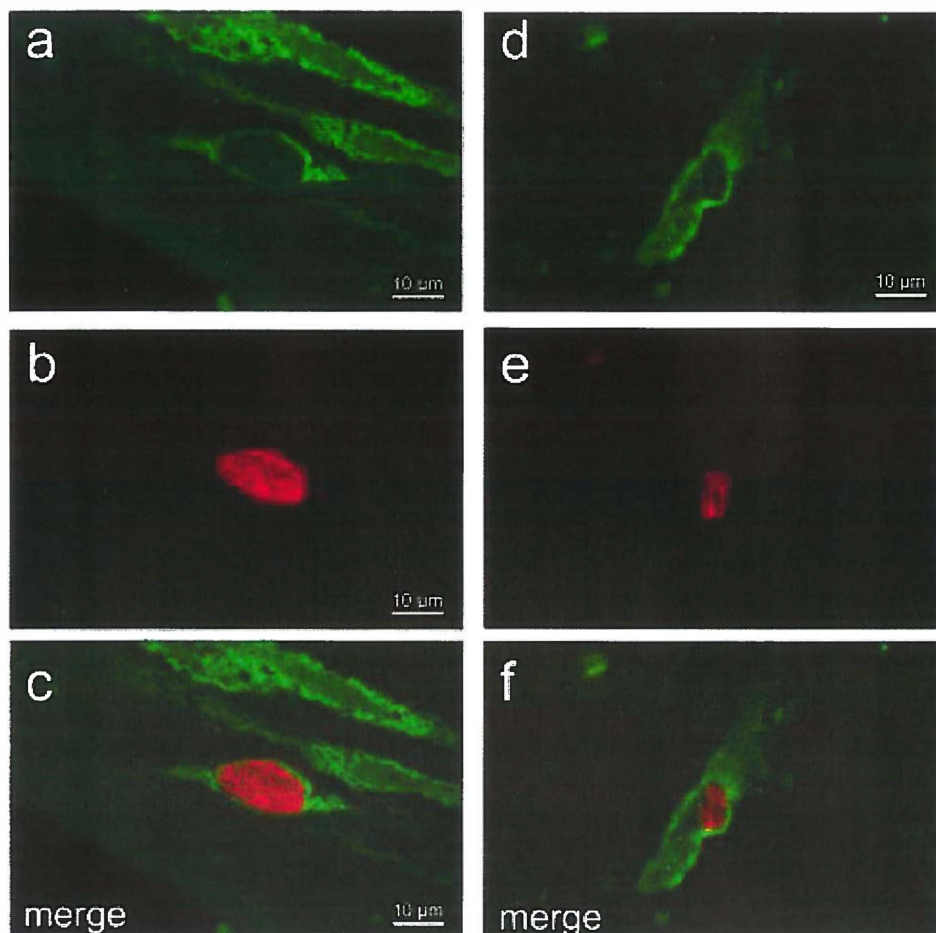


**Figure 4.4: 1C2 and anti-neurofilament double immunofluorescence.**

The oculomotor nerve (a, d) of a representative SCA3 patient shows 1C2 immunopositive aggregates indicating that ataxin-3 with an expanded polyglutamine stretch is a component of these aggregates (b, c, e, f). The low staining intensity of neurofilament indicates that these aggregates occur independently of age related neurofilament aggregation (a, d). (a-f: Anti-neurofilament immunostaining with alexa 488 – green; 1C2 immunostaining with Alexa 594 – red; 10  $\mu$ m paraffin sections).

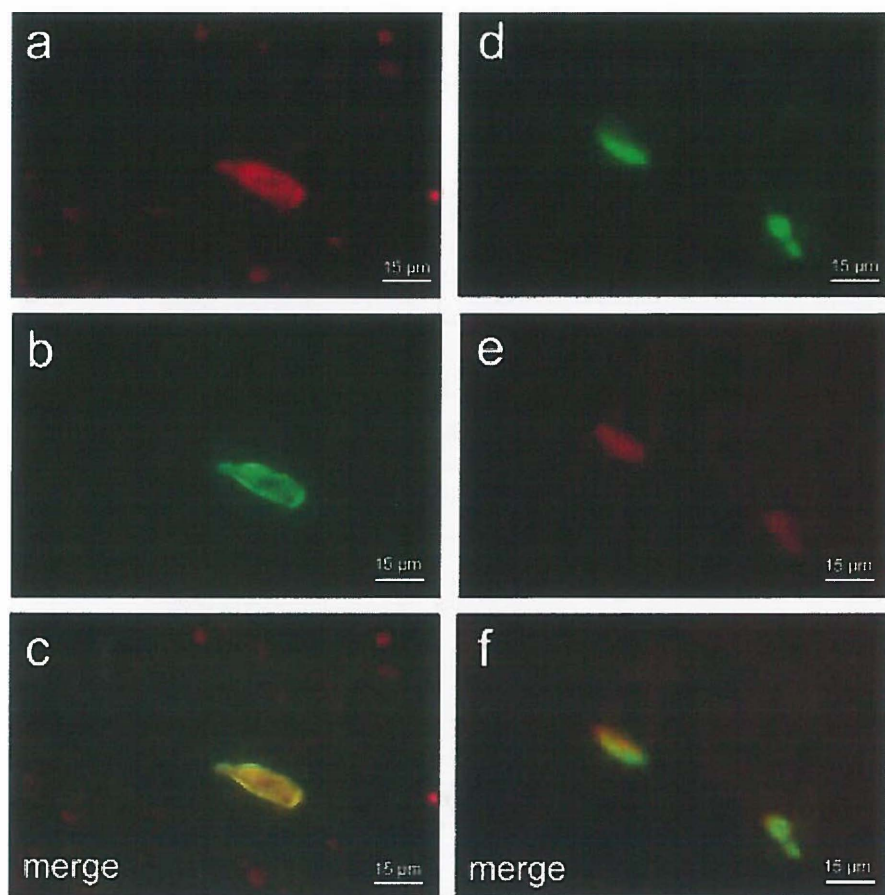


**Figure 4.5: Anti-ataxin-3 and anti-ubiquitin double immunofluorescence.**

Ataxin-3 immunopositive axonal aggregate in the vestibulocochlear nerve of a representative SCA3 patient (a-c). The colocalization of ubiquitin (red) and ataxin-3 (green) indicates polyubiquitination of this axonal aggregate (a-c). Reversed staining pattern of axonal aggregates in the nigrostriatal tract of an additional SCA3 patient (d-f). These aggregates, likewise, show colocalization of ubiquitin (green) and ataxin-3 (red) (d-f). (a-c: Anti-ataxin-3 immunostaining with Alexa 488 - green; Anti-ubiquitin stain with Alexa 568 - red; d-f: Anti-ataxin-3 immunostaining with Alexa 568 - red; Anti-ubiquitin stain with Alexa 488 - green; 100 µm PEG sections)

Combined immunostaining with anti-ataxin-3 antibody and anti-tryptophan hydroxylase PH8 [17] or anti-tyrosine hydroxylase [4] antibodies demonstrated the axonal localization of ataxin-3 immunopositive aggregates in nerve cells of the serotonergic raphe nuclei (Fig. 2a, b), in dopaminergic nigral neurons (Fig. 2c), and in the noradrenergic nerve cells of the locus coeruleus (Fig. 2d). Additional double immunostainings confirmed the presence of expanded polyglutamine stretches in the axonal protein aggregates (Fig. 4), demonstrated their ubiquitination [10] (Fig. 5) and immunopositivity for the shuttle protein p62 [22] (Fig. 3a, b, 6a-f). These staining results were highly similar to those with the anti-ataxin-3/AT270 double staining.

Finally, the axonal inclusions in all of the SCA3 patients were immunonegative for abnormal tau and alpha-synuclein protein aggregations (data not shown), and did not demonstrate significant accumulations of neurofilament (Fig. 4).

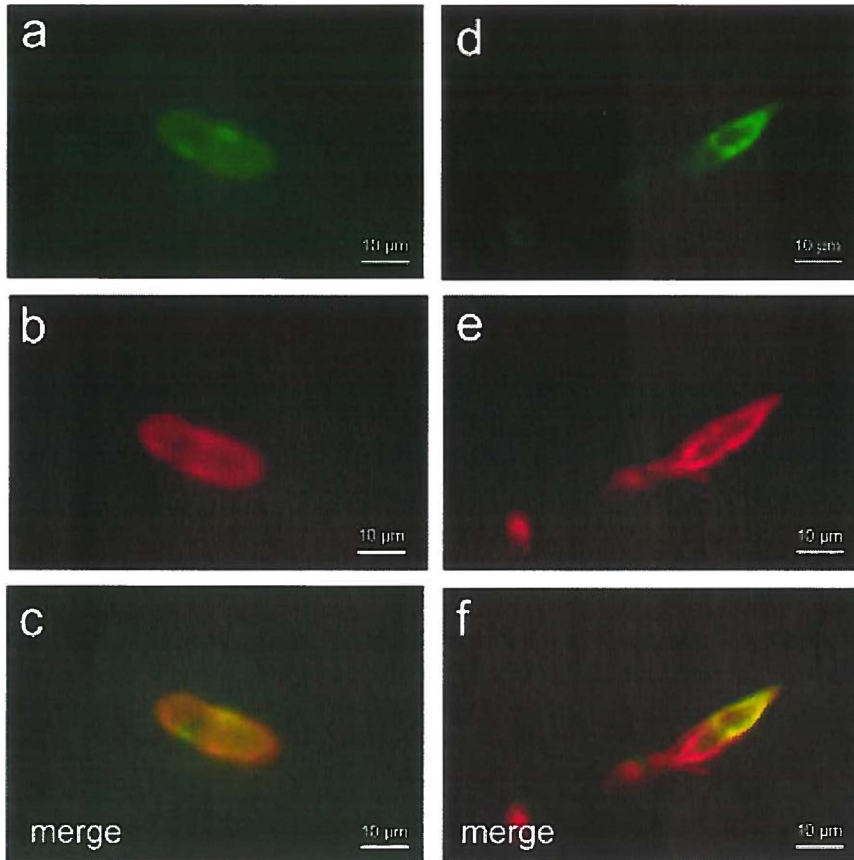


**Figure 4.6 Anti-ataxin-3 and anti-p62 double immunofluorescence.**

Ataxin-3 immunopositive axonal aggregates in the pontocerebellar fibers (a-c) and in nerve cells of the caudal raphe nuclei of a representative SCA3 patient (d-f). The shuttle protein p62 (green) (a, d) is colocalized with ataxin-3 (red) (b, c, e, f) in these axonal aggregates (a-f: Anti-p62 immunostaining with Alexa 488 – green; Anti-ataxin-3 immunostaining with Alexa 568 – red; 100 µm PEG sections)

Statistical analysis revealed a significant negative correlation between the axonal scores of the SCA3 patients and the length of the CAG-repeat in the mutated SCA3 gene (Spearman's Rho -0.793,  $p = 0,033$ ).

| Fiber tract                   | 1         | 2         | 3         | 4         | 5         | 6         | 7         | Axonal scores |
|-------------------------------|-----------|-----------|-----------|-----------|-----------|-----------|-----------|---------------|
| External capsule              | 0         | 0         | 0         | 0         | 0         | 0         | 0         | 0             |
| Extreme capsule               | 0         | 0         | 0         | 0         | 0         | 0         | 0         | 0             |
| Alveus of hippocampus         | 0         | 0         | 0         | 0         | 0         | 0         | 0         | 0             |
| Posterior commissure          | 0         | 0         | 0         | 0         | 0         | 1         | 0         | 1             |
| Optic radiation               | 0         | 0         | 1         | 0         | 0         | 0         | 0         | 1             |
| Acoustic radiation            | 0         | 0         | 1         | 0         | 0         | 0         | 0         | 1             |
| Corpus callosum               | 0         | 0         | 1         | 0         | 0         | 1         | 0         | 2             |
| Mamillothalamic tract         | 0         | 0         | 0         | 0         | 0         | 1         | 1         | 2             |
| Optic tract                   | 1         | 0         | 1         | 0         | 0         | 0         | 0         | 2             |
| Posterior thalamic peduncle   | 0         | 1         | 1         | 0         | 0         | 0         | 0         | 2             |
| Abducens nerve                | 0         | 0         | 1         | 0         | 0         | 1         | 0         | 2             |
| Anterior thalamic peduncle    | 0         | 1         | 0         | 0         | 1         | 0         | 1         | 3             |
| Lateral thalamic peduncle     | 0         | 1         | 1         | 0         | 0         | 1         | 0         | 3             |
| Trochlear nerve               | 0         | 2         | 1         | 0         | 0         | 0         | 1         | 4             |
| Fornix                        | 0         | 0         | 1         | 1         | 1         | 0         | 1         | 4             |
| Lateral vestibulospinal tract | 1         | 0         | 1         | 0         | 0         | 1         | 1         | 4             |
| Inferior cerebellar peduncle  | 0         | 0         | 1         | 0         | 1         | 1         | 1         | 4             |
| Medial cerebellar peduncle    | 1         | 0         | 1         | 1         | 0         | 1         | 1         | 5             |
| Internal capsule              | 0         | 0         | 2         | 1         | 1         | 0         | 1         | 5             |
| Pontocerebellar fibers        | 1         | 0         | 1         | 1         | 0         | 1         | 1         | 5             |
| Medial vestibulospinal tract  | 1         | 1         | 1         | 0         | 0         | 1         | 1         | 5             |
| Trapezoid body                | 1         | 1         | 1         | 1         | 1         | n.d.      | 0         | 5             |
| Acoustic striae               | 1         | 1         | 1         | 1         | 0         | 1         | 0         | 5             |
| Anterior commissure           | 0         | 1         | 1         | 1         | 0         | 1         | 1         | 5             |
| Ventral spinocerebellar tract | 1         | 0         | 1         | 1         | 1         | 1         | 1         | 6             |
| Superior cerebellar peduncle  | 0         | 1         | 1         | 1         | 1         | 1         | 1         | 6             |
| Solitary tract                | 1         | 0         | 1         | 1         | 1         | 1         | 1         | 6             |
| Corticospinal tract           | 0         | 1         | 1         | 1         | 1         | 1         | 1         | 6             |
| Cerebral peduncle             | 1         | 0         | 1         | 2         | 1         | 2         | 0         | 7             |
| Medial lemniscus              | 0         | 1         | 1         | 1         | 1         | 2         | 1         | 7             |
| Ascending tract of Deiters    | 1         | 2         | 1         | 1         | 1         | 0         | 1         | 7             |
| Vestibulocochlear nerve       | 0         | 1         | 1         | 2         | 1         | 1         | 1         | 7             |
| Olivocerebellar fibers        | 1         | 2         | 1         | 1         | 0         | 1         | 1         | 7             |
| Dorsal spinocerebellar tract  | 1         | 1         | 1         | 2         | 1         | 1         | 1         | 8             |
| Inferior thalamic peduncle    | 0         | 2         | 2         | 0         | 1         | 2         | 1         | 8             |
| Oculomotor nerve              | 1         | 0         | 2         | 1         | 0         | 2         | 2         | 8             |
| Internal arcuate fibers       | 0         | 1         | 1         | 1         | 2         | 2         | 2         | 9             |
| Lenticular ansa               | 1         | 1         | 2         | 2         | 1         | 1         | 2         | 10            |
| Cuneate fascicle              | 1         | 1         | 1         | 2         | 2         | 1         | 2         | 10            |
| Central tegmental tract       | 1         | 2         | 2         | 2         | 1         | 1         | 1         | 10            |
| Hypoglossal nerve             | 0         | 0         | 2         | 3         | 1         | 1         | 3         | 10            |
| Lateral lemniscus             | 1         | 1         | 1         | 2         | 1         | 2         | 2         | 10            |
| Vagal nerve                   | 0         | 0         | 3         | 1         | 1         | 3         | 2         | 10            |
| Trigeminal nerve              | 1         | 1         | 2         | 2         | 1         | 1         | 3         | 11            |
| Facial nerve                  | 1         | 1         | 3         | 1         | 1         | 3         | 1         | 11            |
| Gracile fascicle              | 1         | 2         | 1         | 2         | 2         | 1         | 2         | 11            |
| Rubrospinal tract             | 2         | 2         | 2         | 1         | 2         | 1         | 2         | 12            |
| Nigrostriatal tract           | 2         | 3         | 2         | 2         | 1         | 2         | 1         | 13            |
| Medial longitudinal fascicle  | 2         | 2         | 2         | 3         | 2         | 1         | 2         | 14            |
| <b>Axonal scores</b>          | <b>27</b> | <b>37</b> | <b>57</b> | <b>45</b> | <b>33</b> | <b>47</b> | <b>48</b> |               |

**Table 4.3: Distribution and severity of axonal pathology in SCA3 patients.**

Investigated brain fiber tract, rating of axonal ataxin-3 pathology sorted by increasing severity (none: 0; slight: 1-5; marked: 6-10; severe: 11+) indicated by different shades of grey (n.d. not determined)

## Discussion

Aggregation of mutant disease protein is a well known phenomenon in the polyglutamine diseases [21, 26, 40, 45]. In SCA3, mutant ataxin-3 tends to aggregate into NNIs with many affected neurons exhibiting more than one inclusion body, both in and outside of areas affected with neurodegeneration [29, 33, 35, 38]. While the exact role of these aggregates in the pathological mechanisms of SCA3 is still subject to research, they represent an acknowledged pathological hallmark of this disease. NNIs can be recognised by both ataxin-3 specific antibodies as well as the anti-polyglutamine 1C2 antibody, implicating mutant ataxin-3 as the main component of NNI [49]. Furthermore, a variety of additional proteins are found to be associated with NNI (e.g. ubiquitin, p62, heat shock proteins, transcription factors) [18, 26, 29, 30, 38, 51]. Since polyubiquitination is a known prerequisite for proteasomal degradation and the shuttle protein p62 plays a crucial role in cellular pathways handling aberrant protein aggregation (e.g. ubiquitin-proteasome pathway, autophagy), the immunostaining of aggregates with antibodies against ubiquitin and p62 most likely reflects attempts by affected neurons to target the misfolded ataxin-3 into the aforementioned protein degradation pathways [2, 7, 10, 22, 29, 41, 42].

Although many reports have provided detailed analyses of the distribution pattern of NNIs in SCA3 brains, the occurrence of axonal aggregates in SCA3 has remained unreported [29, 35, 38]. In addition to these well described NNIs [28, 29, 38], we were for the first time able to demonstrate intra-axonal aggregations of mutant ataxin-3 protein in SCA3 brain tissue, reminiscent of the neuritic aggregates in Huntington's disease [13]. These novel findings suggest that axonal aggregates represent consistent associated tissue changes of SCA3 present in a large number of brain fiber tracts. SCA3 thus becomes the first spinocerebellar ataxia to be associated with axonal aggregates.

The axonal inclusions detected in the present SCA3 study do not colocalize with and occur independently from neuronal aggregates of other human proteinopathies (e.g. tauopathies, synucleinopathies) and share major biological hallmarks with the long-known NNIs. They can be visualized with antibodies directed against ataxin-3, as well as with the 1C2 polyglutamine antibody, indicating that mutant ataxin-3 with its extended polyglutamine stretch likewise represents a primary component of these axonal aggregates [49]. Ataxin-3/ubiquitin or ataxin-3/p62 double immunoreactions confirmed their similar state of ubiquitination and association with the shuttle protein p62 as has been observed in NNIs, indicating comparable attempts by affected nerve cells to combat intra-axonal aggregation [2, 7, 10, 41]. Only a few axonal inclusions were also TDP-43 immunopositive, indicating that TDP-43 immunopositivity is restricted only to a subset of axonal inclusions. The intra-axonal localization of these axonal aggregates is facilitated by the application of axonal markers (i.e. AT270 and anti-neurofilament antibodies) [15, 43], as well as whole cell markers for serotonergic, dopaminergic and noradrenergic nerve cells (i.e. PH8 and anti-TH antibodies) [4, 17].



Axonal inclusions were present in a large variety of fiber tracts of the SCA3 brains studied, irrespective of the calibre or length of the affected axons. They occurred predominantly in the fiber tracts that belong to the functional and neurotransmitter systems known to undergo neurodegeneration in the progressive neuropathology of SCA3 [9, 19, 31-37]. The affected fiber tracts serve as anatomical interconnections between gray components, which have been shown to be selectively, consistently and severely affected by neurodegeneration (e.g. cerebellar dentate nucleus, primary motor cortex, sensory and motor thalamic nuclei, substantia nigra, precerebellar nuclei, ingestion-related brainstem nuclei, vestibular nuclei, auditory and oculomotor nuclei, somatosensory nuclei) in patients in the advanced clinical stages of SCA3, including several of the patients investigated in the present study [19, 31-37]. In view of the close correlation of the occurrence of intra-axonal aggregates with the consistent demise of nerve cells in the afferent sources and/or efferent targets of these affected fiber tracts it is conceivable that the formation of axonal aggregates, irrespective of their primarily toxic or protective role, is incompatible with and detrimental to normal functions inside these anatomical interconnectivities (e.g. anterograde or retrograde axonal transport processes), thus ultimately impeding the survival of interconnected nerve cells [16] and representing an integral component of and important step in the neurodegenerative process of SCA3. Since it allows several interpretations, the inverse correlation between the axonal pathology and CAG-repeat length unfortunately does not reveal unequivocal answers regarding an immediate detrimental or protective role of the intra-axonal inclusions. Longer CAG-repeats are commonly associated with more severe neurodegeneration [11, 20, 24, 27, 39, 45]. Assuming that intra-axonal aggregates are primarily detrimental to nerve cells, this inverse correlation may be due to a greater fibre loss in more severely affected SCA3 patients [11, 35]. Since protein aggregation might also be primarily protective against soluble and harmful oligomers of the disease proteins [24, 46], the lower frequency of axonal aggregates in more severely diseased SCA3 patients, on the other hand, may reflect a less efficient protein handling in these patients.

In view of the current uncertainties regarding the pathogenic mechanisms of the neurodegenerative process of SCA3 and the possible significance of the newly described intra-axonal aggregates for the demise of affected and interconnected nerve cells, it appears worthwhile to perform additional studies aimed at to test the hypothesis proposed above and to identify the exact pathophysiological causes and consequences of the intra-axonal aggregates in SCA3. These studies should include (1) reconstruction of the spatial and temporal evolution of these axonal aggregates and their relationship to neurodegeneration, (2) investigation of axonal accumulation of cellular organelles and proteins involved in axonal transport mechanisms, (3) systematic investigation of animal models of SCA3 with different disease durations [52], and will contribute to a better understanding of the pathophysiological mechanisms of the neurodegenerative process of SCA3.



**Acknowledgements**

This study was supported by grants from the Deutsche Forschungsgemeinschaft [RU 1215/1-2 to U.R., SCHU 1412/2-1 to C.S.]; the Deutsche Heredo-Ataxie Gesellschaft [DHAG to U.R.]; De Cock-Stichting Groningen [Project number 08-15 to W.d.D.]; the Prinses Beatrix Funds [PBF- WAR05-0129 to H.K. and E.B.]; the ADCA Vereniging Nederland [to U.R. and W.d.D.]; and the National Institutes of Health [NINDS RO1NS38712 to H.P.]. The skillful assistance of M. Babl, B. Meseck-Selchow, M. Bouzrou (processing of tissue sections and immunohistochemistry), J. Vinet (confocal microscopy), M. Hütten (secretary) and I. Szasz (graphics) is gratefully acknowledged. We would like to thank G. Auburger for the donation of the TDP-43 antibody.

## References

1. Abele M, Bürk K, Andres F, Topka H, Laccone F, Bösch S, Brice A, Cancel G, Dichgans J, Klockgether T. Autosomal dominant cerebellar ataxia type I: Nerve conduction and evoked potential studies in families with SCA1, SCA2 and SCA3. *Brain* 1997;120:2141-2148.
2. Arai T, Nonaka T, Hasegawa M, Akiyama H, Yoshida M, Hashizume Y, Tsuchiya K, Oda T, Ikeda K. (2003) Neuronal and glial inclusions in frontotemporal dementia with or without motor neuron disease are immunopositive for p62. *Neurosci Lett* 2003;342:41-44.
3. Berke SJ, Chai Y, Marrs GL, Wen H, Paulson HL. Defining the role of ubiquitin-interacting motifs in the polyglutamine disease protein, ataxin-3. *J Biol Chem* 2005;280:32026-32034.
4. Berod A, Hartman BK, Keller A, Joh TH, Pujol JF. A new double labeling technique using tyrosine hydroxylase and dopamine-beta-hydroxylase immunohistochemistry: evidence for dopaminergic cells lying in the pons of the beef brain. *Brain Res* 1982;240:235-243.
5. Bichelmeier U, Schmidt T, Hübener J, Boy J, Rüttiger L, Häbig K, Poths S, Bonin M, Knipper M, Schmidt WJ, Wilbertz J, Wolburg H, Laccone F, Riess O. Nuclear localization of ataxin-3 is required for the manifestation of symptoms in SCA3: in vivo evidence. *J Neurosci* 2007;27:7418-7428.
6. Biernat J, Mandelkow EM, Schröter C, Lichtenberg-Kraag B, Steiner B, Berling B, Meyer H, Mercken M, Vandermeeren A, Goedert M. The switch of tau protein to an Alzheimer-like state includes the phosphorylation of two serine-proline motifs upstream of the microtubule binding region. *EMBO J* 1992;11:1593-1597.
7. Bjorkoy G, Lamark T, Brech A, Outzen H, Perander M, Overvatn A, Stenmark H, Johansen T. (2005) p62/SQSTM1 forms protein aggregates degraded by autophagy and has a protective effect on huntingtin-induced cell death. *J Cell Biol* 171:602-614.
8. Braak H, Rüb U, Del Tredici K. Involvement of precerebellar nuclei in multiple system atrophy. *Neuropathol Appl Neurobiol* 2003;29:60-76.
9. Bürk K, Fetter M, Abele M, Laccone F, Brice A, Dichgans J, Klockgether T. Autosomal dominant cerebellar ataxia type I: oculomotor abnormalities in families with SCA1, SCA2 and SCA3. *J Neurol* 1999;246:789-797.
10. Ciechanover A. The ubiquitin-proteasome pathway: on protein death and cell life. *EMBO J* 1998;17:7151-7160.

11. Cancel G, Abbas N, Stevanin G, Dürr A, Chneiweiss H, Néri C, Duyckaerts C, Penet C, Cann HM, Agid Y, Brice A. Marked phenotypic heterogeneity associated with expansion of a CAG repeat sequence at the spinocerebellar ataxia 3/Machado-Joseph disease locus. *Am J Hum Genet* 1995;57:809-816.
12. Ciani B, Layfield R, Cavey JR, Sheppard PW, Searle MS. Structure of the ubiquitin-associated domain of p62 (SQSTM1) and implications for mutations that cause Paget's disease of bone. *J Biol Chem* 2003;278:37409-37412.
13. DiFiglia M, Sapp E, Chase CO, Davies SW, Bates GP, Vonsattel JP, Aronin N. Aggregation of huntingtin in neuronal intranuclear inclusions and dystrophic neurites in brain. *Science* 1997;277:1990-1993.
14. Gai WP, Power JHT, Blumbergs PC, Culvenor JG, Jensen PH. Alpha-synuclein immunoprecipitation of glial inclusions from multiple system atrophy brain tissue reveals multiprotein components. *J Neurochem* 1999;73:2093-2100.
15. Goedert M, Jakes R, Crowther RA, Cohen P, Vanmechelen E, Vandermeeren M, Cras P. Epitope mapping of monoclonal antibodies to the paired helical filaments of Alzheimer's disease: identification of phosphorylation sites in tau protein. *Biochem J* 1994;301:871-877.
16. Gunawardena S, Goldstein LSB. Polyglutamine diseases and transport problems: deadly traffic jams on neuronal highways. *Arch Neurol* 2005; 62: 46-51.
17. Haan EA, Jennings IG, Cuello AC, Nakata H, Fujisawa H, Chow CW, Kushinsky R, Brittingham J, Cotton RGH. Identification of serotonergic neurons in human brain by monoclonal antibody binding to all three aromatic amino acid hydroxylases. *Brain Res* 1987;426:19-27.
18. Hayashi M, Kobayashi K, Furuta H. Immunohistochemical study of neuronal intranuclear and cytoplasmic inclusions in Machado-Joseph disease. *Psych Clin Neurosci* 2003;57:205-213.
19. Hoche F, Seidel K, Brunt ER, Auburger G, Schöls L, Bürk K, de Vos RA, den Dunnen W, Bechmann I, Egensperger R, Van Broeckhoven C, Gierga K, Deller T, Rüb U. Involvement of the auditory brainstem system in spinocerebellar ataxia type 2 (SCA2), type 3 (SCA3) and type 7 (SCA7). *Neuropathol Appl Neurobiol* 2008;34:479-491.
20. Kawaguchi Y, Okamoto T, Taniwaki, Aizawa M, Inoue M, Katayama S, Kawakami H, Nakamura S, Nishimura M, Akiguchi I, Kimura J, Narumiya S,

- Kakizuka. CAG expansions in a novel gene for Machado-Joseph disease at chromosome 14q32.1. *Nat Genet* 1994;8:221-228.
21. Klockgether T (2003) Ataxias. In: CG Goetz (ed) Textbook of clinical neurology, 2nd edn. Saunders, Philadelphia, pp 741-757.
  22. Kuusisto E, Kauppinen T, Alafuzoff I. Use of p62/SQSTM antibodies for neuropathological diagnosis. *Neuropathol Appl Neurobiol* 2008;34:169-180.
  23. Kuusisto E, Salminen A, Alafuzoff I. Ubiquitin-binding protein p62 is present in neuronal and glial inclusions in human tauopathies and synucleinopathies. *Neuroreport* 2003;12:2085-2090.
  24. Michalik A, van Broeckhoven C. Pathogenesis of polyglutamine disorders: aggregation revisited. *Hum Mol Genet* 2003;12:173-186.
  25. Orr HT, Zoghbi HY. Trinucleotide repeat disorders. *Annu Rev Neurosci* 2007;30:575-621.
  26. Paulson H. Protein fate in neurodegenerative proteinopathies: Polyglutamine diseases join the (mis)fold. *Am J Hum Genet* 1999;64:339-345.
  27. Paulson HL. Dominantly inherited ataxias: lessons learned from Machado-Joseph disease/spinocerebellar ataxia type 3. *Semin Neurol* 2007;27:133-142.
  28. Paulson H, Das S, Crino P, Perez MK, Patel SC, Gotsdiner D, Fischbeck KH, Pittman RN. Machado-Joseph disease gene product is a cytoplasmic protein widely expressed in brain. *Ann Neurol* 1997;4:453-462.
  29. Paulson H, Perez M, Trottier Y, Trojanowski JQ, Subramony SH, Das SS, Vig P, Mandel JL, Fischbeck KH, Pittman RN. Intranuclear inclusions of expanded polyglutamine protein in spinocerebellar ataxia type 3. *Neuron* 1997;19:333-344.
  30. Perez M, Paulson H, Pendse S, Salonz S, Bonini N, Pittman R. Recruitment and the role of nuclear localization in polyglutamine-mediated aggregation. *J Cell Biol* 1998;143:1457-1470.
  31. Rüb U, Brunt ER, Deller T. New insights into the pathoanatomy of spinocerebellar ataxia type 3 (Machado-Joseph disease). *Curr Opin Neurol* 2008;21:111-116.
  32. Rüb U, Brunt E, Del Turco D, de Vos RAI, Gierga K, Paulson H, Braak H. (2003) Guidelines for the pathoanatomical examination of the lower brain stem in ingestive and swallowing disorders and its application to a dysphagic

- spinocerebellar ataxia type 3 patient. *Neuropathol Appl Neurobiol* 2003;29:1-13.
33. Rüb U, Brunt ER, Petrasch-Parwez E, Schöls L, Theegarten D, Auburger G, Seidel K, Schultz C, Gierga K, Paulson H, van Broeckhoven C, Deller T, de Vos RA. Degeneration of ingestion-related brainstem nuclei in spinocerebellar ataxia type 2, 3, 6 and 7. *Neuropathol Appl Neurobiol* 2006;32:635-649.
  34. Rüb U, Brunt ER, de Vos RA, del Turco D, del Tredici K, Gierga K, Schultz C, Ghebremedhin E, Bürk K, Auburger G, Braak H. Degeneration of the central vestibular system in spinocerebellar ataxia type 3 (SCA3) patients and its possible clinical significance. *Neuropathol Appl Neurobiol* 2004;30:402-414.
  35. Rüb U, de Vos RA, Brunt ER, Sebesteny T, Schöls L, Auburger G, Bohl J, Ghebremedhin E, Gierga K, Seidel K, den Dunnen W, Heinsen H, Paulson H, Deller T. Spinocerebellar ataxia type 3 (SCA3): thalamic neurodegeneration occurs independently from thalamic ataxin-3 immunopositive neuronal intranuclear inclusions. *Brain Pathol* 2006;16:218-227.
  36. Rüb U, Gierga K, Brunt ER, de Vos RA, Bauer M, Schöls L, Bürk K, Auburger G, Bohl J, Schultz C, Vuksic M, Burbach GJ, Braak H, Deller T. Spinocerebellar ataxias types 2 and 3: degeneration of the pre-cerebellar nuclei isolates the three phylogenetically defined regions of the cerebellum. *J Neural Transm* 2005;112:1523-1545.
  37. Rüb U, Seidel K, Özerden I, Gierga K, Brunt ER, Schöls L, de Vos RA, den Dunnen W, Schultz C, Auburger G, Deller T. Consistent affection of the central somatosensory system in spinocerebellar ataxia type 2 and type 3 and its significance for clinical symptoms and rehabilitative therapy. *Brain Res Rev* 2007;53:235-249.
  38. Schmidt T, Landwehrmeyer GB, Schmitt I, Trottier Y, Auburger G, Laccone F, Klockgether T, Völpel M, Epplen JT, Schöls L, Riess O. An isoform of ataxin-3 accumulates in the nucleus of neuronal cells in affected brain regions of SCA3 patients. *Brain Pathol* 1998;8:669-679.
  39. Schöls L, Amoiridis G, Büttner T, Przuntek H, Epplen J, Riess O. Autosomal dominant cerebellar ataxia: phenotypic differences in genetically defined subtypes. *Ann Neurol* 1997;42:924-932.
  40. Schöls L, Bauer P, Schmidt T, Schulte T, Riess O. Autosomal dominant cerebellar ataxias: clinical features, genetics and pathogenesis. *Neurology* 2004;3:291-304.

41. Seibenheimer ML, Babu JR, Geetha T, Wong HC, Krishna NR, Wooten MW. Sequestosome 1/p62 is a polyubiquitin chain binding protein involved in ubiquitin proteasome degradation. *Mol Cell Biol* 2004;24:8055-8068.
42. Seidel K, Brunt ERP, de Vos RAI, Dijk F, van der Want HJL, Kampinga HH, Rüb U and den Dunnen WFA. The p62 antibody reveals cytoplasmic protein aggregates in spinocerebellar ataxia type 6 (SCA6). *Clin Neuropath* 2009;28:344-349.
43. Shaw G, Osborn M, Weber K. An immunofluorescence microscopical study of the neurofilament triplet proteins, vimentin and glial fibrillary acidic protein within the adult rat brain. *Eur J Cell Biol* 1981;26:68-82.
44. Smithson KG, MacVicar BA, Hatton GI. Polyethylene glycol embedding: a technique compatible with immunocytochemistry, enzyme histochemistry, histofluorescence and intracellular staining. *J Neurosci Methods* 1993;7:27-41.
45. Soong BW, Paulson HL. Spinocerebellar ataxias: an update. *Curr Opin Neurol* 2007; 20:438-446.
46. Takahashi T, Kikuchi S, Katada S, Nagai Y, Nishizawa M, Onodera O. Soluble polyglutamine oligomers formed prior to inclusion body formation are cytotoxic. *Hum Mol Genet* 2008;17:345-356.
47. Tan CF, Yamada M, Toyoshima Y, Yokoseki A, miki Y, Hoshi Y, Kaneko H, Ikeuchi T, Onodera O, Kakita A, Takahashi H. Selective occurrence of TDP-43-immunoreactive inclusions in the lower motor neurons in Machado-Joseph disease. *Acta Neuropathol* 2009;118:553-560.
48. Trottier Y, Cancel G, An-Gourfinkel I, Lutz Y, Weber C, Brice A, Hirsch A, Mandel JL. Heterogeneous intranuclear localization and expression of ataxin-3. *Neurobiol Disease* 1998;5:335-347.
49. Trottier Y, Lutz Y, Stevanin G, Imbert G, Devys D, Cancel G, Saudou F, Weber C, David G, Tora L, Agid Y, Brice A, Mandel JL. Polyglutamine expansion as a pathological epitope in Huntington's disease and four dominant cerebellar ataxias. *Nature* 1995;378:403-406.
50. Verschuuren-Bemelmans CC, Brunt ER, Burton M, Mensink RG, van der Meulen MA, Smit NH. Refinement by linkage analysis in two large families of the candidate region of the third locus (SCA3) for autosomal dominant cerebellar ataxia type I. *Hum Genet* 1995;96:691-694.

51. Yamada M, Hayashi S, Tsuji S, Takahashi H. Involvement of the cerebral cortex and autonomic ganglia in Machado Joseph disease. *Acta Neuropathol* 2001;101:140-144.
52. Yamada M, Sato T, Tsuji S, Takahashi H. CAG repeat disorder models and human neuropathology: similarities and differences. *Acta Neuropathol* 2008;115:71-86.



## **Chapter 5**

---

### **Introduction:**

### **The protein quality control system**

---

## Contents

---

|              |  |            |
|--------------|--|------------|
| <b>5.1</b>   | <b>The protein quality control system</b>  | <b>97</b>  |
| <b>5.2</b>   | <b>The chaperones</b>  | <b>97</b>  |
| <b>5.3</b>   | <b>Protein degradation pathways</b>  | <b>101</b> |
| <b>5.3.1</b> | Protein degradation pathways: the proteasome   | 101        |
| <b>5.3.2</b> | Protein degradation pathways: Autophagy  | 103        |
| <b>5.4</b>   | <b>Inclusion formation</b>   | <b>105</b> |
| <b>5.5</b>   | <b>Aim of the studies, Part 2 (Protein aggregation and the protein quality control pathways in the neurodegenerative diseases)</b> | <b>106</b> |

## 1.1 Protein quality control systems

As the protein aggregation observed in several neurodegenerative diseases indicates, protein misfolding can pose a significant threat to cell survival. However the misfolding of proteins does not only occur under pathological conditions. Proteins are produced in an unfolded manner, and many require assistance to assume their final conformations [22]. Furthermore, transient chemical or heat stress may cause protein aggregation without an underlying disease. In these cases, the cellular protein quality control (PQC) system can act upon these conditions, and can either assist proteins in (re)assuming their correct conformation or target them towards degradation [22, 30].

At large, 3 levels in PQC exist: a) refolding, b) proteasomal degradation, c) autophagic degradation. Whereas refolding and proteasomal degradation requires soluble substrates, autophagic degradation can occur for both soluble and insoluble, aggregated proteins. Molecular chaperone proteins of the HSP protein families have been primarily implied in maintaining proteins in a non-aggregated, soluble state to facilitate their refolding or their proteasomal degradation [27, 30, 46]. Chaperones have also been implied to play a role in the so-called chaperone-mediated autophagic route [10], but may also play supporting roles in micro- and macro-autophagy [47]. Finally, if aggregating protein cannot be channeled into the above pathways, aggregated proteins can be stored in inclusions at various positions in the cells, how this storage is regulated and whether or not also this is assisted by chaperones/HSP is yet unclear.

## 1.2. The Chaperones

Molecular chaperones, of which heat shock proteins (HSPs) families form the largest, group, are defined by their ability to transiently interact with a given protein without modifying it on a biochemical level, hereby preventing their aggregation and either facilitating its folding or, if not feasible, assisting its degradation [22, 27, 30]. Chaperones usually work in complexes with cofactors and also in concert with each other. For this project, the small HSPs (HspBs) as well as the Hsp 70 (HspA) groups of molecular chaperones are of interest, as well as the DnaJ and the Bag families of co-chaperones [46].

### *Hsp70/HspA family*

The Hsp70 group of HSPs is one of the most conserved proteins of the proteome. There is a 50% sequence homology between the prokaryotic DnaK and their homologues from the eukaryotic Hsp70 group of proteins [13, 46]. In human, the Hsp70 family contains several proteins with a high sequence homology, some of which are constitutively expressed in differing tissues (HSPA1L, HSPA2, HSPA8), some of which are functional homologues in different intracellular compartments (HSPA8 (cytoplasmic/nuclear), HSPA5 (ER), HSPA9 (Mitochondria), while others are mainly expressed as a response to certain forms of stress (HSPA1A, HSPA1B, HSPA6) [13].

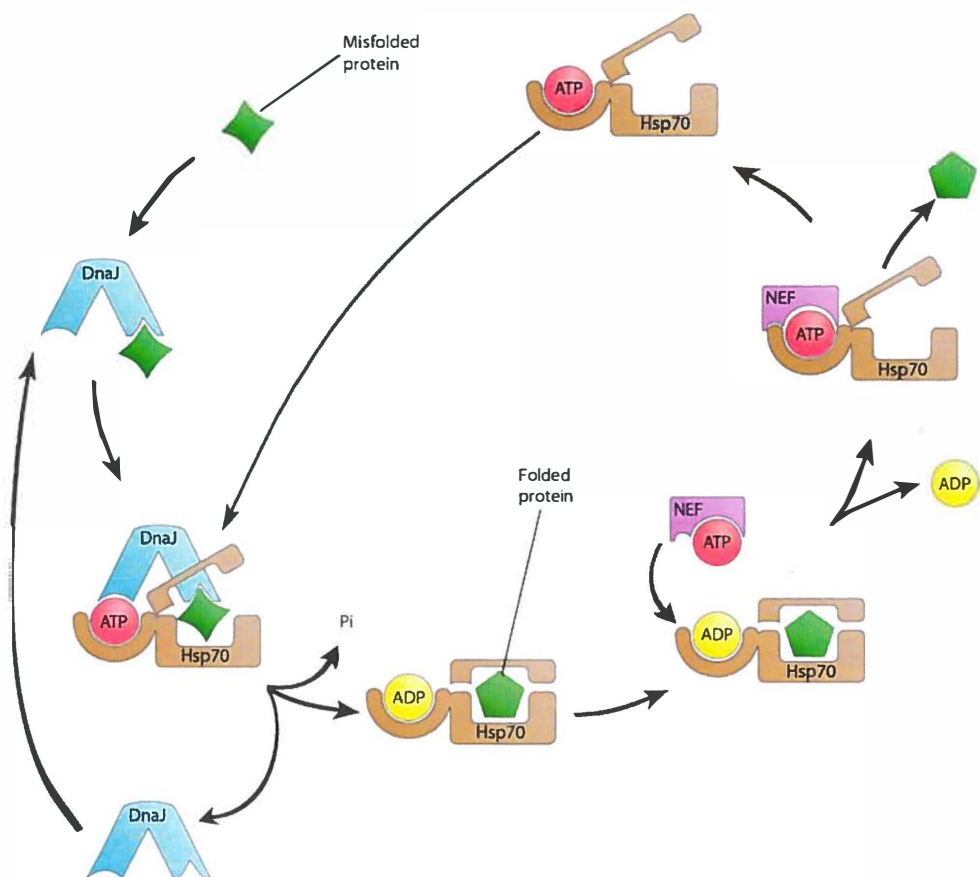


**Figure 5.1: Successful folding of a target protein by the DnaJB1 and HSP70 machinery**

Misfolded proteins (green) are recognized by DnaJ proteins (blue). The protein/DnaJ complex associates with an HSPA protein (brown), the target protein is transferred to the Hsp70 protein, and its ATPase activity is stimulated by the DnaJ protein. The ADP-loaded Hsp70 has a higher affinity for the target which then can refold into its native conformation during the association. After a given period, a nuclear exchange factor (purple) exchanges the bound ADP for an ATP-molecule, whereupon the affinity for the target protein decreases, and it is released into the cytoplasm.

(Adapted from Kampinga & Craig, Nature Reviews, 2010)

Furthermore, all Hsp70 members have a low level ATPase activity. Hsp70 proteins are thought to be fairly unspecific in their capacity to bind clients, specificity is conferred by its co-factors, usually in the form of DnaJ proteins [27, 38] (see below). Upon transferring a client to Hsp70, the co-factor together with the client stimulate hydrolysis of the Hsp70-bound ATP to ADP+P, upon which the co-factor disassociates, while the affinity of the client to the Hsp70 chaperone is increased. After a given time, nucleotide exchange factors facilitate the exchange of the bound ADP for ATP which reduces the clients' affinity to the chaperone, effectively releasing it (Fig.

5.1) [12, 27]. To insure sufficient time for the association between Hsp70 protein and client, the nuclear exchange factors are present at sub-stoichiometric levels [16].

Several Hsp70 family members have been found to be up-regulated in and associated with inclusions in neurodegenerative diseases. In some experimental disease models, overexpression of Hsp70 members indeed reduced disease-related toxicity. Yet, especially suggested on the basis of mouse models in which Hsp70 overexpression alone only marginally reduced disease symptoms [40], Hsp70 may rather be a marker of disease than a good target for therapy.

#### *Hsp40/DnaJ family*

The DnaJ family of proteins, including members like Hsp40 (DnaJB1), is a diverse family of co-chaperones. While initially thought to be clustered around 40kDA, the group displays a large variety in regard to molecular weight and structure [27]. The unifying feature of this group is the J-domain, which is necessary for the association with chaperones from the HSPA group [49]. In this crucial interaction, the DnaJ proteins confer the binding of the client protein to the Hsp70 protein, thus providing the Hsp70 machinery with specificity (Fig. 5.1) [27, 49]. The DnaJ family is subdivided into 3 subfamilies, according to the domain structure of the respective proteins. There is, however, large functional overlap between the different families [20].

Due to their variability, DnaJ proteins can associate with a broad number of clients, which are then targeted to the Hsp70 machinery. The highly conserved J domain facilitates the association with a Hsp70 chaperone and consecutively increases its capacity for hydrolysis of ATP [9, 24, 27]. Apart from this important role in the protein quality control, DnaJ proteins can also interact with fully folded and functional proteins, often involving the remodeling of mature protein complexes, some of which do not require interaction with the HSPA machinery [27].

DnaJ proteins, especially DNAJB1, have also been found in inclusions of patients with neurodegenerative diseases and in many cellular and simple animal models systems, overexpression of DNAJB1 or some other DNAJB members were found to protect against disease [20, 21, 40]. However, to our knowledge, no mouse data are available to date that show that such protective effects are also true in mammals.

#### *Small heat shock proteins/ HspB family*

The human HspB group of small heat shock proteins includes 10 members characterized by the presence of a conserved crystallin sequence [46]. For the rest, the HspB proteins are very diverse. Some exist in cells as higher molecular weight multimers that are highly dynamic and are thought to be storage structures, which dissociate into the active dimers upon stress [43]. Some HspB proteins can form hetero-oligomers [5]. Furthermore, several members of the HspB family can be phosphorylated at specific sites, a mechanism which is thought to be important for

regulating their chaperoning capacity, substrate specificity and for oligomeric redistribution [1, 4, 46].

The dimers are considered to be the active forms of most HspB proteins, which can bind to a variety of substrates. The association with the HspB protein then prevents the aggregation of aggregation-prone proteins. As far as studied, HspB proteins were shown to be ATP independent chaperones: they can bind clients and prevent their aggregation without ATP being needed. For assisted folding, they however require cofactors or other chaperones, like the HSPA family, to dissociate the substrate (e.g. HspB1) [23, 46]. Here, the bound substrate may be targeted towards degradation if refolding is not possible. In fact, several small HspB proteins have been often associated with protein degradation. Aside from the binding of misfolded protein, HspB members have been shown to be important for the stabilization of the cytoskeleton and -related to this- several HspB members are highly expressed in smooth muscle and cardiac tissues and play important function in muscle development [46].

In this thesis, we will spend specific attention to HSPB8. This HspB member has some special, uncommon features that may make it highly relevant to neurodegenerative diseases. Firstly, in cells it does not primarily exist as oligomers but rather associates in a 2:1 ratio with the Hsp70 co-chaperone Bag3 (see also below). HSPB8 depends on BAG3 for its stability, and as a complex HSPB8-BAG3 plays a role in clearance of protein aggregates via autophagy (see also chapter 8) [6].

#### *BAG family of co-chaperones*

The BAG (Bcl2 associated athanogene) family is a variable family of Hsp70 co-chaperones [26]. The unifying feature is the presence of a BAG domain, which confers binding to Hsp70 proteins. Through this domain, BAG proteins can act as nucleotide exchange factors and facilitate the nucleotide exchange of ADP to ATP, which releases the client of the HspA protein (Fig 5.1) [17]. By modulation of this step, the BAG proteins have been suggested to control the activity of Hsp70 proteins and target clients into different pathways. An example of this is BAG1, which aside from the BAG domain, contains an ubiquitin like domain through which it interacts with the proteasome. As such, in a yet to be clarified mechanism BAG1 may form a bridge between Hsp70s and the proteasome and assist in protein degradation [15, 18, 36].

Intriguingly, recent data suggest that several BAG proteins may also interact with several HspB members [5, 6] (Zijlstra and Kampinga, unpublished observations). As stated above, especially the interaction between BAG3 and HSPB8 is worthwhile mentioning here; this complex acts as a global regulator of autophagy [5] and can transfer the substrates for degradation into the autophagosomal protein pathway [6].

### **1.3. Protein degradation pathways**

If refolding of proteins is not possible, misfolded proteins can be directed to the cell's protein degradation machinery, using the same principles as for ongoing turnover of proteins, which are degraded into smaller peptides and amino acids, which then again can be reused by the cellular protein assembly machinery [33]. The two most important degradation pathways are the proteasomal and the autophagosomal pathway.

#### *1.3.1 The proteasomal pathway*

The proteasome is a complex machine consisting of several subunits, in which target proteins are degraded. Indiscriminate digestion however does not take place, as the target proteins are marked specifically [19].

If a protein is to be targeted for degradation by the proteasome, it is tagged with a polyubiquitin flag [8]. Ubiquitin is an evolutionary highly conserved polypeptide of 8 kDa, which is ubiquitously expressed. Through an enzymatically mediated covalent bond to a lysine residue, it can associate with target proteins. Ubiquitin can also be ubiquitinated in seven different positions itself, which enables the formation of polyubiquitin flags in different conformations. (Poly)ubiquitination is mediated by a specific enzyme cascade. The final enzyme in the cascade, the E3 ubiquitin ligase, recognizes the target protein and transfers the ubiquitin onto the target in an enzyme specific manner. A large number of different E3 ligases with different client preferences exist, each conferring different types of polyubiquitin flags that enable the high specificity of this system. Proteins tagged with at least 4 Ubiquitin molecules connected at the K48 residue, are targeted towards degradation by the proteasome. However, not all flags target the protein for degradation. Depending on the conformation of the flag, a given target protein can be modified in its activity or shuttled to different cell compartments [19, 45].



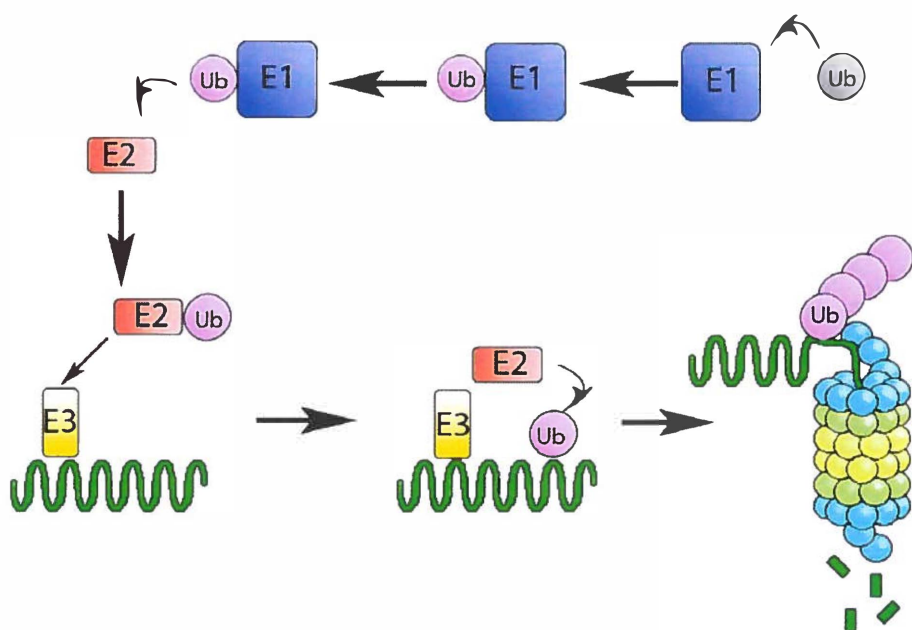


**Figure 5.2: Proteasomal protein degradation**

Depiction of the proteasomal activation pathway. Ubiquitin is activated by an E1 ligase in an ATP dependent manner, is transferred to an E2 ligase which then associates with an E3 ligase at the target protein. The Ubiquitin is then transferred to the target, to build up a polyubiquitin chain of at least 4 K48 linked ubiquitin molecules. The protein is then transferred to the 19S regulatory particle, where it is deubiquitinated and unfolded. It enters the 20S proteasomal particle, where it is degraded into polypeptides.

The proteasome is a macromolecule of approximately 2 mDa consisting of several subunits. It is highly conserved in its function and present in pro- and eukaryotes, and is present in the nucleus as well as in the cytoplasm. Structurally, the proteasome consists of a 20S central unit with a barrel-like structure around a central pore, as well as 1 or 2 19S regulatory units above and below the central barrel structure. The 20S unit consists of 4 ring-like structures of 7 subunits stacked on top of each other. The outer rings are made up of 7 alpha subunits (alpha1-alpha7 in mammals) and are important for transporting the target protein to the catalytic core. The catalytic core consists of the 2 inner rings, which each contain 7 beta subunits (beta1-7 in mammals, although additional beta subunits can be produced under different conditions). The 19S regulatory units consist of 19 subunits. They associate with the proteasome and are responsible for the correct identification and refolding of client proteins compartments (Fig. 5.2) [19, 45].

Ubiquitinated client proteins are recognized by the 19S unit. The protein is then deubiquitinated and unfolded in an ATP dependent manner. Unfolding of the protein is required to enter the 20S unit. The client is then transferred through the alpha-ring into the catalytic core, where it is degraded into peptide fragments between 4-25 amino acid residues. Residues of 7-9 are most common. Once the client is completely degraded, the peptides are released (Fig. 5.2) [19].

The proteasome is responsible for a large portion of the turnover of endogenous proteins, and as such, is a crucial factor to cellular protein homeostasis. However there is mounting evidence that the performance of the proteasome decreases with age [7, 18]. Also, in protein aggregate diseases, the function of the proteasome may either be impaired, or overwhelmed, both posing a threat to cellular protein homeostasis [14].

An efficient way of recognizing proteasomal stress is the study of quickly degraded client proteins. UBB<sup>+</sup> is a frameshift mutant of ubiquitin, which occurs during translation regularly. Under normal conditions, UBB<sup>+</sup> is quickly flagged and degraded by the proteasome and thus remains undetectable by normal immunohistochemical ways. If the proteasome is overwhelmed, the degradation of UBB<sup>+</sup> takes longer, and the protein becomes detectable (see also chapters 7 and 8) [43].

### *1.3.2. The autophagosomal pathway*

Autophagy is an alternate pathway of protein degradation. Used primarily for larger structures up to the size of cellular organelles, this pathway encloses the targets by a plasma double membrane which then fuses with the lysosome to degrade the contents of this structure into smaller peptides and aminoacids [31]. It was first described as part of the lysosomal pathway, a mechanism primarily reserved for the degradation of extracellular material. Autophagy was proven to be involved in manifold functions, such as intracellular protein homeostasis, mass remodeling, immunity reactions and cell division [11, 33, 34].

There are several forms of autophagy, the most common of which is macroautophagy. At the beginning of the macroautophagic pathway, a bulk of cellular material is enclosed within a double plasma membrane. During the process of enclosure, the membranous structure is referred to as phagophore, after the uptake of material and closing of the organelle it is referred to as an autophagosome. To degrade the enclosed mass, the autophagosome fuses with a lysosome into the autolysosome. The acid hydrolyases, originally contained in the lysosome, then enable the degradation of protein contained within the autolysosome. The products of this degradation process are then released into the cellular lumen via permeases (Fig. 5.3) [28, 51].

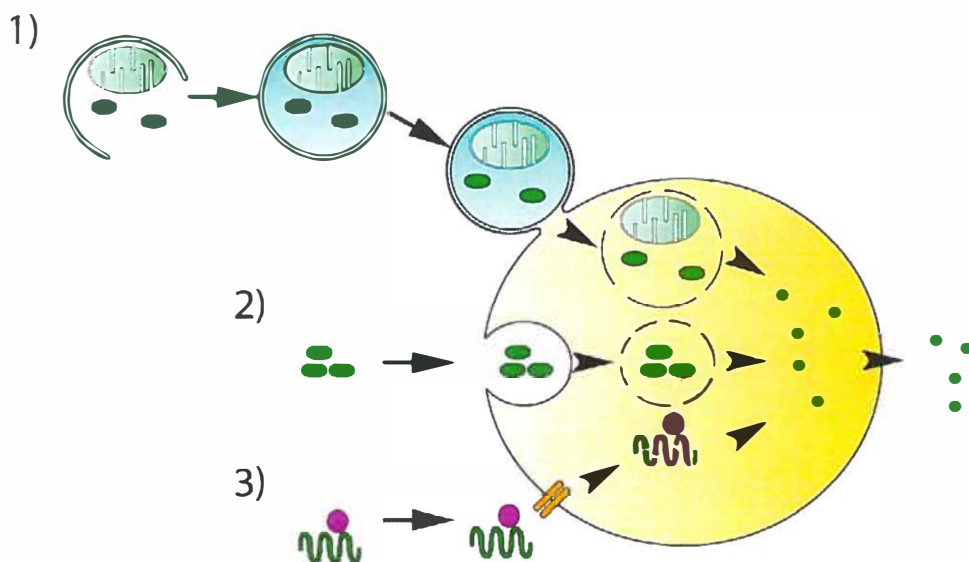


**Figure 5.3: Autophagy Pathways**

Depicted here are the major pathways for protein and bulk degradation via autophagy. 1) depicts the classical macroautophagic pathways, in which a portion of the cytoplasm, containing waste proteins and/or organelles (green) is engulfed in a double membrane, which then associates with the lysosome (yellow) and empties its load together with the inner membrane into the lysosome. 2) shows microautophagy, where waste components (green) of the cytoplasm are directly transported into the lysosome by invagination of the lysosomal membrane. 3) depicts chaperone mediated autophagy, in which a target protein (green) is associated with a chaperone complex (purple), that binds to the LAMP2 complex (orange) and is shuttles into the lysosome.

It is possible for the autophagosome to fuse with endosomes containing extracellular material, before fusing with the lysosome for degradation, though this is technically no longer a purely autophagic pathway. Also, target proteins can enter the lysosome directly, a process called microautophagy. If the client proteins are shuttled into the lysosome by associating with chaperones, this is referred to as chaperone associated autophagy (Fig. 5.3) [20, 28, 32, 41].

Autophagy is tightly regulated by several factors such as mTOR or PKA [51]. A tight regulation is necessary, as excessive autophagy has proven to be harmful to the cell. Since the different autophagic pathways are capable of degrading large quantities of protein, even proteins not degradable by the proteasome, they are interesting objects of research in models of neurodegenerative diseases [3, 25]. Several lines of research involving the upregulation of autophagy demonstrated increased cell survivability and decreased aggregate formation [37]. Similar results were yielded by experiments of a heat shock protein complex of HSPB8 and BAG3, which can recognize and bind target proteins and activate autophagy via the eIF2 $\alpha$ -kinase signaling pathway [6].

#### **1.4. Inclusion formation**

If a cell cannot handle aggregating protein at a given time point, it has the option of depositing it for later degradation. A common example of a cytoplasmic protein inclusion is the aggresome, which forms when the cell's PQC is overwhelmed. In this case, proteins tagged for degradation are transported along the cellular microtubules to the microtubule organizing center, where the aggresome is formed [25, 29]. If and how these are linked to the various inclusions seen in (post-mortem) brain tissues of patients that suffered from neurodegenerative diseases remains an enigma. However, the organized formation of inclusion supports the idea that the initial hypotheses that the protein inclusion encountered in these diseases are harmful, may be incorrect. In parallel to the findings that no direct link between aggregating protein and neurodegeneration could be established, cellular models have now show that formation of (ordered) inclusions are cytoprotective [2] and that knocking out genes involved in inclusion formation enhances disease phenotypes in *C. elegans* [42]. If and how aggresomes/inclusions can be (later) degraded or on the long run still may become toxic is yet unclear. Clearly, in dividing cells, aggresomes are segregated asymmetrically [39] which may ensure rejuvenation of stem cells, further supporting that they serve in a manner protective for the organism.

Notwithstanding the above, inclusion formation still must be interpreted as a marker of an overwhelmed cellular PQC (the first line defender), as the protein the cell can no longer handle is sequestered into the aggregate. Coupled with the fact that most cells exhibit aggregates in the end stage of protein aggregation diseases this may serve as an indicator of the profound and prolonged protein stress of the neurons exhibiting aggregates.

### **1.5. Aim of the studies, Part 2 (Protein aggregation and the protein quality control pathways in the neurodegenerative diseases)**

Chapter 1 demonstrated several links between protein aggregation and neuronal degeneration. The polyglutamine diseases SCA2, 3 and 7 exhibit severe neurodegeneration including their auditory systems. Furthermore, SCA3 exhibits axonal aggregation of the disease protein ataxin-3 in fiber tracts, which are associated with degenerating nuclei. A mutation in the PD disease gene, alpha-synuclein, yields the same phenotype as the idiopathic forms with loss of catecholaminergic neurons as well as widespread protein aggregation.

As the elements of the PQC system are aimed at combating protein misfolding and aggregation causative to the neurodegenerative diseases, we undertook a study of several of the PQC's component proteins in the human brain, both of control cases as well as end stage disease cases, including SCA3, SCA6, HD, PD and AD. While in comparison to diverse disease models, direct observation of disease processes is impossible, studies in human end stage material can be used as a strong indicator of the parts of the PQC which are involved in the disease process, and thus of interest for further investigation. These studies can be facilitated by comparing different sites of degeneration, as later or less seriously affected sites may exhibit specific phenotypes typical for earlier disease processes.

#### **1) The p62 antibody reveals various cytoplasmic protein aggregates in spinocerebellar ataxia type 6**

The polyglutamine disease SCA6 exhibits only minor expansion of the polyQ tract, well below the detection range of the polyglutamine antibody 1C2. The p62 protein is widely involved as a shuttle protein in both proteasomal as well as autophagosomal degradation pathways, as well as in the formation of protein aggregates [3, 50]. Furthermore, it is known to closely associate with proteins aggregates in neurodegenerative diseases. We investigate post mortem SCA6 tissue for the presence of p62-positive aggregates.

#### **2) The evolution of polyglutamine aggregates in spinocerebellar Ataxia type 3 and their relation to cellular protein quality control**

While different forms of protein aggregation have been described in SCA3, there is a lack of investigations into their frequency as well as their relation to the state of neuron. We aim to describe the relative frequency in the pontine nuclei of the different aggregate types and relate them the presence of protein stress.

#### **3) The HSPB8-BAG3 chaperone complex is upregulated in astrocytes in the human brain affected by protein aggregation diseases.**

As has been shown in disease models, the HSPB8-BAG3 complex protects against protein aggregation in polyQ disease models in an autophagy dependent manner. We analyse the presence of HSPB8 and BAG3 in post mortem control brain tissue, as well as in brain tissue afflicted with one of different Neurodegenerative diseases (AD, PD, HD, SCA3).

## References

1. Ahmad MF, Raman B, Ramakrishna T, and Rao C. Effect of phosphorylation on RB-crystallin: Differences in stability, subunit exchange and chaperone activity of homo and mixed oligomers of RB-crystallin and its phosphorylation-mimicking mutant. *J Mol Biol* 2008;375:1040–1051.
2. Arrasate M, Mitra S, Schweitzer ES, Segal MR, Finkbeiner S. Inclusion body formation reduces levels of mutant huntingtin and the risk of neuronal death. *Nature* 2004;431:805-810.
3. Bjorkoy G, Lamark T, Brech A, Outzen H, Perander M, Overvatn A, Stenmark H, Johansen T. p62/SQSTM1 forms protein aggregates degraded by autophagy and has a protective effect on huntingtin-induced cell death. *J Cell Biol* 2005;171:602-614.
4. Bryantsev AL, Kurchashova SY, Golyshev SA, Polyakov VY, Wunderink HF, Kanon B, Budagova KR, Kabakov AE, Kampinga HH. Regulation of stress-induced intracellular sorting and chaperone function of Hsp27 (HspB1) in mammalian cells. *Biochem J* 2007;407:407–417.
5. Carra S, Seguin SJ, Lambert H, Landry J. HspB8 chaperone activity toward poly(Q)-containing proteins depends on its association with Bag3, a stimulator of macroautophagy. *J Biol Chem* 2008a;283:1437-1444.
6. Carra S, Seguin SJ, Landry J. HspB8 and Bag3: a new chaperone complex targeting misfolded proteins to macroautophagy. *Autophagy* 2008b;4:237-239.
7. Carrard G, Bulteau AL, Petropoulos I, Friguet B. Impairment of proteasome structure and function in aging. In *J Biochem Cell Biol* 2002;34:1461-1474.
8. Ciechanover A. The ubiquitin-proteasome pathway: on protein death and cell life. *EMBO J* 1998;17:7151-7160.
9. Craig EA, Huang P, Aron R, Andrew A. The diverse roles of J-proteins, the obligate Hsp70 co-chaperone. *Rev Physiol Biochem Pharmacol* 2006;156:1–21.
10. Cuervo AM. Chaperone-mediated autophagy: selectivity pays off. *Trends Endocrinol Metab* 2010;21:142-150.
11. Cuervo AM, Bergamini E, Brunk UT, Dröge W, French M, Terman A. Autophagy and aging: the importance of maintaining „clean“ cells. *Autophagy* 2005;1:131-140.



12. Cyr DM. Swapping nucleotides, tuning Hsp70. *Cell* 2008;133:945–947.
13. Daugaard M, Rohde M, Jäättelä. The heat shock protein 70 family: Highly homologous proteins with overlapping and distinct functions. *FEBS Lett* 2007;581:3702–3710.
14. Davies JE, Sarkar S, Rubinsztein DC. The ubiquitin proteasome system in Huntington's disease and the spinocerebellar ataxias. *BMC Biochem* 2007;8(Suppl 1): S2.
15. Demand J, Alberti S, Patterson C, Höhfeld J. Cooperation of a ubiquitin domain protein and an E3 ubiquitin ligase during chaperone/proteasome coupling. *Curr Biol* 2001;11:1569–1577.
16. Diamant S, Goloubinoff P. Temperature-controlled activity of DnaK-DnaJ-GrpE chaperones: protein folding arrest and recovery during and after heatshock depends on the substrate protein and the GrpE concentration. *Biochemistry* 1998;37:9688–9694.
17. Doong H, Vrilaas A, Kohn EC. What's in the 'BAG'? – A functional domain analysis of the BAG-family proteins. *Cancer Lett* 2002;188:25–32.
18. Gamerding M, Hajieva P, Kaya AM, Wolfrum U, Hartl FU, Behl C. Protein quality control during aging involves recruitment of the macroautophagy pathway by BAG3. *Embo J* 2009;28:889–901.
19. Glickman MH, Ciechanover A. The ubiquitin-proteasome proteolytic pathway: destruction for the sake of construction. *Physiol Rev* 2002; 82:373–428.
20. Hageman J, Kampinga, HH. Computational analysis of the human HSPH/HSPA/DNAJ family and cloning of a human HSPH/HSPA/DNAJ expression library. *Cell Stress Chaperones* 2009;14:1–21.
21. Hageman J, Rujano MA, van Waarde MA, Kakkar V, Dirks RP, Govorukhina N, Oosterveld-Hut HM, Lubsen NH, Kampinga HH. A DnaJB chaperone subfamily with HDAC-dependent activities suppresses toxic protein aggregation. *Mol Cell* 2010;37:355–369.
22. Hartl FU, Hayer-Hartl M. Converging concepts of protein folding in vitro and in vivo. *Nat Struct Mol Biol* 2009;16:574–581.
23. Haslbeck M, Miess A, Stromer T, Walter S, Buchner J. Disassembling protein aggregates in the yeast cytosol. The cooperation of Hsp26 with Ssa1 and Hsp104. *J Biol Chem* 2005;280:23861–23868.

24. Jiang J, Maes EG, Taylor AB, Wang L, Hinck AP, Lafer EM, Sousa R. Structural basis of J cochaperone binding and regulation of Hsp70. *Mol Cell* 2007;28:422-433.
25. Johnston JA, Ward CL, Kopito RR. Aggresomes: a cellular response to misfolded proteins. *J Cell Biol* 1998;143:1883-1898.
26. Kabbage M, Dickman MB. The Bag proteins: a ubiquitous family of chaperone regulators. *Cell Mol Life Sci* 2008;65:1390-1402.
27. Kampinga HH, Craig EA. The HSP70 chaperone machinery: J proteins as drivers of functional specificity. *Nat Rev Mol Cell Biol* 2010;11:579-592.
28. Klionsky DJ (Ed). *Autophagy*. Georgetown: Landes Bioscience; 2004; pp. 1–303.
29. Kopito RR. Aggresomes, inclusions bodies and protein aggregation. *Trends Cell Biol* 2000;10:524-530.
30. Lee S, Tsai FT. Molecular chaperones in protein quality control. *J Biochem Mol Biol* 2005;38:259-265.
31. Levine B, Klionsky DJ. Development by self-digestion: molecular mechanisms and biological functions of autophagy. *Dev Cell* 2004;6:463-477.
32. Majeski AE, Dice JF. Mechanisms of chaperone-mediated autophagy. *Int Biochem Cell Biol* 2004;36:2435-2444.
33. Mizushima N. The pleiotropic role of autophagy: from protein metabolism to bactericide. *Cell Death Differ* 2005;12 Suppl 2:1535-1541.
34. Mizushima N, Klionsky DJ. Protein turnover via autophagy: implications for metabolism. *Annu rev Nutr* 2007;27:19049.
35. Nair U, Klionsky DJ. Molecular mechanisms and regulation of specific and nonspecific autophagy pathways in yeast. *J Biol Chem* 2005;280:41785–41788.
36. Nollen EA, Brunsting JF, Song J, Kampinga HH, Morimoto R. Bag1 functions in vivo as a negative regulator of Hsp70 chaperone activity. *Mol cell Biol* 2000;20:1083-1088.
37. Ravikumar B, Vacher C, Berger Z, Davies JE, Luo S, Oroz LG, Scaravilli F, Easton DF, Duden R, O’Kane CJ, Rubinsztein DC. Inhibition of mTOR

- induces autophagy and reduces toxicity of polyglutamine expansions in fly and mouse models of Huntington disease. *Nat Genet* 2004;36:585-595.
38. Rüdiger S, Germoth L, Schneide-Mergener J, Bukau B. Substrate specificity of the DnaK chaperone determined by screening cellulose-bound peptide libraries. *EMBO J* 1997;16:1501-1507.
  39. Rujano MA, Bosveld F, Salomons FA, Dijk F, van Waarde MA, van der Want JJ, de Vos RA, Brunt ER, Sibon OC, Kampinga HH. Polarised asymmetric inheritance of accumulated protein damage in higher eukaryotes. *PLoS Biol* 2006;4:e417.
  40. Rujano MA, Kampinga HH, Salomons FA. Modulation of polyglutamine inclusion formation by the Hsp70 chaperone machinery. *Exp Cell Res* 2007;313:3568-3578.
  41. Sattler T, Mayer A. Cell-free reconstitution of microautophagic vacuole invagination and vesicle formation. *J Cell Biol* 2000;151:529-538.
  42. van Ham TJ, Holmberg MA, van der Goot AT, Teuling E, Garcia-Arencibia M, Kim HE, Du D, Thijssen KL, Wiersma M, Burggraaff R, van Bergeijk P, van Rheeën J, Jerre van Veluw G, Hofstra RM, Rubinsztein DC, Nollen EA. Identification of MOAG-4/SERF as a regulator of age-related proteotoxicity. *Cell* 2010;142:601-612.
  43. Van Leeuwen FW, de Kleijn DP, van den Hurk HH, Neubauer A, Sonnemans MA, Sluijs JA, Köycü S, Ramdjielal RD, Salehi A, Martens GJ, Grosveld FG, Peter J, Burbach H, Hol EM. Frameshift mutants of beta amyloid precursor protein and ubiquitin-B in Alzheimer's and Down patients. *Science* 1998;279:242-247.
  44. van Montfort R, Slingsby C, Vierling E. Structure and function of the small heat shock protein/alpha-crystallin family of molecular chaperones. *Adv Protein Chem* 2001;59:105-156.
  45. Voges D, Zwickl P, Baumeister W. The 26S proteasome: a molecular machine designed for controlled proteolysis. *Annu Rev Biochem* 1999;68:1015-1068.
  46. Vos MJ, Hageman J, Carra S, Kampinga HH. Structural and functional diversities between members of the human HSPB, HSPH, HSPA and DNAJ Chaperone families. *Biochemistry* 2008;47:7001-7011.
  47. Vos MJ, Zijlstra MP, Carra S, Sibon OC, Kampinga HH. Small heat shock proteins, protein degradation and protein aggregation diseases. *Autophagy* 2010; 24:101-103.

48. Wacker JL, Huang SY, Steele AD, Aron R, Lotz GP, Nguyen Q, Giorgini F, Roberson ED, Lindquist S, Masliah E, Muchowski PJ. Loss of Hsp70 exacerbates pathogenesis but not levels of fibrillar aggregates in a mouse model of Huntington's disease. *J Neurosci* 2009;29:9104-9114.
49. Walsh P, Bursac D, Law YC, Cyr D, Lithgow T. The J-protein family: modulating protein assembly, disassembly and translocation. *EMBO Rep* 2004;5:567-571.
50. Wooten MW, Hu X, Babu JR, Seibenheimer ML, Geetha T, Paine MG, Wooten MC. Signaling, polyubiquitination, trafficking, and inclusions: sequestosome 1/p62's role in neurodegenerative disease. *J Biomed Biotechnol* 2006;2006:62079.
51. Yorimitsu T, Klionsky DJ. Autophagy: molecular machinery for self-eating. *Cell Death Differ* 2005;12 Suppl 2:1542-1552.



## Chapter 6

---

# **The p62 antibody reveals cytoplasmic protein aggregates in spinocerebellar ataxia type 6 (SCA6)**

---

K. Seidel<sup>1</sup>, E.R.P. Brunt<sup>2</sup>, R.A.I. de Vos<sup>3</sup>, F. Dijk<sup>4</sup>, H.J.L. van der Want<sup>4</sup>, H.H. Kampinga<sup>5</sup>, T. Deller<sup>6</sup>, U. Rüb<sup>6</sup>, W.F.A. den Dunnen<sup>1</sup>.

<sup>1</sup>*Department of Pathology and Medical Biology, University Medical Center Groningen, University of Groningen*

<sup>2</sup>*Department of Neurology, University Medical Center Groningen, University of Groningen, Hanzeplein 1, P.O.Box 30.001, 9700 RB Groningen, the Netherlands*

<sup>3</sup>*Laboratory for Pathology Oost Nederland, Burg. Edo Bergsmalaan 1, P.O.Box 377, 7500 AJ, Enschede, the Netherlands*

<sup>4</sup>*Cell Biology, Electron microscopy, University of Groningen, Antonius Deusinglaan 1, P.O.Box 196, 9700 AD Groningen, the Netherlands*

<sup>5</sup>*Cell Biology, Radiation and Stress Cell Biology, University of Groningen, Antonius Deusinglaan 1, P.O.Box 196, 9700 AD, Groningen, the Netherlands*

<sup>6</sup>*Institute of Clinical Neuroanatomy, J.W. Goethe University, Theodor Stern Kai 7, 60590 Frankfurt/Main, Germany.*

Published in: Clin Neuropathol. 2009 ;28:344-349



## **Abstract**

Neuronal protein aggregates are considered as pathological hallmarks of various human neurodegenerative diseases, including the so-called CAG-repeat disorders, such as spinocerebellar ataxia type 6 (SCA6). Since the immunocytochemical findings of an initial post-mortem study using a specific antibody against the disease protein of SCA6 (i.e. pathologically altered  $\alpha$ -1A subunit of the P/Q type voltage-dependent calcium channel, CACNA1A) have not been confirmed so far, the occurrence and central nervous system distribution of neuronal protein aggregates in SCA6 is still a matter of debate.

Owing to the fact that the antibody against the pathologically altered CACNA1A is not commercially available, we decided to apply a recently generated p62 antibody on brain tissue from two clinically diagnosed and genetically confirmed SCA6 patients. Application of this p62 antibody revealed numerous cytoplasmic neuronal inclusions in the degenerated cerebellar dentate nucleus and inferior olive of both SCA6 patients studied, whereby a subset of these aggregates were also ubiquitin-immunopositive. In view of the known role of p62 in protein degradation as well as aggresome/sequestosome formation, the p62 aggregate formation observed in the present study suggests that SCA6 not only is associated with an impairment of the calcium channel function and an elongated polyglutamine stretch in CACNA1A, but also with a defective protein handling by the protein quality control system.

## **Keywords**

Aggregate formation - CAG-repeat disorder - p62 - SCA6 - protein quality system

## Introduction

Spinocerebellar ataxia type 6 (SCA6) is the 6<sup>th</sup> genetically identified SCA, accounting for 10-15% of all SCAs in the Western countries and occurring with a relative regional prevalence in Japan [13, 20]. The SCA6 gene on chromosome 19p13.2-p13.1 encodes for the  $\alpha$ -1A subunit of the P/Q type voltage-dependent calcium channel (CACNA1A). The CAG-repeat in this gene normally contains 4-19 copies and is expanded to 21-26 copies in affected patients. Thus theoretically, SCA6 is classified both as a CAG-repeat disorder and a channelopathy [7]. SCA6 is clinically characterized by adult disease onset with relative pure cerebellar manifestations [14, 20], and is associated with a consistent degeneration of the cerebellar Purkinje cell layer, dentate nucleus, as well as the inferior olive [6, 19].

Neuronal protein aggregates are considered as pathological hallmarks of various CAG-repeat disorders [4]. In a recent SCA6 study, the presence of neuronal cytoplasmic aggregates, immunoreactive for the pathologically altered CACNA1A, has been reported [6]. However, these initial findings have not been confirmed by further studies and application of the 1C2 antibody, originally developed against the 38-polyglutamine repeat in the TATA box binding protein, up till now revealed conflicting results [6, unpublished observations]. Therefore, the presence, central nervous system distribution and significance of SCA6-related neuronal protein aggregates are still controversial among researchers in the field.

Since the specific antibody against the pathologically altered CACNA1A is not commercially available and the widely used 1C2 antibody according to our experience does not detect the short poly-Q stretch in SCA6, we decided to apply a new p62 antibody to brain tissue from clinically diagnosed and genetically confirmed SCA6 patients. This antibody is directed against a 62 kDA protein (p62), which has also been designated STAP, A170 and ZIP. p62 acts as a shuttling factor of polyubiquitinated proteins to the proteasome [11, 17], regulates autophagy [11, 18] and plays an important role in aggresome/sequestosome formation (i.e. protein aggregate storage) in various neurodegenerative diseases [8-10, 12]. The present study was performed in order to test the hypothesis that the p62 antibody also reveals insoluble protein aggregates in the CAG-repeat disorder SCA6.

## Patients and Methods

### *Patients*

A general overview of the patient characteristics is given in Table 1.

Patient 1. Female diagnosed with 22 CAG repeats in the SCA6 gene. The first symptoms of unsteadiness appeared at age 45. A vertebral angiography for a suspected posterior fossa lesion at age 55 was complicated by cerebral ischemia which left her right hemiplegic, aphasic and wheelchair-bound. At age 94 she died. Autopsy was performed after 21 hours. Brain tissue was also sampled for (immuno) electron microscopy.

Patient 2. Male also diagnosed with 22 CAG repeats in the SCA6 gene. Following recurrent headaches from age 40 onward, slowly progressive unsteadiness appeared at age 52. He died at age 69 from a cardiac arrest. Autopsy was performed after 46 hours.

|                              | Patient 1    | Patient 2           |
|------------------------------|--------------|---------------------|
| Age (years)                  | 94           | 69                  |
| Gender                       | female       | male                |
| CAG-repeat length            | 22           | 22                  |
| Onset of SCA6 (years)        | 45           | 40                  |
| Initial disease symptoms     | unsteadiness | recurrent headaches |
| Progressive disease symptoms | Ataxia       | Ataxia              |
|                              | Dysphagia    | Dysphagia           |
|                              | Dysarthria   | Dysarthria          |
| Cause of death               | Old age      | Cardiac arrest      |
| Brain weight                 | 980          | 1395                |

**Table 6.1: Characteristics of the two SCA6 patients.**

Both patients had given their informed consent for autopsy and research use on their brain tissue. Brain tissue from 4 individuals (aged 46 to 84 years) who died of non-neurological disease (negative controls) and from 3 clinically diagnosed and genetically confirmed SCA3 patients (aged 63 to 75 years) served as controls for the immunohistochemical staining procedures.

### *Preparation techniques*

Following immersion fixation in 4% aqueous formaldehyde, the brainstems were severed at the level of the inferior colliculus and the cerebella were removed. Paraffin embedded tissue blocks from the right cerebral hemispheres, cerebella and brainstems were cut into 5 micron sections, which were routinely stained with haematoxylin and Eosin, Klüver-Barrera and Sevier-Munger. For immunohistochemistry primary antibodies were used against hyperphosphorylated Tau (AT8, Innogenetics, 1:20, no antigen retrieval (AR)), Ubiquitin (polyclonal, DAKO, 1:100, no AR), alpha-synuclein (KM51, Novocastra, 1:40, AR using Tris HCl (pH 9.5) for 30 minutes followed by 100% formic acid for 3 minutes), 1C2 (MAB1574, Chemicon, 1:400, AR using Tris

HCl (pH 9.5) for 30 minutes followed by 100% formic acid for 3 minutes) and p62/sequestosome-1 (sc-28359, Santa Cruz, 1:100, AR using Tris Hcl (pH 9.5) for 30 minutes).

In addition, samples from the dentate nucleus were fixed in Karnovsky, 2 % PF, 0.5% GA in 0.1 M cacodylate buffer, pH 7.4. Fifty micron vibratome sections of were used for immuno-electron microscopy. In free floating sections aldehydes were quenched with 0.5% sodium borohydride, endogenous peroxidase by 1% H<sub>2</sub>O<sub>2</sub>. Antigen retrieval was performed by 0.1 M TRIS pH 9.5, at 37°C (30 min) and 98° C for 5 min. Pre incubation (1 % BSA, 0.1% Glycine, 0,1% Lysine, 0,1% CWFS, 0,1% Triton in TBS, pH 7,6) for 2 hrs , RT. Incubation with ms p62 (1:100) at 4°C, 20 hrs. GaM biotin (1:200), 2 hrs, ABC (1:200) 1hr, DAB 8 min. For EM visualization of DAB, the gold substituted silver peroxidase method was used. After GA and OsO<sub>4</sub> fixation sections were embedded in Epon, and placed between coated glasses in order to select areas of interest for EM analysis.

## Results

Patient 1: the brain weighed 980 gr. The cerebellum, base of the pons and the medial cerebellar peduncle showed marked atrophy. The Purkinje cell layer was nearly devoid of nerve cells and showed pronounced Bergmann gliosis, whereby neurodegeneration of the Purkinje cell layer of this patient was far more severe than in the SCA3 patients and negative controls (Table 6.1). Using the ubiquitin, 1C2 and p62 antibodies, inclusions could not be observed in the remaining Purkinje cells. The dentate nucleus and inferior olive showed signs of neuronal degeneration, astro- and microgliosis. Using the p62 antibody, several stages of intracytoplasmic inclusions were found (Fig. 6.1a-6.1b, 6.1d-6.1h), ranging from punctuate aggregates at the periphery of the neurons to more centrally located fibrillary or globose cytoplasmic structures. The punctuate inclusions were most frequent and present in 5 to 10% of the dentate nerve cells. Whereas the bigger fibrillary and globose inclusions were present in up to 2% of the dentate nerve cells. In contrast to the punctuate inclusions, the fibrillary and globose intracytoplasmic inclusions were also ubiquitin immunopositive (Fig 6.1c). EM confirmed the cytoplasmic localization of fibrillary and globose inclusions and showed clusters of electron dense p62-immunopositive aggregates in somata and in primary dendrites of large neurons in the dentate nucleus (Fig. 6.2a). In between larger clusters (Figs. 6.2b and c), fine dispersed labelling could also be observed along thin filaments (Fig. 6.2d).

Patient 2: the brain weighed 1395 gr. Loss of cerebellar Purkinje cells in this patient was less severe than in Patient 1 and no p62-, 1C2- or ubiquitin-immunopositive inclusions could be detected in his Purkinje cells. However, a marked neuronal loss as well as astro- and microgliosis were observed in the cerebellar dentate nucleus and the inferior olive. In addition, both these nuclei displayed ubiquitin- and p62-immunopositive intracytoplasmic inclusions (frequency: <1% of the total number of neurons examined).



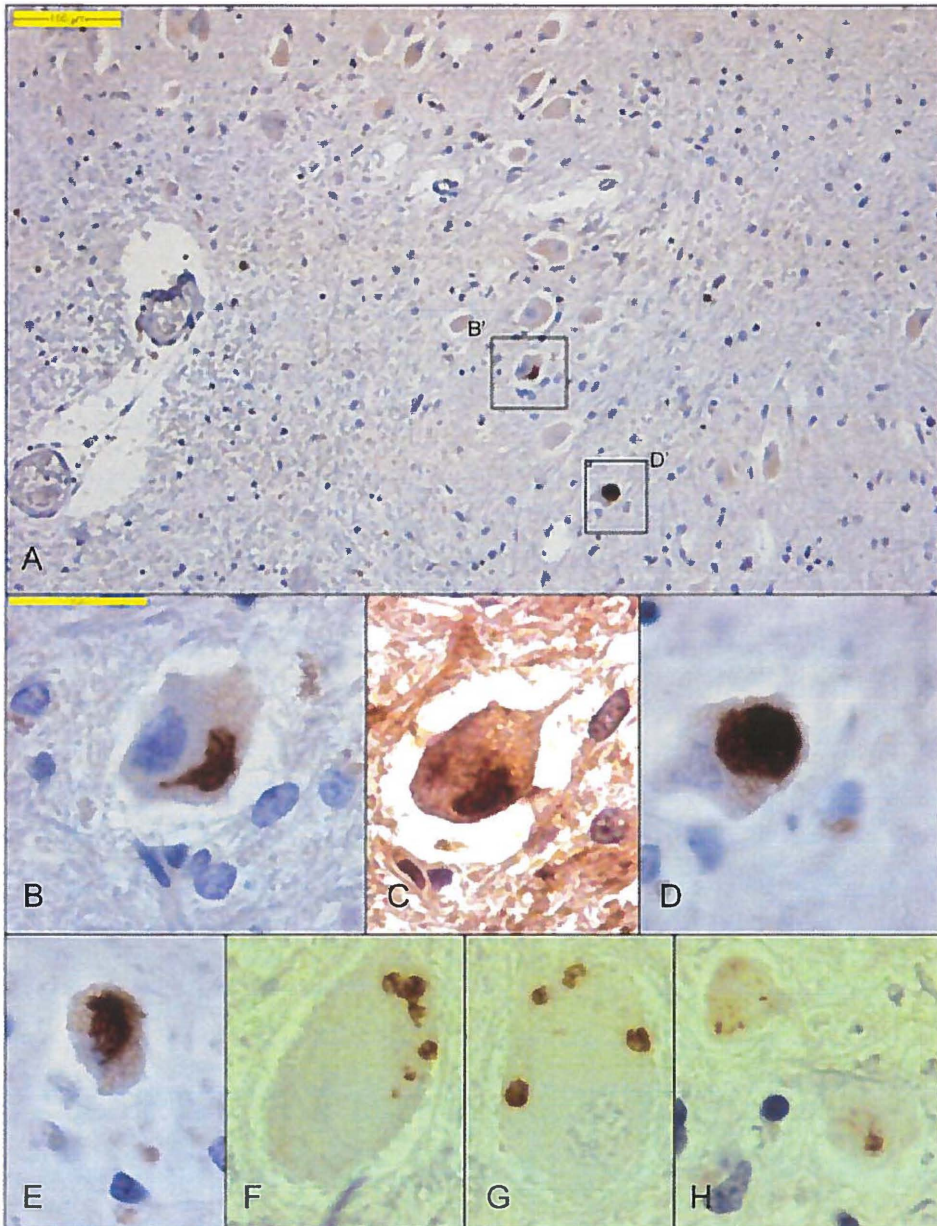


**Figure 6.1: p62 positive aggregates in a SCA6 brain**

(A) Overview showing the dentate nucleus of patient 1 with two big p62 immunopositive cytoplasmic neuronal inclusions. In (B) and (D) these inclusions are shown in more detail. (D) shows a globose inclusion, whereas (B) shows a more irregular inclusion. (C) shows an anti-ubiquitin staining from a serial section of the neuron shown in (B). In (E) to (H) more p62 positive inclusions are shown that were not ubiquitin-positive. (E) shows a fibrillary inclusion centrally located in the cytoplasm. The punctate inclusions in (F) to (H) vary in diameter, are located at the periphery of the cytoplasm and were the most frequently observed type of inclusion. Probably the different types of inclusions represent various stages of aggregate formation, whereby the big globose inclusion could be considered as an end stage. The bar in (A) represents 100  $\mu\text{m}$  and the bar in (B) 25  $\mu\text{m}$ . The micrographs in (C) to (H) were made at the same magnification as (B).

In both SCA6 patients no p62-immunopositive intranuclear neuronal inclusions were found and all of the p62-immunopositive cytoplasmic neuronal inclusions were negative for tau and alpha-synuclein (data not shown), excluding overlap with aggregates of other frequently occurring neurodegenerative diseases. In contrast to the SCA6 patients and negative controls, immunostaining with the 1C2 antibody, which is directed against a polyQ stretch with a length of 38, revealed numerous intranuclear neuronal inclusions in the SCA3 patients studied. Moreover, these intranuclear inclusions were also p62 positive.

| Case           | Number of Purkinje cells/mm <sup>2</sup> | Number of dentate nucleus cells/HPF |
|----------------|--|-------------------------------------|
| Control 1      | 9.1                                      | 18.3                                |
| Control 2      | 10.5                                     | 20.8                                |
| Control 3      | 7.5                                      | 20.2                                |
| Control 4      | 8.9                                      | 21.8                                |
| SCA6 patient 1 | 2.2                                      | 18.9                                |
| SCA6 patient 2 | 2,2                                      | 19.8                                |

**Table 6.2: Number of neurons in the Purkinje cell layer and dentate nucleus.**  
 HPF = High Power Field i.e. 40x objective



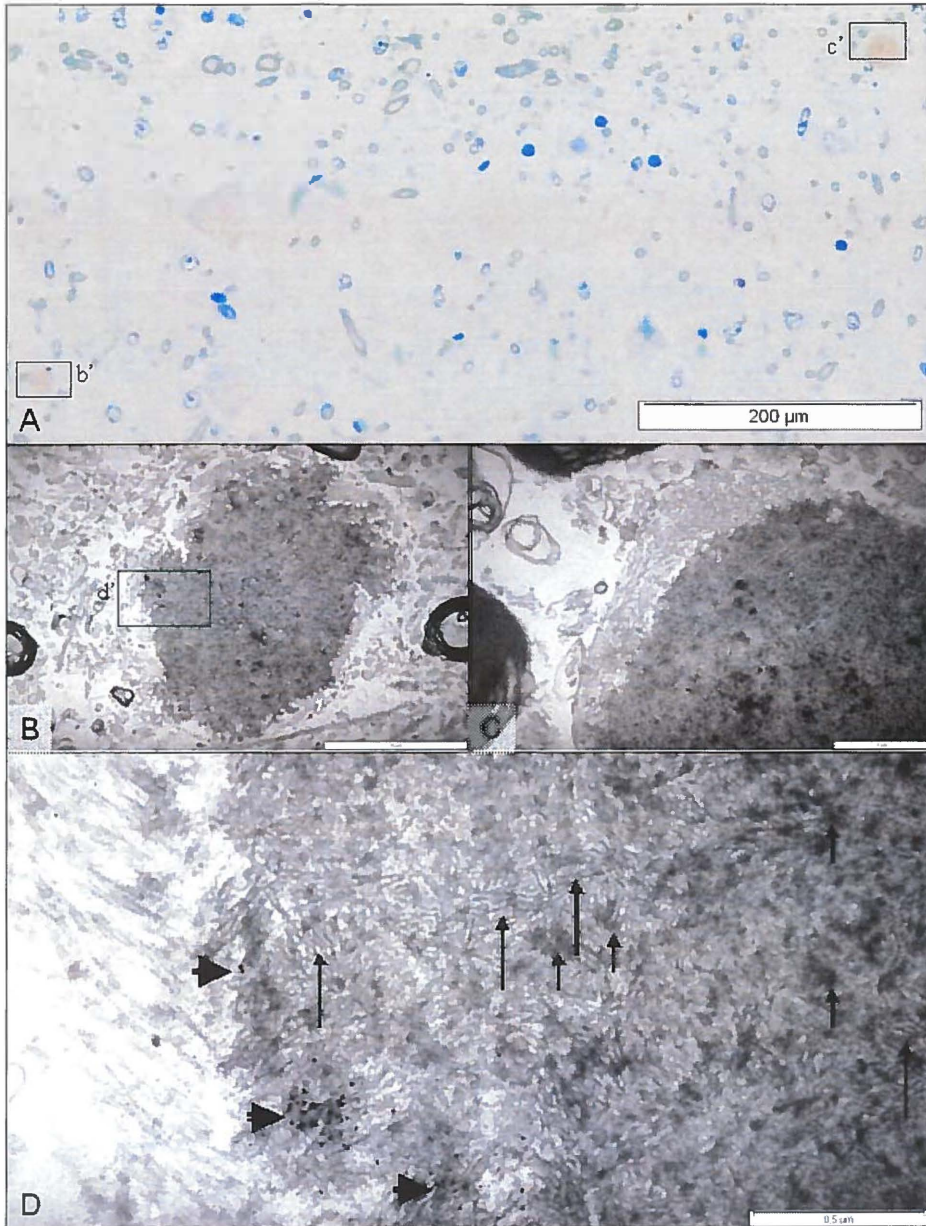


**Figure 6.2: Ultrastructural analysis of p62 positive aggregates**

(A) shows a 1 µm thick Epon section from the dentate nucleus of patient 1 with 2 faint p62 positive round cytoplasmic inclusions (counterstaining with toluidine blue). Figures B and C are transmission electron micrographs from these 2 inclusions. In (B) the inclusion has a somewhat irregular shape, whereas (C) shows a more rounded form. (D) is a higher magnification from the inclusion in (B), showing multiple filamentous structures (long arrows) and more amorphous electron-dense material (short arrows). The small black dots (arrowheads) indicate positive immunoreactivity with the p62 antibody.

## Discussion

The present study demonstrates for the first time, that the p62-antibody is well-suited to detect various stages of intracytoplasmic neuronal inclusions in SCA6. Upon light microscopical investigation these intracytoplasmic neuronal inclusions (1) appeared as punctuate, filamentous or globose structures, most likely reflecting different developmental stages of SCA6-related aggregate formation, and (2) were 1C2-immunonegative and (3) only the larger among them were also ubiquitin-immunopositive. Additional electron microscopical investigation showed that the p62 immunoreactivity was located in dense fibrillar cytoplasmic aggregates.

P62 has been observed in intraneuronal or intraglial inclusions in a number of other neurodegenerative diseases [8-10, 12]. It has been suggested that p62 is capable of non-covalent binding to polyubiquitin chains [3, 15, 17] and may be involved in storage of ubiquitinated proteins. We find Ub-positivity in centrally located fibrillary or globose cytoplasmic p62-positive structures, but not in p62-positive punctated structures. In several neurodegenerative diseases it is hypothesized that small aggregates/protofibrils are more toxic than the larger aggregates [18]. Using the p62 antibody we found both small punctate and bigger globose inclusions in our SCA6 patients, without any overlap with tau- or alpha-synuclein staining. According to the above mentioned hypothesis, the smaller punctuate aggregates could be neurotoxic, thereby playing a role in neurodegeneration in SCA6.

The formation of larger aggregates might be seen as a reaction of the cell to store misfolded proteins, thereby preventing toxicity. On the other hand, the formation of large aggregates might also cause sequestration of ubiquitin, p62 etc, leading to impairment of the protein quality system and defective degradation of unstable proteins, subsequently leading to cell death [2]. Indeed a loss of p62 by antisense oligonucleotides has been shown to lead to neuronal dysfunction [2]. However, further research will be needed to elucidate the function of p62 in the formation of the different aggregates and the precise role of the different aggregates in the pathology of SCA6.

## Conclusion

We suggest that p62 immunoreactivity in SCA6 indicates that aggregate formation in the cytoplasm is a hallmark of SCA6 pathology, providing an additional means to assess the neuropathology in SCA6 and confirming earlier suggestions that SCA6 is not only a channelopathy but also an aggregation disease. Further analysis on the exact composition of these p62 positive aggregates, as well as the distribution throughout the central nervous system in SCA6 will be necessary.

## **Acknowledgements**

We kindly acknowledge the skilful assistance of Mr. B.E. Groenewold, Mr. J. Donga and Mrs. F.A. Kempinga with the tissue processing and the immunohistochemistry. We thank Prof. Dr. H. Hollema for helpful discussions and critical reading of the manuscript and Mrs. J.E. den Dunnen-Briggs for improving the English text as a native speaker. This research is supported by the Deutsche Forschungsgemeinschaft (RU 1215/1-2), the Deutsche Heredo-Ataxie-Gesellschaft (DHAG), the ADCA-Vereniging Nederland, the Bernd Fink-Stiftung (Düsseldorf, Germany) and De Cock-Stichting (project-code 08-15, Groningen, Netherlands).

## References

1. Bjorkoy G, Lamark T, Brech A, Outzen H, Perander M, Overvatn A, Stenmark H, Johansen T. p62/SQSTM1 forms protein aggregates degraded by autophagy and has a protective effect on huntingtin-induced cell death. *J Cell Biol* 2005;171:603-614.
2. Donaldson KM, Li W, Ching KA, Batalov S, Tsai CC, Joazeiro CA. Ubiquitin-mediated sequestration of normal cellular proteins into polyglutamine aggregates. *Proc Natl Acad Sci USA* 2003;100:8892-8897.
3. Geetha T, Wooten MW. Structure and functional properties of the ubiquitin binding protein p62. *FEBS Lett* 2002;512:19-24.
4. Gunawardena S, Goldstein LSB. Polyglutamine diseases and transport problems; Deadly traffic jams on neuronal highways. *Arch Neurol* 2005;62:46-51.
5. Ishikawa K, Fujigasaki H, Saegusa H, Ohwada K, Fujita T, Iwamoto H, Komatsuzaki Y, Toru S, Toriyama H, Watanabe M, Ohkoshi N, Shoji S, Kanazawa I, Tanabe T, Mizusawa H. Abundant expression and cytoplasmic aggregations of  $\alpha$ -1A voltage-dependent calcium channel protein associated with neurodegeneration in spinocerebellar ataxia type 6. *Hum Mol Genet* 1999;8:1185-1193.
6. Ishikawa K, Owada K, Ishida K, Fujigasaki H, Shun Li M, Tsunemi T, Ohkoshi N, Toru S, Mizutani T, Hayashi M, Arai N, Hasegawa K, Kawanami T, Kato T, Makifuchi T, Shoji S, Tanabe T, Mizusawa H. Cytoplasmic and nuclear polyglutamine aggregates in SCA6 Purkinje cells. *Neurology* 2001;56:1753-1756.

7. Kordasiewicz HB, Gomez CM. Molecular Pathogenesis of spinocerebellar ataxia type 6. *Neurotherapeutics* 2007;4:285-294.
  
8. Kuusisto E, Salminen A, Alafuzoff I. Ubiquitin-binding protein p62 is present in neuronal and glial inclusions in human tauopathies and synucleinopathies. *NeuroReport* 2001;12:2085-2090.
  
9. Kuusisto E, Salminen A, Alafuzoff I. Early accumulation of p62 in neurofibrillary tangles in Alzheimer's disease: possible role in tangle formation. *Neuropathol Appl Neurobiol* 2002;28:228-237.
  
10. Kuusisto E, Parkkinen L, Alafuzoff I. Morphogenesis of Lewy bodies: dissimilar incorporation of alpha-synuclein, ubiquitin, and p62. *J. Neuropathol Exp Neurol* 2003;62:1241-1253.
  
11. Mizuno Y, Amari M, Takatama M, Aizawa H, Mihara B, Okamoto K. Immunoreactivities of p62, an ubiquitin-binding protein, in the spinal anterior horn cells of patients with amyotrophic lateral sclerosis. *J Neurol Sci* 2006;249:13-18.
  
12. Nagaoka U, Kim K, Jana NR, Doi H, Maruyama M, Mitsui K, Oyama F, Nukina N. Increased expression of p62 in expanded polyglutamine-expressing cells and its association with polyglutamine inclusions. *J Neurochem* 2004;91:57-68.
  
13. Riess O, Schöls L, Bottger H, Nolte D, Vieira-Saecker AM, Schimming C, Kreuz F, Macek M, Krebsová A, Sen Macek M, Klockgether T, Zühlke C, Laccone FA. SCA6 is caused by moderate CAG expansion in the alpha1A-voltage-dependent calcium channel gene. *Hum Mol Genet* 1997;6:1289-1293.

14. Schöls L, Krüger R, Amoiridis G, Przuntek H, Epplen JT, Riess O. Spinocerebellar ataxia type 6: genotype and phenotype in German kindreds. *J Neurol Neurosurg Psychiatry* 1998;64:67-73.
15. Seibenhener ML, Babu JR, Geetha T, Wong HC, Krishna NR, Wooten MW. Sequestosome 1/p62 is a polyubiquitin chain binding protein involved in ubiquitin proteasome degradation. *Mol Cell Biol* 2004;24:8055-8068.
16. Tsuchiya K, Oda T, Yoshida M, Sasaki H, Haga C, Okino H, Tominaga I, Matsui K, Akiyama H, Hashizume Y. Degeneration of the inferior olive in spinocerebellar ataxia 6 may depend on disease duration: report of two autopsy cases and statistical analysis of autopsy cases reported to date. *Neuropathol* 2005;25:125-135.
17. Vadlamudi RK, Joung I, Strominger JL, Shin J. p62, a phosphotyrosine-independent ligand of the SH2 domain of p56lck, belongs to a new class of ubiquitin-binding proteins. *J Biol Chem* 1996;271:20235-20237.
18. Wooten MW, Hu X, Babu JR, Seibenhener ML, Geetha T, Paine MG, Wooten MC. Signaling, Polyubiquitination, Trafficking, and Inclusions: Sequestosome 1/p62's role in neurodegenerative disease. *J Biomed Biotechnol* 2006;3: Article ID 62079.
19. Yang Q, Hashizume Y, Yoshida M, Wang Y, Goto Y, Mitsuma N, Ishikawa K, Mizusawa K. Morphological Purkinje cell changes in spinocerebellar ataxia type 6. *Acta Neuropathol* 2000;100:371-376.
20. Zhuchenko O, Bailey J, Bonnen P, Ashizawa T, Stockton DW, Amos C, Dobyns WB, Subramony SH, Zoghbi HY, Lee CC. Autosomal dominant cerebellar ataxia (SCA6) associated with small polyglutamine expansions in the alpha 1A-voltage-dependent calcium channel. *Nat Genet* 1997;15:62-69.





# Chapter 7

---

## Cellular protein quality control and the evolution of aggregates in SCA3

---

Kay Seidel<sup>1,2,5</sup>, Melanie Meister<sup>1,2</sup>, George J Dugbartey<sup>1</sup>, Marianne P. Zijlstra<sup>2</sup>, Jonathan Vinet<sup>3</sup>, Ewout Brunt<sup>4</sup>, Fred W van Leeuwen<sup>6</sup>, Udo Rüb<sup>5</sup>, Harm H. Kampinga<sup>2</sup>, Wilfred den Dunnen<sup>1</sup>

<sup>1</sup>*Department of Pathology and Medical Biology, University Medical Center Groningen, University of Groningen*

<sup>2</sup>*Cell Biology, Radiation and Stress Cell Biology, University of Groningen, Antonius Deusinglaan 1, P.O.Box 196, 9700 AD, Groningen, the Netherlands*

<sup>3</sup>*Department of Neuroscience, Section Medical Physiology, University of Groningen, Antonius Deusinglaan 1, 9713 AV, Groningen, the Netherlands*

<sup>4</sup>*Laboratory for Pathology Oost Nederland, Burg. Edo Bergsmalaan 1, P.O.Box 377, 7500 AJ, Enschede, the Netherlands*

<sup>5</sup>*Dr. Senckenberg Chronomedical Institute, J.W. Goethe University, Theodor-stern-Kai 7, 60950 Frankfurt/Main, Germany*

<sup>6</sup>*Dept. of Neuroscience, Maastricht University, Universiteitssingel 50, 6229ER Maastricht, the Netherlands*

Submitted

## Abstract

A characteristic of polyglutamine (polyQ) diseases is the increased propensity of disease proteins to aggregate, which is thought to be a major contributing factor to the underlying neurodegeneration. Healthy cells contain mechanisms by which they can handle protein damage, the protein quality control (PQC), which must be impaired or inefficient to permit proteotoxicity under pathological conditions. We used a quantitative analysis of immunohistochemical stainings of the pons of 8 patients with the polyQ disorder SCA3. We employed the anti-polyglutamine antibody 1C2, antibodies against the autophagy- and aggregation-associated protein p62, the PQC components HSPA1A and DNAJB1 and the proteasomal stress marker UBB<sup>+1</sup>. The 1C2 antibody stained Neuronal Nuclear Inclusions (NNI), Diffuse Nuclear Staining (DNS), Granular Cytoplasmic Staining (GCS) and combinations, with a reproducible distribution. P62 always colocalized with 1C2 in NNI. DNS and GCS co-stained with a lower frequency. UBB<sup>+1</sup> was present in a subset of neurons with NNI. A subset of UBB<sup>+1</sup> containing neurons displayed increased levels of HSPA1A, while DNAJB1 was sequestered into the NNI. Based on our results, we propose a model for the aggregation associated pathology of SCA3: GCS and DNS aggregation likely represents early stages of pathology, which progresses towards formation of p62 positive NNI. A fraction of NNI exhibits UBB<sup>+1</sup> staining, implying proteasomal overload at a later stage. Subsequently, the stress inducible HSPA1A is elevated while DNAJB1 is recruited into NNIs. This indicates that the stress response is only induced late when all endogenous PQC systems have failed.

## Introduction

Protein aggregation can be caused by chemical, oxidative and heat stress as well as by protein misfolding or mutations [22]. It is also a characteristic feature of many neurodegenerative diseases, including the polyQ diseases [27]. In these, an expansion of a poly-CAG repeat sequence within a gene coding for a disease specific protein causes polyQ expansion and aggregation, which is considered to be a major contributing factor to the severe neurodegeneration present in these diseases [21, 22, 27, 33]. Spinocerebellar ataxia type 3 (SCA3), a polyQ disease, is the most frequent dominant spinocerebellar ataxia [25]. In healthy individuals the *ATXN3* disease gene contains 12-40 CAG-repeats, while in patients it encompasses 61-84 CAG-repeats [21]. The best-described protein aggregates in SCA3 are neuronal nuclear inclusions (NNI), which have been demonstrated to sequester numerous other proteins (e.g. transcription factors, heat shock proteins, ubiquitin) [22]. However, the relation between the appearance of NNI and neuronal death remains elusive. While an animal model demonstrates that ataxin-3 toxicity depends on nuclear localization [4], nuclear aggregates are also present in areas otherwise spared in the neurodegenerative process in SCA3 patients [4,23]. Other types of aggregates exist, but received less attention [26, 35].

To deal with aggregating and misfolded protein, cells contain several biological pathways, referred to as the protein quality control (PQC) system, which include refolding (e.g. HSP70 chaperones) and degradation pathways (e.g. ubiquitin-proteasome system, autophagy). The evolutionary highly conserved HSP70 chaperones act together with the DNAJ family of co-chaperones in multiple folding processes [16]. The human HSPA1A is a strongly stress inducible HSP70 member and an excellent marker of proteotoxic stress [32] and, if present at elevated levels, can protect against acute proteotoxic stress by assisting protein refolding [20]. However HSPA1A is not very effective in responding to and protecting against chronic stress, like expression of polyQ disease protein [12]. For the latter, upregulation of DNAJ proteins seems to be more effective [12]. For the present study, we focused on DNAJB1, as it has been reported to be included into polyQ inclusions in post mortem tissue [6] and expression levels in fibroblast cultures of SCA3 patients were associated with the age of onset of these patients [36]. Also, DNAJB1 was found to reduce polyQ aggregation in a HSPA1A dependent manner in a cell model [12, 19], by assisting proteasomal degradation of polyQ proteins [2].

The ubiquitin proteasome system (UPS) degrades target proteins into oligopeptides, thereby eliminating unnecessary or misfolded proteins [7]. Target proteins are tagged with a specific polyubiquitin flag, and are transferred to the proteasome via shuttle proteins containing an ubiquitin associated domain, such as the p62 protein [5, 34]. In polyQ diseases like SCA3, the aggregates are ubiquitinated, indicating that the disease protein may be flagged for UPS degradation [13]. However, once proteins are aggregated, UPS degradation is either inefficient or impossible. The presence of ubiquitinated aggregates therefore likely represents the overloading or failure of the proteasome to degrade soluble polyQ protein [8]. Although it is debated how and at

what stage in disease, general proteasomal overload does seem to occur during polyQ disease progression. This may be deduced from the increased presence of the ubiquitin transcription frameshift mutant UBB<sup>+1</sup> in post-mortem tissue of SCA3 patients. Molecular misreading of ubiquitin to UBB<sup>+1</sup> also occurs in healthy cells, where it is quickly degraded by a normally functioning UPS and thus hardly detectable [30, 31].

In this study, we performed a quantitative analysis of aggregation profiles in the base of the pons of 8 SCA3 patients in relation to changes in components of the PQC. We found a reproducible distribution of the different aggregate types and observed UBB<sup>+1</sup> and aberrant HSPA1A/DNAJB1 expression in a specific co-staining pattern related to aggregate formation, from which we propose a model for neuronal cell pathology and PQC failure in SCA3.

### Materials and Methods

#### *Patients and controls.*

Brains of 8 SCA3 patients (4 males, 4 females, mean age at death  $61 \pm 15$  years) and 5 controls without medical histories of neuropsychiatric diseases (3 males, 2 females, mean age at death  $56 \pm 26$  years) (Table 7.1) were analyzed. Informed consent was obtained from all patients, in accordance with the Medical Ethical Committee of the UMCG where the autopsies were performed. All brains were fixed for 2 weeks in a 4% phosphate-buffered, aqueous formaldehyde solution (pH 7.4). Tissue blocks were embedded in paraffin and cut into 5  $\mu$ m thick sections.

| Patient Number | Age at death | Gender | Disease | CAG-repeats |
|----------------|--------------|--------|---------|-------------|
| 1              | 27           | M      | Control |             |
| 2              | 43           | F      | Control |             |
| 3              | 62           | F      | Control |             |
| 4              | 84           | M      | Control |             |
| 5              | 75           | M      | Control |             |
| 6              | 34           | F      | SCA3    | 14/77       |
| 7              | 42           | F      | SCA3    | 23/75       |
| 8              | 63           | M      | SCA3    | n.d.        |
| 9              | 67           | F      | SCA3    | n.d.        |
| 10             | 70           | M      | SCA3    | 23/68       |
| 11             | 70           | F      | SCA3    | 14/68       |
| 12             | 71           | M      | SCA3    | 24/70       |
| 13             | 73           | M      | SCA3    | 28/65       |

**Table 7.1: Synopsis of the SCA patients and control individuals studied**

Brain materials from control individuals and SCA3 patients. List of patient number, age at death, gender, diagnosis and CAG repeats, if available. Patients 8 and 9 are as of yet not genotyped, but are clinically diagnosed with SCA3 and from known SCA3 families. Control patients were without history of neurodegenerative or psychiatric diseases.

### *Immunohistochemistry*

Sections were deparaffinated and rehydrated with a xylol/ethanol sequence. For antigen retrieval, slides were transferred into tris/HCl buffer (pH 9.5), heated 3 x 10 min to 95°C (p62 (rabbit), HSPA1A). For p62 (mouse), 1C2, UBB<sup>+1</sup>, slides were then transferred into 98% formic acid for 3 min. Endogenous peroxidases were blocked using 0.3% H<sub>2</sub>O<sub>2</sub>/PBS buffer for 30 min at RT, after which sections were incubated 1h at RT with primary antibodies (Table 7.2) diluted in 1% BSA/PBS. Consecutively, the slides were incubated with peroxidase conjugated secondary and tertiary antibodies for 30 min at RT. After staining with 3,3%-DAB (Sigma), sections were counterstained with hematoxylin, dehydrated in ethanol and coverslipped.

| antibody          | clone                   | donor species | Source                 | Working dilution | AR   |
|-------------------|-------------------------|---------------|------------------------|------------------|------|
| p62               | D3                      | mouse         | Santa Cruz             | 1:100            | MW-  |
| 1C2               | 5TF1-1C2-172            | mouse         | Chemicon               | 1:3200           | MW+  |
| Ubiquitin         | Polyclonal              | Rabbit        | Dako                   | 1:200            | None |
| UBB <sup>+1</sup> | Ubi2A (bleeding 180398) | Rabbit        | Van Leeuwen Laboratory | 1:100            | MW+  |
| HSPA1A            | Polyclonal              | Mouse         | Stressgen              | 1:100            | MW-  |
| HSPA1A            | Polyclonal              | Rabbit        | Abcam                  | 1:100            | MW-  |
| DNAJB1            | Polyclonal              | Rabbit        | Stressgen              | 1:100            | MW-  |

**Table 7.2: Information on the primary antibodies.**

AR: antibody retrieval (None; MW-: microwave 3x 10 min Tris/HCl pH9; MW+: microwave 3x 10 min Tris/HCl pH9, followed by 3 min 99% formic acid at RT)

For double immunofluorescent staining, sections were treated with 1% sodium borohydrate (Sigma) for 10 min to quench autofluorescence. The slides were blocked with 5% normal goat serum (Vector) in PBS containing 0.03% Triton X-100 (Sigma) for 30 min. Next, sections were incubated at 4°C overnight with various primary antibody combinations, washed in PBS and incubated for 3h at RT with goat anti-mouse Alexa488 (Invitrogen) and goat anti-rabbit Cy3 (Jackson ImmunoResearch) secondary antibodies. For additional quenching of autofluorescence, sections were treated with 0.05% sudan black solution (Merck) for 10 min at room temperature, washed 8 times in PBS and coverslipped with Mowiol (Sigma). For quantitative evaluation, 100 neurons per case were scored. Non-parametric tests were performed with the SPSS version 16.0 software package.



## Results

### *Characterization of polyQ aggregates in the pons of SCA3 patients*

Using the 1C2 antibody, which recognizes any polyQ repeat of 38+ [28], we first analyzed the types of aggregates present in the basal pons of 8 SCA3 brains (Fig. 7.1). Individual neurons exhibited a variety of staining patterns consistent with earlier observations [35]. Neuronal Nuclear Inclusion bodies (NNI), defined as clearly demarked and strongly stained round objects within the neuronal nucleus, not in contact with the outer membrane, are frequently reported inclusions (Fig. 7.1A). Besides NNI, Diffuse Nuclear Staining (DNS), defined as uncondensed and evenly distributed or slightly grainy (Fig. 7.1B), was detected in a majority neurons. Furthermore, a subset of neurons was found to contain Granular Cytoplasmic Staining (GCS), with the granules being usually smaller than NNIs (Fig. 7.1C).

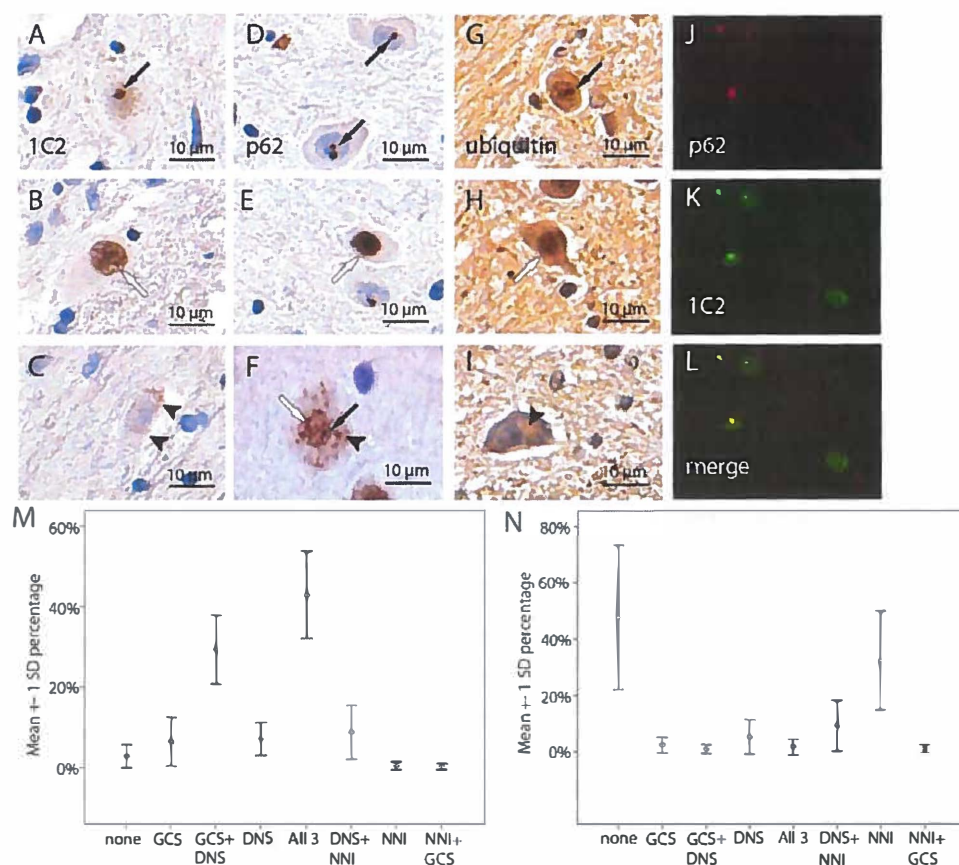


**Figure 7.1: Analysis of aggregate types and frequencies.**

Immunostaining of polyglutamine aggregates with 1C2 (A-C), p62 (D-F) and ubiquitin (G-I) and 1C2/p62 double staining (J-L). NNIs (arrows) (A,D,F,G), DNS (open arrows) (B,E,F,H) and GCS (arrowheads) (C,F,I) exhibit different staining qualities and intensities, depending on the antibody employed. Note the combination of staining patterns in figure F. In all cases, the 1C2/p62 staining co-localizes in NNI (J-L: 1C2 (green) and p62 (red)). Frequency distribution of 1C2- (M) and p62-positive (N) aggregate types (mean  $\pm$  1 SD).

For each patient, the frequency of the aggregate types was scored by 3 independent observers in 100 neurons per patient. Scoring was highly reproducible (Fig. 7.2) and all patients show highly comparable aggregation patterns (Fig. 7.1M), with most neurons containing a mix of NNI, DNS or GCS, and a notable absence of the NNI/GCS combination (Fig. 7.1M). In this study, the average percentage of neurons showing staining patterns including the disease hall-mark NNI was 62% in the fluorescent stainings and 53% in positive contrast.

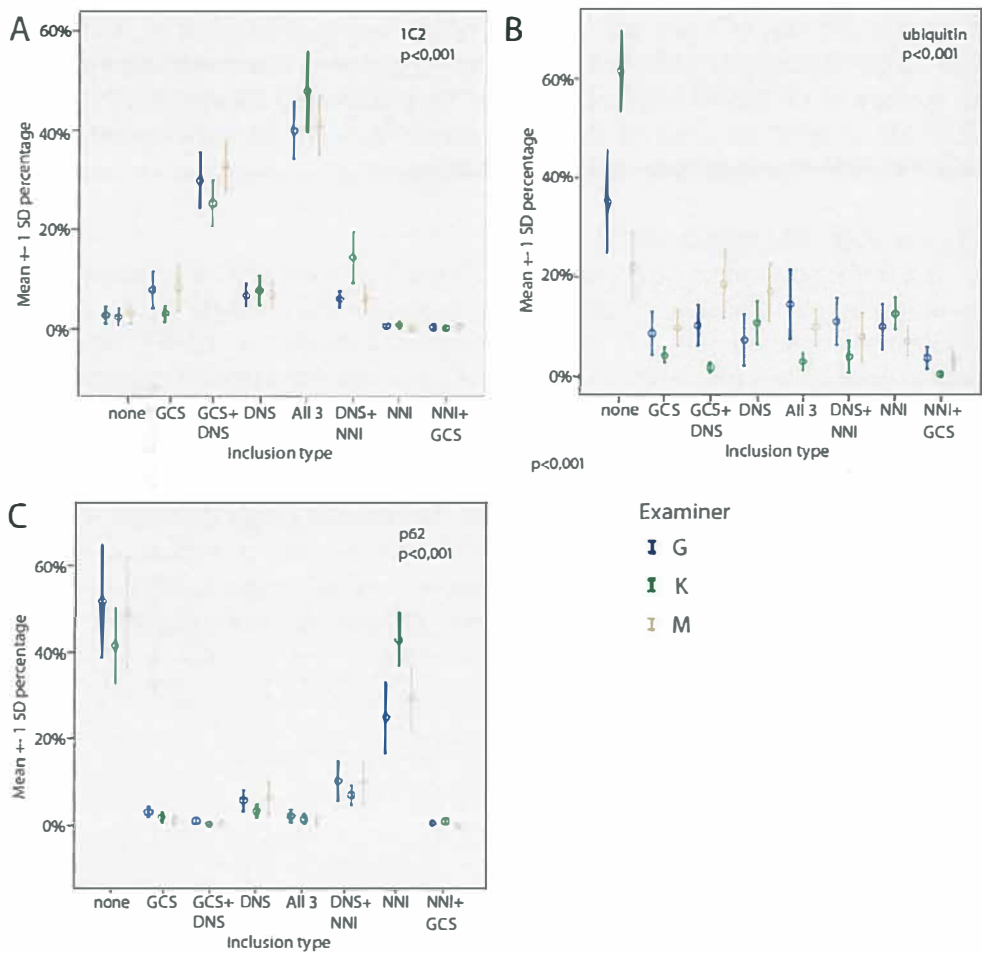


**Fig. 7.2: Scoring reproducibility.** Relative incidence of a given inclusion type as scored by 3 independent researchers. Scoring reproducibility for all stainings, 1C2 (A), Ubiquitin (B) and p62 (C), was highly significant (P values < 0.001). 1C2 and p62, but not ubiquitin staining, (B) showed a distinct distribution of aggregation types.

Another marker frequently used for detection of protein aggregation is the p62 protein [5,34]. P62 is primarily implicated in protein degradation pathways, especially autophagy, but is also known to participate in the formation of inclusions of disease proteins [5,34]. The p62 antibody stains NNIs, DNS as well as GCS (Fig. 7.1D-F) but preferentially detects NNI (Figs. 7.1N and 7.1C). In contrast, a ubiquitin antibody decorated all types of aggregates with no preference (Figs. 7.1G-I and 7.2B).

Comparing the 1C2 and p62 staining pattern with a fluorescent staining protocol (Fig. 7.1J-L) confirmed that 1C2 and p62 staining indeed always overlapped in NNI, while this was rarely the case for DNS and GCS staining patterns. The distribution of these stages, the lack of GCS/NNI combinations, and the preferential staining of NNI by the p62 antibody suggest an order of events in which GCS are an initial event, whilst neurons with NNI represent later stages of pathology.

#### *PolyQ aggregates and protein quality control*

UBB<sup>+1</sup> is a frame shift mutant of ubiquitin, resulting from molecular misreading which occurs at low levels in healthy conditions, and is usually undetectable due to its rapid proteasomal degradation [30, 31]. Upon proteasomal inhibition, UBB<sup>+1</sup> levels can increase to detectable levels and thus can be used as a suitable marker for proteasomal dysfunction in post-mortem tissue [11], and can by itself exert a toxic influence onto the affected neurons [9]. Using double staining with either 1C2 or p62 together with UBB<sup>+1</sup> specific antibodies, we observed that UBB<sup>+1</sup> was found exclusively in neurons containing NNI (Fig. 7.3) but not DNS or GCS, and located primarily in the NNI. All UBB<sup>+1</sup> positive NNI co-stained with either 1C2 or p62, but only a fraction of 1C2/p62 positive NNI (27% of NNI containing neurons, 17% of all neurons, n=300) showed UBB<sup>+1</sup> labeling, suggesting that only a fraction of neurons containing NNI exhibit signs of proteasomal dysfunction.

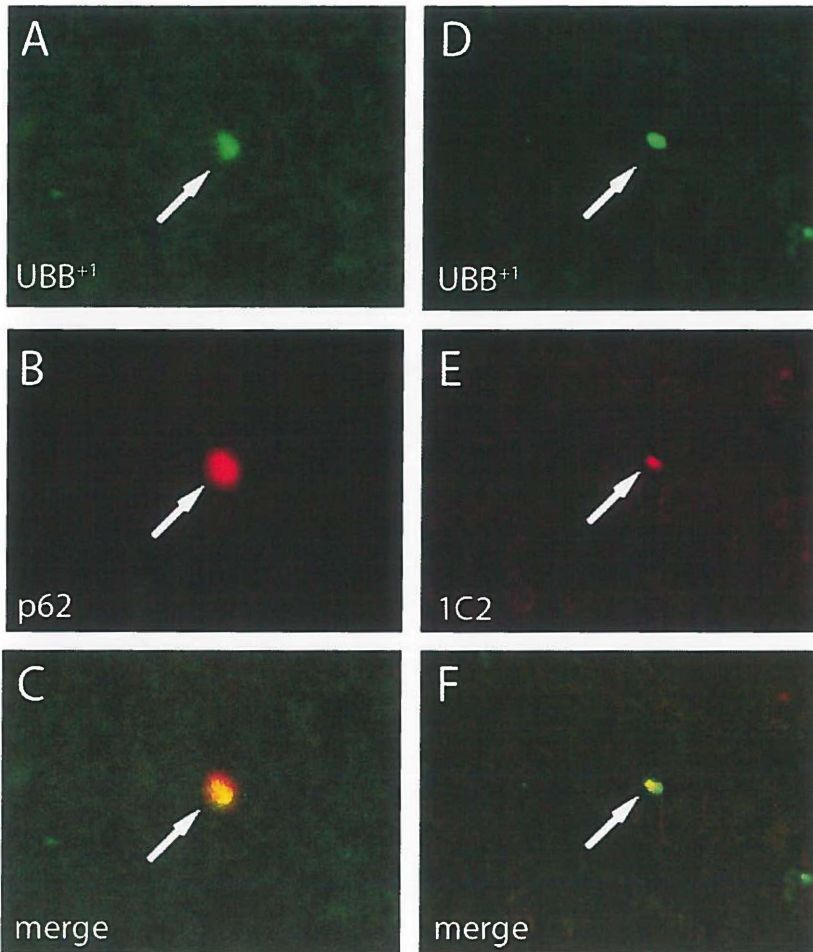


**Figure 7.3: Co localization of UBB<sup>+</sup> with p62 and 1C2.**

Double staining with p62/UBB<sup>+</sup> (A-C) and 1C2/UBB<sup>+</sup> (D-F). UBB<sup>+</sup> staining co localizes with some (arrows) but not all (arrowheads) p62 and 1C2 positive NNI (A-F). (A-C: p62 – red, UBB<sup>+</sup> – green; D-F: 1C2 – red, UBB<sup>+</sup> – green).

A central element in protein homeostasis is formed by molecular chaperones, especially those of the family of heat shock proteins (HSPs). Several HSPs have been implicated in disease processes, especially DNAJB1 as a modifier of age of onset in SCA3 [36]. In the pons of unaffected individuals, all neuronal cells showed moderate DNAJB1 staining primarily in the cytoplasm (Fig. 7.4A). The same was found in most neuronal cells from the SCA3 patients (Fig. 7.4B). Double fluorescent staining of 1C2 and DNAJB1 showed that 85% of all NNI were immunoreactive for DNAJB1 (Fig. 7.5A-C). Most of these neurons still showed a diffuse cytoplasmic and nuclear staining (Fig. 7.5A-C). However, a small fraction of all neurons (6%) showed a marked



decrease of cytoplasmic staining combined with sequestration of the DNAJB1 into the NNI (Fig. 7.5D-F). Cells without a NNI never displayed this absence of cytoplasmic DNAJB1 staining.

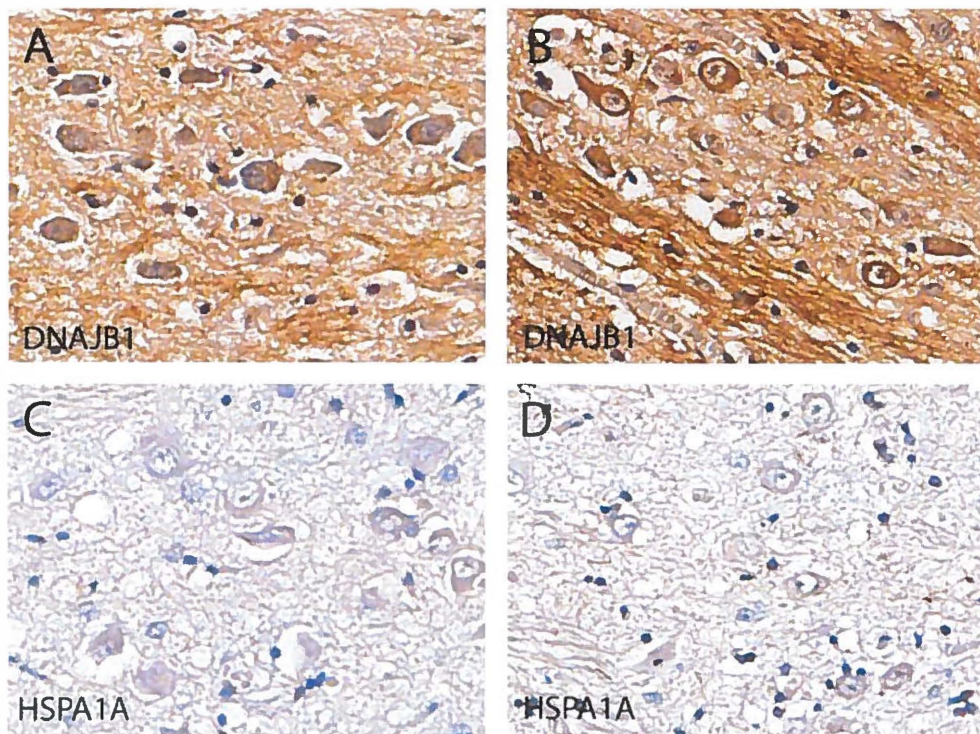


**Figure 7.4: DNAJB1 and HSPA1A stainings in healthy and diseased brain tissue.**

Photomicrograph of a positive contrast single staining of the pontine nuclei with DNAJB1 (A, B) and HSPA1A (C, D) (DAB staining, brown). There is no discernable difference in neuronal staining intensity between healthy (A, C) and diseased tissue (B, D). Counterstaining with hematoxylen.

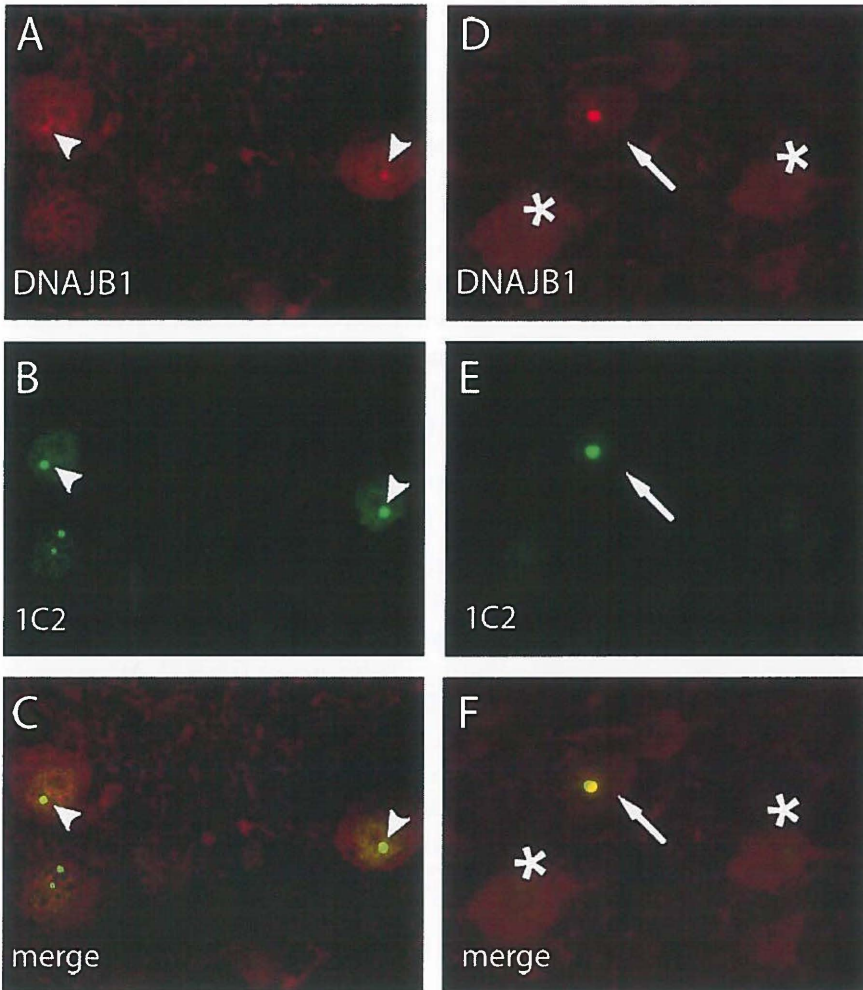


**Figure 7.5: Co-localization of aggregates with DNAJB1 and sequestration of DNAJB1 into the NNI.**

Fluorescent double staining with the 1C2 and DNAJB1 antibodies. The antibody labels the majority (85%) of all NNI (arrowheads). In a subset of neurons (6%), DNAJB1 is largely sequestered into the NNI, as can be seen by a lower intensity of somatic staining (arrow) compared to other neurons (asterisks).

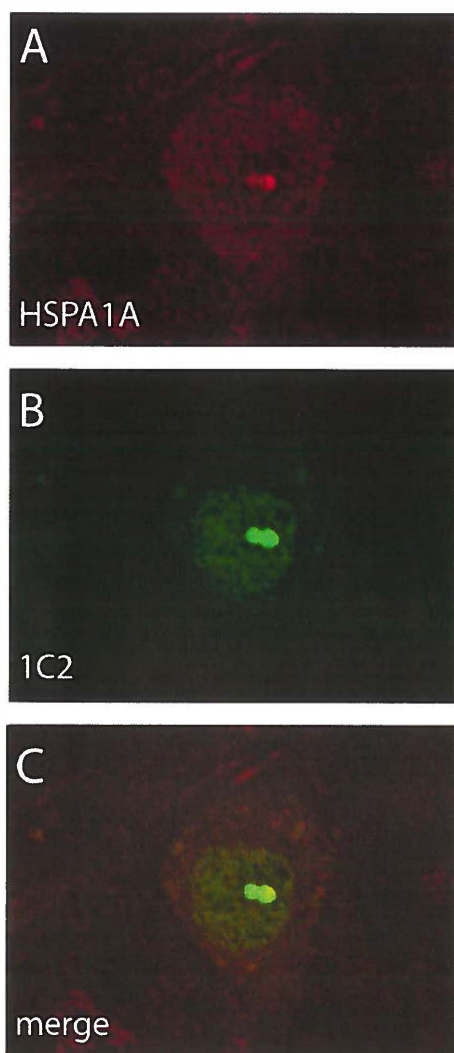


**Figure 7.6: Co-localization of 1C2 with HSPA1A.**

Fluorescent double staining demonstrates co-localization of aggregates (1C2: green) with HSPA1A (red) in the NNI of affected neurons.

Finally, we performed double immunolabelling with antibodies against p62, UBB<sup>+</sup>, or DNAJB1 combined with a specific antibody against the stress-inducible member of the HSP70 family, HSPA1A. In most neurons, HSPA1A is found at low basal levels in the cytoplasm both in control and SCA3 brain (Fig. 7.4C,D). A majority of NNI were HSPA1A immunoreactive as revealed by the 1C2 co-staining (Fig. 7.6), consistent with in vitro data and previous work in human brains [6], indicating that HSPA1A is recruited into the NNI. Interestingly, combined staining of UBB<sup>+</sup> with HSPA1A revealed a subset of UBB<sup>+</sup> positive neurons that exhibited a marked upregulation of HSPA1A (Fig. 7.7A-C). Double staining of DNAJB1 with HSPA1A revealed that particularly in cells lacking cytoplasmic DNAJB1 staining and full sequestration of DNAJB1 into the NNI, HSPA1A intensities were drastically elevated (Fig. 7.7D-F). In fact, we found an inverse correlation between cytoplasmic HSPA1A and DNAJB1 staining intensities (Fig. 7.8).



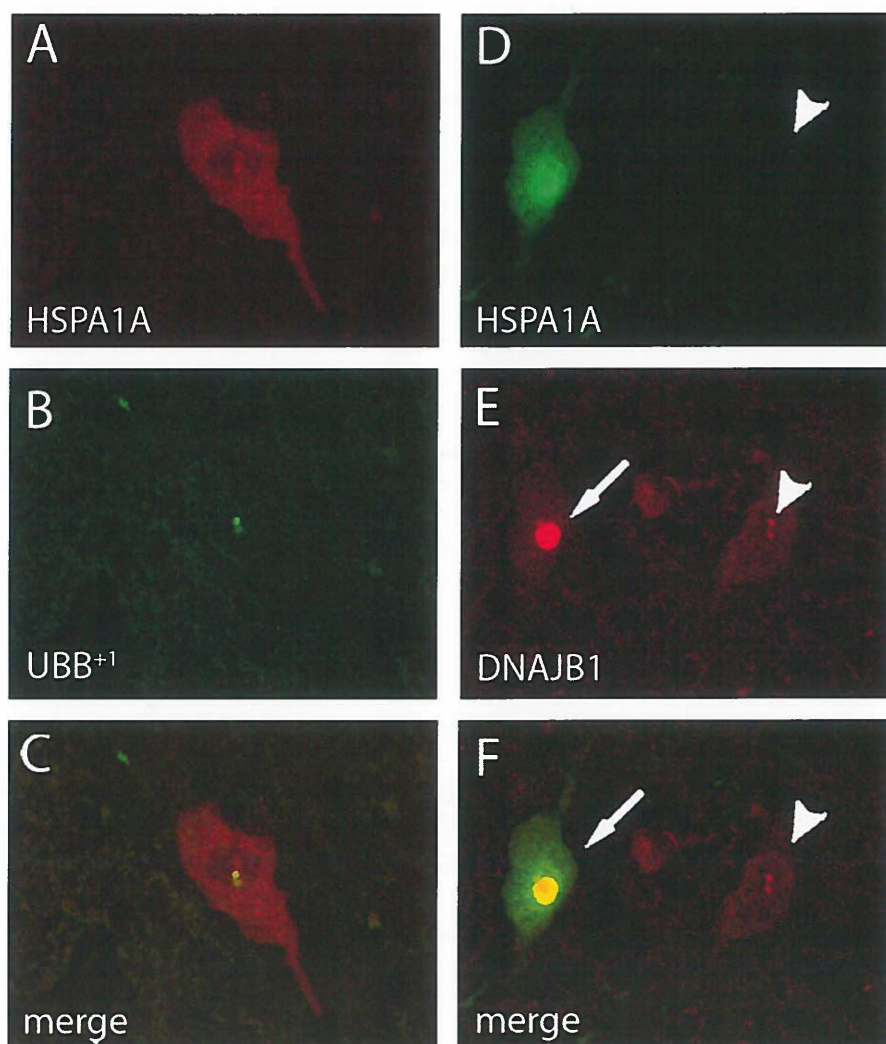


**Figure 7.7: DNAJB1 sequestration into NNI and HSPA1A up-regulation.**

Double staining with UBB<sup>+</sup>/HSPA1A (A-C) and DNAJB1/HSPA1A (D-F) showing positivity of UBB<sup>+</sup> in a subset of neurons both with and without changes in DNAJB1 or HSPA1A in neurons. HSPA1A is strongly up-regulated when DNAJB1 is sequestered from the cytosol into the NNIs (arrow), while other neurons retain their staining (arrowhead). (A-C: p62 – red, UBB<sup>+</sup> – green; D-F: HSPA1A – green, DNAJB1 – red).

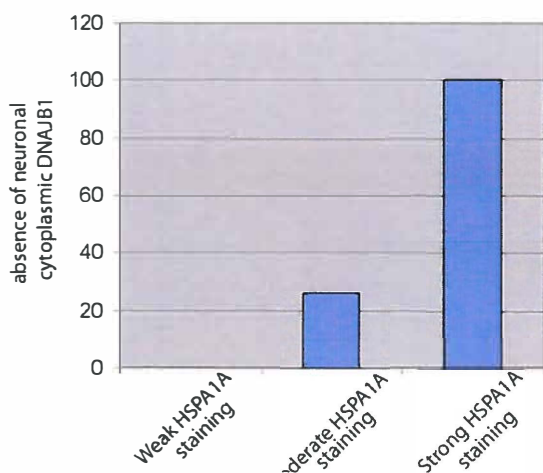


**Figure 7.8: Relative incidence of DNAJB1 sequestration in HSPA1A positive neurons.** Graphical representation of the frequency of NNI entrapped DNAJB1 in relation to the staining intensity of HSPA1A (n=105).

## Discussion

In this manuscript, we quantitatively analyzed different forms of protein aggregates in post-mortem brains of SCA3 patients in relation to differential expression of components of the PQC. Furthermore, our data suggest that components of the PQC only respond to and become impaired at a late stage during the aggregation process. From this, we propose a sequence of events taking place during the aggregation process of SCA3.

Using 1C2 antibodies as protein aggregation marker, we found neurons not only to contain Neuronal Nuclear Inclusion bodies (NNI), the canonical aggregates that hallmark SCA3 [22], but also diffuse aggregates throughout the nucleus (DNS) and granular aggregates in the cytoplasm (GCS), consistent with earlier reports [35]. Frequently, combinations of the 3 staining types were observed, except for the combined CGS/NNI patterns that were never found. Another aggregation marker, the p62 protein, had a clear preference for NNI, with GCS and DNS type labeling being both less frequent and less intensive.

In parallel to these aggregation patterns, we studied the distribution of PQC markers. As marker for proteasomal overload we used UBB<sup>+1</sup> [30 31]. The presence of UBB<sup>+1</sup> in a subset of NNI containing neurons suggests that a fraction of neurons exhibit signs of proteasomal dysfunction and that GCS and DNS may represent earlier, less stressful stages of aggregation pathology, since they do not display detectable levels of UBB<sup>+1</sup>.

As markers for (proteotoxic) stress, we monitored the expression of the stress inducible HSPA1A chaperone and the co-chaperone DNAJB1 [16, 24]. Somewhat surprisingly, HSPA1A was only found to be up-regulated in a subset of UBB<sup>+1</sup> positive neurons: in fact, only those UBB<sup>+1</sup> positive, NNI containing neurons that concomitantly have lost somatic staining of the HSP70 co-chaperone DNAJB1 showed this HSPA1A up-regulation. This shows that neurons do not display a heat shock response in the presumed early stages of aggregation of the polyQ protein (DNS, GCS).

*Staging of the Aggregation process*

Based on these observations, we propose the following model for the sequence of events in SCA3 neurons (Fig. 7.9): Neurons containing 1C2-stained GCS (stage 1) and DNS (stage 2) are only rarely positive for p62. Formation of NNI (stage 3) likely represents a more advanced stage of the aggregation process, as they are constitutively labeled by p62. The progressive protein aggregation next leads to proteasomal impairment (stage 4) as supported by the UBB<sup>+1</sup> staining, only present in neurons with NNI. The final stage (stage 5) is characterized by the up-regulation of HSPA1A, while at the same time the co-chaperone DNAJB1 is sequestered into the NNI.

In this model, the transition from cells exhibiting aggregation of disease protein into GCS towards DNS and NNI during stages 1 to 3 is supported by the lack of GCS/NNI combinations and the preferential staining of NNI by the p62 antibody. P62 is implicated in active aggregation processes, as knocking out p62 in model organisms leads to absence of aggregates and enhanced proteotoxicity [34]. This also suggests that NNI are not necessarily toxic and may even reflect active protective mechanisms of temporal storage of aggregating protein [1, 5, 29]. However, while cytoplasmic inclusions might be subject to autophagosomal degradation [5, 10, 15], this may be less likely for inclusions within the nucleus. While polyQ proteins can be shuttled out of the nucleus [14], it is a highly aggregation-prone environment in which small aggregates may rapidly nucleate to large aggregates which then can no longer be transported through the nuclear membrane [18].

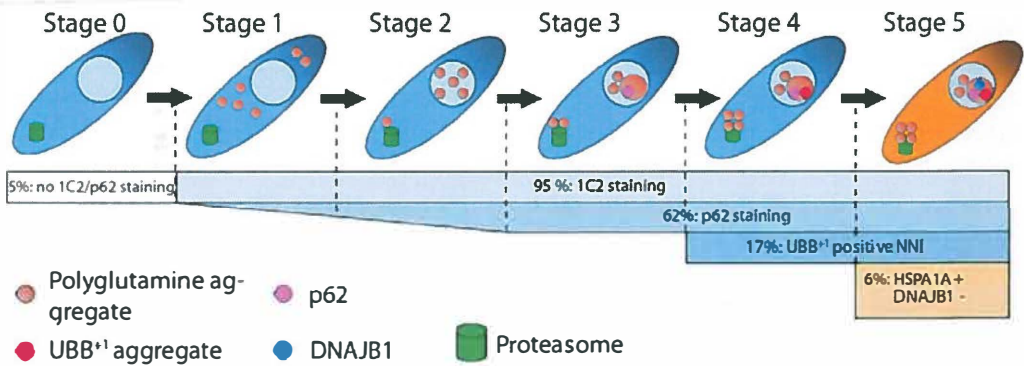


**Figure 7.9: Model for progressive changes in protein quality control in human SCA3.**

Aggregating ataxin3 (brown dots) occurs first as GCS, progresses via DNS to NNI. Proteasomal dysfunction, marked by UBB<sup>+1</sup> (red dots), only occurs in neurons with NNI. Up-regulation of HSPA1A is associated with DNAJB1 sequestration into NNI. Frequencies of all stages as derived from all quantifications are given in the bars.

Although in vitro data are inconclusive regarding the precise interference of polyQ aggregates with the proteasome [8], the presence of UBB<sup>+1</sup> during stage 4 hints at an impairment of the proteasomal system. Its function could either be inhibited due to

saturation of the ability to sequester polyQ aggregates (overloading the proteasome) or due to direct sequestration of elements of the proteasome (loss of function) [3].

The up-regulation of HSPA1A demarks the final stage (stage 5) of the progressive aggregation pathology. The constitutive expression of chaperones might be able to temporarily counterbalance the deficit in proteostasis caused by the impairment of proteasomal function. Long term benefits, however seem unlikely. Indeed, the HSP70 overexpressing neurons showed morphological abnormalities (Fig 7.7) indicative of poor health.

It is striking to note that the stress response seems to be activated only so late during pathogenesis, given its potential to interfere with misfolded proteins. However, the heat shock response (HSR) is self-regulating and induced in a stress-dose dependent manner. Given the chronic nature of the disease and the slow accumulation of misfolded proteins over time, this may just be insufficient to induce the HSR. Only when all other systems fail and misfolded protein or/and aggregates accumulate to high quantities HSR seems activated. At this stage, however, cellular damage may already be too severe and the induction of the HSR, amongst which the elevated expression of HSPA1A, is too late and no longer sufficient to be cytoprotective.

Lastly, it is interesting to note that the HSPA1A induction coincided with a sequestration of the constitutively expressed DNAJB1 in the inclusions. DNAJ proteins are generally found to be good suppressors of polyQ aggregation and toxicity [12]. Moreover, we recently found that differential expression of DNAJB1 in SCA3 patients was correlated to the age at onset in addition to CAG repeat length [36]. This raises the hypothesis that the recruitment of DNAJB1 proteins into the NNI in parallel with its cytosolic disappearance reflects a failure of these chaperones to maintain the misfolded polyQ proteins in a state competent for (proteasomal) degradation, and raises the question of whether the up-regulation of HSP70 alone has any effect on the aggregating polyQ alone [2].

#### *Implications in terms of neurodegeneration and clinical symptoms*

Whereas our data point to an order of events during SCA3 pathology within a single neuron, the implications of the various stages for neuronal dysfunction and clinical symptoms is far from being understood. Based on our data, it seems conceivable, that entrance of ataxin-3 into the nucleus is necessary but not sufficient to cause cell toxicity [4, 23]. Seemingly, additional pathological processes are required to elicit cellular toxicity, such as sequestration of components of the PQC. Furthermore, it is unlikely that this model describes the only pathological pathway at work in SCA3. In the in vitro situation cells forming only DNS type staining degenerate very readily [1], so in all likelihood, our model only observes the neurons that mount an initially successful adaptor response but later in the process suffer from PQC dysregulation. Also, protein aggregation may act independently of the PQC system, e.g. by sequestration of known interactors of polyQ proteins and by blockade of axonal transport processes [17, 26]. Likely, SCA3 and possibly other protein aggregation

diseases exhibit several pathological pathways, running in parallel, but mounting cumulative stress on the long lived neurons.

Although the observed patterns were highly reproducible amongst 8 different patients that all died at different ages, the limitation of our study, is of course, that it has been done in post-mortem tissue where we only see the end stage situation. Therefore, longitudinal studies in animal models will be required to further test our proposed model. Also, it would be interesting to see whether such a chain of events also applies to other polyQ diseases (e.g. HD or SBMA), how this compares to some other SCAs that do not exhibit NNI (e.g. SCA2 and SCA6), or at what stages the disease process can be reversed. Furthermore, since p62 is a well known component of autophagic pathways, an investigation of the state of autophagy in human SCA3 tissue would be of interest. What our data again stress is that PQC impairment is a major issue in polyQ diseases and that, likely due to its chronic nature, these systems are not responsive enough to counteract the ongoing, progressive aggregation. Together with the in vitro data and data with models systems, this therefore reemphasizes that boosting the HSR or components thereof could be of potential clinical relevance.

### **Acknowledgements**

This work was supported by the Prinses Beatrix Foundation (WAR05-0129) awarded to E.R. Brunt and H.H. Kampinga, Jan Kornelis de Cock stichting (08-15) awarded to W.F.A. den Dunnen and by support from the Dutch ADCA patient society and GUIDE/BCN awarded to W.F.A. den Dunnen, U. Rüb and H.H. Kampinga. F.W. Van Leeuwen was supported by ISAO (09514), Hersenstichting Nederland (2008.17 and 15F07.48), the Prinses Beatrix Foundation (MAR 99-0113), IPF 2008 and Van Leersum Foundation KNAW 2008.



## References

1. Arrasate M, Mitra S, Schweitzer ES, Segal MR, Finkbeiner S. Inclusion body formation reduces levels of mutant huntingtin and the risk of neuronal death. *Nature* 2004;431:805-810.
2. Bailey CK, Andriola IF, Kampinga HH, Merry DE. Molecular chaperones enhance the degradation of expanded polyglutamine repeat androgen receptor in cellular model of spinal and bulbar muscular atrophy. *Hum Mol Genet* 2002;11:515-523.
3. Bennett EJ, Shaler TA, Woodman B, Ryu KY, Zaitseva TS, Bekcer CH, Bates GP, Schulman H, Kopito RR. Global changes to the ubiquitin system in Huntington's disease. *Nature* 2007;448:704-708.
4. Bichelmeier U, Bichelmeier U, Schmidt T, Hübener J, Boy J, Rüttiger L, Häbig K, Poths S, Bonin M, Knipper M, Schmidt WJ, Wilbertz J, Wolburg H, Laccone F, Riess O. Nuclear localization of ataxin-3 is required for the manifestation of symptoms in SCA3: in vivo evidence. *J Neurosci* 2007;27:7418-7428.
5. Bjorkoy G, Lamark T, Brech A, Outzen H, Perander M, Overvatn A, Stenmark H, Johansen T. p62/SQSTM1 forms protein aggregates degraded by autophagy and has a protective effect on huntingtin-induced cell death. *J Cell Biol* 2005;171:602-614.
6. Chai Y, Koppenhafer SL, Bonini NM, Paulson HL. Analysis of heat shock protein (HSP) molecular chaperones in polyglutamine disease. *J Neurosci* 1999;19:10338-10347.
7. Ciechanover A. The ubiquitin-proteasome pathway: on protein death and cell life. *EMBO J* 1998; 17:7151-7160.
8. Davies JE, Sarkar S, Rubinsztein DC. The ubiquitin proteasome system in Huntington's disease and the spinocerebellar ataxias. *BMC Biochem* 2007;8(Suppl 1): S2.
9. de Pril R, Hobo B, van Tijn P, Roos RA, van Leeuwen FW, Fischer DF. (2010) Modest proteasomal inhibition by aberrant ubiquitin exacerbates aggregate formation in a Huntington disease mouse model. *Mol Cell Neurosci* 2010;43:281-286.
10. Filimonenko M, Isakson P, Finley KD, Anderson M, Jeong H, Melia TJ, Bartlett BJ, Myers KM, Birkeland HC, Lamark T, Krainc D, Brech A, Stenmark H, Simonsen A, Yamamoto A. The selective macroautophagic



degradation of aggregated proteins requires the PI3P-binding protein Alfy. *Mol Cell* 2010;23:265-279.

11. Fischer DF, De Vos RA, Van Dijk R, De Vrij FM, Proper EA, Sonnemans MA, Verhage MC, Sluijs JA, Hobo B, Zouambia M, Steur EN, Kamphorst W, Hol EM, Van Leeuwen FW. Disease-specific accumulation of mutant ubiquitin as a marker for proteasomal dysfunction in the brain. *FASEB J* 2003;17:2014-2024.
12. Hageman J, Rujano MA, van Waarde MA, Kakkar V, Dirks RP, Govorukhina N, Oosterveld-Hut HM, Lubsen NH, Kampinga HH. A DNAJB chaperone subfamily with HDAC-dependent activities suppresses toxic protein aggregation. *Mol Cell* 2010;37:355-369.
13. Hayashi M, Kobayashi K, Furuta H. Immunohistochemical study of neuronal intranuclear and cytoplasmic inclusions in Machado-Joseph disease. *Psych Clin Neurosci* 2003;57:205-213.
14. Jeong H, Then F, Melia TJ Jr, Mazzulli JR, Cui L, Savas JN, Voisine C, Paganetti P, Tanese N, Hart AC, Yamamoto A, Krainc D. Acetylation targets mutant huntingtin to autophagosomes for degradation. *Cell* 2009;137:60-72.
15. Johnston JA, Ward CL, Kopito RR. Aggresomes: a cellular response to misfolded proteins. *J Cell Biol* 1998;143:1883-1898.
16. Kampinga HH, Craig EA. The HSP70 chaperone machinery: J proteins as drivers of functional specificity. *Nat Rev Mol Cell Biol* 2010;11:579-592.
17. Matilla-Duenas A, Matilla-Dueñas A, Sánchez I, Corral-Juan M, Dávalos A, Alvarez R, Latorre P. Cellular and molecular pathways triggering neurodegeneration in the spinocerebellar ataxias. *Cerebellum* 2010;9:148-166.
18. Michels AA, Nguyen VT, Konings AW, Kampinga HH, Bensaude O. Thermostability of a nuclear-targeted luciferase expressed in mammalian cells. Destabilizing influence of the intranuclear microenvironment. *Eur J Biochem* 1005;234:382-389.
19. Muchowski PJ, Muchowski PJ, Schaffar G, Sittler A, Wanker EE, Hayer-Hartl MK, Hartl FU. HSP70 and hsp40 chaperones can inhibit self-assembly of polyglutamine proteins into amyloid-like fibrils. *Proc Natl Acad Sci USA* 2000;97:7841-7846.
20. Nollen EA, Brunsting JF, Roelofsen H, Weber LA, Kampinga HH. In vivo chaperone activity of heat shock protein 70 and thermotolerance. *Mol Cell Biol* 1999;19:2069-2079.

21. Orr HT, Zoghbi HY. Trinucleotide repeat disorders. *Annu Rev Neurosci* 2007;30:575-621.
22. Paulson H. Protein fate in neurodegenerative proteinopathies: Polyglutamine diseases join the (mis)fold. *Am J Hum Genet* 1999;64:339-345.
23. Rüb U, de Vos RA, Brunt ER, Sebestény T, Schöls L, Auburger G, Bohl J, Ghebremedhin E, Gierga K, Seidel K, den Dunnen W, Heinsen H, Paulson H, Deller T. Spinocerebellar ataxia type 3 (SCA3): thalamic neurodegeneration occurs independently from thalamic ataxin-3 immunopositive neuronal intranuclear inclusions. *Brain Pathol* 2006;16:218-227.
24. Rujano MA, Kampinga HH. The HSP70 chaperone machine as guardian of the proteome: implications for protein misfolding diseases. In *Heat Shock Proteins and Medicine*. Eds Radons J, Multhoff G. Kerela, India: Research Signpost, 2006:59-85.
25. Schöls L, Bauer P, Schmidt T, Schulte T, Riess O. Autosomal dominant cerebellar ataxias: clinical features, genetics and pathogenesis. *Neurology* 2004;3:291-304.
26. Seidel K, den Dunnen WF, Schultz C, Paulson H, Frank S, de Vos RA, Brunt ER, Deller T, Kampinga HH, Rüb U. Axonal inclusions on spinocerebellar ataxia type 3. *Acta Neuropathol* 2010;120:449-460.
27. Soto C. Unfolding the role of protein misfolding in neurodegenerative diseases. *Nat Rev Neurosci* 2003;4:49-60.
28. Trottier Y, Lutz Y, Stevanin G, Imbert G, Devys D, Cancel G, Saudou F, Weber C, David G, Tora L, Agid Y, Brice A, Mandel JL. Polyglutamine expansion as a pathological epitope in Huntington's disease and four dominant cerebellar ataxias. *Nature* 1995;378:403-406.
29. van Ham TJ, Holmberg MA, van der Goot AT, Teuling E, Garcia-Arencibia M, Kim HE, Du D, Thijssen KL, Wiersma M, Burggraaff R, van Bergeijk P, van Rheen J, Jerre van Veluw G, Hofstra RM, Rubinsztein DC, Nollen EA. Identification of MOAG-4/SERF as a regulator of age-related proteotoxicity. *Cell* 2010;142:601-612.
30. van Leeuwen FW, de Kleijn DP, van den Hurk HH, Neubauer A, Sonnemans MA, Sluijs JA, Köycü S, Ramdjielal RD, Salehi A, Martens GJ, Grosveld FG, Peter J, Burbach H, Hol EM. Frameshift mutants of beta amyloid precursor protein and ubiquitin-B in Alzheimer's and Down patients. *Science* 1998;279:242-247.

31. van Tijn P, Verhage MC, Hobo B, van Leeuwen FW, Fischer DF. Low levels of mutant ubiquitin are degraded by the proteasome in vivo. *J Neurosci Res* 2010;88:2325-2337.
32. Vos MJ, Hageman J, Carra S, Kampinga HH. Structural and functional diversities between members of the human HSPB, HSPH, HSPA and DNAJ Chaperone families. *Biochemistry* 2008;47:7001-7011.
33. Williams AJ, Paulson HL. Polyglutamine neurodegeneration: Protein misfolding revisited. *Trends Neurosci* 2008;31:512-518.
34. Wooten MW, Hu X, Babu JR, Seibenhener ML, Geetha T, Paine MG, Wooten MC. Signaling, polyubiquitination, trafficking, and inclusions: sequestosome 1/p62's role in neurodegenerative disease. *J Biomed Biotechnol* 2006;2006:62079.
35. Yamada M, Sato T, Tsuji S, Takahashi H. CAG repeat disorder models and human neuropathology: similarities and differences. *Acta Neuropathol* 2008;115:71-86.
36. Zijlstra MP, Rujano MA, Van Waarde MA, Vis E, Brunt ER, Kampinga HH. Levels of DNAJB family members (HSP40) correlate with disease onset in patients with spinocerebellar ataxia type 3. *Eur J Neurosci* 19 [Epub ahead of print].



## Chapter 8

---

# **The HSPB8-BAG3 chaperone complex is upregulated in astrocytes in the human brain affected by protein aggregation diseases**

---

Kay Seidel<sup>1\*</sup>, Jonathan Vinet<sup>2\*</sup>, Wilfred F.A. den Dunnen<sup>1</sup>, Ewout R. Brunt<sup>3</sup>, Melanie Meister<sup>4</sup>, Alessandra Boncoraglio<sup>4</sup>, Marianne P. Zijlstra<sup>4</sup>, Hendrikus W.G.M. Boddeke<sup>2</sup>, Udo Rüb<sup>5</sup>, Harm H. Kampinga<sup>4</sup> and Serena Carra<sup>4</sup>

<sup>1</sup> *Department of Pathology and Medical Biology, University Medical Centre Groningen, University of Groningen, Hanzeplein 1, 9713 RB, Groningen, the Netherlands.*

<sup>2</sup> *Department of Neuroscience, Section Medical Physiology, University of Groningen, Antonius Deusinglaan 1, 9713 AV, Groningen, The Netherlands.*

<sup>3</sup> *Department of Neurology, University Medical Centre Groningen, University of Groningen, Hanzeplein 1, 9713 RB, Groningen, the Netherlands*

<sup>4</sup> *Department of Cell Biology, University of Groningen, Antonius Deusinglaan 1, 9713 AV, Groningen, the Netherlands.*

<sup>5</sup> *Institute of Clinical Neuroanatomy, Dr. Senckenberg Chronomedical Institute, J. W. Goethe University, Theodor-Stern-Kai 7, D-60950, Frankfurt/Main, Germany.*

\* these authors equally contributed to the work

Neuropathology and applied neurobiology, 2011 Jun 23. doi: 10.1111/j.1365-2990.2011.01198.x.

[Epub ahead of print]

## Abstract

**Aims:** HSPB8 is a small heat shock protein that forms a complex with the co-chaperone BAG3. Overexpression of the HSPB8-BAG3 complex in cells stimulates autophagy and facilitates the clearance of mutated aggregation-prone proteins, whose accumulation is a hallmark of many neurodegenerative disorders. HSPB8-BAG3 could thus play a protective role in protein aggregation diseases and might be specifically upregulated in response to aggregate-prone protein-mediated toxicity. Here we analyzed HSPB8-BAG3 expression levels in post mortem human brain tissue from patients suffering of the following protein conformation disorders: Alzheimer's disease (AD), Parkinson's disease (PD), Huntington's disease (HD) and spinocerebellar ataxia type 3 (SCA3). **Methods:** Western Blotting and immunohistochemistry techniques were used to analyze HSPB8 and BAG3 expression levels in fibroblasts from SCA3 patients and post-mortem brain tissues, respectively. **Results:** In all diseases investigated, we observed a strong upregulation of HSPB8 and a moderate upregulation of BAG3 specifically in astrocytes in the cerebral areas affected by neuronal damage and degeneration. Intriguingly, no significant change in the HSPB8-BAG3 expression levels was observed within neurons, irrespective of their localization or of the presence of proteinaceous aggregates. **Conclusions:** We propose that the upregulation of HSPB8 and BAG3 may enhance the ability of astrocytes to clear aggregated proteins released from neurons, cellular debris, maintain the local tissue homeostasis and/or participate in the cytoskeletal remodeling that astrocytes undergo during astrogliosis.



## Introduction

Protein misfolding and aggregation can occur due to external stressors, ageing or genetic factors, and pose a threat to the survival of cells. A number of genetic or idiopathic diseases are characterized by the formation of fibrillar aggregates containing disease-specific protein and by selective neuronal degeneration. These include Alzheimer's disease (AD), Parkinson's disease (PD) and polyglutamine diseases (e.g. Huntington's disease, HD and spinocerebellar ataxia type 3, SCA3) [10, 17, 59]. Although the mutated proteins and the affected neurons/areas differ, aggregates of AD, PD, HD and SCA3 have similar composition and share a  $\beta$ -sheet-rich fibrillar structure [59]. Additionally to the disease-related protein, these aggregates contain components of the protein quality control system including molecular chaperones and ubiquitin, transcription factors and cytoskeletal elements [3, 4, 26, 54]. Sequestration of these elements into the aggregates may result in impairing the function of the protein quality control system, and may contribute to disruption of the cytoskeletal organization, thereby influencing vesicle trafficking and axonal transport, which may all contribute to the pathogenesis [4, 27, 60].

The protein quality control system includes molecular chaperones and degradative systems (ubiquitin-proteasome system, chaperone-mediated autophagy and macroautophagy) [18, 29, 44, 46, 47, 75]. Molecular chaperones of the heat shock protein (HSP) family recognize misfolded polypeptides and in iterative binding and release cycles can assist in protein (re)folding. If (re)folding is not possible or not successful, these iterative cycles may also keep the protein in a degradation competent state and some HSP members may even directly interact with elements of the ubiquitin-proteasome system to promote substrate polyubiquitination and degradation by the proteasome [14, 29, 75]. As such, molecular chaperones can exert protective functions towards mutated aggregate-prone proteins. This is supported by the findings that their upregulation in both cellular and animal models of protein conformation disorders is beneficial by decreasing mutated aggregate-prone protein mediated toxicity [2, 6, 11, 12, 68, 73, 74]. If proteasomal degradation of (soluble) misfolded proteins fails, microaggregates, which can no longer be degraded by the proteasome, can arise [65]. Those microaggregates, however, can still be disposed very efficiently through macroautophagy [5, 51, 52].

Macroautophagy (here referred to as autophagy) allows the degradation of aggregated cytoplasmic material through its sequestration into double-membrane vesicles, called autophagosomes, and their subsequent fusion with lysosomes, which contain proteolytic enzymes [44, 46]. Autophagy has indeed been shown to be of eminent importance in combating aggregation-related toxicity of polyglutamine diseases in both cellular and animal models [5, 6, 51, 52]. Moreover, loss of autophagy causes neurodegeneration in animal models and leads to the accumulation of polyubiquitinated substrates, further highlighting the critical role of this proteolytic process in cell survival, especially under stress conditions [28]. Several molecular chaperones have been shown to participate in autophagy-like degradation processes,

including members of the DNAJ and HSP70 (HSPA) families, BAG1 [15, 16] and the HSPB8-BAG3 chaperone complex [11]. For example, HSP40/DNAJB1 and BAG1 are located at the membrane of lysosomes, where they participate with HSPA8 (the constitutively expressed HSC70) in chaperone-mediated autophagy, a process that allows the selective degradation of proteins containing the specific pentapeptide motif KFERQ [15, 16]. The HSPB8-BAG3 complex induces global macroautophagy and facilitates the autophagy-mediated clearance of mutated polyglutamine proteins [11]. Interestingly, an increase of BAG3 levels has been documented during aging, a condition characterized by a decline in the proteasomal activity and by the progressive accumulation of misfolded proteins [25]. The age-related increase of BAG3 levels has been correlated with a stimulation of autophagy, suggesting that it might represent a compensatory protective response against the accumulation of misfolded aggregate-prone proteins [25]. On the basis of these results, it might be speculated that HSPB8 and BAG3 are upregulated in protein folding diseases and that this might support/contribute to ensure the appropriate disposal of the aggregated proteins.

To investigate whether the HSPB8-BAG3 complex is indeed activated in response to neurodegenerative protein folding diseases, we investigated their expression levels in control and diseased human brains affected by AD, PD, HD or SCA3. Expression patterns of HSPB8 and BAG3 were analyzed in both neuronal and glial cells. Intriguingly, we found no upregulation of HSPB8 and BAG3 within neurons in any of the diseases, irrespective of the presence of proteinaceous aggregates. In contrast, in all four pathological conditions analyzed, HSPB8 and BAG3 expression were upregulated selectively in astrocytes found within the brain regions characterized by neurodegeneration.

## Materials and Methods

### *Brain tissue and fibroblast cultures*

Fibroblast cultures from control (n=6) and SCA3 (n=19) patients were prepared and grown in DMEM supplemented with 15% fetal calf serum. A detailed description of the control and SCA3 patient's age, length of polyglutamine repeat, age of onset and gender is reported in Table 8.1.

Control brains from 14 subjects without any record of neuropsychiatric diseases and 33 brains from patients afflicted with neurodegenerative diseases (AD, PD, HD, SCA3; Table 8.2) were used for immunohistochemistry. Selected tissue regions were extracted from the brain, fixed for 14 days in 4% formalin and embedded in paraffin blocks. After fixation, the blocks were cut into 5  $\mu$ m thick sections in a consecutive series and transferred onto APES coated glass slides. Additionally, tissue samples of the frontal cortex from disease and control patients were frozen for protein analysis. Informed consent during life was obtained from patients suffering from HD or SCA3. Control tissue, as well as tissue from AD and PD patients was obtained during routine diagnostic practice. These tissue blocks were treated according to a national guideline "Code for good use of patient material". All tissue samples were anonymized. The

investigation was approved by the medical ethical committee of the University Medical Center Groningen (UMCG).

#### *Western Blotting*

A denaturing 12,5% SDS-PAGE gel was used to resolve fibroblasts protein extracts. Gels were blotted overnight in 25 mM ethanolamine/glycine pH 9.5 to Hybond-ECL nitrocellulose membranes (Amersham Biosciences). Blocking in PBST (0.1% Tween), containing 5% low-fat milk powder (Nutricia, The Netherlands) was followed by overnight incubation with either rabbit anti-HSPB8 (1:1000) or rabbit anti-BAG3 (1:1000) or mouse anti-alpha-tubulin (SIGMA, 1:2000). After washing, membranes were incubated at room temperature for 1 h in PBST, containing 5% milk powder and secondary horseradish peroxidase-conjugated antibody (Amersham Biosciences). Chemiluminescence was developed by ECLplus Western blotting Detection System (Amersham Biosciences) and visualised by exposing X-ray films (Kodak). Protein quantification was done with Gelpro32 program and HSPB8 and BAG3 levels were normalized against alpha-tubulin.

#### *Cell culture and transfection*

HEK-293 (human embryonic kidney) cells were grown in Dulbecco's modified Eagle's medium with high glucose (Gibco BRL) supplemented with 10% fetal bovine serum and penicillin/streptomycin. Transfections of cDNAs were performed using Lipofectamine, according to the manufacturer's instructions. 24 hours post-transfection, cells were extracted in 2% SDS-sample buffer, separated by SDS/PAGE and analyzed by Western blotting, using specific antibodies.

#### *Co-immunoprecipitation Assay*

Human brain tissue was homogenized in immunoprecipitation lysis buffer (20 mM Tris-HCl, pH 7.4, 2.5 mM MgCl<sub>2</sub>, 100 mM KCl, 0.5% NP-40, 3% glycerol, 1 mM DTT, complete EDTA-free). After gentle rotation for 30 min at 4 °C, the brain lysates were centrifuged at 14000 rpm for 10 min at 4 °C. The supernatants were divided in two equal aliquots, which were cleared by incubation with Rabbit TrueBlot™ beads (eBioscience) at 4 °C, with gentle agitation, for 1h. At the same time, Rabbit TrueBlot™ beads were incubated either with anti-HSPB8 or nonimmune rabbit serum at 4 °C, with gentle agitation, for 1h. The beads complexed with the HSPB8 specific antibody or with the nonimmune serum were washed and added to the lysates. Samples were incubated at 4 °C, with gentle agitation, for 2h. Immune complexes were briefly centrifuged and beads were washed 4 times in immunoprecipitation lysis buffer. Co-immunoprecipitated proteins were recovered after boiling in 2% SDS-sample buffer. Co-immunoprecipitated proteins (beads) and an aliquot of the precleared supernatants (input) were separated on SDS-polyacrylamide gel electrophoresis and analyzed by western blotting, using specific anti-HSPB8 (1:1000) and anti-BAG3 (1:1000) antibodies.

| Pt nr | CAG  | Age onset of | Gender | Age death at |
|-------|------|--------------|--------|--------------|
| 1     | n.a. | n.a.         | Male   | 29           |
| 2     | n.a. | n.a.         | Male   | 39           |
| 3     | n.a. | n.a.         | Female | 45           |
| 4     | n.a. | n.a.         | Female | 52           |
| 5     | n.a. | n.a.         | Male   | 54           |
| 6     | n.a. | n.a.         | Female | 55           |
| 7     | 80   | 13           | male   | 24           |
| 8     | 71   | 32           | Male   | 32           |
| 9     | 65   | 35           | Female | 40           |
| 10    | 74   | 35           | Female | 42           |
| 11    | 64   | 39           | Male   | 45           |
| 12    | 71   | 29           | Male   | 46           |
| 13    | 70   | 30           | Male   | 51           |
| 14    | 71   | 47           | Male   | 51           |
| 15    | 69   | 36           | Male   | 52           |
| 16    | 71   | 45           | Male   | 55           |
| 17    | 72   | 30           | Male   | 56           |
| 18    | 64   | 49           | male   | 58           |
| 19    | 70   | 35           | Female | 59           |
| 20    | 61   | 49           | Female | 61           |
| 21    | 75   | 22           | Male   | 62           |
| 22    | 73   | 35           | Female | 62           |
| 23    | 78   | 38           | Male   | 65           |
| 24    | 68   | 30           | Male   | 66           |
| 25    | 68   | 47           | Female | 75           |

**Table 8.1: Fibroblast culture material from control individuals and spinocerebellar ataxia type 3 patients**

Patient number (Pt nr), length of polyglutamine repeat of mutated ataxin 3 (CAG), age at disease onset, gender and age at death. Control patients were without history of neuropsychiatric diseases.

| Pt nr | Age at death | Gender | Diagnosis | PM Delay | Braak stage (tau) | Braak stage ( $\alpha$ -syn) | Vonsattel stage |
|-------|--------------|--------|-----------|----------|-------------------|------------------------------|-----------------|
| 26    | 27           | Male   | Control   | 3h       | 0                 | 0                            | 0               |
| 27    | 40           | Male   | Control   | 16h      | 0                 | 0                            | 0               |
| 28    | 43           | Female | Control   | 24h      | 0                 | 0                            | 0               |
| 29    | 48           | Female | Control   | 21h      | 0                 | 0                            | 0               |
| 30    | 54           | Male   | Control   | 16h      | 0                 | 0                            | 0               |
| 31    | 59           | Male   | Control   | 40h      | 0                 | 0                            | 0               |
| 32    | 62           | Female | Control   | 19h      | 0                 | 0                            | 0               |
| 33    | 60           | Female | Control   | 16h      | 0                 | 0                            | 0               |
| 34    | 65           | Female | Control   | 8h       | 3                 | 0                            | 0               |
| 35    | 65           | Male   | Control   | 5h       | 0                 | 0                            | 0               |
| 36    | 69           | Male   | Control   | 3h       | 0                 | 0                            | 0               |
| 37    | 75           | Male   | Control   | 3h       | 0                 | 0                            | 0               |
| 38    | 75           | Male   | Control   | 60h      | 3                 | 0                            | 0               |
| 39    | 81           | Male   | Control   | 3h       | 2                 | 0                            | 0               |
| 40    | 84           | Male   | Control   | 24h      | 3                 | 0                            | 0               |
| 41    | 34           | Female | SCA3      | 5h       | 0                 | 0                            | 0               |
| 42    | 47           | Male   | SCA3      | 5h       | 0                 | 0                            | 0               |
| 43    | 54           | Male   | SCA3      | 8h       | 0                 | 0                            | 0               |
| 44    | 63           | Female | SCA3      | 8h       | 0                 | 0                            | 0               |
| 45    | 63           | Male   | SCA3      | 18h      | 3                 | 0                            | 0               |
| 46    | 70           | Female | SCA3      | 18h      | 1                 | 0                            | 0               |
| 47    | 71           | Male   | SCA3      | 17h      | 2                 | 0                            | 0               |
| 48    | 73           | Male   | SCA3      | 10h      | 1                 | 0                            | 0               |
| 25    | 75           | Female | SCA3      | 8h       | 3                 | 0                            | 0               |
| 49    | 85           | Male   | SCA3      | 11h      | 2                 | 0                            | 0               |
| 50    | 88           | Female | SCA3      | 8h       | 3                 | 0                            | 0               |
| 51    | 61           | Female | HD        | 4h       | 1                 | 0                            | 3               |
| 52    | 64           | Male   | HD        | 4h       | 2                 | 0                            | 2               |
| 53    | 66           | Male   | HD        | 8h       | 3                 | 0                            | 4               |
| 54    | 67           | Male   | HD        | 20h      | 1                 | 0                            | 3               |
| 55    | 68           | Male   | HD        | 17h      | 3                 | 0                            | 3               |
| 56    | 70           | Female | HD        | 6h       | 0                 | 0                            | 2               |
| 57    | 91           | Male   | HD        | 20h      | 3                 | 0                            | 2               |
| 58    | 58           | Female | AD        | 20h      | 6                 | 0                            | 0               |
| 59    | 58           | Male   | AD        | 24h      | 5                 | 0                            | 0               |
| 60    | 63           | Male   | AD        | 24h      | 6                 | 0                            | 0               |
| 61    | 64           | Female | AD        | 24h      | 6                 | 0                            | 0               |
| 62    | 74           | Male   | AD        | 7h       | 5                 | 0                            | 0               |
| 63    | 75           | Female | AD        | 40h      | 5                 | 0                            | 0               |
| 64    | 76           | Female | AD        | 36h      | 5                 | 0                            | 0               |
| 65    | 81           | Female | AD        | 6h       | 5                 | 0                            | 0               |
| 66    | 83           | Female | AD        | 42h      | 5                 | 0                            | 0               |
| 67    | 84           | Female | AD        | 21h      | 4                 | 0                            | 0               |
| 68    | 55           | Male   | PD        | 5h       | 0                 | 5                            | 0               |
| 69    | 62           | Male   | PD        | 6h       | 1                 | 4                            | 0               |
| 70    | 74           | Male   | PD        | 22h      | 0                 | 5                            | 0               |
| 71    | 76           | Female | PD        | 9h       | 3                 | 6                            | 0               |
| 72    | 78           | Female | PD        | 24h      | 3                 | 6                            | 0               |
| 73    | 81           | Male   | PD        | 20h      | 2                 | 4                            | 0               |
| 74    | 84           | Male   | PD        | 20h      | 0                 | 4                            | 0               |
| 75    | 90           | Female | PD        | 24h      | 3                 | 4                            | 0               |
| 76    | 95           | Male   | PD        | 30h      | 3                 | 6                            | 0               |

**Table 8.2 (previous Page): Brain materials from control individuals and patients.**

List of patient number (Pt nr), age at death, gender, diagnosis and post-mortem (PM) delay. Control patients were without history of neuropsychiatric diseases. SCA3: spinocerebellar ataxia type 3; HD: Huntington's disease; AD: Alzheimer's disease; PD: Parkinson's disease.

### *Immunohistochemistry*

Sections were deparaffinated with a descending xylol and ethanol sequence. When antibodies required antigen retrieval (Table 8.3), slides were either transferred into Tris/HCl Buffer (pH 9.5), heated 3 x 10 min to 95°C and cooled to room temperature (microwave antigen retrieval method) or transferred into 98% formic acid for 3 min (formic acid antigen retrieval method). In some instance, a combination of both antigen retrieval methods was used, first starting with the microwave method followed by the formic acid method. Endogenous peroxidases were blocked using 0.3% H<sub>2</sub>O<sub>2</sub>/PBS buffer for 30 min at RT. Sections were then incubated 1h at RT with primary antibodies (Table 8.3) diluted in 1% BSA/PBS. Consecutively, sections were rinsed and incubated with appropriate peroxidase conjugated secondary antibodies for 30 min at RT. Signal amplification was done by incubating sections with an appropriate peroxidase conjugated tertiary antibody directed against the secondary antibody, for 30min at RT. The immunoprecipitate was revealed with 3,3%-diaminobenzidine (Sigma) as the chromogen. Sections were counterstained with hematoxylin, dehydrated in ethanol and coverslipped. Primary antibody omission served as negative controls.

### *Double immunofluorescent staining*

Deparaffination and antigen retrieval was done as described above. Sections were first treated with 1% sodium borohydrate (Sigma) for 10 min to quench autofluorescence and then blocked with 5% normal goat serum (Vector) in PBS containing 0.03% TritonX (Sigma) for 30 min. Subsequently, sections were incubated at 4°C overnight with the various primary antibodies (Table 8.3). The next day, sections were washed in PBS and incubated for 3h at RT with goat anti-mouse Alexa488 (Invitrogen) and goat anti-rabbit Cy3 (Jackson ImmunoResearch) secondary antibodies. Sections were then incubated with 0.05% sudan black solution (Merck) for 10 min, for further quenching of autofluorescence, washed in PBS and coverslipped with Mowiol (Sigma). Primary antibody omission served as negative controls. Sections were analyzed with a Leica AOBs TCS SP2 confocal laser scanning microscope. Images were deconvoluted for background noise correction using Huygens Pro Software (SVI).

### *Statistical analysis*

Student T-Test was performed to analyze the data derived from control and SCA3 fibroblasts. Immunohistochemical staining of astrocytes was independently assessed by two researchers in a semi quantitative manner. For statistical analysis the PASW statistics 18 software package was used. Since the subgroups of the different diseases and controls were not composed of large numbers, non-parametric tests were performed. For comparing 2 groups (for instance HSPB8 staining intensity in one disease area with its control) Mann-Whitney-U tests were carried out. For distribution of age at death and post-mortem delay across the different diseases and controls, we



used Kruskal-Wallis tests. For inter-rater reliability, Kappa scores were calculated. Results were considered significant when  $p < 0.05$ .

| Anti-body       | clone        | donor spec. | source       | Dil.   | AR   | Marker for                      |
|-----------------|--------------|-------------|--------------|--------|------|---------------------------------|
| BAG3            | polyclon     | rabbit      | -            | 1:750  | none | Heat shock protein [23,24]      |
| HSPB8           | polyclon     | rabbit      | -            | 1:750  | none | Heat shock protein [23,24]      |
| p62             | D3           | mouse       | Santa Cruz   | 1:100  | MW-  | Aggregation/degradation [36]    |
| 1C2             | 5TF1-1C2-172 | mouse       | Chemicon     | 1:3200 | MW+  | Polyglutamine [37]              |
| Tau             | AT8          | mouse       | Innogenetics | 1:20   | none | Neurofibrillary tangles [38]    |
| Beta – Amyloid  | GF/3D        | mouse       | DAKO         | 1:400  | FA   | Amyloid plaques [39]            |
| Alpha-synuclein | KM51         | mouse       | Novocastra   | 1:40   | MW+  | Alpha synuclein aggregates [40] |
| CD68            | PGM1         | mouse       | DAKO         | 1:100  | MW-  | Phagocytic lysosomes [41]       |
| GFAP            | polyclon     | rabbit      | DAKO         | 1:800  | none | Astrocytes [42]                 |
| MAP2            | HM-2         | mouse       | Sigma        | 1:500  | none | Neurons [43]                    |

**Table 8.3: List of primary antibodies used.**

AR: Antigen retrieval method; FA: 3 min treatment with 98% formic acid at RT; MW: microwave treatment 3 times for 10 min in Tris/Hcl buffer (pH 9); MW+: a combined retrieval protocol with microwave treatment followed by formic acid treatment as described above.

## Results

HSPB8 is a member of the human small heat shock protein family (HSPB1-HSPB10), which forms in mammalian cells a stable complex with the HSC70/HSP70 co-chaperone BAG3, a member of the BAG family of proteins (BAG1-6). The expression of HSPB8 and BAG3 is upregulated by treatments which induce the accumulation of denatured/misfolded proteins (e.g. heavy metal treatment and heat shock) [48, 61]. To investigate whether this is also true when disease-associated misfolded proteins are expressed, we analyzed the expression levels of HSPB8 and BAG3 in fibroblast cultures derived from control (n=6) and SCA3 patients (n=19) by Western blotting. Interestingly, both HSPB8 and BAG3 levels were significantly higher in SCA3-derived fibroblasts as compared to control fibroblasts (Fig. 8.1). On the basis of these results, we decided to investigate whether HSPB8 and BAG3 levels could also be upregulated in the post-mortem brain of patients suffering of SCA3 and other age-related neurodegenerative disorders.

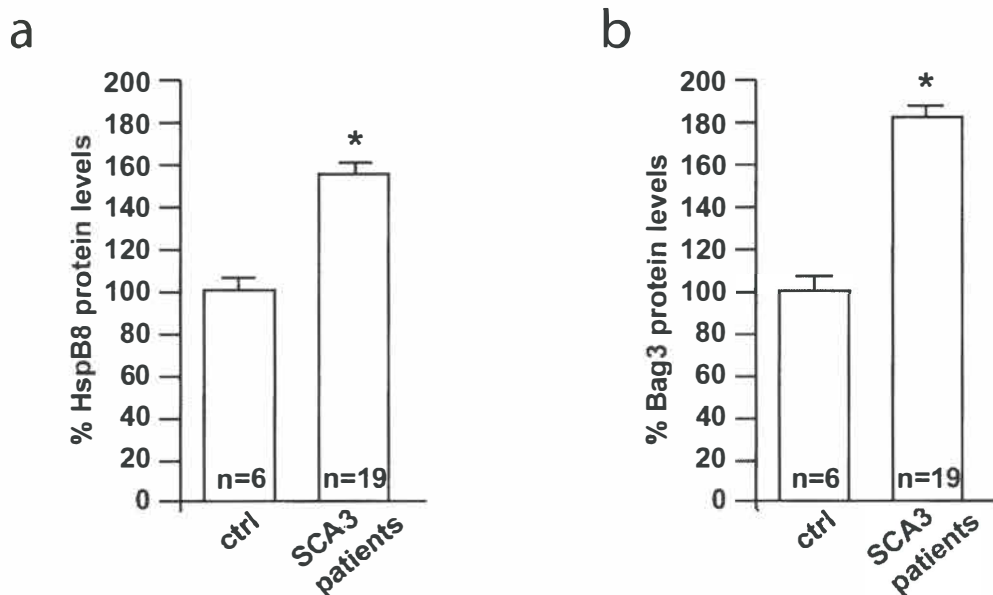


**Figure 8.1: HSPB8 and BAG3 are upregulated in fibroblasts from patients affected by SCA3.**

A, B: Total protein extracts were prepared from fibroblasts obtained from 6 control patients and 19 patients affected by SCA3 (with age comprised between 30 and 75 years-old). HSPB8 and BAG3 expression levels in the healthy versus SCA3 affected populations were analyzed by Western blotting and subsequently quantified using the Gelpro32 program. % of HSPB8 or BAG3 expression levels, normalized against  $\gamma$ -tubulin is reported. (\* =  $p < 0,05$ ; average values  $\pm$  s.e.m. of  $n = 6-19$  independent samples).

### *Specificity of the HSPB8 and BAG3 antibodies.*

In order to address the question whether HSPB8 and BAG3 expression may be upregulated under neuropathological conditions, characterized by the accumulation of misfolded aggregate-prone proteins, we first verified the specificity (for further use in

immunohistochemistry) of the HSPB8 and BAG3 antibodies. The rabbit polyclonal antibody anti-HSPB8 used in this study was raised against the C-terminal peptide KNELPQDSQEVTCT of the human HSPB8 protein [12], while the rabbit polyclonal antibody anti-BAG3 was directed against the C-terminal peptide CSSMTDTPGNPAAP of human BAG3 [11]. HSPB8 shares a high sequence homology with the other members of the HSPB family, especially in the C-terminal  $\alpha$ -crystallin domain [34] and the BAG domain at the C-terminus of BAG3 is highly conserved in all members of the BAG family [63]. This raises the possibility that our HSPB8 and BAG3 antibody might also recognize other members of the HSPB and BAG families, respectively. Cross-reactivity with other HSPB/BAG proteins was tested in HEK293 cells transfected with cDNAs encoding for the V5 tagged HSPB1-HSPB8 proteins (Figure 8.2a), HA or myc tagged BAG family members (Figure 8.2b) and detection of the proteins was carried out using either the HSPB8, BAG3 or the tag (V5, HA, myc) specific antibodies. HSPB9 and HSPB10, which are expressed selectively in testis [24, 35], were excluded from our crossreactivity screen. Supplementary Fig. 1A and 1B show that anti-HSPB8 and anti-BAG3 recognize specifically HSPB8 and BAG3, respectively.

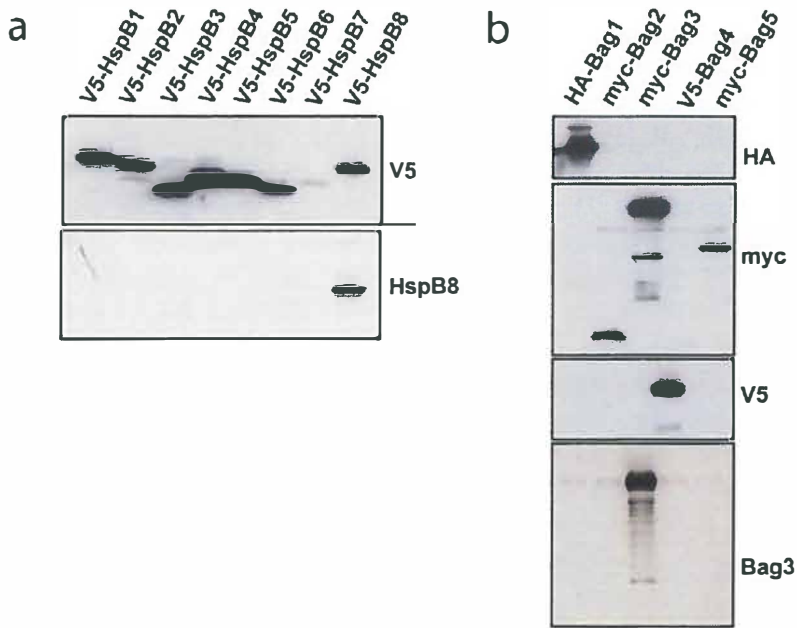


**Figure 8.2: The BAG3 and HSPB8 antibodies are specific for the corresponding epitopes.**

HSPB8 and BAG3 antibodies do not cross react with the other members of the HSPB family (A) or the Bag family (B), respectively. HEK-293 cells were transfected overnight with vectors encoding for several members of the HSPB family (A; V5-HSPB1-8) or of the Bag family (B; HA-Bag1, myc-Bag2-5). Total protein extracts were processed for Western blotting and protein expression levels/crossreactivity were measured using HSPB8, BAG3 or tag specific antibodies.

Next, we verified by co-immunoprecipitation technique whether HSPB8 and BAG3 also co-immunoprecipitate from human healthy (Fig. 8.3) and diseased (SCA3, data not shown) human brain extract. Fig. 8.3 shows that HSPB8 and BAG3 form a complex also in the human brain.

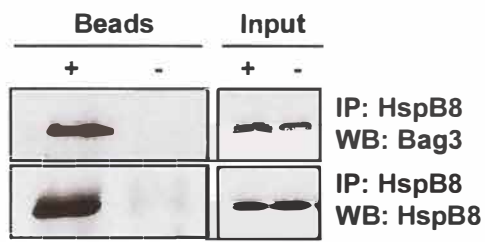


**Figure 8.3: Co-immunoprecipitation of HSPB8 and BAG3 from human brain.**  
A total protein extract from human healthy brain was immunoprecipitated using either anti-HSPB8 (+) or a pre-immune rabbit serum (-). Immunoprecipitated proteins were probed by Western with specific antibodies for BAG3 and HSPB8.

*Pattern and intensity of HSPB8 and BAG3 expression in neurons and astrocytes of human control individuals.*

After having established the specificity of our antibodies (Fig. 8.2) [34-37] and confirming that HSPB8 and BAG3 form a complex also in the human brain (Fig. 8.3), we next examined HSPB8 and BAG3 expression in human brain material from healthy patients (Table 8.2). Considering that the scope of our study was to assess whether HSPB8 and BAG3 are selectively upregulated in affected brain areas featuring protein aggregation, we restricted our analysis of HSPB8 and BAG3 expression to one area from each disease, which is known to be consistently affected by neurodegeneration: entorhinal cortex for Alzheimer’s Disease (AD) [8], the midbrain at the level of the substantia nigra for Parkinson’s Disease (PD) [9], the caudate nucleus affected in Huntington’s Disease (HD) [56], and the base of the pons at the level of the locus coeruleus for SCA3 [55]. Investigation of these specific areas in brains from control individuals revealed positive immunoreaction for both HSPB8 and BAG3 in neuronal and astroglial cell populations (Fig. 8.4). Neurons were identified by immunostaining of the microtubule associated protein (MAP2; Fig. 8.4B-D, F-H) and astroglia by immunostaining against the glial fibrillary acidic protein (GFAP; Fig. 8.4J-L, N-P). In neurons, staining intensity of HSPB8 and BAG3 was homogenous within the whole cell soma and extended well into the processes, such that large axons were visibly stained (Fig. 8.4A, E). Astroglial cells preferentially expressed HSPB8, which was mainly confined to their perinuclear cytoplasm, with minimal staining of their processes (Fig. 8.4I). BAG3 was only rarely expressed in control astrocytes (Fig. 8.4M). Nuclear staining with either antibody was only rarely encountered. The staining of the astrocyte nucleus in (J) is either due to an overlay by the strongly positive perinuclear cytoplasm, or due to genuine but rare nuclear staining.





expressed moderate levels of BAG3 (Fig. 8.4M-P). This expression pattern was observed in all control sections.

*Astroglial HSPB8 and BAG3 expression is increased in degenerating central nervous areas.*

We next addressed the question whether HSPB8 and BAG3 expression may be upregulated in brain under neuropathological conditions characterized by the accumulation of misfolded aggregate-prone proteins, including AD, PD, HD and SCA3 (Table 8.2). Under all these four pathological conditions, neurodegeneration is usually also accompanied by astrogliosis and microglia activation in the degenerating areas [17, 21, 41, 45, 58]. As mentioned earlier, for each disease we selected the major brain area known to exhibit early and serious neurodegeneration and compared it with the same area from age-matched controls, as well as with another disease, where the analyzed area is known to be spared from neurodegeneration (e.g. pons in HD). These comparative analyses were done to investigate whether changes in HSPB8-BAG3 staining levels are a generalized response of the brain in the presence of a neurodegenerative disease or are confined/localized specifically where neurodegenerative processes occur.

Interestingly, astrocytes in the respective degenerating areas of all four diseases exhibited increased immunoreactivity for HSPB8 accompanied by a moderate increase in BAG3 staining (Fig. 3, 4). In all disease cases, the staining intensity of the perinuclear soma of astrocytes was increased compared to control situation (Fig. 3C-D, K-L; Fig. 4C-D, K-L). Furthermore, the staining in glial processes was more intense and extended further into the processes compared to control condition.



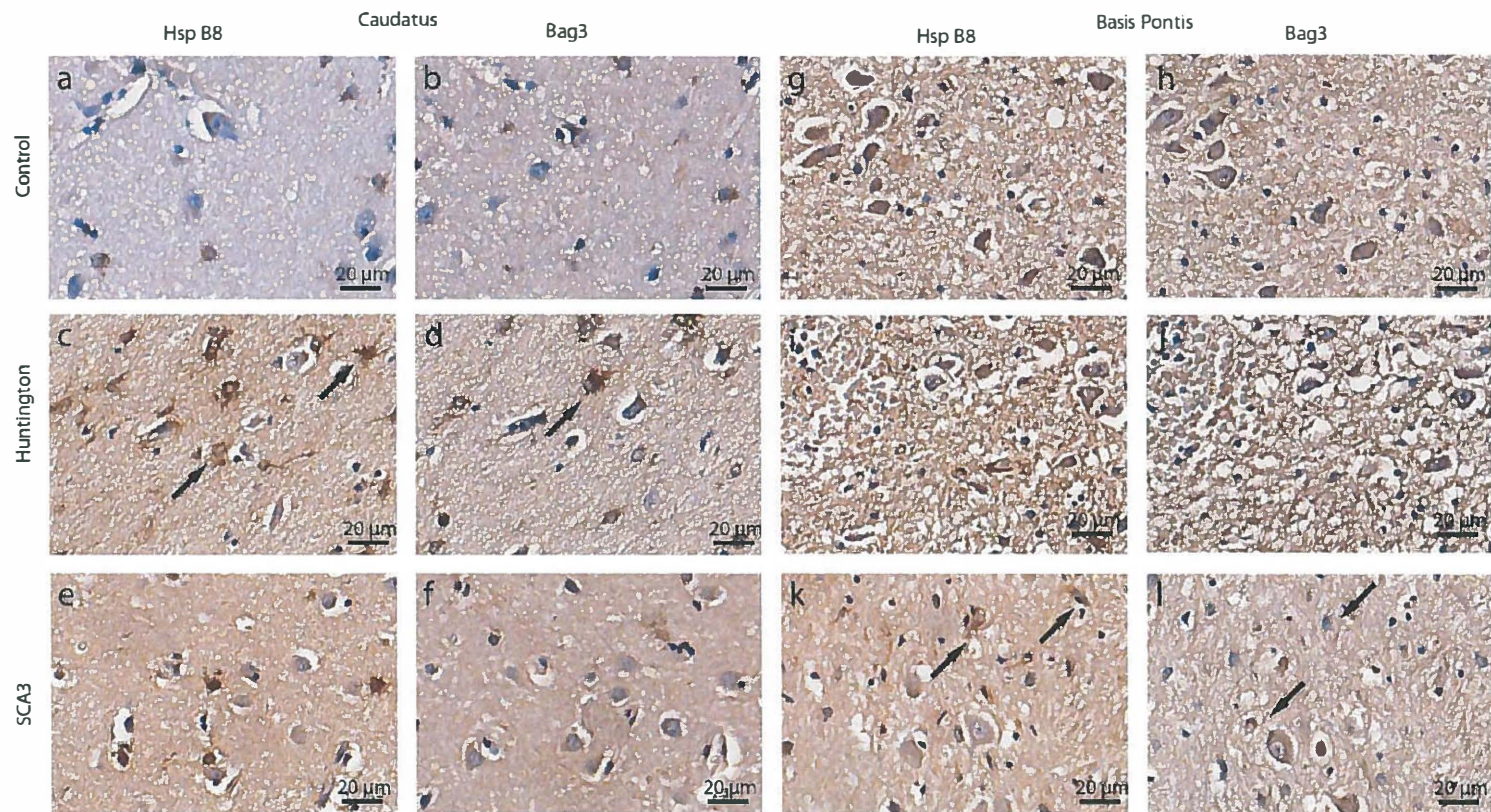


**Figure 8.5: Astroglia in areas of neurodegeneration display enhanced reactivity for both HSPB8 and BAG3 in HD and SCA3**

Astrocytes of the caudate nucleus of a HD patient display strong immunoreactivity for HSPB8 (C) and moderate staining for BAG3 (D), compared to the control case (A, B), whereas astrocytes of the caudate nucleus of a SCA3 case show weaker staining of HSPB8 (E) and BAG3 (F). In SCA3, the glia of the base of the pons display a marked increase in HSPB8 (K) staining and a mild increase in Bag 3 staining (L), as compared with control and Huntington cases (G, H, I, J).



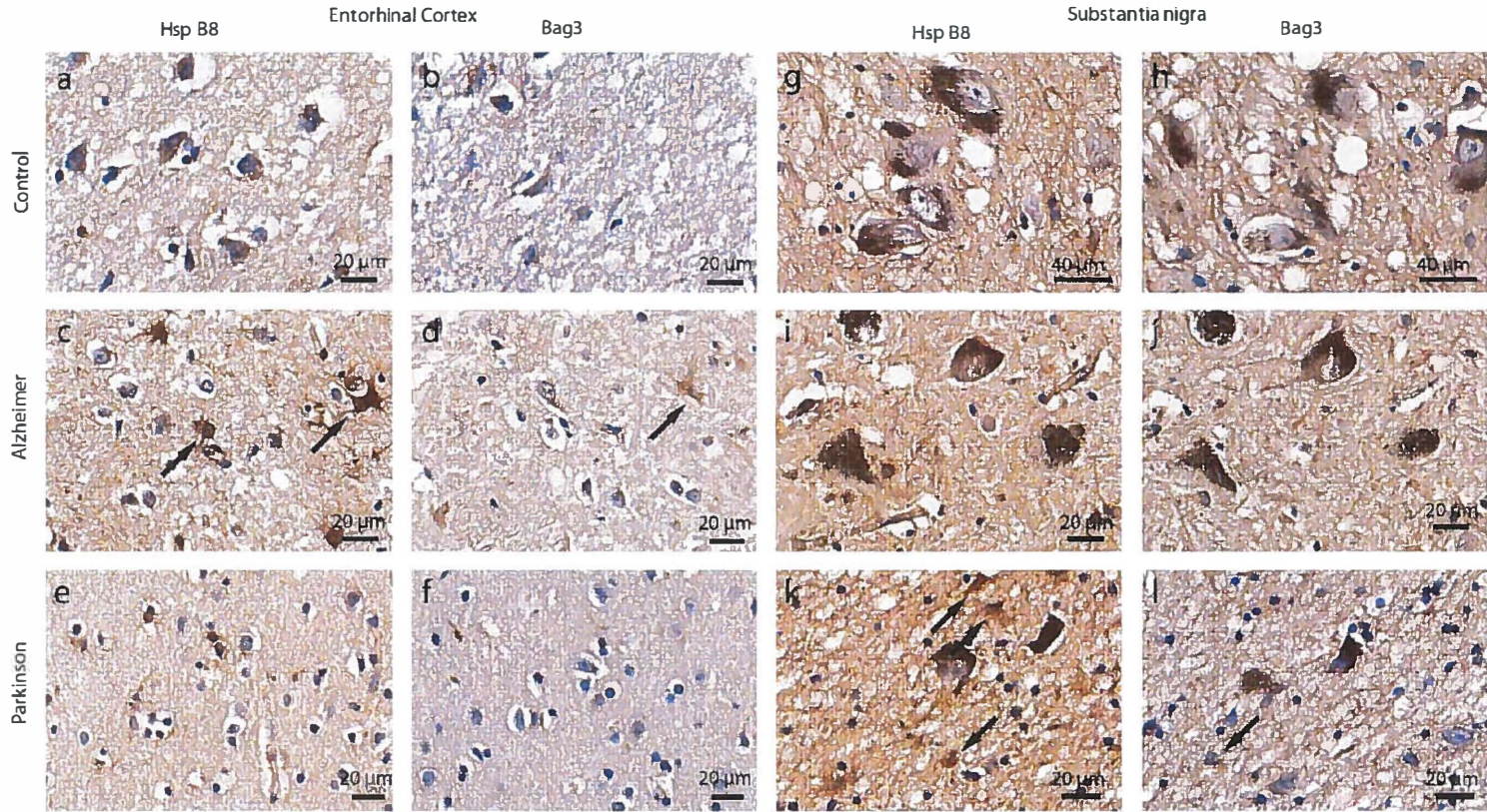


**Figure 8.6: Glial cells of degenerating areas in Alzheimer's and Parkinson's diseases express high levels of HSPB8 and BAG3.**

The transentorhinal cortex of an AD patient displays a marked upregulation of HSPB8 (C) and BAG3 in the glial cells of this affected area (arrows) (D). The control region and the unaffected transentorhinal cortex of a PD patient displayed significantly weaker staining (A, B, E, F). The substantia nigra of a PD patient displayed a moderate upregulation of HSPB8 (K) and marginal upregulation of BAG3 (arrows) (L) compared the control case and the substantia nigra of an AD patient with early A $\beta$  and tau pathology (data not shown) in the mesencephalon (G, H, I, J).

These changes were visible in the majority of astrocytes within an affected area (Fig. 8.5, 8.6) and were clearly due to an increase in staining intensities of individual astrocytes and not because of the increase of numbers of astrocytes occurring during astrogliosis. Most importantly, the increase in HSPB8 and BAG3 expression was confined to the brain areas that do exhibit neurodegeneration. In the case of polyglutamine diseases, the increase in expression of both proteins was visible in the caudate nucleus of HD patients (Fig. 8.5C-D) and the basis pontis of SCA3 patients (Fig. 8.5K-L), while no change was observed in the basis pontis of HD patients (Fig. 8.5I-J) and only minor up-regulation was visible in the caudate nucleus of SCA3 patients, which is known to exhibit slight degeneration in late cases (Fig. 8.5E-F). Similar results were obtained in AD and PD: elevated levels of HSPB8 and BAG3 were present in astrocytes in the entorhinal cortex of AD patients (Fig. 8.6C-D) and in the substantia nigra of PD patients (Fig. 8.6K-L) but not in unaffected areas (Fig. 8.6E-F; Fig. 8.6I-J). These results were confirmed by a semi quantitative assessment showing a consistent and significant upregulation of both HSPB8 and BAG3 only in degenerating areas (Fig. 8.7; Table 8.4-7). Kappa scores for the 2 independent investigators were 0.77 for HSPB8 ( $p < 0.001$ ) and 0.85 for BAG3 ( $p < 0.001$ ) (Table 8.8). Kappa scores for all the disease subgroups and controls were also highly significant (Table 8.8).

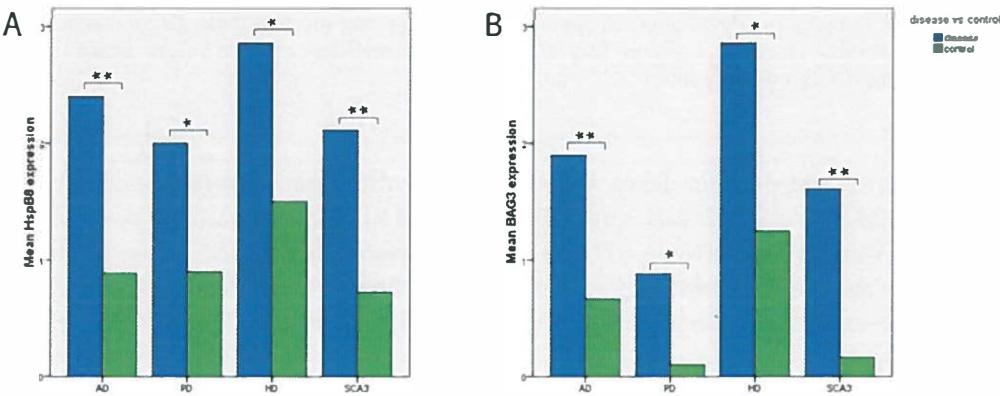


**Figure 8.7: Semi quantitative assessment of astroglial HSPB8 and BAG3 staining.** Tissue sections were scored for astroglial expression of HSPB8 (A) and BAG3 (B) in areas with neurodegeneration (blue columns) and corresponding control tissue (green columns). Statistical analysis displays a significant difference between degenerating and unaffected tissue sections (Mann-Whitney-U-test; \*  $p < 0.05$ , \*\*  $p < 0.001$ ).

The distribution of age at death was not significantly different across the disease and control groups (Fig. 8.8). The upregulation of HSPB8 and BAG3 was also independent of the age of the patients, since even two young SCA3 subjects (34 and 42 years-old, respectively) displayed the same change in HSPB8 and BAG3 expression levels in astroglia (Fig. 8.9A-D) compared to older patients. Furthermore we observed no visible changes in HSPB8 and BAG3 expression in the tissue of a 90 year old patient diagnosed with Braak 3 stage PD, showing Lewy pathology but no visible loss of nigral neurons (Fig. 8.9E-F).

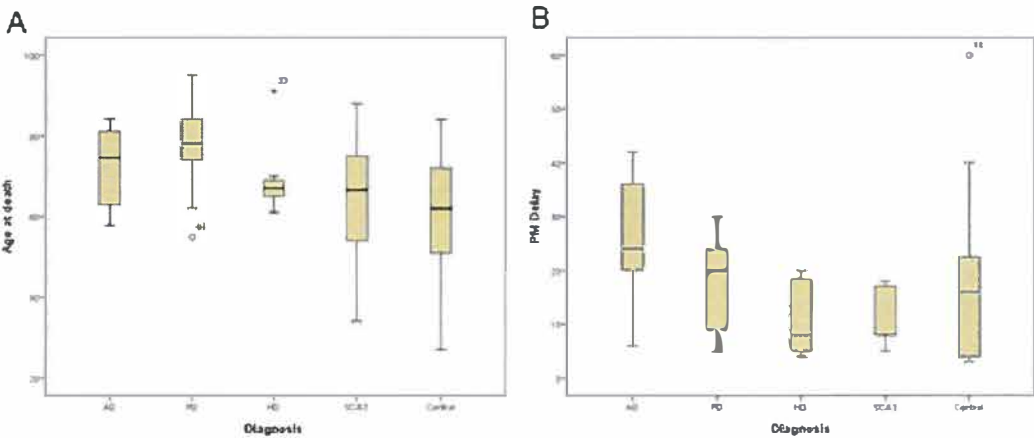


**Figure 8.8: Distribution of age of Death and post mortem delay in patient samples.** Boxplots showing the distribution of age at death (A) and post-mortem delay (B) across the various diseases and control groups. Star and circle shapes represent extreme values, which lie outside the 95% confidence intervals.

Distribution of post-mortem delay was significantly different amongst the disease and control groups (Kruskal-Wallis test  $p=0.04$ ) (Fig. 8.8). More specifically, significant differences were found between AD and HD and between AD and SCA3 ( $p=0.015$  and  $p=0.004$ , respectively). However, the control group did not significantly differ from the various disease groups. Thus post-mortem delay did not influence HSPB8 or BAG3 staining intensity.



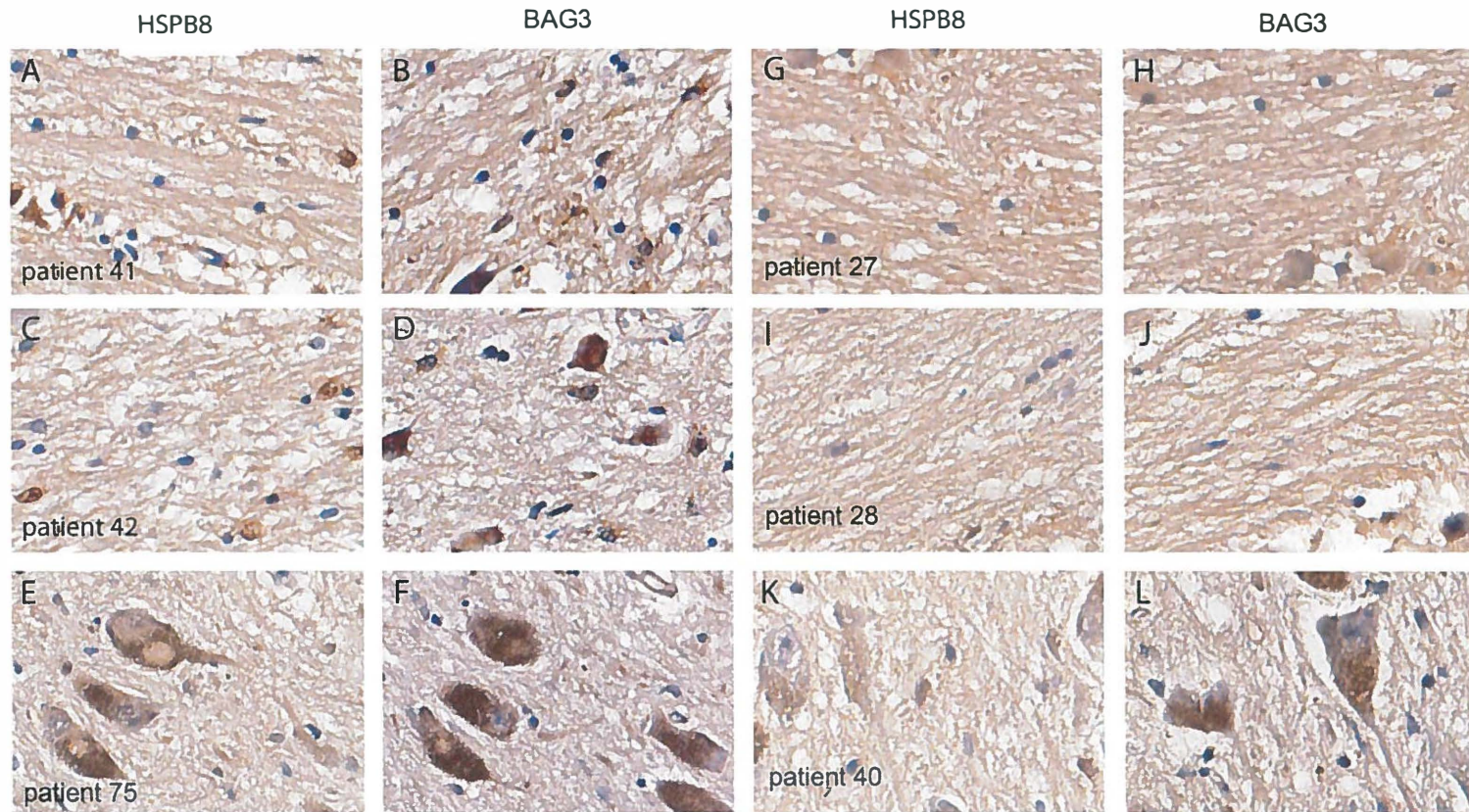


**Figure 8.9. Upregulation of HSPB8-BAG3 occurs independently of age or protein aggregation.**

Staining of pontine tissue from young SCA3 patients (patient 41, 34 years; patient 42, 42 years) shows moderate upregulation of glial HSPB8 (A, C) and BAG3 (B, D) as compared to control subjects 27 (G, H, 40 years) and 28 (I, J, 43 years). Early PD case without nigral neurodegeneration (E, F) do not demonstrate marked changes in HSPB8 and BAG3 expression compared to control cases (K, L).

*Expression levels of HSPB8 and BAG3 in neurons and co-localization with proteinaceous aggregates.*

Surprisingly, in all diseases investigated, neurons did not exhibit changes in HSPB8 or BAG3 expression, even in areas affected by neurodegeneration (Fig. 8.5, 8.6). Also, the expression levels of HSPB8 or BAG3 in neurons bearing protein aggregates did not differ in comparison to the rest of the neuronal population. Considering the ability of HSPB8 to recognize and bind to misfolded substrates *in vitro*, we next investigated whether HSPB8 and BAG3 colocalized with the mutated aggregate-prone proteins present in the diseased human brain. Interestingly, the neuronal nuclear inclusion bodies (NNIs) typical for SCA3 and HD were immunonegative for HSPB8 or BAG3 (Fig. 8.10).

In AD, astrocytes associated with amyloid- $\beta$  enriched extracellular mature plaques expressed high levels of HSPB8 and BAG3 (Fig. 8.11), whereas intraneuronal neurofibrillary tangles, composed of hyperphosphorylated tau proteins, were devoid of HSPB8 and BAG3 signal (data not shown). The mature amyloid plaques contain dystrophic neurites, which again links the upregulation of HSPB8 and BAG3 in astrocytes to neurodegenerative processes. Furthermore, HSPB8 and BAG3 were associated with Lewy bodies, but not with Lewy neurites (Fig. 8.12).



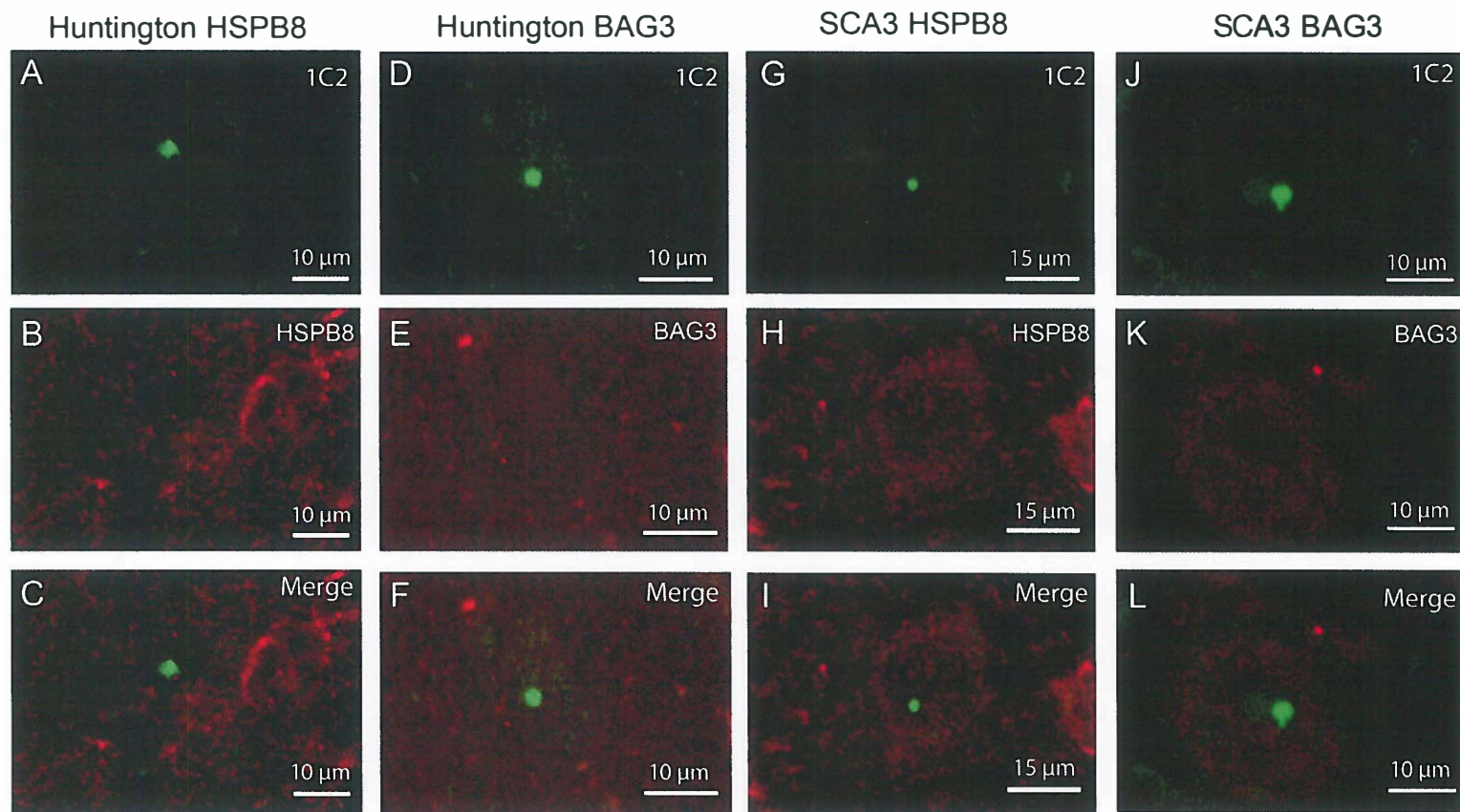


**Fig. 8.10: HSPB8 and BAG3 do not colocalize with 1C2-positive polyglutamine aggregates.**  
 Double immunostaining revealed no colocalization between 1C2 positive polyglutamine aggregates and HSPB8 in either HD (A-C) or SCA3 (G-I). BAG3 also did not colocalized with polyglutamine aggregates (D-F; J-L).

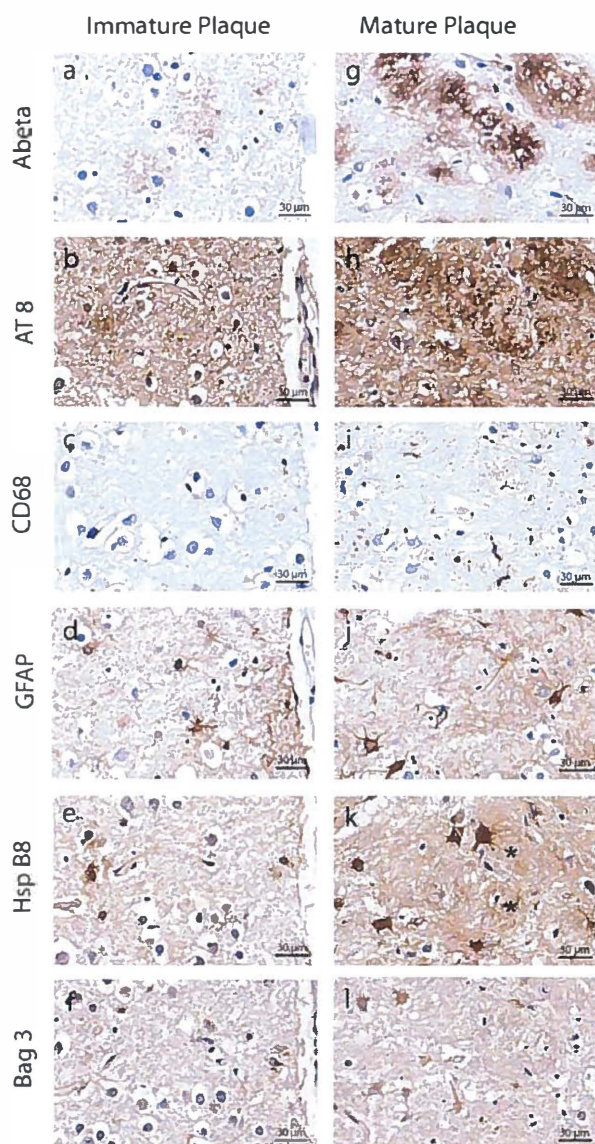


**Figure 8.11: HSPB8 and BAG3 are strongly expressed in glial cells associated with mature AD plaques.** Immature plaques in the entorhinal cortex of an AD patient display diffuse A $\beta$  staining (A), no tau positive neurites (B), no elevated CD68 immunoreaction (C) and no elevated GFAP (D) in astroglia. Associated astrocytes show a slight increase in staining with HSPB8 around the nucleus (E) but no visible BAG3 upregulation (F), compared to control cases. Astroglia associated with mature plaques, characterized by a dense  $\beta$ -amyloid core (G), tau immunopositivity (H), a large number of CD68 positive structures (I) and upregulated GFAP staining of neighbouring Glia (J), display a strong whole cell staining for HSPB8 (K) and a moderate staining for BAG3 (L). Extracellular material is also positive for HSPB8 (asterisk; K).

### Lewykörper + Hsps

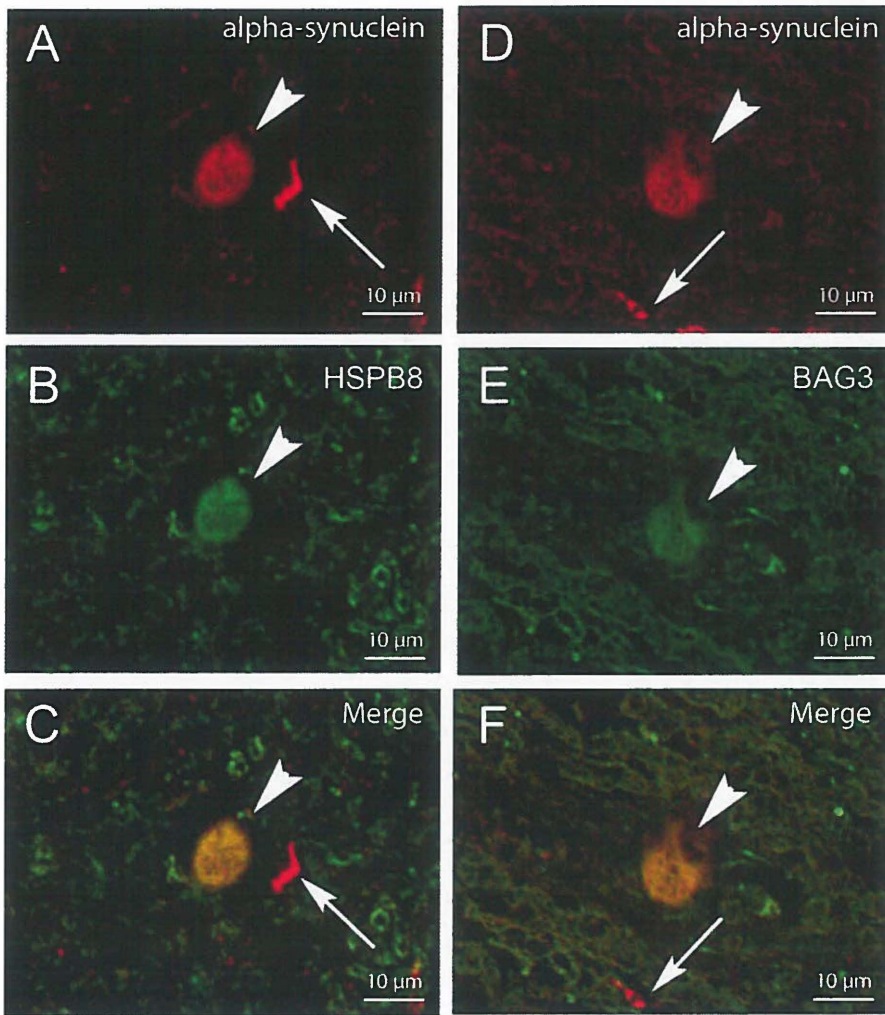


**Figure 8.12: Lewy bodies are immunopositive for HSPB8 and BAG3.**

*Lewy bodies are immunopositive for HSPB8 and BAG3. Double fluorescence staining confirmed co-localization of alpha-synuclein with both HSPB8 (A-C) and BAG3 (D-F) in Lewy bodies (arrowheads) but not in Lewy neurites (arrows) and granular alpha synuclein.*



| Alzheimer's disease / Entorhinal Cortex |       |     |      |    |             |
|---|-------|-----|------|----|-------------|
| Pt Nr                                   | HspB8 |     | BAG3 |    | Braak Stage |
|   | R1    | R2  | R1   | R2 |             |
| Patient 58                              | +++   | +++ | ++   | ++ | 6           |
| Patient 59                              | +++   | ++  | +    | +  | 5           |
| Patient 60                              | +++   | +++ | ++   | ++ | 6           |
| Patient 61                              | +++   | +++ | ++   | ++ | 5           |
| Patient 62                              | ++    | ++  | ++   | ++ | 5           |
| Patient 63                              | ++    | ++  | ++   | ++ | 5           |
| Patient 64                              | +     | +   | ++   | ++ | 5           |
| Patient 65                              | +++   | ++  | ++   | ++ | 5           |
| Patient 66                              | +++   | +++ | ++   | ++ | 5           |
| Patient 67                              | ++    | ++  | ++   | ++ | 4           |
|   |       |     |      |    |             |
| Patient 27                              | 0     | 0   | 0    | 0  | 0           |
| Patient 28                              | 0     | 0   | 0    | 0  | 0           |
| Patient 30                              | ++    | ++  | +    | ++ | 0           |
| Patient 32                              | +     | +   | +    | +  | 0           |
| Patient 34                              | 0     | 0   | 0    | 0  | 3           |
| Patient 36                              | +     | +   | 0    | 0  | 0           |
| Patient 38                              | ++    | ++  | ++   | ++ | 3           |
| Patient 39                              | +     | +   | +    | +  | 2           |
| Patient 40                              | +     | +   | +    | 0  | 3           |

**Table 8.4: Semiquantitative assessment of astroglial staining intensities in AD tissue and corresponding controls.**

Patient number (Pt nr), staining intensities of HSPB8 and BAG3 staining as assessed by 2 independent Researchers (R1, R2). Semiquantitative scores are: 0: not discernable, +: light, ++: moderate, +++: intense. Control patients were without history of neuropsychiatric diseases.

| Parkinson's disease / Substantia Nigra |       |     |      |    |             |
|--|-------|-----|------|----|-------------|
| Pt Nr.                                 | HspB8 |     | BAG3 |    | Braak Stage |
|  | R1    | R2  | R1   | R2 |             |
| Patient 68                             | +++   | +++ | ++   | ++ | 5           |
| Patient 69                             | ++    | ++  | +    | +  | 4           |
| Patient 70                             | ++    | ++  | 0    | 0  | 5           |
| Patient 71                             | +++   | +++ | +    | +  | 6           |
| Patient 72                             | +++   | +++ | ++   | ++ | 6           |
| Patient 73                             | ++    | ++  | +    | +  | 4           |
| Patient 74                             | +     | +   | 0    | 0  | 4           |
| Patient 75                             | +     | 0   | 0    | 0  | 4           |
| Patient 76                             | +     | ++  | +    | +  | 6           |
|  |       |     |      |    |             |
| Patient 26                             | +     | ++  | 0    | 0  | 0           |
| Patient 28                             | +     | +   | 0    | 0  | 0           |
| Patient 30                             | +     | +   | +    | +  | 0           |
| Patient 32                             | +     | 0   | 0    | 0  | 0           |
| Patient 33                             | +     | 0   | 0    | 0  | 0           |
| Patient 34                             | +     | +   | 0    | 0  | 0           |
| Patient 36                             | +     | ++  | 0    | 0  | 0           |
| Patient 38                             | +     | +   | 0    | 0  | 0           |
| Patient 39                             | +     | +   | 0    | 0  | 0           |
| Patient 40                             | 0     | 0   | 0    | 0  | 0           |

**Table 8.5: Semiquantitative assessment of astroglial staining intensities in PD tissue and corresponding controls.**

Patient number (Pt nr), staining intensities of HSPB8 and BAG3 staining as assessed by 2 independent Researchers (R1, R2). Semiquantitative scores are: 0: not discernable, +: light, ++: moderate, +++: intense. Control patients were without history of neuropsychiatric diseases. Note that patient 73 and 74 displayed no visible nigral degeneration at the level investigated.

| Huntington's disease / Caudate nucleus |       |     |      |     |                 |
|--|-------|-----|------|-----|-----------------|
| Case                                   | HspB8 |     | BAG3 |     | Vonsattel Stage |
|  | R1    | R2  | R1   | R2  |                 |
| Patient 52                             | +++   | +++ | +++  | +++ | 2               |
| Patient 53                             | +++   | +++ | +++  | +++ | 4               |
| Patient 54                             | +++   | +++ | +++  | +++ | 3               |
| Patient 55                             | +++   | +++ | +++  | +++ | 3               |
| Patient 56                             | +++   | +++ | +++  | +++ | 2               |
| Patient 57                             | +++   | +++ | +++  | +++ | 2               |
|  |       |     |      |     |                 |
| Patient 31                             | +     | +   | +    | ++  | 0               |
| Patient 37                             | ++    | ++  | +    | +   | 0               |

**Table 8.6: Semiquantitative assessment of astroglial staining intensities in HD tissue and corresponding controls**

Patient number (Pt nr), staining intensities of HSPB8 and BAG3 staining as assessed by 2 independent Researchers (R1, R2). Semiquantitative scores are: 0: not discernable, +: light, ++: moderate, +++: intense. Control patients were without history of neuropsychiatric diseases.

| Spinocerebellar ataxia type 3 / Basis pontis |       |     |      |     |           |
|--|-------|-----|------|-----|-----------|
| Pt Nr.                                       | HspB8 |     | BAG3 |     | Diagnosis |
|  | R1    | R2  | R1   | R2  |           |
| Patient 25                                   | ++    | +   | +    | +   | SCA3      |
| Patient 41                                   | ++    | ++  | ++   | ++  | SCA3      |
| Patient 42                                   | ++    | ++  | ++   | ++  | SCA3      |
| Patient 43                                   | +++   | +++ | +    | +   | SCA3      |
| Patient 45                                   | +++   | ++  | ++   | ++  | SCA3      |
| Patient 46                                   | +++   | +++ | ++   | ++  | SCA3      |
| Patient 47                                   | ++    | ++  | ++   | +++ | SCA3      |
| Patient 48                                   | +     | +   | +    | +   | SCA3      |
| Patient 49                                   | ++    | ++  | +    | +   | SCA3      |
|  |       |     |      |     |           |
| Patient 27                                   | +     | +   | +    | 0   | Control   |
| Patient 28                                   | +     | +   | 0    | 0   | Control   |
| Patient 30                                   | +     | ++  | 0    | +   | Control   |
| Patient 32                                   | 0     | 0   | 0    | 0   | Control   |
| Patient 33                                   | +     | +   | 0    | 0   | Control   |
| Patient 36                                   | +     | +   | +    | 0   | Control   |
| Patient 38                                   | 0     | 0   | 0    | 0   | Control   |
| Patient 39                                   | +     | +   | 0    | 0   | Control   |
| Patient 40                                   | 0     | 0   | 0    | 0   | Control   |

**Table 8.7: Semiquantitative assessment of astroglial staining intensities in SCA3 tissue and corresponding controls.**

Patient number (Pt nr), staining intensities of HSPB8 and BAG3 staining as assessed by 2 independent Researchers (R1, R2). Semiquantitative scores are: 0: not discernable, +: light, ++: moderate, +++: intense. Control patients were without history of neuropsychiatric diseases.



|           | HspB8          | BAG3           |
|-----------|----------------|----------------|
| AD        | 0,67 (p=0,004) | 1,00 (p=0,002) |
| PD        | 0,83 (p<0,001) | 1,00 (p<0,001) |
| HD        | 1,00 (p=0,008) | 1,00 (p=0,008) |
| SCA3      | 0,63 (p=0,009) | 1,00 (p=0,003) |
| Controls  | 0,71 (p<0,001) | 0,56 (p=0,001) |
| All cases | 0,77 (p<0,001) | 0,85 (p<0,001) |

**Supplementary Table 8.8: Interobserver variability (kappa scores).**  
 Variability in scoring the intensity of both the HspB8 and BAG3 staining by 2 independent researchers (K.S. and M.M.).

**Discussion**

In this report we analyzed the expression pattern of the HSPB8-BAG3 chaperone complex in human post-mortem brain tissue from four different protein conformation disorders: Alzheimer’s disease (AD), Parkinson’s disease (PD), Huntington’s disease (HD) and spinocerebellar ataxia type 3 (SCA3). In these neurodegenerative diseases, we observed upregulation of HSPB8 and BAG3 selectively in astrocytes located within the degenerated areas, with no detectable change in their expression levels in neurons. In addition, we also observed that fibroblasts from SCA3 patients upregulate HSPB8-BAG3. These fibroblasts have no disease-related phenotype nor develop inclusions, not even upon prolonged culturing, suggesting that the elevated HSPB8-BAG3 expression might represents a protective adaptation to combat this chronic stress condition.

Astrocytes are glial cells which initially were thought to mainly provide structural support to neurons, but later were shown to release important neuronal growth factors, actively maintain neuronal homeostasis, to regulate the neuronal production of synapses and growth of neuronal extension and to control the rate of proliferation of neuronal stem cells in the adult brain [20, 22, 49, 62, 67]. Under stressful conditions characterized by neuronal metabolic dysfunction and/or neuronal death, astrocytes undergo a process named reactive gliosis. Reactive gliosis plays an essential role for the maintenance of local homeostasis and participates in the protection of the remaining neurons and restoration of their metabolic functions [53].

Following neuronal cell death, reactive astrocytes may acquire phagocytic properties and participate together with microglia in the clearance of injured neurons and thus of the potentially toxic cellular debris [1, 37, 43, 66, 69, 72]. Microglia represent the first line of defense against neuronal damage and pathogens [50]; however, experimental evidence suggests that also astrocyte-mediated phagocytosis may contribute to the repair process of the nervous system aimed at confining neurodegeneration and

maintaining the local tissue homeostasis [37, 43, 58, 72]. Interestingly, we recently published a role for the HSPB8-BAG3 complex in autophagy activation and in the degradation of misfolded aggregate-prone proteins [11].

In particular, overexpression of HSPB8 and BAG3 in mammalian cells significantly increases the formation of autophagic vacuoles, whereas their knock-down impairs autophagy activation upon proteotoxic stress conditions, suggesting that they might modulate the biogenesis of these vacuoles [11]. Moreover, HSPB8 has been largely localized to the plasma membrane and has been found associated with lipids *in vitro* [13]. Autophagy and phagocytosis are ancient and highly conserved cellular processes that share many functional aspects, such as the engulfment and digestion of material found within the intracellular or extracellular space, respectively [19]. In both autophagy and phagocytosis, the degradation of the sequestered material is achieved through the maturation of autophagosomes or phagosomes, respectively, into acidified organelles called autophagolysosomes or phagolysosomes [19]. Finally, recent evidence suggests cooperation between autophagy and phagocytosis in infection and immunity [57, 64]. On the basis of these findings, it could be envisioned that the selective upregulation of HSPB8 and BAG3 observed in astrocytes surrounding damaged neurons may participate in the stimulation of their autophagic/phagocytic properties, which may also contribute to the protective effect of the HSPB8-BAG3 complex.

In addition to the digestion of debris from dead neurons, the upregulation of HSPB8 and BAG3 in astrocytes may facilitate the clearance of extracellular aggregated proteins. In particular, it has been recently shown that neurons can release microaggregated proteins (e.g.  $\alpha$ -synuclein), which can be taken up through endocytosis by astrocytes [42, 43]. Once it has entered the astrocytes, the aggregated  $\alpha$ -synuclein travels along the endosomal pathway and is degraded by the lysosomes [42, 43]. Similarly, astrocytes have been shown to bind and clear amyloid- $\beta$  deposits [37, 72], suggesting that astrocytes may represent important sites for the clearance of potentially harmful extraneuronal protein aggregates. It is thus tempting to speculate that increased expression levels of HSPB8 and BAG3 might serve to ensure high phagocytic capacity of the reactive astrocytes surrounding degenerating neurons and aggregated proteins. In this respect, it is intriguing to note that HSPB8 and BAG3 were highly expressed in astrocytes located adjacent to the amyloid- $\beta$  enriched extracellular mature plaques in AD (our observation and [70]).

Another important aspect of reactive gliosis is that in the presence of neuronal damage, reactive astrocytes undergo a dramatic reorganization of the cytoskeleton as well as hypertrophy of their cellular processes and can migrate towards the injured areas. This process is evidenced by e.g. an increased expression of intermediate filament proteins, such as glial fibrillary acidic protein (GFAP), vimentin and nestin [21, 23]. In mammalian cells, some members of the small heat shock protein family, like HSPB1 and HSPB5 interact with and stabilize the elements of the cytoskeleton [32, 39, 40, 70, 71]. The selective upregulation of HSPB1 and HSPB5 within reactive astrocytes may

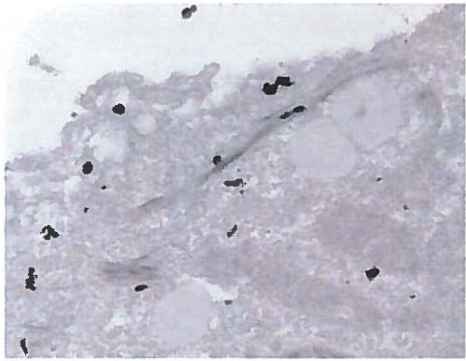
participate to ensure stability to the cytoskeleton during their structural reorganization. Such a hypothesis could apply also for HSPB8. In fact we could observe that HSPB8 is highly associated with cytoskeletal elements in human cells (data not shown) and, most importantly, it colocalizes with GFAP-positive filament like structures in primary astrocytes (Supplementary Fig. 7). Concerning BAG3, it also colocalizes with cytoskeletal elements and participates in the modulation of cell migration [7, 31, 33, 36]. Thus, aside from being upregulated for the (phagocytic) clearance of neuronal debris and extracellular protein aggregates, the upregulation of HSPB8 and BAG3 in reactive astrocytes may also reflect their requirement for cytoskeletal remodeling needed for the activation of the astrocytes, for migration to their target area and for the functional changes of these cells.

Regarding the expression levels of HSPB8 and BAG3 in neurons located in brain regions characterized by neurodegeneration, it was surprising to find no major changes, irrespective of the presence or absence of visible protein aggregates. Moreover, HSPB8 and BAG3 were not colocalizing with polyglutamine aggregates neither in HD nor in SCA3 brains, but in contrast were highly expressed in astrocytes adjacent to the amyloid- $\beta$  enriched extracellular mature plaques in AD (our observation and [70]). Furthermore, both HSPB8 and BAG3 were present in Lewy bodies, but not Lewy neurites. Interestingly, Lewy neurites also do not stain for the p62 protein, which is involved in aggregate formation and protein degradation [7]. This implies that basic differences between Lewy bodies and Lewy neurites might exist regarding their composition and structure [38]. Since HSPB8 and BAG3 were also elevated in fibroblasts from SCA3 patients, which (yet) lack visible protein aggregates, one could speculate that the upregulation of the complex necessary for the clearance of endogenous (mini)aggregates may occur at an early stage of disease, e.g. before the onset of inclusion formation. So at later stages (such in the brains that we investigated), neuronal cells are beyond this point and at this later stage of disease, neuronal rescue is beyond the point of no return. The upregulation of HSPB8 and BAG3 may then take place in the active astrocytes to prevent further damage to the surrounding neurons. Alternatively, neurons may simply lack the correct signaling pathways to induce HSPB8 and BAG3 in response to intraneuronal damage.

BAG3 has been recently reported to be upregulated in brain during aging [25]. Most of the brain sections analyzed in our study were from relatively old patients; thus one could assume that the upregulation of HSPB8 and BAG3 observed could merely be due to the aging process. However, within the brain tissues from old patients affected by proteinopathies (AD, HD, SCA3 or PD), the upregulation of HSPB8 and BAG3 was confined only to areas characterized by the presence of neurodegeneration, whereas no change in HSPB8 and BAG3 expression was found in unaffected areas of the same old-aged patient. Moreover, we could observe a significant increase in HSPB8 and BAG3 expression levels, again selectively in areas affected by neurodegeneration, in two relatively young SCA3 patients (34 and 42 years-old, respectively). Finally, no upregulation of HSPB8 and BAG3 was found in the brain of a 90 years old patient diagnosed with presymptomatic PD, showing Lewy pathology but no visible loss of

nigral neurons. All together these observations strongly suggest that the increase in HSPB8 and BAG3 observed in our study is most likely unrelated to the aging process.

A



B

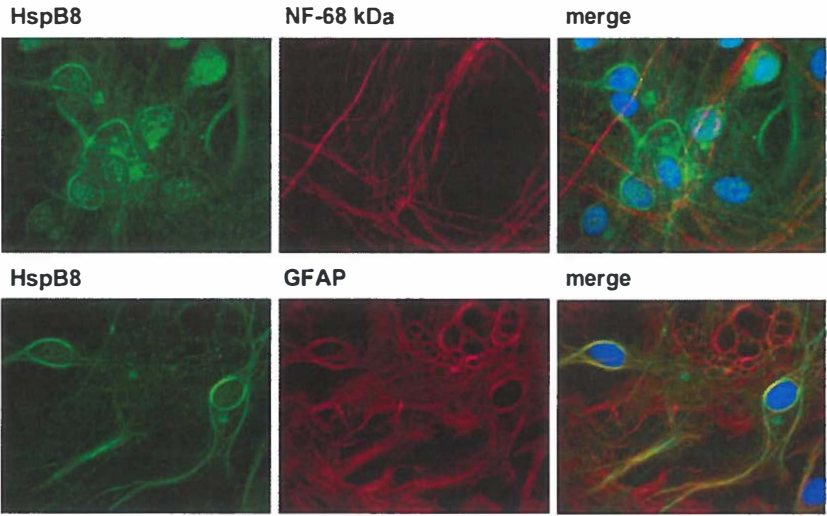


**Figure 8.13: Association of endogenous HSPB8 with the cytoskeleton.** Primary rat hippocampal neuronal culture showing that endogenous HSPB8 is expressed in astrocytes, where it colocalizes with GFAP and showed a filament like-staining; in contrast, HSPB8 did not colocalize with the axonal marker neurofilament light polypeptide 68 kDa (NF-68 kDa).

Considering the ability of HSPB8 and BAG3 to facilitate the clearance of aggregated proteins in mammalian cells, pharmacological upregulation of these chaperones in neurons at early stage of disease might represent a valid therapeutic tool to slow-down the progression of protein conformational disorders. However, it is still unclear whether the upregulation of HSPB8 and BAG3 in astrocytes during the late stage of disease may also effectively participate to decrease the severity of neurodegeneration and to tissue repair process. Future studies are needed to investigate the pathophysiological significance and function of HSPB8-BAG3 upregulation in astrocytes in neurodegenerative disorders.

## **Acknowledgments**

This work was supported by the National Ataxia Foundation Young Investigator Award, by the Marie Curie International Reintegration Grant (PIRG-03-GA-2008-230908) and by the Prinses Beatrix Fonds/Dutch Huntington Association (WAR09-23) awarded to S. Carra, by the Prinses Beatrix Fonds (WAR05-0129) awarded to E.R. Brunt and H.H. Kampinga, by the Jan Kornelis de Cock stichting (08-15) awarded to W.F.A. den Dunnen, by the Dr. Senckenbergische Stiftung and the Stiftung Hoffnung awarded to U. Rüb and by support from the Dutch ADCA patient society and GUIDE/BCN awarded to W.F.A. den Dunnen, U. Rub and H.H. Kampinga.

## References

1. al-Ali SY, al-Hussain SM. An ultrastructural study of the phagocytic activity of astrocytes in adult rat brain. *Journal of anatomy* 1996;188:257-262.
2. Bailey CK, Andriola IF, Kampinga HH, Merry DE. Molecular chaperones enhance the degradation of expanded polyglutamine repeat androgen receptor in a cellular model of spinal and bulbar muscular atrophy. *Hum Mol Genet* 2002;11:515-523.
3. Barral JM, Broadley SA, Schaffar G, Hartl FU. Roles of molecular chaperones in protein misfolding diseases. *Semin Cell Dev Biol* 2004;15:17-29.
4. Bence NF, Sampat RM, Kopito RR. Impairment of the ubiquitin-proteasome system by protein aggregation. *Science* 2001;292:1552-1555.
5. Berger Z, Ravikumar B, Menzies FM, Oroz LG, Underwood BR, Pangalos MN, Schmitt I, Wullner U, Evert BO, O'Kane CJ, Rubinsztein DC. Rapamycin alleviates toxicity of different aggregate-prone proteins. *Hum Mol Genet* 2006;15:433-442.
6. Bilen J, Bonini NM. Genome-wide screen for modifiers of ataxin-3 neurodegeneration in *Drosophila*. *PLoS genetics* 2007;3:1950-1964.
7. Bjorkoy G, Lamark T, Brech A, Outzen H, Perander M, Overvatn A, Stenmark H, Johansen T. p62/SQSTM1 forms protein aggregates degraded by autophagy and has a protective effect on huntingtin-induced cell death. *J Cell Biol* 2005;171:603-614.
8. Braak H, Braak E. Staging of Alzheimer's disease-related neurofibrillary changes. *Neurobiol Aging* 1995;16:271-278; discussion 8-84.
9. Braak H, Del Tredici K, Bratzke H, Hamm-Clement J, Sandmann-Keil D, Rub U. Staging of the intracerebral inclusion body pathology associated with idiopathic Parkinson's disease (preclinical and clinical stages). *J Neurol* 2002;249 Suppl 3: III/1-5.
10. Bucciantini M, Giannoni E, Chiti F, Baroni F, Formigli L, Zurdo J, Taddei N, Ramponi G, Dobson CM, Stefani M. Inherent toxicity of aggregates implies a



common mechanism for protein misfolding diseases. *Nature* 2002;416:507-511.

11. Carra S, Seguin SJ, Lambert H, Landry J. HspB8 chaperone activity toward poly(Q)-containing proteins depends on its association with Bag3, a stimulator of macroautophagy. *J Biol Chem* 2008;283:1437-1444.
12. Carra S, Sivilotti M, Chavez Zobel AT, Lambert H, Landry J. HspB8, a small heat shock protein mutated in human neuromuscular disorders, has in vivo chaperone activity in cultured cells. *Hum Mol Genet* 2005;14:1659-1669.
13. Chowdary TK, Raman B, Ramakrishna T, Rao Ch M. Interaction of mammalian Hsp22 with lipid membranes. *Biochem J* 2007;401:437-445.
14. Connell P, Ballinger CA, Jiang J, Wu Y, Thompson LJ, Hohfeld J, Patterson C. The co-chaperone CHIP regulates protein triage decisions mediated by heat-shock proteins. *Nat Cell Biol* 2001;3:93-96.
15. Cuervo AM, Dice JF. Lysosomes, a meeting point of proteins, chaperones, and proteases. *Journal of molecular medicine (Berlin, Germany)* 1998;76:6-12.
16. Cuervo AM, Dice JF. Age-related decline in chaperone-mediated autophagy. *J Biol Chem* 2000;275:31505-31513.
17. Cummings CJ, Zoghbi HY. Trinucleotide repeats: mechanisms and pathophysiology. *Annu Rev Genomics Hum Genet* 2000;1:281-328.
18. Demand J, Alberti S, Patterson C, Hohfeld J. Cooperation of a ubiquitin domain protein and an E3 ubiquitin ligase during chaperone/proteasome coupling. *Curr Biol* 2001;11:1569-1577.
19. Deretic V. Autophagosome and phagosome. *Methods in molecular biology (Clifton, NJ)* 2008;445:1-10.
20. Doetsch F, Caille I, Lim DA, Garcia-Verdugo JM, Alvarez-Buylla A. Subventricular zone astrocytes are neural stem cells in the adult mammalian brain. *Cell* 1999;97:703-716.

21. Eddleston M, Mucke L. Molecular profile of reactive astrocytes--implications for their role in neurologic disease. *Neuroscience* 1993;54:15-36.
22. Emsley JG, Arlotta P, Macklis JD. Star-cross'd neurons: astroglial effects on neural repair in the adult mammalian CNS. *Trends Neurosci* 2004;27:238-240.
23. Eng LF, Ghimikar RS. GFAP and astrogliosis. *Brain Pathol* 1994;4:229-237.
24. Fontaine JM, Rest JS, Welsh MJ, Benndorf R. The sperm outer dense fiber protein is the 10th member of the superfamily of mammalian small stress proteins. *Cell Stress Chaperones* 2003;8:62-69.
25. Gamerdinger M, Hajieva P, Kaya AM, Wolfrum U, Hartl FU, Behl C. Protein quality control during aging involves recruitment of the macroautophagy pathway by BAG3. *Embo J* 2009;28:889-901.
26. Goldberg AL. Protein degradation and protection against misfolded or damaged proteins. *Nature* 2003;426:895-899.
27. Gunawardena S, Goldstein LS. Polyglutamine diseases and transport problems: deadly traffic jams on neuronal highways. *Archives of neurology* 2005;62:46-51.
28. Hara T, Nakamura K, Matsui M, Yamamoto A, Nakahara Y, Suzuki-Migishima R, Yokoyama M, Mishima K, Saito I, Okano H, Mizushima N. Suppression of basal autophagy in neural cells causes neurodegenerative disease in mice. *Nature* 2006;441:885-889.
29. Hartl FU. Molecular chaperones in cellular protein folding. *Nature*;381: 571-579.
30. Head MW, Goldman JE. Small heat shock proteins, the cytoskeleton, and inclusion body formation. *Neuropathol Appl Neurobiol* 2000;26:304-312.
31. Homma S, Iwasaki M, Shelton GD, Engvall E, Reed JC, Takayama S. BAG3 deficiency results in fulminant myopathy and early lethality. *Am J Pathol* 2006;169:761-773.

32. Iwaki T, Iwaki A, Tateishi J, Goldman JE. Sense and antisense modification of glial alpha B-crystallin production results in alterations of stress fiber formation and thermoresistance. *J Cell Biol* 1994;125:1385-1393.
33. Iwasaki M, Homma S, Hishiya A, Dolezal SJ, Reed JC, Takayama S. BAG3 regulates motility and adhesion of epithelial cancer cells. *Cancer Res* 2007; 67:10252-10259.
34. Kappe G, Franck E, Verschuure P, Boelens WC, Leunissen JA, de Jong WW. The human genome encodes 10 alpha-crystallin-related small heat shock proteins: HspB1-10. *Cell Stress Chaperones* 2003;8:53-61.
35. Kappe G, Verschuure P, Philipsen RL, Staaldin AA, Van de Boogaart P, Boelens WC, De Jong WW. Characterization of two novel human small heat shock proteins: protein kinase-related HspB8 and testis-specific HspB9. *Biochim Biophys Acta* 2001;1520:1-6.
36. Kassis JN, Guancial EA, Doong H, Virador V, Kohn EC. CAIR-1/BAG-3 modulates cell adhesion and migration by downregulating activity of focal adhesion proteins. *Exp Cell Res* 2006;312:2962-2971.
37. Koistinaho M, Lin S, Wu X, Esterman M, Koger D, Hanson J, Higgs R, Liu F, Malkani S, Bales KR, Paul SM. Apolipoprotein E promotes astrocyte colocalization and degradation of deposited amyloid-beta peptides. *Nat Med* 2004;10:719-726.
38. Kuusisto E, Parkkinen L, Alafuzoff I. Morphogenesis of Lewy bodies: dissimilar incorporation of alpha-synuclein, ubiquitin, and p62. *J Neuropathol Exp Neurol* 2003;62:1241-1253.
39. Lavoie JN, Gingras-Breton G, Tanguay RM, Landry J. Induction of Chinese hamster HSP27 gene expression in mouse cells confers resistance to heat shock. HSP27 stabilization of the microfilament organization. *J Biol Chem* 1993;268:3420-3429.
40. Lavoie JN, Lambert H, Hickey E, Weber LA, Landry J. Modulation of cellular thermoresistance and actin filament stability accompanies phosphorylation-induced changes in the oligomeric structure of heat shock protein 27. *Mol Cell Biol* 1995;5:505-516.

41. Lee VM, Goedert M, Trojanowski JQ. Neurodegenerative tauopathies. *Annu Rev Neurosci* 2001;24:1121-1159.
42. Lee HJ, Suk JE, Bae EJ, Lee JH, Paik SR, Lee SJ. Assembly-dependent endocytosis and clearance of extracellular alpha-synuclein. *Int J Biochem Cell Biol* 2008;40:1835-1849.
43. Lee HJ, Suk JE, Patrick C, Bae EJ, Cho JH, Rho S, Hwang D, Masliah E, Lee SJ. Direct transfer of alpha-synuclein from neuron to astroglia causes inflammatory responses in synucleinopathies. *J Biol Chem* 2010;285:9262-9272.
44. Levine B, Klionsky DJ. Development by self-digestion: molecular mechanisms and biological functions of autophagy. *Dev Cell*;6:463-477.
45. Murray C, Viehman A, Lippa CF. The corpus callosum in Pick's disease, Alzheimer's disease, and amyotrophic lateral sclerosis: gliosis implies possible clinical consequence. *Am J Alzheimers Dis Other Dement* 2006;21:37-43.
46. Ohsumi Y. Molecular dissection of autophagy: two ubiquitin-like systems. *Nat Rev Mol Cell Biol* 2001;2:211-216.
47. Orenstein SJ, Cuervo AM. Chaperone-mediated autophagy: Molecular mechanisms and physiological relevance. *Semin Cell Dev Biol* 2010;21:719-726.
48. Pagliuca MG, Leroise R, Cigliano S, Leone A. Regulation by heavy metals and temperature of the human BAG-3 gene, a modulator of Hsp70 activity. *FEBS Lett* 2003;541:11-15.
49. Parri R, Crunelli V. An astrocyte bridge from synapse to blood flow. *Nat Neurosci* 2003;6:5-6.
50. Ransohoff RM, Perry VH. Microglial physiology: unique stimuli, specialized responses. *Annual review of immunology* 2009;27:119-145.

51. Ravikumar B, Duden R, Rubinsztein DC. Aggregate-prone proteins with polyglutamine and polyalanine expansions are degraded by autophagy. *Hum Mol Genet* 2002;11:1107-1117.
52. Ravikumar B, Vacher C, Berger Z, Davies JE, Luo S, Oroz LG, Scaravilli F, Easton DF, Duden R, O'Kane CJ, Rubinsztein DC. Inhibition of mTOR induces autophagy and reduces toxicity of polyglutamine expansions in fly and mouse models of Huntington disease. *Nat Genet* 2004;36 585-595.
53. Ridet JL, Malhotra SK, Privat A, Gage FH. Reactive astrocytes: cellular and molecular cues to biological function. *Trends Neurosci* 1997;20:570-577.
54. Ross CA, Pickart CM. The ubiquitin-proteasome pathway in Parkinson's disease and other neurodegenerative diseases. *Trends Cell Biol* 2004;14: 703-711.
55. Rüb U, Gierga K, Brunt ER, de Vos RA, Bauer M, Schols L, Burk K, Auburger G, Bohl J, Schultz C, Vuksic M, Burbach GJ, Braak H, Deller T. Spinocerebellar ataxias types 2 and 3: degeneration of the pre-cerebellar nuclei isolates the three phylogenetically defined regions of the cerebellum. *J Neural Transm* 2005;112:1523-1545.
56. Rüb U, Heinsen H, Brunt ER, Landwehrmeyer B, Den Dunnen WF, Gierga K, Deller T. The human premotor oculomotor brainstem system - can it help to understand oculomotor symptoms in Huntington's disease? *Neuropathol Appl Neurobiol* 2009;35:4-15.
57. Shintani T, Klionsky DJ. Autophagy in health and disease: a double-edged sword. *Science* 2004;306:990-995.
58. Sofroniew MV. Molecular dissection of reactive astrogliosis and glial scar formation. *Trends Neurosci* 2009;32:638-647.
59. Soto C. Unfolding the role of protein misfolding in neurodegenerative diseases. *Nat Rev Neurosci* 2003;4:49-60.
60. Sugars KL, Rubinsztein DC. Transcriptional abnormalities in Huntington disease. *Trends Genet* 2003;19 233-238.

61. Sun X, Fontaine JM, Bartl I, Behnam B, Welsh MJ, Benndorf R. Induction of Hsp22 (HspB8) by estrogen and the metalloestrogen cadmium in estrogen receptor-positive breast cancer cells. *Cell Stress Chaperones* 2007;12:307-319.
62. Svendsen CN. The amazing astrocyte. *Nature* 2002;417:29-32.
63. Takayama S, Reed JC. Molecular chaperone targeting and regulation by BAG family proteins. *Nat Cell Biol* 2001;3:E237-241.
64. Tal MC, Iwasaki A. Autophagy and innate recognition systems. *Current topics in microbiology and immunology* 2009;335:107-121.
65. Verhoef LG, Lindsten K, Masucci MG, Dantuma NP. Aggregate formation inhibits proteasomal degradation of polyglutamine proteins. *Hum Mol Genet* 2002;11:2689-2700.
66. Viores SA, Herman MM. Phagocytosis of myelin by astrocytes in explants of adult rabbit cerebral white matter maintained on Gelfoam matrix. *J Neuroimmunol* 1993;43:169-176.
67. Volterra A, Meldolesi J. Astrocytes, from brain glue to communication elements: the revolution continues. *Nat Rev Neurosci* 2005;6:626-640.
68. Warrick JM, Chan HY, Gray-Board GL, Chai Y, Paulson HL, Bonini NM. Suppression of polyglutamine-mediated neurodegeneration in *Drosophila* by the molecular chaperone HSP70. *Nat Genet* 1999;23:425-428.
69. Watabe K, Osborne D, Kim SU. Phagocytic activity of human adult astrocytes and oligodendrocytes in culture. *J Neuropathol Exp Neurol* 1989;48:499-506.
70. Wilhelmus MM, Boelens WC, Otte-Holler I, Kamps B, Kusters B, Maat-Schieman ML, de Waal RM, Verbeek MM. Small heat shock protein HspB8: its distribution in Alzheimer's disease brains and its inhibition of amyloid-beta protein aggregation and cerebrovascular amyloid-beta toxicity. *Acta Neuropathol (Berl)* 2006;111:139-149.
71. Wisniewski T, Goldman JE. Alpha B-crystallin is associated with intermediate filaments in astrocytoma cells. *Neurochem Res* 1998;23:385-392.



72. Wyss-Coray T, Loike JD, Brionne TC, Lu E, Anankov R, Yan F, Silverstein SC, Husemann J. Adult mouse astrocytes degrade amyloid-beta in vitro and in situ. *Nat Med* 2003;9:453-457.
73. Wyttenbach A, Carmichael J, Swartz J, Furlong RA, Narain Y, Rankin J, Rubinsztein DC. Effects of heat shock, heat shock protein 40 (HDJ-2), and proteasome inhibition on protein aggregation in cellular models of Huntington's disease. *Proc Natl Acad Sci U S A* 2000;97:2898-2903.
74. Wyttenbach A, Sauvageot O, Carmichael J, Diaz-Latoud C, Arrigo AP, Rubinsztein DC. Heat shock protein 27 prevents cellular polyglutamine toxicity and suppresses the increase of reactive oxygen species caused by huntingtin. *Hum Mol Genet* 2002;11:1137-1151.
75. Young JC, Agashe VR, Siegers K, Hartl FU. Pathways of chaperone-mediated protein folding in the cytosol. *Nat Rev Mol Cell Biol* 2004;5:781-791.



## **Chapter 9**

---

### **Discussion and future perspectives**

---

**Contents**

---

|            |  |            |
|------------|--|------------|
| <b>9.1</b> | <b>Pathological pathways in protein aggregation diseases</b> | <b>191</b> |
| <b>9.2</b> | <b>Relevance of the study</b>                                | <b>196</b> |
| <b>9.3</b> | <b>Future perspectives</b>                                   | <b>198</b> |

## Discussion

A large number of the neurodegenerative diseases are characterized by protein aggregation, which can be recognized by histochemical and immunohistochemical methods. The diseases described in this thesis, Alzheimer's disease, Parkinson's disease, Huntington's disease and Spinocerebellar Ataxia type 3, all exhibit several types of protein aggregations. As the aggregation of disease proteins is the unifying mechanism of these diseases, I will here discuss the possible underlying processes which result in neurodegeneration.

### 9.1. Pathological pathways in protein aggregation diseases

#### *Primary causes*

At the basic levels of the neurodegenerative diseases, there are several ways through which a pathologically altered protein can cause damage to a given cell. The first pathway is damage due to the pathological alteration of the protein, which is the focus of this thesis. In the polyQ diseases, the expansion of the glutamine sequence leads to aggregation, a function not intrinsic to the disease protein in question and therefore not specific to any polyQ protein [17]. Likewise, the tau protein of AD gains its aggregation properties by aberrant phosphorylation [21]. This can affect the cell by overloading the PQC, inhibiting transport and by nonspecific sequestration of proteins (e.g. polyQ proteins sequester glutamine rich transcription factors), thus inhibiting their function [10, 16, 31].

Other pathways involve the normal protein functions and interaction. Pathological alteration of a protein can lead to loss of function, as the protein is no longer fit to fulfill its role in the cellular metabolism. An example is ataxin-7, which is part of the STAGA complex regulating transcription function, which is disrupted upon glutamine expansion in the protein [20]. Alternatively to this, a protein may experience a toxic gain of function by expansion of its normal function. An example of this is ataxin-3, which through its intrinsic de-ubiquitinating function regulates the degradation of parkin [13]. Upon elongation of the polyQ tract the rate of degradation of parkin actually increases.

So, although especially the heritable neurodegenerative diseases are monogenic, neurodegeneration likely occurs through multiple pathways including both toxic gain and loss of function mechanisms.

Whereas the effects of dominant gain of aggregation may be rather disease non-specific (and thus require generic treatments), effects due to gain of protein function as well as haploinsufficiency effects related to loss of function likely contribute to disease and brain area specific features of each individual disease. Also, the relative contribution of each of these aspects may be different for the various diseases, e.g., in the polyQ disorders due to a very long expansion (e.g. SCA2, 3, 7) toxic aggregation may be the highly dominant effects, since the propensity to aggregate increases with the length of the polyQ sequence. Inversely, in diseases with shorter CAG repeats (e.g.

SCA6, HD) symptoms associated with gain or loss of the disease protein may play a prominent role as well.

Additionally to the effects caused by the different pathological intracellular processes there are the systemic aspects to neurodegeneration. Neuronal survival depends on the interplay between connected neurons. If one cell is lost from a given neuronal circuit, the whole system is weakened and the survivability of direct interactors is compromised [9]. Additionally, glial cells, which normally lend trophic support to neurons, can exhibit disease phenomena, and loss of glial support is just as detrimental, as is loss of neuronal interconnections [45].

Finally, several modifiers, in the form of external and internal, patient specific factors, which are not directly linked to the disease process, can ameliorate or exacerbate neurodegenerative diseases. External factors include overall health of the patient and exposure to toxins (e.g. certain pesticides raise the probability of developing Parkinson's disease) [3]. Polymorphisms inherent to the patient can also act as modifiers of the disease (e.g. the ApoE polymorphism is a well known modifier of the lifetime risk for AD, and DnaJB1 expression levels modify age of onset of SCA3) [34, 49].

#### *Secondary effects*

The primary proteotoxic pathways listed above may damage cells in a number of ways. Several of these, which are of relevance in regard to this thesis, are listed below.

##### *(1) Transport Blockage and Neurotrophic factors*

Whereas most research has been focused on the formation of aggregates in the soma or in the nucleus of neurons, one must be aware that aggregation also occurs in axonal processes, exemplified by the tau tangles of AD (Figure 1.2), the Lewy neurites of PD (Figure 1.3) and the axonal aggregates of HD and SCA3 (Figure 1.6, Figure 4.1) (Chapter 4). While many lines of research indicate a primary protective effect of the formation of nuclear or somatic macroaggregates, the axon seems to be a less than ideal place to enact this process [2, 16]. Transport processes running through the axon are vital for the correct functioning of the neuron. Vital protein components moved via anterograde transport ensure correct function of the neuronal synapses, while at the same time, neurotrophic factors as well as messenger molecules transported retrogradely towards the neuronal soma ensure cell survival and plasticity. An example of the importance of growth factors for neuronal survival can be deduced from neuronal lesion experiments, where application of neural growth factor (NGF) improved neuronal survivability in the cholinergic basal forebrain nuclei after lesion of afferent pathways, mimicking neuronal degeneration in AD [9]. Macroaggregates impairing these transport pathways are likely to obstruct these vital processes, resulting in cellular stress and decreased chance of survival of these cells [16]. This is underscored by the fact that fiber tracts affected in SCA3 by aggregation correspond well with systems known to be affected and to degenerate in the process of the disease (Chapter 4).



## *(2) Protein quality control*

As mentioned in the introduction, the cell has a large array of pathways to counter protein aggregation, which is important in stress conditions, but also for normal cell homeostasis [19] (See Chapter 5). Yet, the appearance of visible protein aggregates themselves is a basic indicator of a failed PQC. However, as our data suggest (Chapter 7), despite this failure to handle the disease protein, proteasomal function seems to remain intact for a prolonged period even after neuronal nuclear inclusions (NNI) are formed. Similarly, several NNI containing cells have not mounted a stress response, suggesting that the PQC indeed did not recognize and/or counteract polyQ aggregation and thus, that the inclusion formation per se serves as a back-up and protective mechanism to deposit smaller oligomeric material that would otherwise impede the survival of the cell [2, 24], even though this may impair some neuronal functions as described before (chapters 1 and 4). That this indeed likely represents a secondary mechanism as a result of failure of the primary PQC system is underscored by the fact that the protein aggregates found in most neurodegenerative diseases are ubiquitinated, meaning they were originally tagged for degradation via the proteasome, which was unable to do so [8, 10]. The finding of proteasomal components which are in or associated with these macro-aggregates [31] further supports this. The sequestration of proteasomal components does not directly inhibit proteasomal function, as accumulation of UBB<sup>+1</sup> only occurs in a few cells, (Chapter 7) probably at a late stage of disease. Subsequently, degeneration may rapidly progress as UBB<sup>+1</sup> accumulation itself may impair proteasomal activity [12], and as such proteostasis may decline fast from this point onwards. This, rather than the polyQ inclusion as such, may then trigger the stress response, consistent with what we observed in presumed later stages when HSPA1A is up-regulated in neuronal cells (Chapter 7). This occurs when an important cofactor of HSPA1A, DnaJB1, is sequestered into the nuclear aggregates (Chapter 7). DNAJB1 can maintain proteins in a state competent for both refolding and degradation [23] and assist polyQ protein degradation through the proteasome [4]. If, as suggested by the UBB<sup>+1</sup> data, the proteasome function is impaired, DNAJB1 and its clients may aggregate consistent with the observed recruitment in the inclusion and thus reflecting failed function. The decreased availability of DNAJB1 as vital HSPA1A/HSPA8 co-factor, next causes the acute stress that initiates the Heat shock response. However, this is likely too late to rescue the neuron from dying. In summary, our data indicate that the chronic expression of the polyQ proteins themselves does not activate the stress response, meaning that polyQ protein by itself is not (so) misfolded and that its aggregation initially does not have a significant impact on proteostasis. It is not until late in the disease process, that the impairment of the PQC reaches detectable levels (chapter 7).

Another important component of the PQC that is often present in protein inclusions is the p62 protein. P62 acts as a shuttle protein towards both autophagosomal and lysosomal degradation, and importantly, adds in the formation of inclusions/macroaggregates [5, 47]. The early presence of p62 within inclusions/macroaggregates suggests that the cells indeed primarily and actively

sequester polyQ proteins or small oligomeric aggregates into larger inclusions, rather than handling it via the proteasome (Chapter 7) [5]. The observation of p62 positive aggregates in SCA6 was of special interest in this regard, as this also hints at PQC disturbances in SCA6, which was beforehand thought of primarily as a channelopathy (Chapter 6) [25].

However, even in the same disease not all kinds of aggregates display the same staining pattern. As was shown previously in PD, Lewy bodies are positive for p62. However, Lewy neurites, which like Lewy bodies consist of alpha-synuclein, do not stain for p62 [26]. Similarly, we observed HSPB8/BAG3 association only with Lewy bodies, but not with Lewy neurites (Chapter 8). In SCA3 we also observed association of p62 with NNI, but not with more diffuse staining patterns (chapter 7). These different staining properties may be explained by a maturation process, where the p62-positive aggregate is the more mature form, or that those aggregates are fundamentally different.

### *(3) Interaction with other proteins*

As stated above, aggregating disease protein can affect other proteins both specifically (gain/loss of function) as well as unspecifically (gain of aggregation), leading to different consequences. Several disease proteins are known to be involved in transcription (e.g. SCA7) or protein stability (e.g. tau, SCA3) [13, 20, 21, 29]. Their interacting partners may co-aggregate, leading to loss of function. Furthermore, polyQ sequence extensions may give rise to new interactions with other non-mutated proteins containing polyglutamine sequences, most notably several transcription factors [29, 32, 40]. For example, Shimohata et al. demonstrated the strong binding of the TAF4 (TAFII130) to expanded polyQ sequences, which in a reporter essay resulted in decreased CREB-dependent translation of reporter genes. Similarly, Perez et al. showed many other regulatory proteins being recruited in polyQ aggregates in fly and cell models [32, 40]. It is important to note, that these interactions are unspecific and not related to normal protein functions, but rather and likely cause their loss of function.

The exact phenotype resulting from these altered interactions depends on the nature of the interactor. Cross comparison between the role of interactors of disease proteins and neuropathological data could elicit the pathophysiological underpinnings of the selective vulnerability often observed in neurodegenerative disease [13, 20, 41].

### *(4) Oxidative Stress*

Oxidative stress is caused by an overabundance of oxidative molecules, such as reactive oxygen species (ROS) or reactive nitrogen species (RNS), resulting from higher production than breakdown rates of these molecules. They can result from light or ionizing radiation or can be taken up from the environment [43]. But, more importantly, they can be formed by biological processes, especially by the respiratory chain. Since the human brain has extremely high energy consumption, oxidative

species are abundant in neurons. However, cells have numerous defenses against oxidative stresses.

Aggregating protein can cause oxidative stress by damaging components of the respiratory chain or of antioxidant systems. In AD and PD, patient tissue and model organisms display signs of oxidative stress [7, 33] and the aggregating amyloid-beta protein itself may contribute to the formation of oxidative stress by disrupting the structure of mitochondria [36]. Likewise, idiopathic cases of PD presented a reduction in complex 1 activity and PINK1, a protein known to be causative for familial parkinsonism, is a known interactor of complex 1 [46].

#### *(5) Neuron-neuron and neuron-glia interactions*

As stated above, neurodegeneration is not just a cell autonomous process. Often whole neuronal systems are affected in disease, with the targets of an affected system also degenerating somewhat later in the disease process. There are at least two plausible reasons for this. One is the transmission of toxic protein species to neighboring neurons via axonal transport or transsynaptic transmission [27]. Transmission of proteotoxic species from diseased to healthy tissue has been demonstrated in several cases of PD, where the patients received neuronal grafts. After the death of the patients, severe Lewy pathology within the grafts was detectable [28]. Aside from transmission of pathologically altered protein species, the simple loss of the targets of neurons also compromises their survivability. Neurons require trophic factors from their targets to function correctly. If a given neuron loses contact to its target it will receive less trophic factors, similarly to when axonal transport is blocked (Chapter 4) [9]. If the neuron is also affected by other sources of stress, such as ongoing protein aggregation, an additive effect of both stressors may eventually lead to the death of this cell.

Outside of the neuronal systems, glial cells, and especially astrocytes may be an important aspect of neurodegenerative disease. In their normal function they provide structural support, trophic factors, a suitable environment and may add in neuronal differentiation. In neurodegenerative diseases, apart from the well-documented formation of the gliotic scar, they are known to aid neurons, but can also release detrimental factors [45]. Interestingly, astroglia can endocytose certain disease proteins and even transmit alpha-synuclein to other neurons, several neurodegenerative disease even exhibit astroglial protein aggregates. Furthermore, as we show in chapter 8, a part of the astroglial chaperone system is activated in degenerating areas. Taken together all this hints at a profound astroglial involvement in the processes of neurodegenerative diseases [14, 48].

#### *Conclusion*

The emerging picture is, that neurodegenerative diseases may very well not be caused by a single stressor or pathway, but that there are cumulative effects on the affected cells. Since neurons are postmitotic it is very conceivable that they are especially

vulnerable to cumulative stresses, resulting in the often late onset of the neurodegenerative diseases. Since there seem to be different stages of aggregation, each with their own “phenotype” it is conceivable that neurons experience different types of stress depending on the stage they are in (Chapter 7) (figure 9.1).

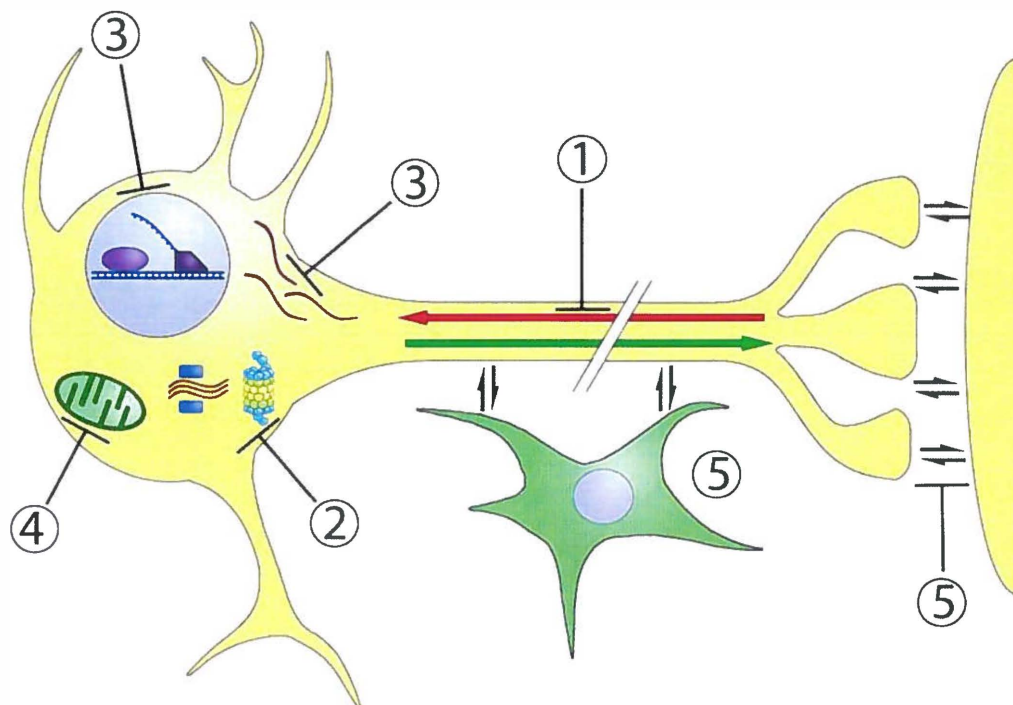


**Figure 9.1: Several different types of stress affect neurons in neurodegenerative diseases**

Depending on the neurodegenerative disease, neurons may be affected by (1) blockage of anterograde and retrograde axonal transport, (2) sequestration and/or overloading of specific parts of the PQC, (3) aberrant interaction with proteins, resulting in altered protein stability, and, in case of transcription factors, in altered protein production, (4) damage to mitochondria, resulting in oxidative stress, (5) disruption of trophic support by the target neuron and transmission of toxic protein species via cell/cell interaction.

## 9.2. Relevance of the studies in this thesis

Investigations into the pathological processes underlying neurodegenerative diseases serve several ends, among them a completion of the clinical picture, setting a baseline for animal models as well as elucidation of disease processes.

### *Protein aggregation and neurodegeneration*

The pathoanatomical investigation of brains afflicted with neurodegenerative diseases can directly elucidate affected systems, and link affected systems to the according symptoms. Our investigation of the hearing tracts improves upon knowledge gained from affected evoked auditory potentials in SCA [1] and confirms that the auditory

tract is indeed affected and SCA patients suffer from hearing problems [39] (Chapter 2).

Using the results of pathoanatomical investigations, new symptoms can be discovered in the neurodegenerative diseases, as in their advanced stages their cardinal symptoms dominate the clinical picture and psychiatric symptoms, which manifest in AD, PD and HD, add to the difficulty of a correct diagnosis. Also early symptoms of the disease may not be recognized as such, like the loss of the sense of smell and constipation in PD and the early eye movement disorders in HD [35], because they may be overshadowed later in the course of the disease or might entirely disappear due to the impairment of other systems. The knowledge of additional symptoms and their underlying pathologies, gained from pathoanatomical studies can provide clues for medical examinations and importantly, enhance the quality of patient care, as has been shown by investigation of the swallowing process in SCA cases [37, 38].

Our pathoanatomical investigation of a brain affected with A30P familial PD (chapter 3) shed light on the pathology of this disease, which indeed proved to be highly similar to idiopathic PD. This is also of interest for the generation of animal models of PD, as A30P mutants are shown to be appropriate to generate models resembling idiopathic PD (Chapter 3) [11, 22].

The consistent presence of axonal aggregates in SCA3 described in chapter 4 adds a new aspect to the SCA3 pathology, as axonal blockage is added as a possible disease mechanism [16]. The actual relevance and impact on the disease process of these aggregates is underscored by their good correlation with degenerating neuronal systems (chapter 4).

#### *Protein aggregation and protein quality control*

In SCA6, we were able to stain masses of aggregating protein with the p62 antibody. Up until now, there was no antibody available to label expanded ataxin-6, since even the pathologically altered polyQ sequence is below 39, and thus too short to be recognized by the 1C2 antibody (chapter 6) [42]. Also, the actual presence of p62 aggregated protein implicates a strong proteostasis component in the pathology of the disease, which was beforehand considered to be primarily a channelopathy. Together with chapter 4 and 7, the discovery also sheds light on the tendency of neurons to sequester pathologically altered protein into aggregates in all intracellular compartments, possibly with different consequences for the cell.

The careful (semi)quantitative investigation undertaken in chapter 7 furthered our understanding of aggregation pathology of SCA3. It describes a possible sequential pathological pathway to the polyglutamine diseases. Moreover, it shows that the primary PQC system may not act upon polyQ aggregation initially. Yet, we do show that the aggregating proteins overload the neuronal PQC, but only in a late stage of the disease. This system next becomes unavailable for normal folding tasks, resulting in



severely stressed neurons. Also, it establishes a method of quantitative analysis for human post-mortem for further studies on other protein aggregation diseases.

Our investigation of the HSPB8/BAG3 complex, which was shown to be a powerful regulator of autophagic degradation of polyQ proteins [6], showed that both HSPB8 and BAG3 are upregulated in astrocytes of degenerating areas. Astrocytes, which are important interactors of neurons, clearly respond to pathological alterations, and may be involved in the disease process themselves. Astrocytes which were initially conceived as cells providing structural support to neurons, have been shown to provide essential support to neurons on different levels, even drive differentiation and act in neurodegenerative diseases [14, 45, 48]. In what precise way the response of the astroglia might be beneficial to the affected neurons (if at all) has to be further researched. However, the implications for phagocytic clearance of neuronal debris are quite strong (chapter 8) [6, 48].

### **9.3. Future perspectives**

The results of the studies presented here provide hints at pathological processes, both on systemic and cellular level, but rarely provide true final answers to the problems at hand. As a matter of fact, while many processes have been implicated, the primary connection between protein aggregation and neuronal degeneration is still not resolved, and it is plausible that more pathways to neuronal death exist. From the results presented here, several new questions and lines of research have emerged.

#### *Examination of transport Problems*

As inhibition of the axonal transport seems to be of relevance in HD, SCA3 and possibly PD (in the form of Lewy Neurites) a more in-depth approach is of interest [16]. A validation of the presence of aggregating protein within axons in the different protein aggregation diseases could easily be undertaken using standard immunohistochemical methods. Possible targets of interest are the amyloid precursor proteins (APP), which is a client of axonal transport and is known to aggregate in axonal lesions, as well as mitochondria, which are being transported to the synaptic terminals.

Furthermore, the knowledge of protein aggregation pathology would greatly profit from an investigation of the underlying processes of axonal clotting. However, normal immunohistochemical methods are only of limited use here. While it is certainly feasible to investigate accumulations of substrates of axonal transport in direct proximity to the aggregates, for investigation of the actual formation of the aggregate and its impact on axonal transport and neuronal health, in vivo imaging techniques provide a better toolset. Transfected, cultured neurons or acute slice cultures from animals expressing the disease protein could be used to monitor axonal aggregates.



### *Cross examination of different protein aggregation diseases*

Most of the studies in this work were undertaken in patient tissue of polyQ disease patients, primarily SCA3. However, protein aggregation also occurs in several other diseases, all of which would be interesting for a cross comparison.

For our initial observations of aggregation related disease pathology, we used the basal pontine area in SCA3, as the area is affected early during the disease process, yet retains enough cells for analysis, opposed to e.g. the major brain nerve nuclei which suffer an extreme loss of neurons. Thus, our primary investigations were undertaken in early pathological areas. A comparison with other early affected sites could either confirm the phases of aggregation as a universal property of early affected areas, or could reveal differences in the distribution of different phases, which may be interesting with regard to selective vulnerability. Similarly, investigation of sites which are known to be affected at different time points during the pathophysiological process may be informative with regard to the progression of the aggregation pathology. Additionally to providing information about possible differences in the progression of aggregation, the information gathered during such an investigation may actually give rise to a staging of SCA3, and possibly other polyQ disorders.

Other protein aggregation diseases are interesting subjects for an investigation of aggregation-related changes. With respect to the polyQ disorders, the difference between diseases with NNI (SCA1, SCA3, SCA7, HD) and without NNI (SCA2, SCA6) is an interesting point of research, since one crucial step of the original aggregation pattern (Figure 7.9), is the formation of a p62-positive aggregate within the neuronal nucleus, which is an environment highly permissive of aggregate formation [30]. This implies differences in the aggregation patterns between those two groups and makes investigation into the aggregation of disease protein and the behavior of elements of the PQC in SCA2 and SCA6 all the more interesting. Even other protein aggregation diseases, which are not related to polyQ disorders, might see similar processes during aggregate formation, and alterations of PQC components. Taken even further, the investigation of the (possible) differences in the specific disease processes, and a comparison with the affected areas may shed some light of the selective vulnerabilities in the respective diseases.

During this work, we were not able to do a complete survey of all PQC components, in relation to the ongoing protein aggregation. Investigations on other HSP family members, most notably DNAJB6 and DNAJB8 [18] and HSPB7 and HSPB9 [44] all shown to be strong suppressors of polyQ aggregation, is opportune as soon as suitable antibodies have become available.

### *Analysis of tissue*

Apart from immunohistochemical analysis of patient tissue, molecular biology offers additional approaches. According to the progressive aggregation model presented in chapter 7, neurons affected with aggregation pathology exhibit characteristic changes to their protein load. The expression pattern of the excised neurons can then be

analysed via mRNA blots, qPCR and micro arrays. However in order to do this, neurons at different stages have to be sampled specifically, as cross sampling a whole section of tissue would include neurons at all stages of aggregation related pathology. Lasermicrodissection (LMD) might provide a solution to the selectivity problem. By using consecutive sections, one 5 $\mu$ m section stained for a suitable marker and a 20 $\mu$ m section for the actual sampling, it is theoretically possible to accurately sample neurons in a specific state of aggregation pathology (Figure 9.2). Pilot studies have to be executed, to determine whether this approach is feasible. This may also allow to do analyses on either neuronal cells or glial cells selectively.

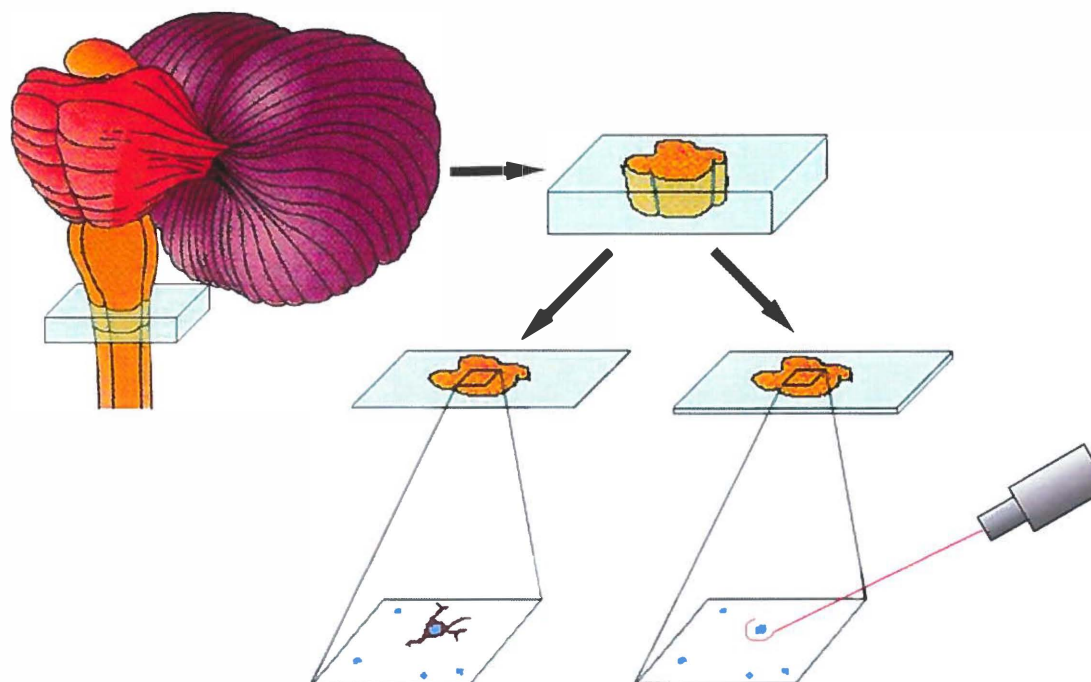


**Figure 9.2: Identifying areas of interest and LMD processing**

Tissue is cryosectioned, alternating in 5 $\mu$ m and 20 $\mu$ m sections. The 5 $\mu$ m are then stained against the protein of interest. Targets are identified, tracked to the subsequent 20 $\mu$ m section, and cut out for later analysis.

### *Animal and cell models*

To complement the other lines of research, in vivo studies of aggregation processes, proteotoxicity and the resulting changes in neuronal or glial cells are of interest. For this, cell and animal models of the disease can be used. By comparing the phenotype described in human pathological material of the available models it can be assessed, how precisely a model mirrors the disease process in question. However, disease models are not without problems.

The short lifespan of lab animals and the even shorter lifespan of cell cultures present a difficult obstacle to modeling neurodegenerative diseases. Neurodegenerative diseases often have a clinical course of over 10 years, with a possibly equally long preclinical phase before that. Still, disease models can be put to very good use to answer specific research questions and monitor specific processes. By combining information from the human pathological situation with detailed information on specific disease processes from a variety of animal and cell models, one can construct detailed models of the complex processes during neurodegenerative diseases, which will deepen our understanding of the diseases and may even result in the development of therapies and, perhaps even cures.

## References

1. Abele M, Bürk K, Andres F, Topka H, Laccone F, Bösch S, Brice A, Cancel G, Dichgans J, Klockgether T. Autosomal dominant cerebellar ataxia type I. Nerve conduction and evoked potential studies in families with SCA1, SCA2 and SCA3. *Brain* 1997;120:2141-2148.
2. Arrasate M, Mitra S, Schweitzer ES, Segal MR, Finkbeiner S. Inclusion body formation reduces levels of mutant huntingtin and the risk of neuronal death. *Nature* 2004;431:805-810.
3. Ascherio A, Chen H, Weisskopf MG, O'Rielly E, McCullough ML, Calle EE, Schwarzschild MA, Thun MJ. Pesticide exposure and risks for Parkinson's disease. *Ann Neurol* 2006;60:197-203.
4. Bailey CK, Andriola IF, Kampinga HH, Merry DE. Molecular chaperones enhance the degradation of expanded polyglutamine repeat androgen receptor in cellular model of spinal and bulbar muscular atrophy. *Hum Mol Genet* 2002;11:515-523.
5. Bjorkoy G, Lamark T, Brech A, Outzen H, Perander M, Overvatn A, Stenmark H, Johansen T. p62/SQSTM1 forms protein aggregates degraded by autophagy and has a protective effect on huntingtin-induced cell death. *J Cell Biol* 2005;171:603-614.
6. Carra S, Seguin SJ, Lambert H, Landry J. HspB8 chaperone activity toward poly(Q)-containing proteins depends on its association with Bag3, a stimulator of macroautophagy. *J Biol Chem* 2008;283:1437-1444.
7. Cassarino DS, Bennett JP Jr. An evaluation of the role of mitochondria in neurodegenerative diseases: mitochondrial mutations and oxidative pathology, protective nuclear responses, and cell death in neurodegeneration. *Brain Res Rev* 1999;29:1-25.
8. Ciechanover A. The ubiquitin-proteasome pathway: on protein death and cell life. *EMBO J* 1998;17:7151-7160.
9. Connor B, Dragunow M. The role of neuronal growth factors in neurodegenerative disorders of the human brain. *Brain Res Rev* 1998;77:1-39.
10. Davies JE, Sarkar S, Rubinsztein DC. The ubiquitin proteasome system in Huntington's disease and the spinocerebellar ataxias. *BMC Biochem* 2007; 8(Suppl 1): S2.

11. Dawson TM, Ko HS, Dawson VL. Genetic animal models of Parkinson's disease. *Neuron* 2010;66:646-661.
12. De Pril R, Hobo B, van Tijn P, Roos RA, van Leeuwen FW, Fischer DF. Modest proteasomal inhibition by aberrant ubiquitin exacerbates aggregate formation in Huntington disease Mouse model. *Mol Cell Neurosci* 2010;43: 281-289.
13. Durcan TM, Kontogiannea M, Thorarinsdottir T, Fallon L, Williams AJ, Diamati A, Fantaneanu T, Paulson FL, Fon EA. The Machado-Joseph disease-associated mutant form of ataxin-3 regulates parkin ubiquitination and stability. *Hum Mol Genet* 2010; Oct 25 [Epub ahead of print]
14. Eddleston M, Mucke L. Molecular profile of reactive astrocytes--implications for their role in neurologic disease. *Neuroscience* 1993;54:15-36.
15. Elden AC, , Kim HJ, Hart MP, Chen-Plotkin AS, Johnson BS, Fang X, Armakola M, Geser F, Greene R, Lu MM, Padmanabhan A, Clay-Falcone D, McCluskey L, Elman L, Juhr D, Gruber PJ, Rüb U, Auburger G, Trojanowski JQ, Lee VM, Van Deerlin VM, Bonini NM, Gitler AD. Ataxin-2 intermediate-length polyglutamine expansions are associated with increased risk for ALS. *Nature* 2010;466:1069-1075.
16. Gunawardena S, Goldstein LSB. Polyglutamine diseases and transport problems: deadly traffic jams on neuronal highways. *Arch Neurol* 2005;62:46-51.
17. Gusella JF, MacDonald ME. Molecular genetics: unmasking polyglutamine triggers in neurodegenerative disease. *Nat Rev Neurosci* 2000;1:109-115.
18. Hageman J, Rujano MA, van Waarde MA, Kakkar V, Dirks RP, Govorukhina N, Oosterveld-Hut HM, Lübsen NH, Kampinga HH. A DnaJB chaperone subfamily with HDAC-dependent activities suppresses toxic protein aggregation. *Mol Cell* 2010;37:355-369.
19. Hartl FU, Hayer-Hartl M. Converging concepts of protein folding in vitro and in vivo. *Nat Struct Mol Biol* 2009;16:574-581.
20. Helmlinger D, Tora L, Devys D. Glutamine-expanded ataxin-7 alters TFTC/STAGA recruitment and chromatin structure leading to photoreceptor dysfunction. *PLoS Biol* 2006;4:e67.
21. Iqbal K, Liu F, Gong CX, Alonso Adel C, Grundke-Iqbal I. Mechanisms of tau-induced neurodegeneration. *Acta Neuropathol* 2009;118:53-69.

22. Kahle PJ, Neumann M, Ozmen L, Müller V, Odoy S, Okamoto N, Jacobsen H, Iwatsubo T, Trojanowski JQ, Takahashi H, Wakabayashi K, Bogdanovic N, Riederer P, Kretschmar HA, Haass C. Selective insolubility of alpha synuclein in human Lewy body disease is recapitulated in a transgenic mouse model. *Am J Pathol* 2001;159:2215-2225.
23. Kampinga HH, Craig EA. The HSP70 chaperone machinery: J proteins as drivers of functional specificity. *Nat Rev Mol Cell Biol* 2010;11:579-592.
24. Kopito RR. Aggresomes, inclusions bodies and protein aggregation. *Trends Cell Biol* 2000;10:524-530.
25. Kordasiewicz HB, Gomez CM. Molecular Pathogenesis of spinocerebellar ataxia type 6. *Neurotherapeutics* 2007;4:285-294.
26. Kuusisto E, Parkkinen L, Alafuzoff I. Morphogenesis of Lewy bodies: dissimilar incorporation of alpha-synuclein, ubiquitin, and p62. *J Neuropathol Exp Neurol* 2003;62:1241-1253.
27. Lee SJ, Desplats P, Sigurdson C, Tsigelny I, Masliah E. Cell-to-cell transmission of non-prion protein aggregates. *Nat Rev Neurol.* 2010;6:702-706.
28. Li JY, Englund E, Holton JL, Soulet D, Hagell P, Lees AJ, Lashley T, Quinn NP, Rehnkrone S, Björklund A, Widner H, Revesz T, Lindvall O, Brundin P. Lewy bodies in grafted neurons in subjects with Parkinson's disease suggest host to-to-graft disease propagation. *Nat Med* 2008;14:501-503.
29. Matilla-Duenas A, Sanchez I, Corral-Juan M, Davalos A, Alvarez R, Latorre P. Cellular and molecular pathways triggering neurodegeneration in the spinocerebellar ataxias. *Cerebellum* 2010;9:148-266.
30. Michels AA, Nguyen VT, Konings AW, Kampinga HH, Bensaude O. Thermostability of a nuclear-targeted luciferase expressed in mammalian cells. Destabilizing influence of the intranuclear microenvironment. *Eur J Biochem* 1995;234:382-389.
31. Paulson H. Protein fate in neurodegenerative proteinopathies: Polyglutamine diseases join the (mis)fold. *Am J Hum Genet* 1999;64:339-345.
32. Perez M, Paulson H, Pendse S, Salonz S, Bonini N, Pittman R. Recruitment and the role of nuclear localization in polyglutamine-mediated aggregation. *J Cell Biol* 1998;143:1457-1470.



33. Pratico D. Oxidative stress hypothesis in Alzheimer's disease: a reappraisal. *Trends Pharmacol Sci* 2008;29:609-615.
34. Price DL, Sisodia SS. Mutant genes in familial Alzheimer's disease and transgenic models. *Annu Rev Neurosci* 1998;21:479-505.
35. Ramijt AL, Sedig L, Leibner J, Wu SS, Dai Y, Okun MS, Rodriguez RL, Malaty IA, Fernandez HH. The relationship between anosmia, constipation, and orthostasis and Parkinson's disease duration: results of a pilot study. *Int J Neurosci* 2010;120:67-70.
36. Reddy PH, Beal MF. Amyloid beta, mitochondrial dysfunction and synaptic damage: implications for cognitive decline in aging and Alzheimer's disease. *Trends Mol Med* 2008;14:45-53.
37. Rüb U, Brunt ER, Del Turco D, de Vos RA, Gierga K, Paulson H, Braak H. Guidelines for the pathoanatomical examination of the lower brain stem in ingestive and swallowing disorders and its application to a dysphagic spinocerebellar ataxia type 3 patient. *Neuropathol Appl Neurobiol* 2003;29:1-13.
38. Rüb U, Brunt ER, Petrasch-Parwez E, Schöls L, Theegarten D, Auburger G, Seidel K, Schultz C, Gierga K, Paulson H, van Broeckhoven C, Deller T, de Vos RA. Degeneration of ingestion-related brainstem nuclei in spinocerebellar ataxia type 2, 3, 6 and 7. *Neuropathol Appl Neurobiol* 2006;32:635-649.
39. Seidel K, Hoche F, Brunt ER, Auburger G, Schöls L, Bürk K, de Vos RA, den Dunnen W, Bechmann I, Egensperger R, Van Broeckhoven C, Gierga K, Deller T, Rüb U. Involvement of the auditory brainstem system in spinocerebellar ataxia type 2 (SCA2), type 3 (SCA3) and type 7 (SCA7). *Neuropathol Appl Neurobiol*. 2008;34:479-491.
40. Shimohata T, Nakajima T, Yamada M, Uchida C, Onodera O, Naruse S, Kimura T, Koide K, Sano Y, Ishiguro H, Sakoe K, Ooshima T, Sato A, Ikeuchi T, Oyake M, Sato T, Aoyagi Y, Hozumi I, Nagatsu T, Takiyama Y, Nishizawa M, Goto J, Kanazawa I, Davidson I, Tanese N, Takahashi H, Tsuji S. Expanded polyglutamine stretches interact with TAFII130, interfering with CREB- dependent transcription. *Nat Genet* 2000;26:29-36.
41. Thomas EA. Striatal specificity of gene expression dysregulation in Huntington's disease. *J Neurosci Res* 2006;84:1151-1164.
42. Trottier Y, Lutz Y, Stevanin G, Imbert G, Devys D, Cancel G, Saudou F, Weber C, David G, Tora L, Agid Y, Brice A, Mandel JL. Polyglutamine

- expansion as a pathological epitope in Huntington's disease and four dominant autosomal cerebellar ataxias. *Nature* 1995;378:403-406.
43. Valko M, Rhodes CJ, Moncol J, Izakovic M, Mazur M. Free radicals, metals and antioxidants in oxidative stress induced cancer. *Chem Biol Interact* 2006;160:1-40.
  44. Vos MJ, Hageman J, Carra S, Kampinga HH. Structural and functional diversities between members of the human HSPB, HSPH, HSPA and DNAJ Chaperone families. *Biochemistry* 2008;47:7001-7011.
  45. Volterra A, Meldolesi J. Astrocytes, from brain glue to communication elements: the revolution continues. *Nat Rev Neurosci* 2005;6:626-640.
  46. Winklhofer KF, Haass. Mitochondrial dysfunction in Parkinson's disease. *Biochim Biophys Acta* 2010;1802:29-44.
  47. Wooten MW, Hu X, Babu JR, Seibenheimer ML, Geetha T, Paine MG, Wooten MC. Signaling, polyubiquitination, trafficking, and inclusions: sequestosome 1/p62's role in neurodegenerative disease. *J Biomed Biotechnol* 2006;2006:62079.
  48. Wyss-Coray T, Loike JD, Brionne TC, Lu E, Anankov R, Yan F, Silverstein SC, Husemann J. Adult mouse astrocytes degrade amyloid-beta in vitro and in situ. *Nat Med* 2003;9:453-457.
  49. Zijlstra MP, Rujano MA, Van Waarde MA, Vis E, Brunt ER, Kampinga HH. Levels of DNAJB family members (HSP40) correlate with disease onset in patients with spinocerebellar ataxia type 3. *Eur J Neurosci* 2010;32:760-770.

# Nederlandse Samenvatting

## Neurodegeneratieve ziekten

Omdat in de westerse wereld mensen een steeds oudere leeftijd bereiken, neemt de incidentie van ouderdomsziekten steeds meer toe. Een groep van bijzonder slopende ouderdomsziekten zijn de neurodegeneratieve ziekten. Hierbij degenereren bepaalde onderdelen van het centrale zenuwstelsel geleidelijk in de tijd. Sommige van de neurodegeneratieve ziekten treden sporadisch op, zonder 1 specifieke oorzaak (idiopathisch genoemd), terwijl andere te wijten zijn aan bekende genetische mutaties. De getroffen neuronale systemen alsmede de volgorde en snelheid van de progressie zijn afhankelijk van de ziekte in kwestie. Net als het degeneratieve proces, zijn ook de symptomen progressief, zoals ernstige problemen met het evenwicht, gedeeltelijke verlamming, onwillekeurige bewegingen en gedeeltelijke verlies van de zintuigen en problemen met slikken, eten, praten en ademen.

De onderzoeken in dit proefschrift richten zich vooral op de polyglutamine ziekten (polyQ ziekten), een groep die wordt gekenmerkt door de verlenging van een aminozuur sequentie, die uitsluitend bestaat uit glutamine. Deze sequenties zijn gelegen in verschillende, niet gerelateerde genen. De polyQ ziekten die in dit proefschrift worden bestudeerd, zijn de ziekte van Huntington en de spinocerebellaire ataxieën 1, 2, 3, 6 en 7. Dit zijn zeldzame, progressieve ziekten van de hersenen en het ruggenmerg met een zeer uitgebreid degeneratie patroon.

Een andere ziekte, die in dit proefschrift wordt onderzocht, is de ziekte van Parkinson. Deze aandoening wordt gekenmerkt door het verlies van zwart-gepigmenteerde neuronen in een bepaald gebied van de hersenen, de zgn substantia nigra, en de wijdverbreide aggregatie van het ziekte typische alfa-synucleïne eiwit. Patiënten ervaren een karakteristieke combinatie van klachten: tremor, stijfheid, traagheid van de bewegingen en houdingsinstabiliteit. De ziekte van Parkinson kan zich manifesteren zonder bekende oorzaak (idiopathisch) of als gevolg van een specifieke genetische aanleg.

## Deel I: Eiwit aggregatie en neurodegeneratie:

De degeneratieve patronen van de verschillende neurodegeneratieve ziekten zijn zeer divers. Door een enorme hoeveelheid klinisch-neurologisch en anatomisch onderzoek met elkaar te verbinden kan men nu de meeste van de symptomen koppelen aan het verlies van bepaalde gebieden binnen het centrale zenuwstelsel. Omgekeerd kan pathologisch onderzoek van de degeneratie juist aanleiding geven tot onderzoek van specifieke symptomen bij een bepaald type ziekte, die soms over het hoofd worden gezien in de standaard klinische praktijk en die eventueel zelfs als vroeg diagnosticum gebruikt zouden kunnen worden.

Veel neurodegeneratieve ziekten worden gekenmerkt door het klonteren van ziekte-specifieke eiwitten in microscopisch zichtbare brokjes (zgn aggregaten), die vaak in zenuwcellen zijn gelegen. De vorm, samenstelling en plaats binnen het neuron is afhankelijk van het ziekte-specifieke eiwit. Dit samengeklonterde eiwit blijkt vaak voor te komen in een ongebruikelijke 'verkeerd gevouwen' vorm. Hoewel de aggregaten frequent worden aangetroffen, bestaat er veel discussie over de directe verbinding met neuronale celdood.

Naarmate de ziekte eiwitten samenklonteren tot grotere brokken, worden ook andere eiwitten in deze aggregaten ingevangen (sneeuwbaaleffect). Een klein verlies van een aantal essentiële eiwitten kan al een verstoring van de celfunctie en bedreiging van de gezondheid van een cel geven, vooral als de verloren eiwitten een regulerende functie hebben.

Bovendien kan een deel van de toxiciteit van een aggregaat afhangen van de lokalisatie. Neuronen hebben zeer lange uitlopers, die doorgaans worden aangeduid als neurieten (dendriten en axonen). Hiermee hebben zenuwcellen onderling en met hun doelorganen (spieren, klieren etc) contact. Axonen zijn vele centimeters lang. Voor een correcte werking moeten cellulaire componenten en boodschapper moleculen (bijv neurotransmitters) bewegen door deze neurieten. Eiwit aggregaten op deze plek in de zenuwcel veroorzaken transport problemen en zorgen zodoende voor neuronale dysfunctie.

Het is niet alleen de eigenschap van de aggregatie van eiwitten, maar in ieder geval voor een deel ook de aard van het neuron zelf, waardoor deze gevoelig zijn voor degeneratieve processen. Neuronen kunnen niet delen, hetgeen betekent dat een afgestorven neuron niet kan worden vervangen. Doordat celdeling niet mogelijk is, kan een neuron zich niet ontdoen van aggregaten naar 1 dochtercel, terwijl de andere gezond blijft (een proces dat is beschreven in andere celtypen). Een neuron moet dus het gehele leven mee, waarin verschillende vormen van celstress zich kunnen voordoen. Zenuwcellen zijn zeer actief, waardoor druk kan ontstaan op hun cellulaire stofwisseling. Daarnaast zijn neuronen afhankelijk van contact met andere neuronenvan hun eindorganen. Dit kan betekenen dat een neuron deze steun verliest wanneer het contact met zijn omgeving wegvalt t.g.v. het degeneratieve ziekteproces.

In de hoofdstukken 1-4 wordt voornamelijk vanuit de neuropathologische hoek gekeken naar ziekte-typische aggregatie en degeneratie patronen binnen verschillende neurodegeneratieve ziekten.

Het is al enige tijd bekend, dat het gehoor in de spinocerebellaire ataxieën is aangetast. In hoofdstuk 2 hebben we geprobeerd dit te betrekken bij het degeneratieve pathologische patroon van deze ziekten. Onze studie toont aan dat er inderdaad een uitgebreide degeneratie van auditieve zenuwen en kerngebieden aanwezig is.

Zoals eerder vermeld bestaan er zeldzame genetische (familiaire) vormen van de ziekte van Parkinson. Bij enkele mutaties kan dat leiden tot afwijkingen van de standaard-symptomen en patronen van degeneratie, zoals die te zien zijn in de idiopathische vorm. In hoofdstuk 3 hebben we de gelegenheid gehad om voor het eerst de hersenen van een patiënt te onderzoeken met een specifieke mutatie in het alfa-synucleïne gen. Uit ons onderzoek naar de hersenen van deze patiënt blijkt dat deze specifieke vorm van familiair parkinsonisme lijkt op de idiopathische vorm. Deze mutatie zou dus zeer nuttig kunnen zijn om ziektemodellen te creëren en zo de idiopathische ziekte van Parkinson na te bootsen.

In spinocerebellaire ataxie type 3 vormt het ziekte-specifieke eiwit ataxine-3 kleine puntvormige aggregaten in de celkern van de neuronen. Deze zijn uitvoerig bestudeerd, maar ze correleren niet goed met het degeneratiepatroon van deze ziekte. In hoofdstuk 4 beschrijven we een nieuw soort aggregaat bij deze ziekte, die zich bevindt binnen het axon. Deze nieuwe aggregaten komen goed overeen met het patroon van degeneratie, hetgeen een direct nadelig effect van deze aggregaten doet vermoeden.

## **Deel II: Eiwit aggregatie en het Proteïne Kwaliteits-Controle-systeem**

Verkeerd opvouwen van eiwitten en aggregatie zijn typische kenmerken, die gezien kunnen worden in cellen die worden blootgesteld aan externe stress zoals hitte of zware metalen of fysiologische processen die anders interfereren met de juiste eiwitvouwing of samenstelling. Cellen hebben een aantal coping-mechanismen ontwikkeld als antwoord op verkeerd gevouwen eiwitten, gewoonlijk aangeduid als Proteïne Kwaliteits-Controle-systeem (PKC).

Centraal in het PKC-systeem is een grote familie van gespecialiseerde eiwitten, aangeduid als heat shock proteins (HSP's) of als moleculaire chaperones. Ze voorkomen aggregatie door te binden aan blootgestelde oppervlakken van eiwitten, waardoor deze correct gevouwen kunnen worden of kunnen worden afgebroken wanneer de correcte vouwing is mislukt. Er zijn verschillende HSP families, zoals de kleine energie-onafhankelijke HSPs (HSPB) of de energieafhankelijke Hsp70 (HSPA) familie. De HSPA-familie wordt gereguleerd door de DNAJ familie van cofactoren, die zorgdragen voor de specificiteit en activiteit van de processen, en de familie van Nucleotide Exchange Factors (NEF), die daarbij assisteren.

De beste verdediging tegen verkeerd gevouwen eiwitten in neurodegeneratieve ziekten is het verwijderen daarvan. Er zijn in wezen twee afbraak systemen in cellen, die ook vaak worden gebruikt voor de normale eiwit omzet (verwijderen van oude eiwitten en recyclen van hun onderdelen): via het proteasoom of het autofagosoom.

Proteasomen zijn kleine tonvormige structuren, die alleen oplosbare eiwitten kunnen degraderen. Het doelwit moet echter eerst worden gelabeld met een ander molecuul (ubiquitine). Een proteasoom is echter inefficiënt in het afbreken van grotere eiwitfragmenten en kan worden belemmerd in zijn functie door pogingen om juist die grotere deeltjes te verteren.

Voor bulkdegradatie van structuren tot de grootte van celorganellen staat het autofagosoom ter beschikking. Het af te breken fragment wordt eerst omgeven door een membraan. Dit fuseert met een ander celorganel (het lysosoom), dat de enzymatische activiteit bezit om degradatie van deze grotere structuren te bewerkstelligen.

Omdat het PKC een grote rol speelt in de klaring van eiwitten, kunnen onderdelen van het PKC worden betrokken bij de pathologische processen van de ziektespecifieke eiwitten. Van verschillende HSP's is al aangetoond dat ze aanwezig zijn in eiwitaggregaten. Aan de andere kant blijken de ziekte typische aggregaten moeilijk te verwijderen. Vooral het proteasoom heeft problemen met de klaring van grote geaggregeerde massa's en kan daardoor zelfs worden uitgeschakeld. Daarnaast kunnen eiwitaggregaten onderdelen van het PKC-systeem wegvangen, wat kan leiden tot problemen in de algemene cellulaire huishouding. Het blokkeren van het PKC door aggregaten kan derhalve een grote bedreiging voor de neuronale gezondheid vormen.

In de hoofdstukken 5-8 van dit proefschrift worden veranderingen in het PKC in neurodegeneratieve ziekten gekarakteriseerd om het inzicht in de betrokkenheid van onderdelen van het PKC in de pathologische processen binnen deze ziektes verder te vergroten.

Om neurodegeneratieve ziektes te onderzoeken, is het zichtbaar maken van specifieke eiwitten een belangrijke stap. In sommige ziektes is dit niet zo eenvoudig. De (vermeende) eiwit aggregaten in spinocerebellaire ataxie type 6 waren tot nu toe niet op te sporen. In hoofdstuk 6, hebben we gebruik gemaakt van een specifieke component van het PKC, p62, waarvan bekend is dat dit geassocieerd is met eiwit aggregaten in een aantal andere neurodegeneratieve ziektes. Met behulp van een kleurmethode tegen p62 konden we neuronale eiwit aggregaten bij SCA6 gemakkelijk aantonen.

Naar het aggregatie proces in spinocerebellaire ataxie type 3 wordt nog uitgebreid onderzoek gedaan. In hoofdstuk 7 beschrijven we in hersenweefsel van SCA3 patiënten verschillende typen aggregaten, die opeenvolgende stadia lijken te zijn. Daarnaast tonen we aan dat aggregaten in deze ziekte in eerste instantie kunnen "ontsnappen" uit de aandacht van het PKC. In latere stadia worden verschillende componenten van dit kwaliteitssysteem ernstig ontregeld. Dit kan nog een andere bron van stress voor de neuronen worden.



Interessant was, dat een andere set van moleculaire chaperones, HSPB8 (een kleine HSP) en BAG3 (een NEF), opgereguleerd bleek te zijn in vervallende hersengebieden van SCA3 patiënten. Deze reactie werd echter niet gezien in neuronen, maar in de gliale cellen, met name in de stervormige astrocyten (hoofdstuk 8). Dezelfde respons werd vervolgens ook waargenomen bij patiënten met Huntington, Parkinson en de ziekte van Alzheimer. Omdat gliale cellen hoofdzakelijk dienen ter ondersteuning van neuronen, speculeren wij dat de opregulatie van HSPB8 en BAG3 dient ter bevordering van (1) het opruimen van celpuin en geaggregeerd eiwit afkomstig van neuronen, (2) het onderhouden van de plaatselijke homeostase en / of (3) de omvorming te verbeteren die astrocyten ondergaan bij de reactie op beschadiging van nabijgelegen weefsel.

## Conclusie

De resultaten van dit onderzoek schetsen een zeer divers beeld van de degeneratieve processen in de zogenaamde eiwitaggregatie ziekten. We waren in staat om nieuwe degeneratie- en eiwitaggregatie patronen te beschrijven in de onderzochte ziekten. Verder vonden we aanwijzingen voor twee pathologische processen, namelijk de verstoring van neuronale processen door axonale aggregaten en de geleidelijke ontregeling van vitale cellulaire componenten tijdens de progressieve stadia van aggregatie. Tot slot vonden we bewijs voor de betrokkenheid van niet-neuronale cellen binnen het centrale zenuwstelsel, die op de een of andere manier deelnemen aan de processen van neurodegeneratie.

Met de identificatie van deze pathologische paden, zowel beschreven in dit proefschrift alsook in andere recente lijnen van onderzoek, lijkt het erop dat in de meeste neurodegeneratieve ziekten meerdere schadelijke mechanismen naast elkaar aan het werk zijn. Na verloop van tijd zouden de verschillende effecten een cumulatieve belasting kunnen vormen voor het neuron. Op een bepaald punt van cumulatieve stress schiet de huishouding van het neuron tekort en sterft deze af. Aangezien neuronen van elkaar afhankelijk zijn voor ondersteuning, kan het verlies van een enkel neuron extra stress geven op de andere neuronen in hetzelfde circuit, leidend tot verdere cumulatieve stress.

Voor de meeste neurodegeneratieve ziekten is geen remedie bekend en zijn de behandelingen daarom puur symptomatisch. Dit proefschrift, samen met vele andere lijnen van onderzoek, draagt bij aan het begrip van deze processen, wat gebruikt kan worden als uitgangspunt voor nieuw onderzoek en de opzet van therapieën. Terwijl zaken zoals axonale blokkade misschien moeilijk zijn te bestrijden, lijken onderdelen van het eiwit kwaliteitscontrole-systeem de moeite waard te zijn voor verder onderzoek. Het is al bekend dat het niveau van bepaalde HSPs de activiteit van de afbraaksystemen gunstig kan beïnvloeden. Precieze aanpassingen in dit systeem zouden progressie van de ziekte en symptomen kunnen verminderen en daardoor een

drastische verbetering van de kwaliteit van leven van patiënten met een neurodegeneratieve aandoening kunnen geven.

## English summary

### Neurodegenerative diseases

In the western world, people are progressively reaching older ages, and thus diseases of old age are becoming more prevalent. A group of particularly debilitating diseases of old age are the neurodegenerative diseases. Here, certain components of the central nervous system degenerate progressively over time. Some of the neurodegenerative diseases occur sporadically without any known cause (referred to as idiopathic) while others are due to known genetic mutations. The affected neuronal systems as well as the sequence and speed of the progression are dependent on the disease in question. Just like the degenerative process, the symptoms are progressive, and can include, but are not limited to, severe balance problems, partial paralysis, involuntary movements and partial loss of senses as well as difficulties with eating, talking and breathing.

This study focuses primarily on the polyglutamine diseases (PolyQ diseases), a group characterized by the expansion of an amino acid sequence, which solely consists of glutamine amino acids. These sequences are situated in different and otherwise unrelated disease specific proteins. The PolyQ diseases of relevance here are Huntington's disease and spinocerebellar ataxia 2, 3, 6 and 7. They are rare, progressive and degenerative diseases of the brain and the spine with a very widespread degeneration pattern.

Another disease of relevance is Parkinson's disease. It is characterized by the loss of darkly pigmented neurons in a certain midbrain area, aptly labelled substantia nigra, and the widespread aggregation of the disease typical alpha-synuclein protein. Patients experience a variety of movement symptoms, like a characteristic tremor, rigidity, slowness of movements and postural instability. It can manifest either without known cause (idiopathic) or due to a genetic predisposition.

### Part I: Protein aggregation and neurodegeneration

The degenerative patterns exhibited by the neurodegenerative diseases are very diverse. Thanks to the vast body of neurological and anatomical research assembled in the past decades, one can now link most of the symptoms that a patient experiences to the loss of certain areas within the central nervous system. At the same time, one can use a pathological examination of the degeneration in a patient brain to look for hints for minor or late symptoms of a given type of disease, which are sometimes overlooked in standard clinical practice.

Many neurodegenerative diseases are hallmarked by the aggregation of a disease typical protein into microscopically visible lumps of protein (aggregates) which are often situated in neurons. The form, composition, and position within the neuron are dependent on the disease in question, and the protein within these aggregations is often found in an unusual form, and is thus referred to as "misfolded". While these aggregates are common, no direct connection to neuronal death has been established.

As the disease proteins aggregate into larger lumps, they often also include other proteins into these aggregates. An even small loss of some vital proteins may disturb cellular function and threaten cellular health, especially if the lost proteins have a regulatory function.

Furthermore, some of the toxicity of a protein aggregate can depend on its' localization. Neurons have several very long processes, which are commonly referred to as neurites, with the longest one, the axon, extending to the targets of the neuronal cells (e.g. other neurons, muscles, glands, etc.), sometimes being over 30cm long. For their correct function, neurons need to move cellular components and messenger molecules through these neurites and especially through the axon. Protein aggregates that arise within the axon can inhibit the movement of these particles causing neuronal dysfunction.

It is not only the property of the aggregating proteins, but, at least in some part, the nature of the neuron itself, which makes it susceptible to degenerative processes. Neurons can not divide, meaning that a dying neuron cannot be replaced, nor can a neuron divide to get rid of toxic substances in one daughter, while the other one remains damage-free and healthy (a process described in other cell types). Furthermore, a neuron has to last for the whole lifetime of an organism, during which different stresses can accumulate. They are also very active cells, which puts stress on their cellular metabolism. Additionally neurons depend on certain molecules from their target cells, a process which culls unnecessary neurons early in development. This, however, means that a neuron loses this support when its target cell dies due to degenerative processes.

Chapters 1-4 are primarily concerned with this neuropathological angle and aim to describe disease typical aggregation and degeneration patterns within several neurodegenerative diseases.

It has been known for some time, that the auditory system in the spinocerebellar ataxias are affected. In chapter 2, we tried to associate this to the degenerative pathological pattern of these diseases. Our study shows that there is indeed a widespread degeneration of auditory nerves and sites within the central nervous system.

As stated before, there are rare familial forms of Parkinson's disease. Several mutations in different proteins can cause it, and they do sometimes deviate from the standard symptoms and patterns of degeneration as seen in the idiopathic form. In chapter 3, we had the opportunity to investigate the first brain of one patient with a specific mutation within the alpha-synuclein gene. Our investigation of this patient shows that this specific form of familial Parkinsonism closely resembles the idiopathic form. Thus this mutation is very useful to create disease models mimicking the idiopathic Parkinsonism.

In Spinocerebellar Ataxia type 3, the disease protein ataxin-3 aggregates into small, dot-like aggregates within the core of neurons. These have been extensively studied, but they do not correlate well to the degeneration pattern of the disease. In chapter 4 we describe a novel kind of aggregate within the neuronal axon. These new aggregates correspond well with the pattern of degeneration, hinting at a direct detrimental effect of these aggregates.

## **Part II: Protein aggregation and the Protein Quality Control system**

Protein aggregation and misfolding also are a typical feature, seen in cells exposed to external stresses like heat or heavy metals or physiological processes that otherwise interfere with correct protein folding or assembly. Cells have developed several coping mechanisms in response to protein folding dysfunction, commonly referred to as Protein Quality Control system (PQC).

Central to PQC systems are a large family of specialized proteins, referred to as Heat Shock Proteins (HSPs) or as molecular chaperones. They primarily combat aggregation by binding to exposed surfaces of proteins, thereby enabling the correct folding of misfolded proteins or allowing their degradation if folding is unsuccessful. There are several HSP families, such as the small energy-independent HSPs (HSPB) or the energy-dependent HSP70 (HSPA) family. The HSPA family is regulated by the DNAJ family of co-factors, which drive the specificity and activity, and the family of Nucleotide Exchange Factors (NEF), which also influence activity and can direct proteins, which cannot be successfully refolded, to the protein degradation machinery.

For aggregating protein in neurodegenerative diseases, the best defence may be removal of the disease protein, either before or after it has aggregated. There are essentially two protein degradation systems in cells, which are also commonly used for the normal protein turnover (removal of old protein and recycling their components): the proteasomal and autophagosomal pathway.

Proteasomes are small barrel-shaped cellular components that can only digest soluble proteins. The target proteins have to be tagged with a certain particle (ubiquitin). However, a proteasome is inefficient in clearing larger protein particles, and may be hindered in its function by attempts to digest those particles.

For bulk disposal up to the size of cell organelles, the autophagy pathway is available. In this process the target is engulfed in a membrane, and then fuses to a cellular component, the lysosome, which contains biochemical machinery capable of degrading all kinds of protein.

As the PQC plays a large part in protein aggregate clearance, its components may be involved in the pathological processes of protein degradation disease. Different HSPs have already been shown to be present in protein aggregates, and some HSPs have an effect on cellular health and protein aggregation. On the other hand, the disease typical

aggregates have been shown to be difficult to dispose of. Especially the proteasome has problems with clearing large aggregated masses of protein and can even be incapacitated by this. Additionally, protein aggregates can sequester elements of the PQC, which would lead to an inhibition of refolding and degradation pathways. At the same time, these pathways are important to maintain cellular functions by refolding new and disposing of old protein. Because of this, blocking of the PQC by aggregate formation can pose a significant threat to neuronal health.

In chapters 5-8 of this thesis, we characterized changes to the PQC in neurodegenerative disease, to further the understanding of the involvement of elements of the PQC in pathological processes.

If one wants to analyse neurodegenerative diseases, visualizing the protein is an important step. In some diseases this isn't all that easy. The (putative) protein aggregates in Spinocerebellar Ataxia type 6 were until now undetectable. In chapter 6, we utilized a specific component of the Protein Quality Control system, p62, which is known to associate with protein aggregates in a number of diseases and is easily detectable. Using p62, we were able to demonstrate neuronal protein aggregates.

The aggregation process in Spinocerebellar Ataxia type 3 is still undergoing extensive research. In chapter 7, we describe several seemingly progressive stages of aggregation in human brain material. In addition, we demonstrate that aggregation in this disease initially may "escape" from the attention of the normal stress-regulated protein quality control system. At later stages, several components of the protein quality control do become severely deregulated in this process. This deregulation might be yet another source of stress to the neurons.

Interestingly, another set of the molecular chaperones, HSPB8 (a small HSP) and BAG3 (a NEF), was found to be up-regulated in degenerating areas of the brain of Spinocerebellar Ataxia type 3 patients, but this response was not seen in neurons but in glial cells, specifically in the star shaped astrocytes (chapter 8). The same response was next also observed in patients with Huntington's, Parkinson's, and Alzheimer's disease. As glial cells are the supporting cells of neurons, we speculate that the upregulation of HSPB8 and BAG3 may enhance the ability of these cells to clear aggregated proteins released from neurons, cellular debris, maintain the local homeostasis and/or participate in the remodeling that astrocytes undergo when reacting to nearby tissue damage.

## **Conclusion**

The results of this study paint a very diverse picture of the degenerative processes in the protein aggregation diseases. We were able to describe novel degeneration and protein aggregation patterns in the diseases investigated. Furthermore, we found several strong hints to two of the pathological pathways discussed above, namely the



clotting of neuronal processes by axonal aggregates and the progressive dysregulation of vital cellular components during the progressive aggregation processes. Finally, we found evidence for the involvement of non-neuronal cells within the central nervous system, which somehow partake in the processes of neurodegeneration.

With the identification of these pathological pathways, both in these thesis but also in other recent lines of research, it seems that in most neurodegenerative diseases several damaging mechanisms are at work. Over time, these different effects would enact a cumulative stress on the neuron. At a certain point of cumulative stress, the neuron can no longer maintain itself, and dies. Since neurons are dependent on each other for support, the loss of a single neuron puts additional stress onto all of its interactors, resulting in even more cumulative stress.

For most neurodegenerative diseases, there is no known cure and treatments are purely symptomatic. This thesis, along with many other lines of current research, adds to our understanding of these processes, which may be used as a starting point for future research and conception of therapies. While things like axonal blockage are possibly difficult to counter, elements of the protein quality control seem to be worthwhile targets for further investigation. It is already known that certain HSP levels and the activity of degradation pathways can be influenced, and precise alterations could decrease symptoms and/or disease progression and drastically improve a patients' quality of life.

# Deutsche Zusammenfassung

## Neurodegenerative Erkrankungen

In der westlichen Welt erreicht die Bevölkerung progressiv höheres Alter, weswegen Krankheiten des hohen Alters immer prävalenter werden. Eine Gruppe besonders schwerer Krankheiten des hohen Alters sind neurodegenerative Erkrankungen. In diesen degenerieren spezifische Teile des zentralen Nervensystems über einen längeren Zeitraum hinweg. Manche dieser Erkrankungen ereignen sich ohne erkennbare Ursache (bezeichnet als idiopathisch), andere aufgrund von Mutationen und genetischer Prädisposition. Dabei sind die betroffenen neuronalen Systeme sowie die Reihenfolge und Geschwindigkeit, in der sie degenerieren, krankheitsspezifisch. Entsprechend der progressiven Degeneration sind auch die Symptome der Erkrankungen progressiv, und können unter anderem folgendes enthalten: schwere Balanceprobleme, teilweise oder komplette Lähmung, unfreiwillige Bewegungen, teilweiser Verlust diverser Sinneswahrnehmungen sowie Einschränkungen bei der Nahrungsaufnahme, beim Sprechen und bei der Atmung.

Ein Fokus dieser Studie sind die Polyglutamin (PolyQ) Erkrankungen. Diese Gruppe von Neurodegenerativen Krankheiten wird durch die Verlängerung einer Aminosäuresequenz im entsprechenden Krankheitsprotein definiert, die allein aus einer Aneinanderreihung der Aminosäure Glutamin besteht. Die hier relevanten PolyQ Erkrankungen sind die Spinozerebellären Ataxien 2, 3, 6 und 7. Es handelt sich bei diesen um seltene Neurodegenerative Erkrankungen mit einem weit reichenden Degenerationsmuster und einer ebenso diversen Symptomatik.

Eine weitere relevante Krankheit ist Parkinsons Krankheit. Diese ist charakterisiert durch den Verlust von dunkel pigmentierten Nervenzellen in einem spezifischen Areal des Mittelhirns, das passender Weise als Substantia Nigra – schwarze Substanz – bezeichnet wird. Patienten legen dabei eine Reihe von spezifischen Symptomen an den Tag: Tremor, Steifheit, langsame Bewegungen und eine unsichere Postur. Parkinson kann sowohl ohne erkennbaren Grund, als auch aufgrund diverser Mutationen auftreten, was dann als familiärer Parkinson bezeichnet wird.

### Teil I: Proteinaggregation und Neurodegeneration

Die Neurodegenerativen Erkrankungen betreffen verschiedenste Regionen des zentralen Nervensystems. Dank einem großen Wissensschatz neurologischer und neuroanatomischer Daten, die in den letzten Jahrzehnten gesammelt wurden, kann man die meisten Symptome, die Patienten neurodegenerativer Krankheiten an den Tag legen, direkt mit dem Verlust spezifischer Hirnregionen in Verbindung bringen. Der Umkehrschluss ist auch möglich: Durch die Analyse der Degeneration des Patientengehirns können Rückschlüsse auf Symptome gezogen werden, die entweder

spät auftreten oder nicht sehr stark sind, und so in der klinischen Praxis nicht erkannt werden.

In vielen Neurodegenerativen Erkrankungen kommt es zu mikroskopisch sichtbaren Verklumpungen eines krankheitstypischen Proteins. Diese Klumpen, auch Aggregate genannt, befinden sich oft im Inneren von Neuronen. Die genaue Form, Zusammensetzung und Lage ist ebenfalls von der jeweiligen Krankheit abhängig. Das krankheitstypische Protein liegt dabei oft in einer ungewöhnlichen Form vor, und wird als „falsch gefaltet“ bezeichnet. Und obwohl diese Aggregate sehr häufig sind, war es bis jetzt nicht möglich einen direkten Zusammenhang zu der Neurodegeneration her zu stellen.

Während das Krankheitsprotein verklumpt, absorbiert es oft zusätzlich andere Proteine. Schon kleine Verluste von wichtigen, eventuell regulatorischen Proteinen können das innere Gleichgewicht einer Zelle auf eine gefährliche Art und Weise durcheinander bringen und so die Gesundheit einer Zelle direkt gefährden.

Zusätzlich kann ein Aggregat durch seine Lage gefährlich für die Wirtszelle sein. Nervenzellen haben mehrere lange Fortsätze, Neuriten, und das längste dieser Neuriten, das Axon das zu dem Ziel einer Nervenzelle reicht (z.B. andere Nervenzellen, Muskeln, Sinneszellen), kann über 30 cm lang sein. Damit sie korrekt funktionieren müssen Neurone Zellbestandteile und Botenstoffe durch diese Neuriten bewegen, gerade durch das sehr lange Axon. Bildet sich ein Proteinaggregat innerhalb des Axons, würde der Transport gestört, was die Funktion und Überlebensfähigkeit der Nervenzelle einschränken würde.

Nicht nur die Eigenschaften des aggregierenden Proteins, sondern auch die Natur der Neuronen an sich macht sie anfällig für degenerative Erkrankungen. Neuronen können keine Zellteilung mehr vollführen, was einerseits bedeutet das beim Ausfall eines Neurons keine Tochterzelle dessen Aufgabe übernehmen kann, andererseits kann ein Neuron auch nicht toxische Substanzen oder Proteinaggregate an eine Tochterzelle weitergeben und abschnüren (ein Prozess, der bei anderen Zelltypen beobachtet wird). Des Weiteren muss ein Neuron genau so lange überleben wie der entsprechende Organismus, und während dieser Zeit können sich Stress und toxische Substanzen ansammeln. Neurone sind auch sehr aktive Zellen was ihren zellulären Metabolismus stark beansprucht. Zusätzlich benötigen Neurone spezielle Botenstoffe von ihren Zielzellen, ein Vorgang, der in frühen Entwicklungsphasen unnötige Neurone aussortiert. Das bedeutet allerdings, dass wenn ein Neuron seine Zielzelle verliert, es diese Botenstoffe verliert, und möglicherweise zu Grunde geht.

Kapitel 1-4 beschäftigen sich primär mit dem Neuropathologischen Blickwinkel. Es werden krankheitstypische Proteinaggregations- und Degenerationsprozesse beschrieben.

Es ist bekannt, dass das Hörsystem bei den Spinozerebellären Ataxien 2, 3 und 7 betroffen ist. In Kapitel 2 wird der Zusammenhang zwischen den Hörbeeinträchtigungen und der beobachteten Neurodegeneration beschrieben. Es zeigt sich, dass viele Elemente des Hörsystems in diesen Krankheiten schwer degenerieren.

Wie bereits oben beschrieben, existieren familiäre Formen von Parkinson. Diverse Mutationen in verschiedenen Proteinen können es verursachen, und diese Formen weichen manchmal von der verbreiteten, idiopathischen Form ab. In Kapitel 3 hatten wir die seltene Gelegenheit das erste Patientengehirn mit einer seltenen Mutation des Alpha-synuclein Gens zu studieren. Die Untersuchung zeigt, dass diese spezifische Form des familiären Parkinsonismus tatsächlich deckungsgleich zur idiopathischen Form ist. Diese Mutation kann sehr nützlich bei dem Versuch sein, Tiermodelle von idiopathischem Parkinson zu erzeugen.

In Spinozerebellärer Ataxie typ 3 ist es bekannt, dass das Krankheitstypische Protein Ataxin-3 kleine Punktförmige Aggregate im Zellkern der Neurone bildet. Diese wurden zwar ausführlich beschrieben, sie korrelieren allerdings nicht mit der beobachteten Neurodegeneration. Kapitel 4 widmet sich einem neuen Typ von Aggregat, der in den Axonen von Neuronen auftritt. Das Vorkommen dieser Aggregate korrespondiert wesentlich besser mit der Neurodegeneration. Dies weist auf einen toxischen Effekt dieser Aggregate hin.

## **Teil II: Proteinaggregation und die Zelluläre Proteinqualitätskontrolle**

Aggregation und fehlerhafte Faltung von Proteinen ereignet sich nicht nur bei neurodegenerativen Erkrankungen. Typischerweise passiert es auch in Zellen, die einem externen Stress ausgesetzt werden, wie z.B. Schwermetallen, Hitze oder anderen Prozessen die mit der Neubildung von Proteinen interferieren. Zellen haben allerdings mehrere Abwehrmechanismen gegen diese Sorte von Stress, die man zusammen als die zelluläre Proteinqualitätskontrolle bezeichnet (Protein Quality Control, PQC).

Eine zentrale Rolle im PQC-System nimmt eine Familie von spezialisierten Proteinen ein, die als Hitzeschock Proteine (HSPs) oder Molekulare Chaperone bezeichnet werden. Primär bekämpfen diese die Aggregation von Proteinen, indem sie an deren exponierte Oberflächen binden und ihnen dabei die Möglichkeit geben, in die richtige Form über zu gehen. wenn eine Neufaltung nicht funktioniert, können sie ihren Abbau ermöglichen. Es gibt mehrere HSP Subfamilien: die kleinen, Energieunabhängigen HSPs (HSPB) oder die energieabhängige HSP70 (HSPA) Familie. Letztere wird durch eine Reihe von Co-faktoren reguliert, einerseits die DNAJ Familie, die die Spezifität und Aktivität der HSPA Gruppe erhöht, andererseits die Familie der Nucleotide Exchange Factors (NEF), die ebenfalls die Aktivität beeinflussen, und Substrate, die nicht erfolgreich neu gefaltet werden können, an die Zellulären Abbaumechanismen weitergeben können.

Einer der wichtigsten Abbaumechanismen sind Proteasome. Hierbei handelt es sich um Fassförmige Zelluläre Komponenten die lösliche Proteine abbauen können. Die

Zielpoteine müssen dafür mit einem spezifischen Marker (Ubiquitin) markiert werden. Allerdings sind Proteasome sehr ineffizient dabei größere Proteinpoteikel ab zu bauen, und können tatsächlich von diesen in ihrer Funktion gehindert werden.

Für den Abbau von Komponenten mit größerem Volumen, bis hin zu kompletten Zellorganellen, gibt es Autophagie. Bei diesem Prozess wird das Ziel von einer doppelwandigen Membran eingeschlossen, die dann mit dem Lysosom fusioniert, einer Zellulären Komponente die mit einer Biochemischen Maschinerie ausgestattet ist, um jede Form von Protein ab zu bauen.

Da die PQC eine wichtige Rolle beim Abbau von aggregierendem Protein hat, ist es wahrscheinlich, das Komponenten der PQC in die Pathologie von Neurodegenerativen Erkrankungen involviert ist. Bei verschiedenen Hitzeschockproteinen ist es bereits nachgewiesen, dass sie in Proteinaggregaten vorkommen, andere wieder rum haben einen nachweisbaren Effekt auf Zelluläre Gesundheit und Proteinaggregation. Allerdings hat sich immer wieder gezeigt, dass die Aggregate in Neurodegenerativen Erkrankungen schwer ab zu bauen sind. Besonders das Proteasom hat große Probleme beim Abbau größerer Aggregate und kann durch solche außer Gefecht gesetzt werden. Zusätzlich können Proteinaggregate PQC-Komponenten absorbieren, die dann für ihre normalen Funktionen nicht mehr zur Verfügung stehen. Diese sind allerdings wichtig für die normale Funktion einer Zelle, was die korrekte Proteinfaltung und Wiederverwertung alter Proteine betrifft. Deswegen kann eine Blockade der PQC Funktion durch Aggregate den Gesundheitszustand einer Zelle direkt bedrohen.

In den Kapiteln 5-8 dieser These charakterisieren wir Veränderungen an Komponenten des PQC-Systems in neurodegenerativen Erkrankungen, um das Wissen um die Involvierung dieser Elemente in den pathologischen Prozessen von Neurodegenerativen Erkrankungen zu vertiefen.

Wenn man eine Neurodegenerative Krankheit untersuchen will, ist es wichtig, mögliche Proteinaggregate sichtbar zu machen. In manchen Fällen ist das aber nicht trivial. In Spinocerebellärer Ataxie typ 6 wurde die Anwesenheit von Proteinaggregaten angenommen, allerdings waren bis dato technisch nicht nachweisbar. In Kapitel 6 wird die Verwendung eines Elements des PQC Systems, des Proteins p62, beschrieben. P62 ist bereits dafür bekannt, an Proteinaggregate verschiedener Neurodegenerativer Erkrankungen zu binden. Mit der Hilfe von p62 waren wir in der Lage, Proteinaggregate in Neuronen in SCA6 nach zu weisen.

Der Prozess der Proteinaggregation in Spinozerebellärer Ataxie typ 3 wird immer noch erforscht. In Kapitel 7 beschreiben wir mehrere, anscheinend progressive Stadien der Aggregation in menschlichem, pathologischem Material. Zusätzlich zeigen wir, dass die Aggregate der „Aufmerksamkeit“ des PQC-Systems, das normalerweise stark auf Stress reagiert, entkommen können. Zusätzlich werden in späteren Phasen einige Elemente des PQC-Systems stark dereguliert. Diese Deregulation kann eine weitere Quelle von Stress für die Nervenzelle darstellen.

Interessanterweise zeigt sich, dass ein weiteres Set von PQC Elementen, die molekularen Chaperone HSPB8 (aus der Gruppe der kleinen HSPs) und BAG3 (ein Nucleotide Exchange Factor), in degenerierenden Arealen von Patienten mit Spinozerebellärer Ataxie typ 3 hoch reguliert wird. Derselbe Effekt ist auch in Gehirnen von Parkinson-, Alzheimer- und Huntingtonpatienten sichtbar. Allerdings ist diese Erhöhung nicht in Neuronen sichtbar, sondern in den sogenannten Gliazellen, genauer gesagt in den sternförmigen Astrocyten (Kapitel 8). Da Gliazellen Neurone unterstützen, spekulieren wir, dass die Hochregulation von HSPB8 und BAG3 die Fähigkeit der Gliazellen verstärkt von Neuronen freigesetztes, aggregiertes Protein oder Zelltrümmer abzubauen, die lokale Homeostase stabil zu halten und/oder den Gliazellen bei dem Umbau ihrer Zellstruktur zu assistieren, den sie bei der Reaktion auf nahe Verletzungen des Zentralen Nervensystems durchmachen.

### **Schlussfolgerungen**

Die Resultate, die in dieser Studie erarbeitet wurden, zeigen ein sehr diverses Bild von den Neurodegenerativen Krankheiten. Wir konnten bis dato unbeschriebene Arten von Neurodegeneration und Proteinaggregation beschreiben. Des Weiteren haben wir in humanem Gewebe Hinweise auf 2 der oben erwähnten Pathologischen Pathways gefunden. Nämlich das blockieren des Axonalen Transports durch die Bildung von Aggregaten und die progressive Deregulation von wichtigen Komponenten des zellulären Stoffwechsels durch die ebenfalls progressive Aggregation von Krankheitsprotein. Zu letzt haben wir Indizien für die Involvierung nicht neuronaler Zellen, der Astrocyten, in die neurodegenerativen Prozesse gefunden.

Die Identifizierung von diversen pathologischen Vorgängen, sowohl in dieser These, als auch in anderen aktuellen Arbeiten, lässt den Schluss zu, dass in den meisten Neurodegenerativen Erkrankungen mehrere pathologische Prozesse gleichzeitig ablaufen. Diese Prozesse können über die ganze Lebensdauer eines Neurons hinweg kumulativen Stress aufbauen. An einem gewissen Punkt geht das Neuron dann durch den kumulativen Stress zugrunde. Da Neurone innerhalb ihrer Netzwerke von einander abhängig sind, verursacht der Tod eines Neurons in einem Netzwerk weiteren Stress für alle anderen Neurone im Netzwerk, was weitere Ausfälle begünstigt.

Für die meisten Neurodegenerativen Erkrankungen gibt es noch immer keine Heilung, lediglich Symptome können behandelt werden. Die vorliegende These leistet zusammen mit vielen anderen laufenden Forschungsreihen einen Beitrag zum Verständnis der pathologischen Vorgänge. Dieses Verständnis kann als Startpunkt für weitere Forschung und für das Erarbeiten von effektiven Therapiemethoden dienen. Während es wahrscheinlich schwierig ist, Prozesse wie axonale Blockaden direkt zu kontern, scheinen PQC-Elemente lohnende Zeile zu sein. Es ist bereits bekannt, dass diverse HSPs und die verschiedenen Abbauelemente extern beeinflusst werden könnten. Präzise Eingriffe in diese Systeme könnten Krankheitssymptome abschwächen und



eine weitere Progression verlangsamen oder aufhalten, und damit die Lebensqualität von Patienten nachhaltig verbessern.

## Acknowledgements

Ah, yes: finally, the doctorate shaped light at the end of the tunnel (most certainly not a freight train, no?). It took me only, like 5 ½ years. That's not that long right? Well, it actually is, but it was a very fine time. But the years I spent in Frankfurt and in Groningen wouldn't have been as good without the mighty fine people I had the pleasure of working with.

First of all, I want to thank my supervisors Harrie, Udo and Wilfred. You were (and still are) very supportive, enthusiastic and friendly. I think that a nice workplace atmosphere simply can't be overestimated, and thanks to you three, I had the best. Also, you introduced me to an interesting field of research with the added moral benefit of maybe helping some patients who actually have the diseases we analyzed. And especially to Wilfred, I want to congratulate you on your very fine taste in music. Because it matches mine. And that's awesome.

I'd also like to acknowledge the members of the reading committee: the professors Georg Auburger, Erik Boddeke and Berry Kremer, for the time they put in judging my thesis.

But it's not only at the level of the "bosses" where the puppies and rainbows and assorted niceness are at. I had some of the most splendid colleagues and co-operations during my career that one can imagine. And I want to thank you all for that, especially Andreas, Christian, Dominico, Franziska, Estifanos, Mariette, Mohammed, Wagma and basically everyone I worked with the Anatomy I department. And the same goes for all my dear colleagues at the UMCG, who I only mention later, because I am doing this kinda chronologically. Thank you, Alessandra, Edwin, George, Jing, Jonathan, Marianne, Melanie, Melania, Sander, Serena, Tineke and Vaishali and everyone else at the neurobiology, cell biology and pathology departments, and my numerous (and somewhat changing) roommates at pathology.

There is also a number of people from other institutions, who I co-operated with, and who I want to acknowledge for that: Alex Kern and Prof. Helmut Oelschläger from Anatomy III at Frankfurt University; Prof. Henry Paulson from the University of Michigan; Elisabeth Petrasch-Parwez from the University of Bochum; Rejko Krüger, Prof Lutger Schöls and Prof. Olaf Riess from Tübingen;

Every country has its bureaucracy, and although I think, Germany is still the undisputed leader in this regards, the Netherlands do have a fair bit of paperwork themselves. So, I want to use this opportunity to thank all the people who helped me with that paperwork. Thank you, Martina of the Department Anatomy I in Frankfurt; thank you Diana, Evelyn, Gerry and Janine of BCN; Annet from the cell biology department, and José, Ellen, Marijke and Harriët from the pathology, for all the help.

Beside supportive colleagues and supervisors, I also want to thank my friends and family for their support and time. First and foremost, this one goes out to my parents, from whom I got everything I ever needed, and so much more. I wouldn't be here without you, in more than the obvious regard. And I also want to thank my friends in Daaden, Marburg and Siegen, for being there and providing me with a good time. I also want to thank my landlords in Groningen, the Luttikhuizens, for making me feel welcome in their House, and by extension, in the Netherlands.

And finally, to whoever came up with that "Schengen-area" idea: That's one damn nice thing to have. I mean, I could just drive over to Groningen and start studying. Please, don't let fearmongers and rightwingers ruin this for everyone.

## Curriculum vitae

Surname: Seidel  
First Name: Kay  
Nationality: German  
Date and place of Birth: 13.02.1978, Siegen, Germany

### Scientific career and education

---

|           |  |
|-----------|--|
| 2009-2010 | PhD student at the University of Groningen /UMCG (Netherlands)   |
| 2005-2008 | Scientific Assistant at the Department of Anatomy II at the University Clinic Frankfurt/Main (Germany) |
| 1998-2004 | Graduate in Biology at the Philips University Marburg (Germany)  |

### Research activities

---

|           |  |
|-----------|--|
| 2009-2010 | PhD studies at the UMCG. Subject:<br>Characterization of protein aggregates and components of the cellular protein quality control in neurodegenerative diseases in human tissue.  |
| 2005-2008 | Scientific Assistance at the university clinic, Frankfurt:<br>Subjects:<br>Analysis of the axonal aggregation pathology in spinocerebellar ataxia type 3.<br>Analysis of the pathoanatomy of spinocerebellar ataxia types 1-3, 6 and 7.<br>Comparative pathonatomical study of idiopathic and familial Parkinsonism (A30P).<br>Descriptive study of a case of complex hereditary spastic paraplegia. |

Comparative study of the vestibular nuclei in the human and in the dolphin (*Delphinus delphis*, *Ponoporia blainvillei*)

2003-2004

Diploma Thesis at the department of animal physiology at the Philips University (Marburg, Germany).

Subject:

Characterization of luminal cells in the developing antenna of the tobacco hornworm (*Manduca sexta*)

2002

Major Laboratory course at the department of animal physiology at the Philips University (Marburg, Germany). Subject:

Characterization of luminal cells in the developing antenna of the tobacco hornworm (*Manduca sexta*)

2001

Genetics main course at the department of Genetics, at the Philips University (Marburg, Germany).

Subject:

Basic Techniques of genetic research.

2000

Animal physiology main course at the department of Animal physiology at the Philips University (Marburg, Germany)

Subject:

Cloning of a cytoplasmatic oxygen receptor in the djungarian hamster (*Phodopus sungorus*)

Electrophysiology of the accessory medulla of the common roach (*Leucophaea maderae*)

## Publications

### First and Joint first authorships

---

**Seidel K**, Vinet J, Den Dunnen WF, Brunt ER, Meister M, Boncoraglio A, Zijlstra MP, Boddeke HW, Rüb U, Kampinga HH, Carra S. The HSPB8-Bag3 chaperone complex is upregulated in astrocytes in the human brain affected by protein aggregation diseases. *Neuropathol Appl Neurobiol* 2011 Jun 23. doi: 10.1111/j.1365-2990.2011.01198.x. [Epub ahead of print]

**Seidel K**, den Dunnen WF, Schultz C, Paulson H, Frank S, de Vos RA, Brunt ER, Deller T, Kampinga HH, Rüb U. Axonal inclusions in spinocerebellar ataxia type 3. *Acta Neuropathol* 2010;120:449-460

**Seidel K**, Schöls L, Nuber S, Petrasch-Parwez E, Gierga K, Wszolek Z, Dickson D, Gai WP, Bornemann A, Riess O, Rami A, Den Dunnen WF, Deller T, Rüb U, Krüger R. First appraisal of brain pathology owing to A30P mutant alpha-synuclein. *Ann Neurol* 2010;67:684-689

**Seidel K**, Brunt ER, de Vos RA, Dijk F, van der Want HJ, Rüb U, den Dunnen WF. The p62 antibody reveals various cytoplasmic protein aggregates in spinocerebellar ataxia type 6. *Clin Neuropathol* 2009;28:344-349

**Seidel K**, de Vos R, Derksen L, Bauer P, Riess O, den Dunnen W, Deller T, Hageman G, Rüb U. Widespread thalamic and cerebellar degeneration in a patient with a complicated hereditary spastic paraplegia (HSP). *Ann Anat* 2009;191:203-211

**Seidel K**, Kern A, Oelschläger HH. The central vestibular complex in dolphins and humans: functional implications of Deiters' nucleus. *Brain Behav Evol* 2009;73:102-110

**Seidel K**, Hoche F, Brunt ER, Auburger G, Schöls L, Bürk K, de Vos RA, den Dunnen W, Bechmann I, Egensperger R, von Broeckhoven C, Gierga K, Deller T, Rüb U. Involvement of the auditory brainstem system in spinocerebellar ataxia type 2 (SCA2), type 3 (SCA3) and type 7 (SCA7). *Neuropathol Appl Neurobiol* 2008;34:479-491

### Co-Authorships

---

Carra S, Boncoraglio A, Kanon B, Brunsting JF, Minoia M, Rana A, Vos MJ, **Seidel K**, Sibon OC, Kampinga HH. Identification of the *Drosophila* ortholog of HSPB8: implication of HSPB8 loss of function in protein folding diseases. *J Biol Chem* 2010 Sep 21 [Epub ahead of print]

Gierga K, Schelhaas HJ, Brunt ER, **Seidel K**, Scherzed W, Egensperger R, de Vos RA, den Dunnen W, Ippel PF, Petrasch-Parwez E, Deller T, Schöls L, Rüb U.



Spinocerebellar ataxia type 6 (SCA6): neurodegeneration goes beyond the known brain predilection sites. *Neuropathol Appl Neurobiol* 2009;35:515-527

Rüb U, Brunt ER, **Seidel K**, Gierga K, Mooy CM, Kettner M, Van Broeckhoven C, Bechmann I, La Spada AR, Schöls L, den Dunnen W, de Vos RA, Deller T. Spinocerebellar ataxia type 7 (SCA7): widespread brain damage in an adult-onset patient with progressive visual impairments in comparison with an adult-onset patient without visual impairments. *Neuropathol Appl Neurobiol*. 2008;34:155-168

Schiesling C, Kieper N, **Seidel K**, Krüger R. Review: Familial Parkinson's disease--genetics, clinical phenotype and neuropathology in relation to the common sporadic form of the disease. *Neuropathol Appl Neurobiol* 2008;34:255-271

Rüb U, Brunt ER, Petrasch-Parwez E, Schöls L, Theegarten D, Auburger G, **Seidel K**, Schultz C, Gierga K, Paulson H, van Broeckhoven C, Deller T, de Vos RA. Degeneration of ingestion-related brainstem nuclei in spinocerebellar ataxia type 2, 3, 6 and 7. *Neuropathol Appl Neurobiol* 2006;32:635-649

Rüb U, **Seidel K**, Ozerden I, Gierga K, Brunt ER, Schöls L, de Vos RA, den Dunnen W, Schultz C, Auburger G, Deller T. Consistent affection of the central somatosensory system in spinocerebellar ataxia type 2 and type 3 and its significance for clinical symptoms and rehabilitative therapy. *Brain Res Rev* 2007;53:235-249

Rüb U, de Vos RA, Brunt ER, Sebestény T, Schöls L, Auburger G, Bohl J, Ghebremedhin E, Gierga K, **Seidel K**, den Dunnen W, Heinsen H, Paulson H, Deller T. Spinocerebellar ataxia type 3 (SCA3): thalamic neurodegeneration occurs independently from thalamic ataxin-3 immunopositive neuronal intranuclear inclusions. *Brain Pathol* 2006;16:218-227

Rüb U, Brunt ER, Gierga K, **Seidel K**, Schultz C, Schöls L, Auburger G, Heinsen H, Ippel PF, Glimmerveen WF, Wittebol-Post D, Arai K, Deller T, de Vos RA. Spinocerebellar ataxia type 7 (SCA7): first report of a systematic neuropathological study of the brain of a patient with a very short expanded CAG-repeat. *Brain Pathol* 2005;15:287-295

11013355